16th AIVC Conference
Implementing the Results of Ventilation Research

held at Palm Springs, California, USA
19-22 September 1995

Proceedings
Volume 1

Preface

International Energy Agency

The International Energy Agency (IEA) was established in 1974 within the framework of the Organisation for Economic Co-operation and Development (OECD) to implement an International Energy Programme. A basic aim of the IEA is to foster co-operation among the twenty-one IEA Participating Countries to increase energy security through energy conservation, development of alternative energy sources and energy research development and demonstration (RD&D). This is achieved in part through a programme of collaborative RD&D consisting of forty-two Implementing Agreements, containing a total of over eighty separate energy RD&D projects. This publication forms one element of this programme.

Energy Conservation in Buildings and Community Systems

The IEA sponsors research and development in a number of areas related to energy. In one of these areas, energy conservation in buildings, the IEA is sponsoring various exercises to predict more accurately the energy use of buildings, including comparison of existing computer programs, building monitoring, comparison of calculation methods, as well as air quality and studies of occupancy. Seventeen countries have elected to participate in this area and have designated contracting parties to the Implementing Agreement covering collaborative research in this area. The designation by governments of a number of private organisations, as well as universities and government laboratories, as contracting parties, has provided a broader range of expertise to tackle the projects in the different technology areas than would have been the case if participation was restricted to governments. The importance of associating industry with government sponsored energy research and development is recognized in the IEA, and every effort is made to encourage this trend.

The Executive Committee

Overall control of the programme is maintained by an Executive Committee, which not only monitors existing projects but identifies new areas where collaborative effort may be beneficial. The Executive Committee ensures that all projects fit into a pre-determined strategy, without unnecessary overlap or duplication but with effective liaison and communication. The Executive Committee has initiated the following projects to date (completed projects are identified by *. The final reports for these projects can be obtained from AIVC):

ANNEX 1	Load Energy Determination of Buildings*
ANNEX 2	Ekistics and Advanced Community Energy Systems*
ANNEX 3	Energy Conservation in Residential Buildings*
ANNEX 4	Glasgow Commercial Building Monitoring*
ANNEX 5	Air Infiltration and Ventilation Centre
ANNEX 6	Energy Systems and Design of Communities*
ANNEX 7	Local Government Energy Planning*
ANNEX 8	Inhabitant Behaviour with Regard to Ventilation*

ANNEX 9	Minimum Ventilation Rates*
ANNEX 10	Building HVAC Systems Simulation*
ANNEX 11	Energy Auditing*
ANNEX 12	Windows and Fenestration*
ANNEX 13	Energy Management in Hospitals*
ANNEX 14	Condensation*
ANNEX 15	Energy Efficiency in Schools*
ANNEX 16	BEMS - 1: Energy Management Procedures*
ANNEX 17	BEMS - 2: Evaluation and Emulation Techniques*
ANNEX 18	Demand Controlled Ventilating Systems*
ANNEX 19	Low Slope Roof Systems*
ANNEX 20	Air Flow Patterns within Buildings*
ANNEX 21	Thermal Modelling*
ANNEX 22	Energy Efficient Communities
ANNEX 23	Multizone Air Flow Modelling (COMIS)
ANNEX 24	Heat Air and Moisture Transfer in Envelopes
ANNEX 25	Real Time HEVAC Simulation
ANNEX 26	Energy Efficient Ventilation of Large Enclosures
ANNEX 27	Evaluation and Demonstration of Domestic Ventilation Systems
ANNEX 28	Low Energy Cooling Systems
ANNEX 29	Daylighting in Buildings
ANNEX 30	Bringing Simulation to Application

Annex V Air Infiltration and Ventilation Centre

The IEA Executive Committee (Building and Community Systems) has highlighted areas where the level of knowledge is unsatisfactory and there was unanimous aggreement that infiltration was the area about which least was known. An infiltration group was formed drawing experts from most progressive countries, their long term aim to encourage joint international research and increase the world pool of knowledge on infiltration and ventilation. Much valuable but sporadic and uncoordinated research was already taking place and after some initial groundwork the experts group recommended to their executive the formation of an Air Infiltration and Ventilation Centre. This recommendation was accepted and proposals for its establishment were invited internationally.

The aims of the Centre are the standardisation of techniques, the validation of models, the catalogue and transfer of information, and the encouragement of research. It is intended to be a review body for current world research, to ensure full dissemination of this research and based on a knowledge of work already done to give direction and firm basis for future research in the Participating Countries.

The Participants in this task are Belgium, Canada, Denmark, Germany, Finland, France, Italy, Netherlands, New Zealand, Norway, Sweden, Switzerland, United Kingdom and the United States of America.

16th AIVC Conference
"Implementing the Results of Ventilation Research"

CONTENTS: VOLUME 1 **Page**

SESSION 1: Energy Efficient Ventilation

Energy Requirements for Conditioning of Ventilating Air 1
D Colliver

Comparative Trials of Ventilation Systems for Humidity Control 13
D A McIntyre, S L Palin, R E Edwards

Applying Ventilation Related Research to ASHRAE Standard 62 23
G Tucker, S T Taylor

Performance of Natural Ventilation in Dwellings.A Longitudinal Computational Simulation Study 25
J Kronvall, A Blomsterberg

Energy Demand for the Conditioning of the Supply Air in Ventilation 37
F Steimle

SESSION 2: Measurement and Modelling

Short Term and Long Term Measurements of Ventilation in Dwellings 47
A Blomsterberg, T Carlsson, J Kronvall

Temperature and Velocity Distributions for Slot Devices 59
U Kruger

The Southampton Survey on Asthma and Ventilation:Humidity Measurements During Winter 69
D A McIntyre, F R Stephen

A Low Cost Technique for the Measurement of High Ventilation Rates 79
D K Alexander, S Lannon

Quantification of Radon Migration from a Uranium Mine Through the Soil into Buildings by the Use of Tracer Techniques 87
W Raatschen, R A Grot, W Lobner

The Effect of Ventilation & Pressure Differences on Concentrations of Radon at Workplaces. 105
P Korhonen, H Kokotti, P Kalliokoski

Ventilation Effectiveness Measurements in Selected NZ Office Buildings 115
M R Bassett, N Isaacs

Natural Ventilation Design at the Welsh School of Architecture 125
P J Jones, D K Alexander, H Jenkins

Application of Air Flow Models to Aircraft Hangars with Very Large Openings 127
J van der Maas, A Schaelin

Ventilation and Air Movement within Factories.A Comparison of CFD Predictions with Measured Data. 143
P J Jones, R Waters, G Powell, C Byabagambi

Predicting Indoor Airflow by Combining Network Approach, CFD and Thermal Insulation 145
J A Clarke, J L M Hensen, C O R Negrao

Experimental Validation of ASHRAE SPC-129 "Standard Method of Measuring Air Change Effectiveness". 155
F J Offermann III, M T O'Flaherty, M A Waz, N B Erlin

Fan Pressurization Measurements by Four Protocols 165
S N Flanders

The Combined Use of CFD and Zonal Modelling Techniques to Aid the Prediction and Measurement of Ventilation Effectiveness Parameters 175
M W Simons, J R Waters, J Leppard

The Use of Tracer Gas Methods for Detailed Airborne Moisture Transport Study in Buildings 191
D Ducarme, A Bossaer, P Wouters

The Dutch E'Novation Program: Indoor Air Quality in Dwellings Before and After Renovation 201
P J M Op't Veld, H G Slijpen

SESSION 3: Modelling

NRC Indoor Environment Research Facility 209
C Y Shaw, S A Barakat, G R Newsham, J A Veitch, J Bradley

A Simple Calculation Method for Attic Ventilation Rates 221
I S Walker, T W Forest, D J Wilson

Pressure Simulation Program 233
B Knoll, J C Phaff, W F de Gids

Determining IAQ Dynamic Response to Emissions 243
M Meckler

Modelling Coupled Heat and Airflow: Ping Pong Vs. Onions 253
J L M Hensen

Effectiveness of a Heat Recovery Ventilator, an Outdoor Air Intake Damper and an Electrostatic Particulate Filter at Controlling Indoor Air Quality in Residential Buildings 263
S J Emmerich, A K Persily

A Laboratory for Investigation of the Air Quality in Simulated Indoor Environments 277
L E Ekberg, J B Nielsen

Measurement and CFD Modelling of IAQ Indexes 287
M Regard, F R Carrie, A Voeltzel, V Richalet

VOLUME II

SESSION 4: Energy Efficient Ventilation

The Design and Development of Two Energy & Environmentally Sustainable Prototype Office Buildings 295
E M Sterling, T Coady, J Cook, G Shymko, K Newburt, J Cordonier

Field Survey of Heat Recovery Ventilation Systems: Occupant Interactions 305
D Hill

Improvement of a Mechanical Ventilation Systems Regarding the Utilization of Outdoor Air 315
T Carlsson, A Blomsterberg

Efficient Work Environment Ventilation 327
S Holmberg, I-M Andersson, R Niemela

Air Dehumidification by Absortive & Evaporative Cooling 341
J Roeben, S Y Kourouma

The New Energy Conservation Code in the Federal Republic of Germany 351
G Mertz

Automatic Control of Natural Ventilation and Passive Cooling 359
A Martin

Air Flow Distribution in a Mechanically Ventilated High Rise Residential Building 369
R C Diamond, H E Feustel

Energy Impacts of Air Leakage in US Office Buildings 379
D VanBronkhorst, A K Persily, S J Emmerich

TWINFACE - First Results About a New Developed Double Facade System 393
W Raatschen

Design and Installation of Passive Stack Ventilation in Retrofitted Apartment Buildings 395
J Riberon, J-G Villenave, J-R Millet, S Moutet

SESSION 5: Maintenance and Long Term Performance

The Impact of Various Ventilation Remedies on Radon Levels and Local Building Environment in a UK Test House - Some Preliminary Results 405
P A Welsh

Particulate Deposition on Indoor Surfaces - its Role with Ventilation in Indoor Air Quality Prediction 415
M A Byrne, A J H Goddard, F C Lockwood, M Nasrullah

Occupant Response to Passive Stack Ventilation: A UK Postal Survey 425
N Oseland

Evaluation and Demonstration of Domestic Ventilation: State of the Art 435
L-G Mansson

Indoor Climate and User Interaction in Modern Swedish One-Family Houses - Results Using a Questionnaire. 447
A Blomsterberg, T Carlsson

Feasibility of Ventilation Heat Recovery in Retrofitting Multi-Family Buildings 461
J Sateri, J Heikkinen, M-L Pallari

The Indoor Air Quality and the Ventilation Performance of Two Occupied Residential Buildings with Dynamic Insulation 471
J T Brunsell

Criteria for Heat Recovery and Dehunidification 483
F Dehli

A New Ventilation Strategy for Humidity Control in Dwellings - A Demonstration Project 493
J B Nielsen, I Ambrose

SESSION 6: Workshop on Standardisation

3 part Workshop discussing new developments on Standardisation in (i) Europe, (ii) North America, and (iii) Global standards. Comprising informal presentations with discussion and question time.

SESSION 7: Measurement

Trickle Ventilators: Effective Natural Background Ventilation for Offices 507
M Kolokotroni, S G Marshall, M D A E S Perera

Evaluation of an IR-Controlled Ventilation System in an Occupied Office Building 517
D Ducarme, P Wouters, D L'Heureux

Cooling Performance of Silent Cooling Systems Built by Free Convective Coolers 527
F Steimle

High Resolution Particle-Imaging Velocimetry for Full Scale Indoor Air Flows 537
M M Cui, C Topp, S Pedersen, L L Christianson, R J Adrian, K W Leovic

Reducing the Permeability of Residential Duct Systems 551
F R Carrie, M P Modera

A Report on the Radon Measurement in a Single Family House 561
F Wang, I C Ward

Implementing the Results of Ventilation Research
16th AIVC Conference, Palm Springs, USA
19-22 September, 1995

Energy Requirements for Conditioning of Ventilating Air

Donald G Colliver, Ph.D., P.E.

Visiting Specialist at AIVC

Associate Professor, University of Kentucky, USA

Energy Requirements for Conditioning of Ventilating Air
Donald G. Colliver, Ph.D., P.E.

SYNOPSIS

The energy impact involved between bringing in outdoor air for indoor air pollution reduction and the energy required to condition this air are investigated in this report. Long-term hourly weather data from several European and American locations were analyzed to determine the average conditions of air over the period of record of the data. These data were then analyzed to determine the psychrometric process theoretical heating, cooling and moisture removal energy requirements for a constant mass of airflow per hour (MJ·h/kg). This paper summarizes the information contained in a longer report [3].

It was found that a significant amount of energy is required to condition air which is used for ventilation. The annual energy required per kg-dry-air/hr of airflow varied from 22.1 MJ·h/kg for Los Angeles to 102.5 MJ·h/kg for Omaha. In Europe the range was from 45.6 MJ·h/kg for Nice to 101.1 MJ·h/kg for Saint-Hubert. In Europe most of the energy was used to heat the air to the desired setpoint. In America there were significant amounts of both heating and cooling required. Much of the variation was due to the amount of moisture in the air which had to be removed in air conditioning. In situations where air conditioning is used, a significant amount of this energy is used in dehumidifying the air. For example, in Miami 86% of the energy is used for moisture removal. It was also found that the energy used was highly sensitive to the heating, cooling and relative humidity setpoints.

1. INTRODUCTION

Outdoor air is brought into buildings for many different reasons such as free cooling, "fresh air" and pollution reduction. Over the last several years structures have been built tighter to reduce air infiltration and conserve energy used to heat the air coming into the building. Several standards and organizations have been specifying minimum amounts of "fresh" outdoor air for indoor air quality purposes. There have been several questions however about the energy impact and/or tradeoffs involved between bringing in outdoor air (for pollution reduction) and the energy required to condition this air. This work is intended to provide an initial estimate of the theoretical energy required.

2. OBJECTIVES

The objectives of this work are: first to determine the theoretical energy requirements per constant mass unit of outdoor air used for ventilation for a number of different climates and locations in North America and Europe; and secondly to determine the variation of this annual ventilation heating and cooling energy requirements due to the setpoints for temperature and humidity.

3. PSYCHROMETRIC PROCESSES ASSOCIATED WITH VENTILATION

A psychrometric chart is a visual presentation of the possible characteristics of an air-water vapor mixture and is often used to describe the possible conditions or statepoints which may be obtained by the air. The psychrometric chart is commonly used to determine the heat and moisture changes in the air as it goes from one condition (such as 32 °C, 65% relative humidity outdoor air) to another condition (26 °C, 40% relative humidity) such as inside a building.

The psychrometric chart can also be used to determine the heat and moisture which must be added or subtracted from the air. Therefore if the average conditions of the outdoor air are known, the theoretical energy which must be added or subtracted from the air to heat, cool and/or dehumidify it when the air enters the building may be determined.

The amount of sensible energy need to heat or cool air is calculated from:

$$\text{Sensible} = (C_{pa} + W * C_{pw})(t_{db\text{-}setpt} - t_{db\text{-}outside}) \qquad (1)$$

where:

C_{pa} = Specific heat of dry air (1.0056 kJ/kg-dry air·°C)
W = Amount of moisture in the air (kg)
C_{pw} = Specific heat of water vapor (1.86 kJ/kg water·°C)
$t_{db\text{-}setpt}$ = Setpoint dry-bulb temperature (°C)
$t_{db\text{-}outside}$ = Outside dry-bulb temperature (°C)

Latent heat is that energy which must be added or withdrawn when water is vaporized (in the case of humidification) or condensed (in the case of dehumidification) from the air. The latent heat transfer, or the energy which must be used for moisture control with humidification/dehumidification, can be determined from the amount of moisture which must be added or removed as:

$$\text{Latent} = L * \Delta W \qquad (2)$$

where:

L = Latent heat of vaporization (2501.3 kJ/kg water)

The amount of water which must be subtracted from the air is:

$$\Delta W = H_{setpt} - H_{outside} \qquad (3)$$

where:

H_{setpt} = Humidity ratio of the air at the setpoint (kg water vapor/kg dry air)
$H_{outside}$ = Humidity ratio of the outside air (kg water vapor/kg dry air)

If two independent measurements (such as dry-bulb and relative humidity) and the air pressure are known, the others characteristics (such as humidity ratio, wet-bulb temperature, dew-point temperature, etc) may be determined from the psychrometric chart or from equations which mathematically describing it. The computerized psychrometric routines used in this work [5, 9] are available via anonymous ftp in the directory /pub/bae/psych at the site: ftp.ca.uky.edu.

The psychrometric chart may be divided into several regions where the air being described by that region undergoes the same psychrometric process to reach the desired condition of temperature and moisture content. If the average condition (over all the hours the air is within that region) for the air within that region is known, then the energy and moisture which must be added or subtracted may then be determined. The conditions of the outdoor air fall into six different regions on the chart with respect to the desired condition of the air in the building (see Figure 1).

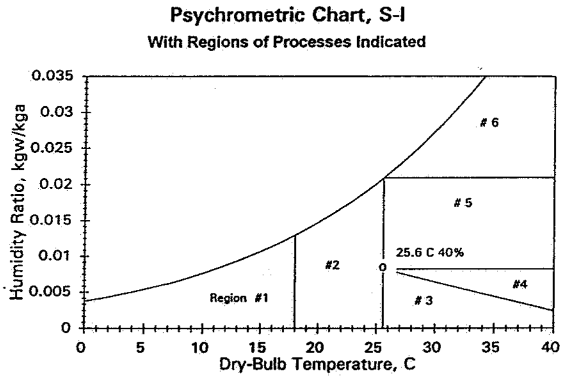

Figure 1. Psychrometric Chart with Regions of Processes Used to Reach Desired Statepoint

Region 1: Outdoor Dry-Bulb Temperature Less Than Heating Setpoint $(T_{db\text{-}outdoor} < T_{dbh\text{-}setpt})$ (Heating Region)

This is the typical wintertime condition when heat is being added to the ventilation air. In this case only sensible heat is added to the air to reach the desired statepoint since typically moisture is not controlled in heating situations. There is no intentional latent heat exchange in this region.

Region 2: Outdoor Dry-Bulb Temperature Greater Than Heating Setpoint but Less Than Cooling Setpoint $(T_{dbh\text{-}setpt} < T_{db\text{-}outdoor} < T_{dbc\text{-}setpt})$ (No Heating or Cooling Region)

This is the condition when the outdoor air does not need to be either heated or cooled. It represents the moderate weather conditions typically encountered during the spring and fall or at other times when neither heating or cooling are needed. This also represents the situation when the outdoor air is being introducing into the building for natural ventilation. In this case there is no sensible or latent energy exchange required to condition the air.

Region 3: Dry-Bulb Temperature Greater Than Cooling Setpoint Temperature and Wet-Bulb Less Than Desired Wet-Bulb $(T_{db\text{-}outdoor} > T_{dbc\text{-}setpt}, T_{wb\text{-}outdoor} < T_{wbc\text{-}setpt})$ (Evaporative Cooling Region)

The air in this region has a higher dry-bulb temperature than desired, however the outdoor wet-bulb temperature is less than the wet-bulb of the design setpoint. This condition is typically associated with hot, dry weather. Evaporative cooling (a process which approximately follows the wet-bulb line) can be used in this psychrometric region to provide the desired reduction in dry-bulb temperature. The sensible energy used to cool the air comes from the latent heat of evaporization of the water added to the air. Since there is an exchange of sensible and latent heat in this region and in practice the energy required is for pumping/spraying which has comparatively small energy expenditure, the sensible and latent energy requirements for this region will not be included in the total energy requirements.

Region 4: Outdoor Dry-Bulb and Wet-Bulb Temperatures Greater Than Cooling Setpoint Temperatures, Dew-Point Less Than Setpoint ($T_{db\text{-}outdoor} > T_{dbc\text{-}setpt}$, $T_{wb\text{-}outdoor} > T_{wbc\text{-}setpt}$, $T_{dp\text{-}outdoor} < T_{dpc\text{-}setpt}$) (Refrigerative and Evaporative Cooling Region)

Air in this region may be partially cooled with evaporate cooling (up to the dew-point of the setpoint) and then external energy must be used to remove the remaining sensible heat if moisture conditioning is achieved. In many cases, cooling is only controlled based upon dry-bulb temperature and moisture is controlled with the system design. For the purposes of this study, the total energy required is the net of the sensible and latent heats.

Region 5: Outdoor Dry-Bulb Temperature Greater Than Cooling Setpoint Temperature, Outdoor Dew-Point Greater than Setpoint and Less Than Saturation ($T_{db\text{-}outdoor} > T_{dbc\text{-}setpt}$, $T_{wb\text{-}outdoor} > T_{wbc\text{-}setpt}$, $T_{dpc\text{-}setpt} < T_{dp\text{-}outdoor} < T_{dpc\text{-}sat}$)
(Refrigerative Cooling Region, Dew-point less than Setpoint Saturation Temperature)

Air in this region must have both sensible heat and moisture (latent heat) removed to maintain the desired setpoint. The amount of moisture removed may be used to determine the amount of latent heat which is removed for humidity control. The sensible and latent energy requirements in this region are defined by eqns 1 and 2.

Region 6: Outdoor Dry-Bulb and Dew-Point Temperatures Greater Than Cooling Dry-Bulb Setpoint Temperature and Dewpoint at Saturation ($T_{db\text{-}outdoor} > T_{dbc\text{-}setpt}$, $T_{wb\text{-}outdoor} > T_{wbc\text{-}setpt}$, $T_{dp\text{-}outdoor} > T_{dpc\text{-}sat}$) (Refrigerative Cooling Region, Dew-point greater than Setpoint Saturation Temp)

Air in this region is hot and humid. The latent (moisture) heat removal is the significant energy requirement to maintain the desired conditions. The sensible and latent energy requirements in this region are defined by eqns 1 and 2.

It should be recognized that the energy values presented are for the minimum theoretical enthalpy changes of the air and the total amount of equipment energy used in Regions 4,5 and 6 may be larger than the theoretical energies given due to the system design and equipment efficiencies.

4. PROCEDURE

Estimates were made of the theoretical amount of energy needed to condition a constant airflow rate of one kg of dry air per hour (kg/hr) of outdoor air used for ventilation. These estimates were made using measured hourly weather data from a number of locations and the theoretical energy and moisture change needed to condition the air to the desired statepoint. The weather data for each location were analyzed to determine the number of hours the outdoor air conditions fell within each psychrometric process region and the weighted average air property for each region. The sensible and latent energies required in each of the psychrometric process regions were then determined by calculating the energy difference between the air statepoint representing the average condition for all the hours within that region and the air at the desired setpoint. Energy values from each of the processes were then combined to determine the total energy per unit mass of ventilation. The effects of equipment and different heating and/or cooling techniques are not included due to the wide variety and efficiencies of possible equipment. Summary weather data are provided in [3] to determine these effects if desired.

4.1 ENERGY TRANSFER SUMMARY

The sensible energy which must be used over all the psychrometric regions to heat to the desired heating setpoint and cool to the desired cooling setpoint is the sum of the heating and cooling energy requirements, or:

$$Sen_{total} = S_1 + | S_4 + S_5 + S_6 | \tag{5}$$

where S represents equation 1 and the subscript represents the region.

The total latent energy which must be removed to obtain the desired cooling humidity conditions is:

$$Lat_{total} = | L_4 + L_5 + L_6 | \tag{6}$$

where L represents equation 2 and the subscript represents the region.

The theoretical total energy which must be supplied to maintain the desired conditions is the sum of the sensible and latent heat transfers or:

$$Energy_{Total} = Sen_{total} + Lat_{total} \tag{7}$$

4.2 WEATHER DATA SOURCES

Measured hourly weather data from a number of locations in North America and Europe were used to determine the average outdoor weather conditions. Long-term (30 years) hourly weather data for 238 US locations are available in the SAMSON data set [8]. A subset of these weather data sets was selected based upon their climate classification region [4, 7] to be representative of the range of climates and weather conditions experienced in America [2]. European locations were selected based upon the availability of hourly weather data. Hourly weather data for most of the British locations were obtained from the CIBSE Example Weather Years, EWY [6]. Weather data for other European locations and four additional UK locations were obtained from the CEC Test Reference Years [1]. The selected American and European locations are presented in Table 1.

4.3 DETERMINATION OF THE AVERAGE CONDITION FOR EACH PSYCHROMETRIC REGION

The "average air" in each psychrometric region for each location was determined by analyzing the measured weather data. Coincident matrices or arrays were made which contained the number of hours each dew-point temperature occurred coincidentally with each dry-bulb temperature. These X-Y arrays (X dry-bulb temperature vs Y dew-point temperature) contained the number of occurrences of Y dew-point temperature which had occurred at X dry-bulb temperature. Thirteen (12 monthly and one yearly total) matrices were determined from the long-term weather data for each location. One °C bins were used for both dry-bulb and dew-point temperatures.

The "average air" statepoint for each region was then determined from the matrices by assuming that it was a mixing process of all the occurrences of conditions within a psychrometric region. In this situation each dry-bulb/dew-point combination was weighted by the number of hours of occurrence of that condition in the historical data set. Dry-bulb and absolute humidity for the given dew-point were the psychrometric parameters used in the mixing routines. The psychrometric properties were calculated using C^{++} routines [5,9]. Standard air pressure based upon station elevation was used for all the mixing calculations.

The average percentage of the annual hours in each psychrometric region and the corresponding average dry-bulb temperature and humidity ratio are given in [3] for each of the locations investigated. The percentage of the total number of hours in each region is given for four locations in the pie charts in Figure 2.

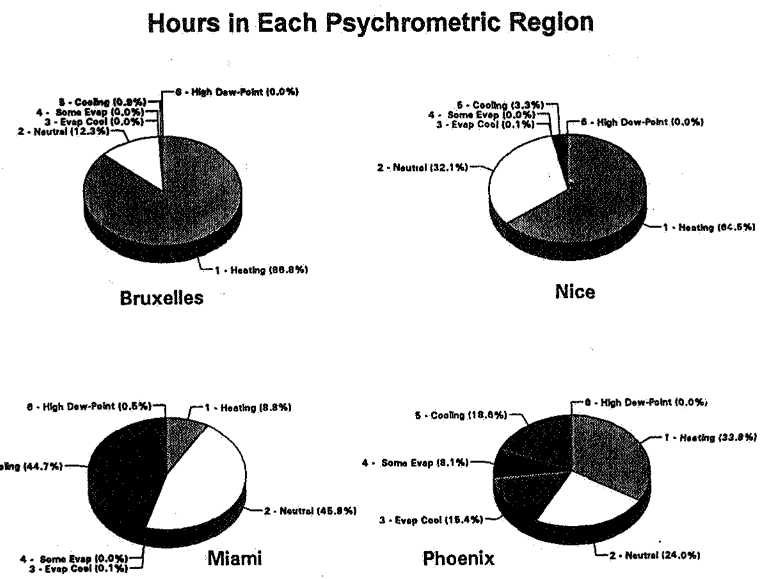

Figure 2. Pie Chart with Percentage of Hours in Each Psychrometric Region

5. RESULTS AND DISCUSSION

5.1 ANNUAL HEATING ENERGY REQUIREMENTS

The amount of sensible heating required for conditioning a constant airflow of one kgdryair/hr of ventilating air to 18 °C was determined for each of the locations and is presented in Table 1. This setpoint was used to closely correspond to a setpoint commonly used in some American standards which relate to air infiltration and ventilation (ASHRAE Standards 119 and 136).

There is a significant amount of energy used to heat the incoming air. For the 18°C setpoint it varies from approximately 101 MJ·h/kg for Saint-Hubert, Belgium (cold climate) to 3.3 MJ·h/kg for Miami, USA (warm climate). These account for 99.6% and 2.3% of the total energy for each location respectively.

Sometimes it is assumed that the entering air needs to be heated to a temperature less than the setpoint due to solar and internal heat gains. A sensitivity analysis of the energy required to heat the air to 1,2, and 3 degrees less than the setpoint (i.e. 17, 16, & 15 °C respectively) was conducted. It was found that for the locations selected in this work which had a significant amount of heating required that there was approximately a 10% (7.2 MJ·h/kg) reduction in this energy for every °C of reduction in the setpoint. The expanded version of this work [3] also contains an equation with location dependent coefficients which describe the variation of the heating requirements over a range of setpoints from 5 to 40 °C.

5.2 ANNUAL SENSIBLE AND LATENT COOLING ENERGY REQUIREMENTS

The total theoretical sensible and latent energy exchange required for humidity control and cooling to the desired statepoint of 25.6 °C and 40% RH for psychrometric regions 4 through 6 are presented in Table 1. The sensible and latent energy exchange for each of the regions 3 through 6 are contained in [3].

These results indicate that conditioning of air to provide cooling and dehumidification can require significant amounts of energy. The greatest amount of sensible cooling was required in Phoenix, AZ (20.2 MJ·h/kg dry air) and the greatest amount of latent cooling was required in Miami, FL (82.2 MJ·h/kg). The total cooling load (combined sensible and latent) is highest in Miami (92.1 MJ·h/kg) which has a hot humid climate.

On the average (each station weighted evenly), latent cooling required 65.3% of the total cooling load for all the locations investigated. When only those locations requiring more than 5 MJ·h/kg are considered (i.e. consider only those locations typically requiring air conditioning), the latent cooling required 79.7% of the total cooling load. This implies that more energy is used in air conditioning for moisture control than dry-bulb temperature control.

Variation of Energy Required due to Setpoint:

The effect of the cooling dry-bulb temperature setpoint on the energy required was determined by changing the setpoint plus and minus two °C for those locations which had greater than 5 MJ·h/kg cooling load. A great sensitivity of the cooling energy requirements to the control setpoint selected was found [3]. The greatest change in energy requirements was for Miami where the cooling energy required at 2 higher and lower setpoints was 151.4% and 49.5% of the energy required at 25.6 °C.

Variation of Energy Required due to Humidity Design Setpoint:

The latent energy requirements previously identified indicate that a significant amount of the energy used is for dehumidifying the air to the desired condition. Thus the design relative humidity greatly impacts the energy requirements. (The energy requirements were determined initially for a 40% relative humidity design.) In order to determine the sensitivity of the relative humidity setting, the energy required for relative humidity designs of 60% and 80% were also determined for the 25.6 °C setpoint.

Increasing the relative humidity setpoint from 40% to 60% had a significant impact on the energy requirements for those locations with significant cooling requirements. The energy requirements at 60% RH relative to that required at 40% RH ranged from 15.2% for Carpentras to 59.0% for Brownsville. When the setpoint was raised to 80% there was an even greater reduction in the energy requirements. The fraction of energy required at 80% RH ranged from 0.0% to 21.2% of that when the setpoint was 40% RH.

5.3 COMBINED ANNUAL SENSIBLE, LATENT AND TOTAL ENERGY REQUIREMENTS PER UNITARY AIRFLOW RATE

The combined heating and cooling sensible, latent and total energy requirements (based on the 18°C heating, and 25.6°C, 40% cooling setpoints) are presented for each of the locations in Table 1 and Figure 3. This is the total theoretical energy required over the entire year which must be supplied to condition the ventilation air to the desired conditions. The total energy required ranged from 22.1 to 102.5 MJ·h/kg in America (Los Angeles and Omaha) and from 45.6 to 101.1 in Europe (Nice and Saint-Hubert). Heating accounted for almost all the energy used for conditioning ventilating air in Europe with the maximum air conditioning load being 5.5 MJ·h/kg (12.1% of total) in Nice. In America the fraction of the total energy used for cooling varied from 96.5 to 0.1% (92.1 to 0.1 MJ·h/kg for Miami and Cheyenne respectively). The latent load was larger than the sensible load for air conditioning in all the locations with a significant cooling load except Phoenix which has a hot dry climate.

6. SUMMARY

Estimates were made of the theoretical amount of energy needed to condition a constant airflow rate of one kg of dry air per hour (kg/hr) of outdoor air used for ventilation. These estimates were made using measured hourly weather data from a number of locations and the theoretical energy and moisture change needed to condition the air to the desired statepoint. It was found that a significant amount of energy is required to condition air used for ventilation. The annual energy required per kg/hr of airflow varied in America from 22.1 MJ·h/kg for Los Angeles to 102.5 MJ·h/kg for Omaha. In Europe the range was from 45.6 MJ·h/kg for Nice to 101.1 MJ·h/kg for Saint-Hubert. In Europe most of the energy was used to heat the air to the desired setpoint. In America there were significant amounts of both heating and cooling required. Much of the variation was due to the amount of moisture in the air which had to be removed in air conditioning. In situations where air conditioning is used, a significant amount of this energy is used in dehumidifying the air. For example in Miami 86.1% of the energy is used for moisture removal.

Table 1. Annual Sensible, Latent and Total Energy Requirements (MJ·h/kg dry-air)

			Total Heating (MJ·h/kg)	Cooling Sensible (MJ·h/kg)	Cooling Latent (MJ·h/kg)	Total Cooling (MJ·h/kg)	TOTAL HEATING & COOLING (MJ·h/kg)
1	BEL	Bruxelles	73.4	-0.1	-1.0	-1.1	74.5
2	BEL	Oostende	76.0	0.0	0.0	0.0	76.0
3	BEL	Saint-Hubert	101.1	0.0	0.0	0.0	101.1
4	DK	Copenhagen	89.6	0.0	-0.1	-0.1	89.7
5	FR	Carpentras	55.0	-1.8	-3.5	-5.3	60.3
6	FR	Limoges	70.3	-0.3	-0.7	-1.0	71.3
7	FR	Macon	72.4	-0.6	-1.7	-2.3	74.7
8	FR	Nancy	78.7	-0.2	-0.9	-1.1	79.7
9	FR	Nice	40.1	-0.4	-5.1	-5.5	45.6
10	FR	Trappes	74.5	0.0	-0.3	-0.3	74.8
11	GB	Aberdeen	88.2	0.0	0.0	0.0	88.2
12	GB	Aberporth	72.7	0.0	-0.1	-0.1	72.8
13	GB	Aberporth,CEC	73.9	0.0	0.0	0.0	73.9
14	GB	Aldergrove	82.2	0.0	0.0	0.0	82.2
15	GB	Birmingham	77.0	0.0	-0.1	-0.1	77.1
16	GB	Bristol	82.1	0.0	0.0	-0.1	82.2
17	GB	Camborne	67.0	0.0	0.0	0.0	67.0
18	GB	Dundee	84.6	0.0	0.0	0.0	84.6
19	GB	Eskdalemuir	95.1	0.0	0.0	0.0	95.1
20	GB	Eskdalemuir,CEC	96.1	0.0	0.0	0.0	96.1
21	GB	Glasgow	81.2	0.0	-0.1	-0.1	81.2
22	GB	Heathrow	67.6	0.0	-0.2	-0.2	67.8
23	GB	Kew	71.7	0.0	0.0	0.0	71.7
24	GB	Kew, CEC	70.4	0.0	0.0	-0.1	70.5
25	GB	Lerwick, CEC	97.5	0.0	0.0	0.0	97.5
26	GB	Manchester	78.6	0.0	-0.1	-0.1	78.7
27	GB	Newcastle	88.0	0.0	0.0	0.0	88.0
28	GB	Norwich	79.5	0.0	-0.3	-0.4	79.8
29	GB	Sheffield	80.4	0.0	-0.1	-0.1	80.5
30	NL	DeBilt	77.5	-0.1	-0.2	-0.3	77.9
31	NL	Eelde	83.2	0.0	-0.1	-0.1	83.2
32	NL	Vlissingen	69.8	0.0	0.0	0.0	69.9
33	USA	Boston, MA	77.3	-1.4	-5.8	-7.2	84.5
34	USA	Brownsville, TX	10.7	-11.7	-76.4	-88.1	98.7
35	USA	Cheyenne, WY	100.0	-0.1	0.0	-0.1	100.1
36	USA	Ft. Worth, TX	34.9	-10.4	-34.5	-44.9	79.8
37	USA	Lexington, KY	64.9	-2.5	-12.0	-14.5	79.4
38	USA	Los Angeles, CA	20.9	-0.3	-1.0	-1.2	22.1
39	USA	Miami, FL	3.3	-9.9	-82.2	-92.1	95.4
40	USA	Omaha, NE	84.7	-3.6	-14.1	-17.8	102.5
41	USA	Phoenix, AZ	19.5	-20.2	-8.7	-28.8	48.3
42	USA	Salt Lake City, UT	79.2	-2.4	0.7	-1.6	80.8
43	USA	Seattle, WA	67.2	-0.4	-0.4	-0.7	67.9

Note: Negative energy represents energy extracted in cooling.
The total is the sum of the absolute values of heating and cooling.

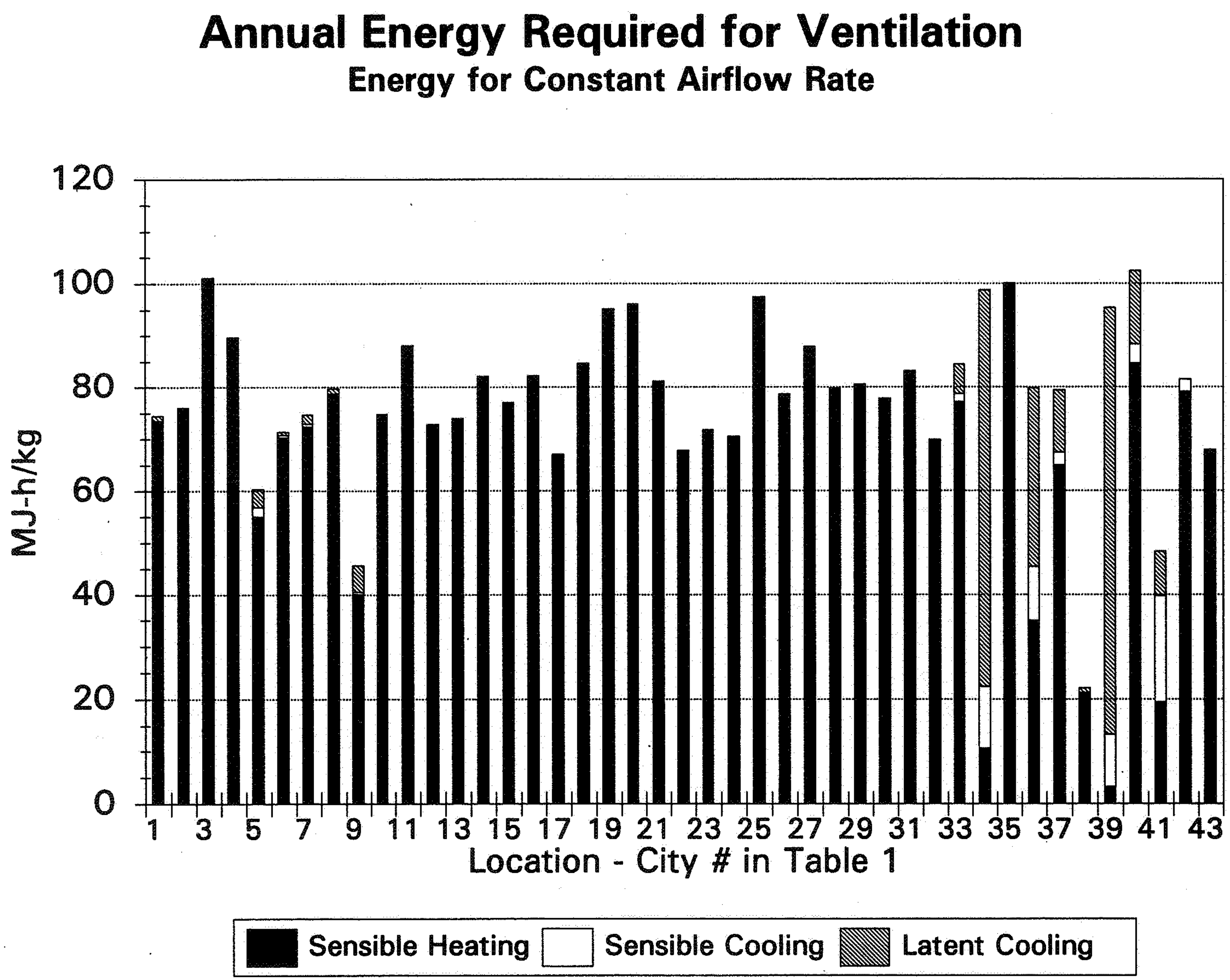

Figure 3. Total Energy Required for Ventilation Based Upon Constant Airflow Rate (Setpoints: Heating = 18 °C, Cooling 25.6 °C, 40%RH)

7. ACKNOWLEDGEMENTS

The investigation reported within this paper No. 95-05-116 is in connection with a project of the Kentucky Agricultural Experiment Station and is published with the approval of the Director.

This work was conducted at the Air Infiltration and Ventilation Centre while the author was on sabbatical from the University of Kentucky. Appreciation is expressed to the IEA, The Oscar Faber Partnership, and especially the AIVC for its support and hospitality during this sabbatical.

8. REFERENCES:

[1] CEC. 1985. Test Reference Years TRY, Weather Data Sets for Computer Simulations of Solar Energy Systems and Energy Consumption in Buildings. Commission of the European Communities, Directorate General XII for Science, Research and Development. Brussels.

[2] COLLIVER, D.G., H. ZHANG., R.S. GATES, and K.T. PRIDDY. 1995. Determination of the 1, 2½, and 5% Occurrences of Extreme Dew-Point Temperature and Mean Coincident Dry-Bulb Temperatures (RP-754). *ASHRAE Transactions* 101(2) Paper No. 3904.

[3] COLLIVER, D.G. 1995. Energy Requirements for Conditioning Ventilating Air - AIVC Technical Note 47. Air Infiltration and Ventilation Centre. Coventry, Great Britain.

[4] CRITCHFIELD, H.J. 1983. *General Climatology, Fourth Ed.* Prentice-Hall.

[5] GATES, R.S., S.H. ZHANG, H. ZHANG and D.G. COLLIVER. 1994. Medium Temperature Psychrometric Routines in C^{++}. Biosystems and Agricultural Engineering Department, University of Kentucky, Lexington.

[6] IRVING, S.J. 1988. The CIBSE Example Weather Year. in Weather Data and Its Applications - A Symposium for Building Service Engineers. 9 March 1988. CIBSE. Balham, Great Britain.

[7] MüLLER, M. J. 1982. *Selected Climatic Data for a Global Set of Standard Stations for Vegetation Science*, *Tasks for vegetation science* 5. Dr. W. Junk Publishers, The Hague.

[8] NCDC. 1993. Solar and Meteorological Surface Observation Network 1961-1990 Version 1.0 (SAMSON). U.S. Department of Commerce, National Climatic Data Center, Ashville, NC and U.S. Department of Energy, National Renewable Energy Laboratory, Golden, CO.

[9] ZHANG, H., R.S. GATES and D.G. COLLIVER.1995. Development and Documentation of a Psychrometric Turning Machine. Dept. Publication 95--05-098. Biosystems and Agricultural Engineering Dept. , Univ of Kentucky, Lexington, KY.

Implementing the Results of Ventilation Research
16th AIVC Conference, Palm Springs, USA
19-22 September, 1995

Comparative Trials of Ventilation Systems for Humidity Control

D A McIntyre*, S L Palin, R E Edwards*****

*E A Technology, Capenhurst, Chester CH1 6ES, UK
**UMIST/EA Technology Post Graduate Training Partnership
***UMIST, P O Box 88, Sackville Street, Manchester M60 1QD, UK

1 Synopsis

Three ventilation systems were installed in the EA Technology Ventilation Test House: passive stack ventilation (PSV), mechanical ventilation with heat recovery (MVHR) and extract fans. Humidifiers were used to simulate occupancy and the performance of the systems monitored over the winter of 1993/94. The aim was to assess the effectiveness of different ventilation systems in controlling indoor humidity at a level that will inhibit the growth of house dust mites.

The PSV system produced low ventilation rates in typical winter weather; excessive ventilation loss in cold windy weather was prevented by the high standard of air tightness in the house. The MVHR system has the advantage of producing consistent ventilation in all weathers. Total energy consumption of the systems was similar. MVHR was the most effective in reducing indoor humidity and in coping with peaks of moisture production; this is to be expected given its greater ventilation rate. Extract fans dealt well with moisture peaks, but should continue to run after moisture production has finished. Detailed results are presented for the variation in humidity between rooms for each ventilation system.

2 Introduction

Control of humidity in dwellings is necessary for a number of reasons, condensation and mould growth being amongst the most well-known. Mould growth is likely if relative humidity exceeds 70% for a significant period[1]. High indoor humidity also helps ensure the survival of the house dust mite, a major cause of asthma. It is generally accepted that humidity levels below 7 g/kg are detrimental to the house dust mite population[2]. This corresponds to a relative humidity of 48% at 20°C, a more stringent requirement than that for avoidance of mould growth. Ventilation of a dwelling with drier outside air acts to reduce indoor humidity levels. The possibility of maintaining humidity below 7 g/kg during winter by ventilation alone in the UK climate depends on the rate of moisture production in the house, ventilation system design and operation, and on ambient weather conditions. A pilot study[3] found fewer mites in houses where continuous mechanical ventilation with heat recovery (MVHR) was used than in similar houses where it was not used.

This paper describes ventilation and humidity measurements made in a ventilation test house[4], as part of a larger project concerned with the effect of ventilation strategy on asthma. This semi-detached house was refurbished to a high standard of air tightness and equipped with a range of ventilation systems, so that effective comparisons could be made on the selection of a ventilation system and its operation for the effective control of humidity and dust mites. A series of measurements was taken during the 1993/94 winter season, which compared the effect of different ventilation systems on humidity in the house.

3 Experimental

The experiments were carried out at 16 Manorfield Close, Capenhurst, one of a group of six test houses. The house has recently been refurbished with particular attention paid to airtightness in order to monitor ventilation systems effectively. House airtightness was tested periodically by the fan-pressurisation technique. Results were less than 3 ac/h at 50 Pa increasing to 5 ac/h with all trickle ventilators open; both results being considerably lower than the mean value of 11.5 for UK housing[5].

Three ventilation systems have been installed: MVHR, passive stack ventilation (PSV) and extract fans.

The PSV system was installed according to then current good practice and comprised two stacks leading from kitchen and bathroom to separate ridge terminals. Two types of room terminal were used. The standard conical extract provides a smooth entry and minimum resistance to air flow. For some runs, the room terminals were replaced with humidity sensitive extracts, which close progressively at low humidities, thus reducing flow in the stack and reducing excess ventilation when not required.

The MVHR system chosen was a standard loft-mounted heat recovery system incorporating cross-flow heat exchanger unit. This is capable of ventilation rates up to one air change per hour, supplying air to lounge, dining room and bedrooms and extracting from kitchen and bathroom. The MVHR unit was operated at approximately either 0.5 or 1 air changes per hour, i.e. approximately 100 or 200 m^3/h, with a slight excess of extract over supply.

Both kitchen and bathroom two speed extract fans were installed through-the-wall at high level and comply with the building regulations[6]. When under test, both extract fans were switched on and off by the central controller at the same times as the humidifiers. The high speed setting was used for almost all tests; flow rates are quoted by the manufacturer as 225 m^3/h (kitchen) and 102 m^3/h (bathroom).

The three ventilation systems were operated sequentially over a period from January to May 1994. All systems were tested with all internal doors either open or closed; all internal doors contain transfer grilles with an open area of 17,500 mm^2 to give a standard leakage between rooms. Windows were kept permanently closed. Trickle ventilators of 4000 mm^2 are installed in all rooms; these were closed only when the MVHR was operational, except for kitchen and bathroom ventilators that were kept closed at all times. A target temperature of 20°C was maintained throughout the house for most of the time. Lower temperatures were occasionally recorded in the kitchen and bathroom. As these did not contain heaters the temperature depended largely on air transferred from the other rooms. Humidifiers in the kitchen, bathroom and one bedroom were used to simulate occupancy, giving a total daily moisture input of approximately 5 kg. This represents four people living in conditions of 'dry' occupancy[1].

Temperature and humidity measurements in all rooms, at three locations in the stairwell and outside in a Stevenson screen were performed by a transmitter consisting of a platinum resistance thermometer and a capacitative humidity sensor. The humidity sensor measures relative humidity directly and is converted later to give absolute humidity.

Measuring bends were used to monitor flow rate in the intake and extract MVHR ducts. Velocity in each stack was monitored by a hot wire anemometer. The conical inlet gave a uniform velocity profile at the entrance to the stack; the volume flow was therefore calculated by multiplying the velocity measured at the inlet by its cross-sectional area. The humidity sensitive inlet, however, consists of louvers that open and close to regulate the flow; this results in a non-uniform velocity profile and the same method of measurement was therefore not possible. In this case, the centre-line velocity was measured further up the stack, enabling calculation of mean velocity using[7] and hence volume flow. This was not possible in the bathroom stack due to a lack of straight ducting.

Weather data (insolation on a horizontal surface, wind speed and direction) was collected from a weather station above roof level at a neighbouring house. Energy consumption on the following circuits was monitored: ground floor heating, first floor heating, ring main, MVHR and total.

4 Results and Discussion

4.1 Energy consumption

Neglecting energy stored in the mass of the building, the energy balance reduces to electrical energy supplied + solar gain = transmission and ventilation losses. Figure 1 shows the daily energy input to the house against average daily temperature difference. Solar gain was estimated from the measured insolation and detailed estimates of the solar performance of the test house made in[8].

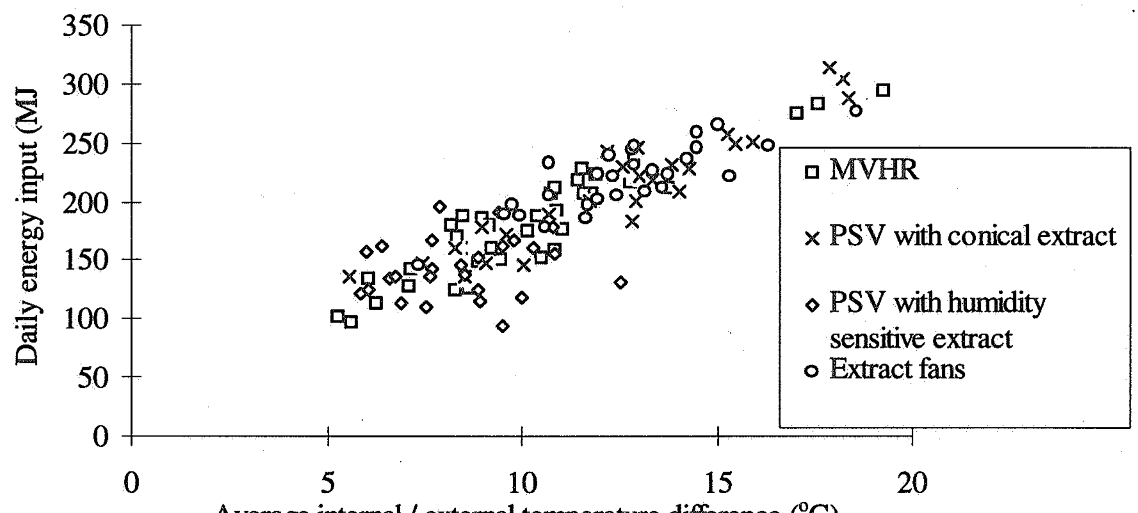

Figure 1. Gross energy input vs. temperature difference (24 hour mean values)

For the ventilation systems used in these trials, there was little difference in gross energy consumption between the systems, i.e. the increased ventilation rate and fan power consumption of the MVHR system was compensated by the heat recovery, to produce an overall energy cost of ventilation similar to the lower ventilation rate produced by the unpowered PSV system. Energy costs due to ventilation would therefore seem to be a less important factor in the choice of a ventilation system than other considerations such as humidity control, capital and installation costs.

4.2 Passive Stack Flow Rates

The flow in a PSV duct is driven by a combination of temperature gradient, resulting from the difference between indoor and outdoor air temperatures, and the pressure resulting from wind speed. Previous research[9] has found that stack flow rates are proportional to square root of internal - external temperature difference at low wind speeds.

The average daily stack flows against square root of temperature difference can be seen in Figure 2. As mentioned earlier, results for flows in the bathroom stack with humidity sensitive extract are unavailable. Stack flows with the conical extract are largely proportional to square root of internal - external temperature difference as expected; the scatter of points would indicate additional variation in flow due to wind speed. The humidity sensitive extract tends to restrict the flow at higher temperature differences; however more measurements at low external temperatures would be desirable.

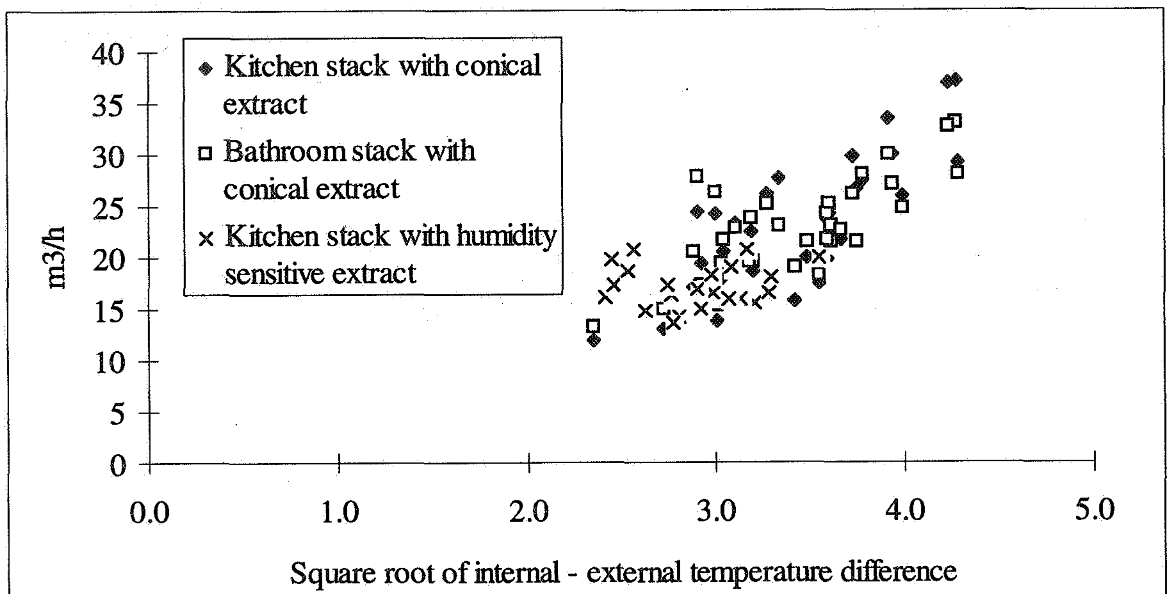

Figure 2. Average Daily Stack Flows

4.3 Humidity

Absolute humidity expressed as the mixing ratio, g, (g/kg) is calculated from the measured relative humidity and air temperature using[10]

$$g = 10\phi \exp\{11.56 - 4030/(T_a + 235)\}$$

where ϕ is the percentage relative humidity and T_a is the air temperature. This is a good approximation within the ranges of temperature and humidity involved.

4.3.1 Whole house

The results for absolute humidity in each room are averaged to give the internal absolute humidity. This and the external absolute humidity are then averaged over each twenty-four hour period. These values for each day are shown in Figure 3. The lowest values of internal humidity tend to be when MVHR is operating, the highest with humidity sensitive PSV. All systems, except humidity sensitive PSV, kept average internal humidity below 7 g/kg for most of the time. External humidity was higher when humidity sensitive PSV was operating, as this was towards the end of the winter, whereas the other systems were tested during the colder, drier months.

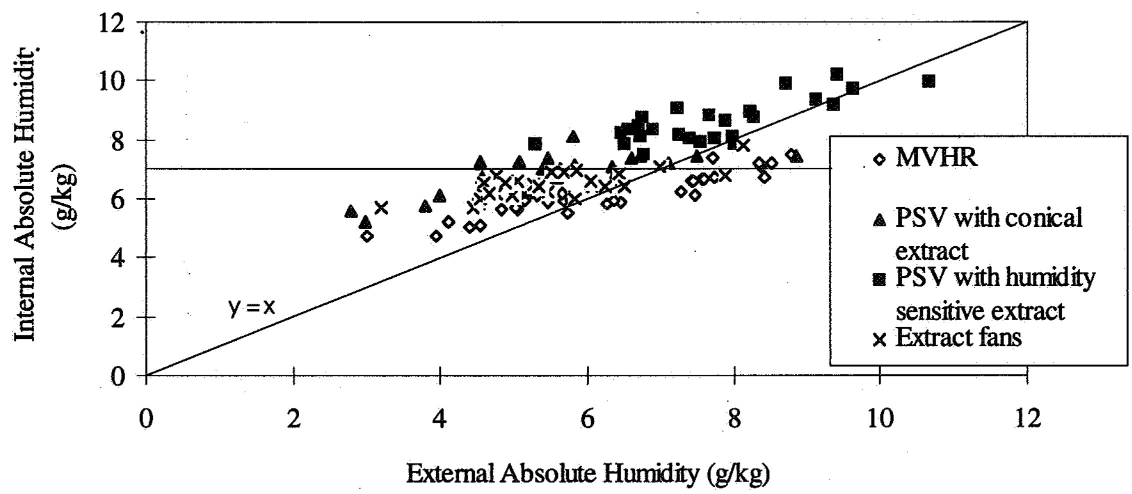

Figure 3. Daily Mean Humidity Levels

Occasionally the internal absolute humidity is less than external absolute humidity. This occurs more often when MVHR is operational than with the other systems, and could be explained by the house and / or MVHR system acting as a buffer, moderating the effect of temporary increases in external humidity by absorption into the building fabric and furnishings.

4.3.2 Room by room

The values of absolute humidity in each room and outside the house are shown in Figures 4(a) and 4(b). A representative twenty-four hour period of operation of each system was taken - these were not consecutive. All internal doors were open in each case. There is considerable humidity transport between rooms, whatever the ventilation system. PSV with conical extract and extract fans exhibit similar performance. MVHR maintains lower humidity than the other systems. Again it can be seen that internal humidity is lower than external humidity for a significant period of MVHR operation. PSV with humidity sensitive extract would seem to have the poorest performance; however the external humidity was higher in this case.

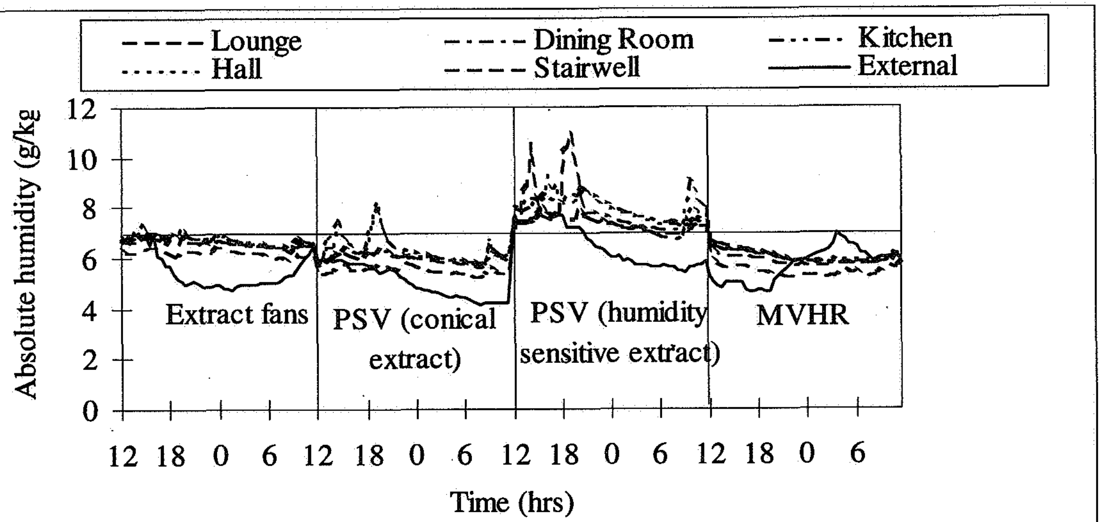

(a) Downstairs rooms

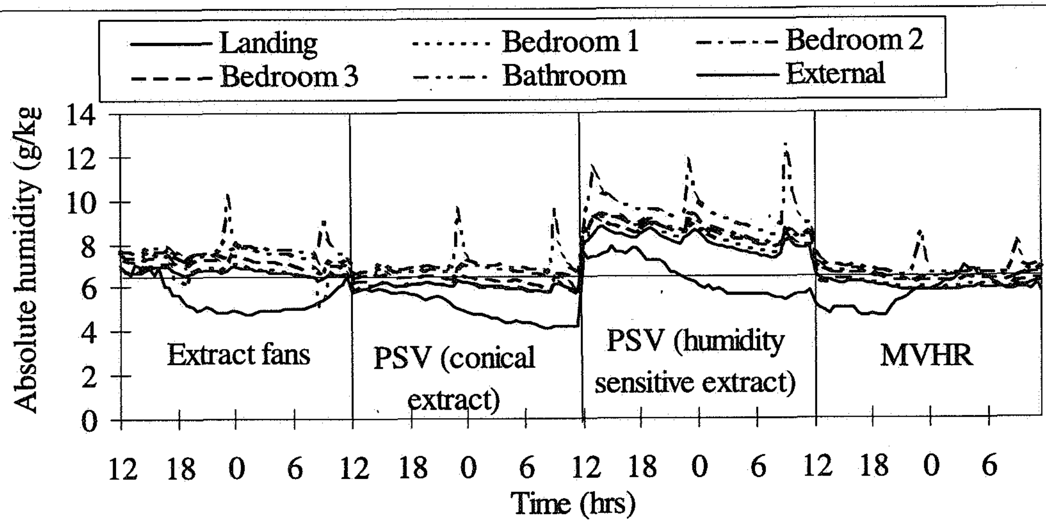

(b) Upstairs rooms

Figure 4. Room by Room Variation of Humidity with Internal Doors Open

5 Conclusions

Energy consumption of the systems tested was similar. An important factor in the comparison of ventilation systems is house airtightness, which is essential for the benefits of MVHR to be realised, and also desirable for other systems. The test house construction ensured a relatively high level of airtightness, which was maintained throughout these tests.

The mechanical ventilation system performed well. The passive stack system showed the expected variation of stack flow with temperature and wind speed. Total house ventilation with a PSV system is affected by general infiltration. For the test house fitted with 4000 mm^2 trickle ventilators, the house under ventilated in typical winter weather. The use of humidity sensitive extracts reduced stack flow in cold weather and would act to prevent over ventilation. The low driving force of passive stack ventilation makes the system sensitive to variation in design, installation and the geometry of house and surroundings.

Total energy consumption for the MVHR and PSV systems was very similar, reflecting the lower ventilation rate of PSV against the higher ventilation and heat recovery of the MVHR system.

MVHR proved the most effective of the systems in reducing indoor humidity levels. This was primarily because of the higher ventilation rate compared with PSV. Opening doors of moisture producing rooms promotes the spread of moisture to the rest of the house, regardless of choice of ventilation system. The fresh air supply to the bedrooms provided by a MVHR system was effective in reducing humidity in occupied bedrooms.

There were strong indications that the dynamic effects of moisture absorption and desorption in the house structure and ventilation system may play an effect in modifying the internal humidity. The effects may be diurnal or seasonal.

7 Acknowledgements

This work was funded as part of the EA Technology Members' Core Research Programme. The authors wish to acknowledge the Members' support.

S L Palin was in receipt of a Postgraduate Training Partnership Award.

8 References

[1] "British Standard Code of Practice for Control of Condensation in Buildings"
BS 5250 British Standards Institution, 1989.

[2] PLATTS-MILLS, T A E AND DE WECK, A L
"Dust mite allergens and asthma -A world wide problem"
J Allergy Clin Immunol 83 1989, pp416 - 427.

[3] MCINTYRE, D A
"The control of house dust mites by ventilation: a pilot study"
13th AIVC Conference, Nice. Coventry, UK. 1992, pp497 - 507.

[4] MCINTYRE, D A, PALIN, S L, AND EDWARDS, R E
"The Capenhurst ventilation test house"
15th AIVC Conference, Buxton. Coventry, UK. 1994, pp343 - 351.

[5] "Domestic draughtproofing: ventilation considerations"
Digest 306 Building Research Establishment, 1986.

[6] "Building Regulations 1985 (1990 Edition) Approved Documents F1, F2"
HMSO, 1991.

[7] MILLER, D S
"Internal Flow Systems"
British Hydromechanics Research Association, The Fluid Engineering Centre, 1986.

[8] SIVIOUR, J B
"Theoretical and experimental heat losses of a well-insulated house"
ECRC/N1537 EA Technology, 1982.

[9] PARKINS, L M
"Experimental Passive Stack Systems for Controlled Natural Ventilation"
CIBSE National Conference. University of Kent, Canterbury. 1991, pp508 - 518.

[10] MCINTYRE, D A
"Indoor Climate"
Applied Science, London, 1980.

Implementing the Results of Ventilation Research
16th AIVC Conference, Palm Springs, USA
19-22 September, 1995

Applying Ventilation Related Research to ASHRAE Standard 62

W Gene Tucker

Air Pollution Prevention and Control Division
National Risk Management Laboratory
US Environmental Protection Agency
Research Triangle Park, NC 27711, USA

APPLYING VENTILATION-RELATED RESEARCH TO ASHRAE STANDARD 62

W. Gene Tucker[1]
Steven T. Taylor[2]

The American Society of Heating, Refrigerating and Air-Conditioning Engineers (ASHRAE) Standard 62--Ventilation for Acceptable Indoor Air Quality--is in an active phase of revision. The current version of the standard (62-89 with addendum 62a-1990) has been available since 1990. Changes proposed by the revision committee are intended primarily to provide more specificity about certain requirements, and to put more emphasis on factors other than dilution ventilation that affect indoor air quality.

The authors of this paper are the former and current chairmen, respectively, of the revision committee. The paper describes some of the changes in Standard 62 that are being considered, and describes the research and field experience that are being used as bases for those changes. Current thinking of the committee on prescriptive ventilation rates, alternative ventilation rates, and design requirement details are discussed. Areas of emphasis for future research are suggested.

---

[1]National Risk Management Research Laboratory
U. S. Environmental Protection Agency
Research Triangle Park, NC USA

[2]Taylor Engineering
Oakland, CA USA

**Implementing the Results of Ventilation Research
16th AIVC Conference, Palm Springs, USA
19-22 September, 1995**

Performance of Passive Stack Ventilation in a Single-Family House. A Computational Simulation Study

Johnny Kronvall*,Ake Blomsterberg**

* J & W Bygg & Anlaggning AB, Consulting Engineers,
Slagthuset, S211 20 Malmo, Sweden
** Swedish National Testing and Research Institute,
Box 857, S 501 15 BORAS, Sweden

Synopsis

The paper presents the results of a simulation study performed by means of the COMIS multizone infiltration and ventilation model. The simulations were carried out for a two-storey single-family passive-stack-ventilated house in a cold climate (Stockholm, Sweden). Main conclusions of the study include the following: it is possible - during at least 75 % of the heating season - to achieve a ventilation rate in the whole house of at least 0.5 ach or approx. 30 l/s only if the house has a leakage rate above approx. 10 m3/m2,h@50 Pa or has purpose-provided supply air devices in the facade with a total area (far) greater than 400 cm^2; that the flow rates in the vertical shafts from kitchen, WC and bathroom are small but quite stable, in the range of appr. 3-4 l/s each; that all bedrooms (on the first floor) are under-ventilated as far as outdoor air is concerned; and that the living room (on the ground floor) is the only room in the house with - in most cases - adequate ventilation.

Possibly, but this was not proven, the performance of the passive stack ventilation could be improved, especially in the bedrooms, if the air supply devices in the facade were to be placed lower than in the simulations (2.1 m above floor level) and/or each bedroom was equipped with an individual exhaust shaft combined with a more or less airtight door. In order to increase the shaft flows it would, of course, also be possible to increase the height of the shafts above roof level and/or use a cowl of a special design.

The work was undertaken as part of the IEA Annex 27 project.

Background

Within the IEA program "Energy Conservation in Buildings and Community Systems", there are several on-going international collaboration projects, one of these being Annex 27, "Evaluation and Demonstration of Domestic Ventilation Systems", MÅNSSON (ed.), (1995). The overall scope of the work in this annex is to establish a general evaluation tool, which will make it possible to pre-evaluate the overall performance of different ventilation systems for different domestic buildings in different climates. A number of performance criteria are dealt with within the annex. They include, e.g. air quality, thermal comfort, energy, noise, life-cycle costs, moisture and reliability. The Swedish part of the research in the annex covers the reliability aspect of domestic ventilation.

In this context, ***reliability*** is defined as:

the probability that the ventilation system provides certain specified air flow rates in each habitable part of the building under specific climatic conditions and during the time between scheduled maintenance occasions.

Especially with natural ventilation strategies - with or without so-called passive stacks - the influence of weather conditions on the ventilation performance is paramount.

In order to study the performance aspect of reliability, the method chosen in this project was firstly to investigate the reliability under the influence of climatic- and building-specific factors by means of computer simulations, and secondly to perform a system safety analysis on the performance of mechanical ventilation systems. The simulation procedure is going to be checked by comparing results of simulations with results of field measurements (constant concentration tracer gas and PFT measurements).

The results of the first parametric study of the performance of a passive stack natural ventilation system in a two-storey single-family house are reported in this paper.

Simulation Procedure

The computer simulations were performed by means of the multi-zone ventilation and infiltration computer program COMIS (version 3.1a). The program was originally developed as an international joint research project - Conjunction of Multizone Infiltration Specialists. The work was led by Dr. Helmut Feustel at the Energy Performance of Buildings Group at Lawrence Berkeley Laboratory's Applied Science Division. The documentation of the program includes FEUSTEL & SMITH (1992) and FEUSTEL & RAYNOR-HOOSEN, (ed.) (1990). Further development of the COMIS model has been undertaken within IEA Annex 23 during the past three years.

Input data for the model are based on assumptions which are described below. Essentially, the building and its ventilation system are described and the climatic conditions for which the model is to perform the calculations are given as a weather file. The output of the simulation is quite extensive, so it must be condensed in some way. For this particular case, the output was condensed by running a couple of specially dedicated computer programs, finally producing cumulative frequency diagrams. This method of expressing the simulation results coincides perfectly with the definition of reliability given above.

Simulation Assumptions

The Building and the Passive Stacks

The building modelled in the simulations is a two-storey single-family house assumed to have a low-slope roof. It is located in a built-up area with other similar houses surrounding it. The floor plan of the house is given in Figure 1. The ceiling height is 2.50 m and the intermediate floor has a thickness of 0.30 m. The overall floor area is 88 m^2 and the corresponding volume of the house is thus 88 x 2.5 = 220 m^3.

The specific leakage rate of the house envelope was chosen to be 2.5, 5.0 or 10.0 m^3/m^2,h@50 Pa. The leakage was evenly distributed over all outer walls and the roof. The house was assumed to be built on a floor slab on the ground, so no leakage paths from the ground were included in the calculations. According to Scandinavian standards, these figures correspond to a rather airtight, a leaky and a very leaky house, respectively.

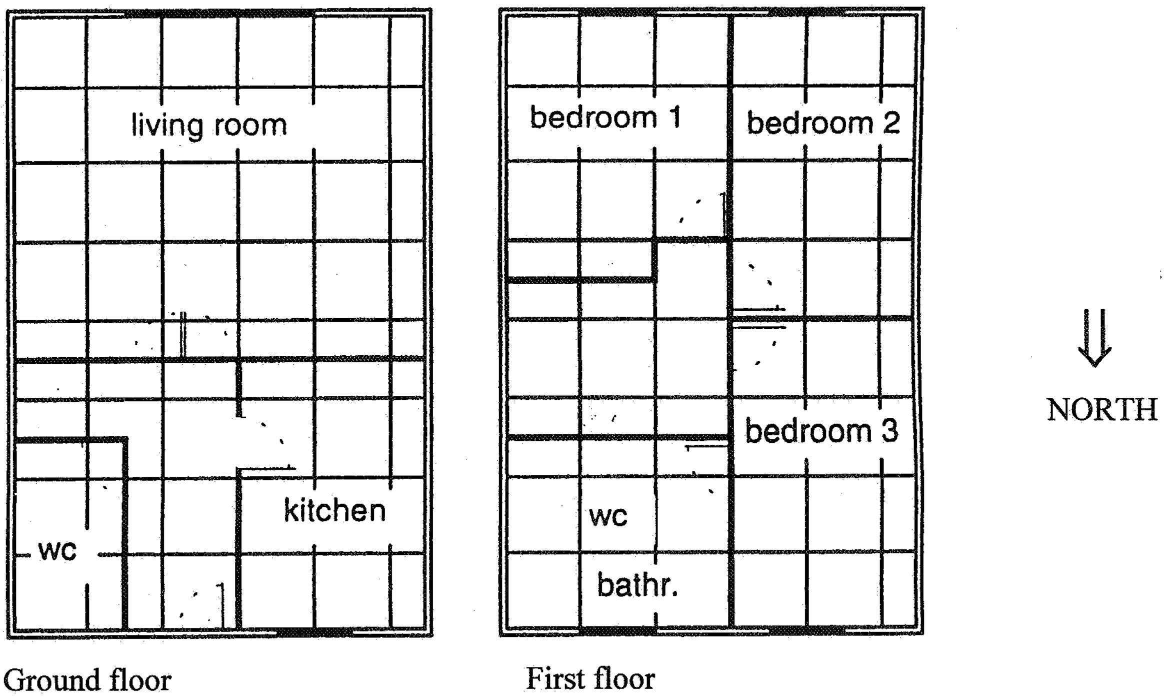

Figure 1 Floor plan of house for simulations.

The total free area of supply air devices (placed 2.1 m above floor level) was chosen to be 0, 200 or 400 cm^2. The area was evenly distributed between the living room and the three bedrooms. The opening area was hydrodynamically treated as the area of a sharp-edged hole in a thin wall. For real devices, the nominal area should be reduced by means of a reduction factor - in many cases roughly 0.5. The three levels chosen are equivalent to closed supply vent openings, normal openings (according to building regulations in many countries) and large vent openings.

The passive ventilation shafts from the kitchen, the WC and the bathroom must be modelled as individual zones in the COMIS model (and, incidentally, in all other single- and multi-zone models). This implies that the small flow resistance in the ductwork must be included in the resistance of the air terminal devices. The flow coefficient chosen for a single exhaust air terminal device in either of the three rooms mentioned was 0.004 kg/s @ 1Pa with a flow exponent of 0.5. For the outer end of the shaft (0.5 m above roof level) the flow coefficient chosen was 0.014 kg/s @ 1 Pa.

Internal doors were assumed to be closed, except for the kitchen door. This door was treated in the model as a large opening, while the closed doors were assumed to have transferred air devices (20 mm x 700 mm) on top of, and small air gaps (appr. 2 mm) at the sides and bottom of, the door-leaf.

Climatic Conditions

The simulations for the parametric study were performed for a cold climate and for the heating season (5400 h/a). Actual weather data for Stockholm 1971 were used. The indoor temperature was chosen to be +20 °C. The weather data were condensed into 84 cases, each one consisting of an interval for corresponding values of wind velocity and temperature. In Figure 2, the frequency distribution for the weather data used is shown. The frequencies for different cases were taken into account when producing the final cumulative frequency diagrams.

Wind pressure coefficients according to Table 3.5 (ii), AIVC Technical Note 44, were used for the simulations. The wind pressure coefficient for the top of the shafts was chosen to be -0.3, according to praxis among many ventilation simulation specialists, e.g. de GIDS (1995) and with certain support in AIVC Technical Note 44, p 6.11.

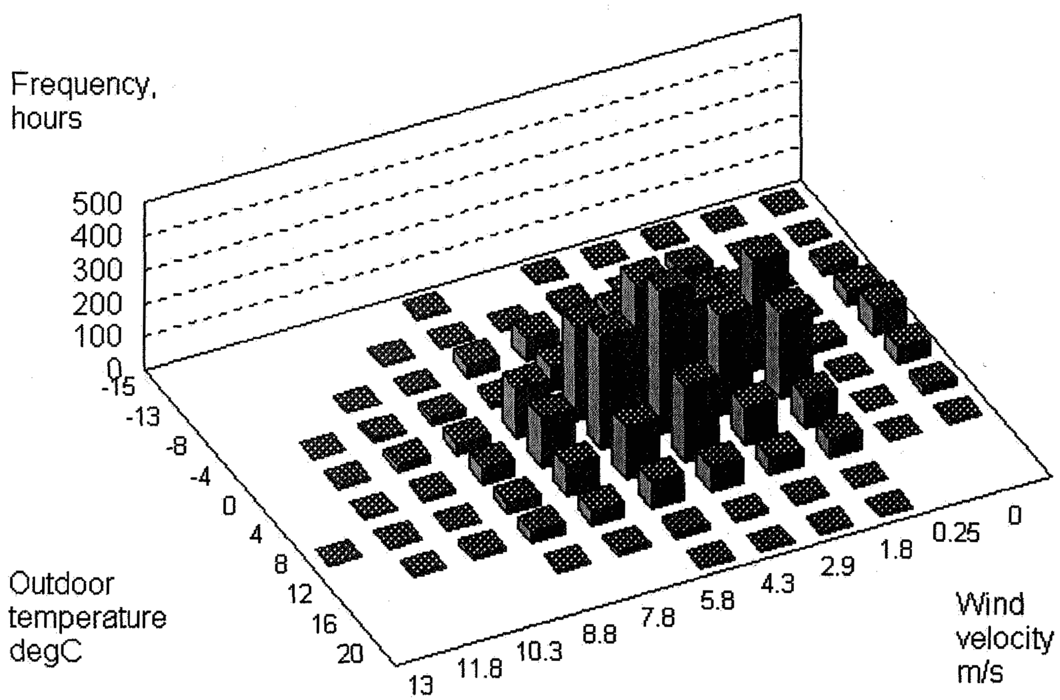

Figure 2 Frequency distribution of weather data used for the simulations.

Simulation Results

Principal Behaviour of Passive Stack Ventilation

In order to illustrate the principal ventilation behaviour in the investigated house, some initial simulations were performed. The scope of this exercise was primarily to check the air flow balances of the four habitable rooms, the shaft flows and the total air exchange for the whole house. Four weather situations, W1 - W4, were used for the simulations, see Table 1. The wind direction was chosen to be Southwest.

Wind velocity	Temp. 0 °C	Temp. 10 °C
0 m/s	**W2** Winter, calm	**W4** Spring/fall, calm
4 m/s	**W1** Winter, windy	**W3** Spring/fall, windy

Table 1 Weather conditions for the initial simulations.

The envelope leakage was chosen to be 5.0 m^3/m^2,h @ 50 Pa and the total free area of supply air devices in the facades 200 cm^2.

The air flow balances for the four habitable rooms are shown in Figure 3. When studying the diagrams, it should be kept in mind that regulations in most countries prescribe ventilation flow rates for bedrooms of the order of 4 litres per second per person (outdoor air). Air originating from locations outside the room (staircase, hall, etc.) can only in certain cases be treated as ”clean” air and added to the flow of outdoor air. The most apparent limitation is associated with the presence of tobacco smokers in the house. In such cases the transferred air flow should definitely not be included in the ”fresh air” supply.

In Figure 3 the shaft flows and the total air exchange of the house are also shown.

Legend for forthcoming diagrams (# 4 - 6)

L#.# A###

means:

L = Envelope leakage; 2.5, 5.0 or 10.0 m^3/m^2,h @ 50 Pa
A = Total free area of supply air devices in facades; 0, 200 or 400 cm^2

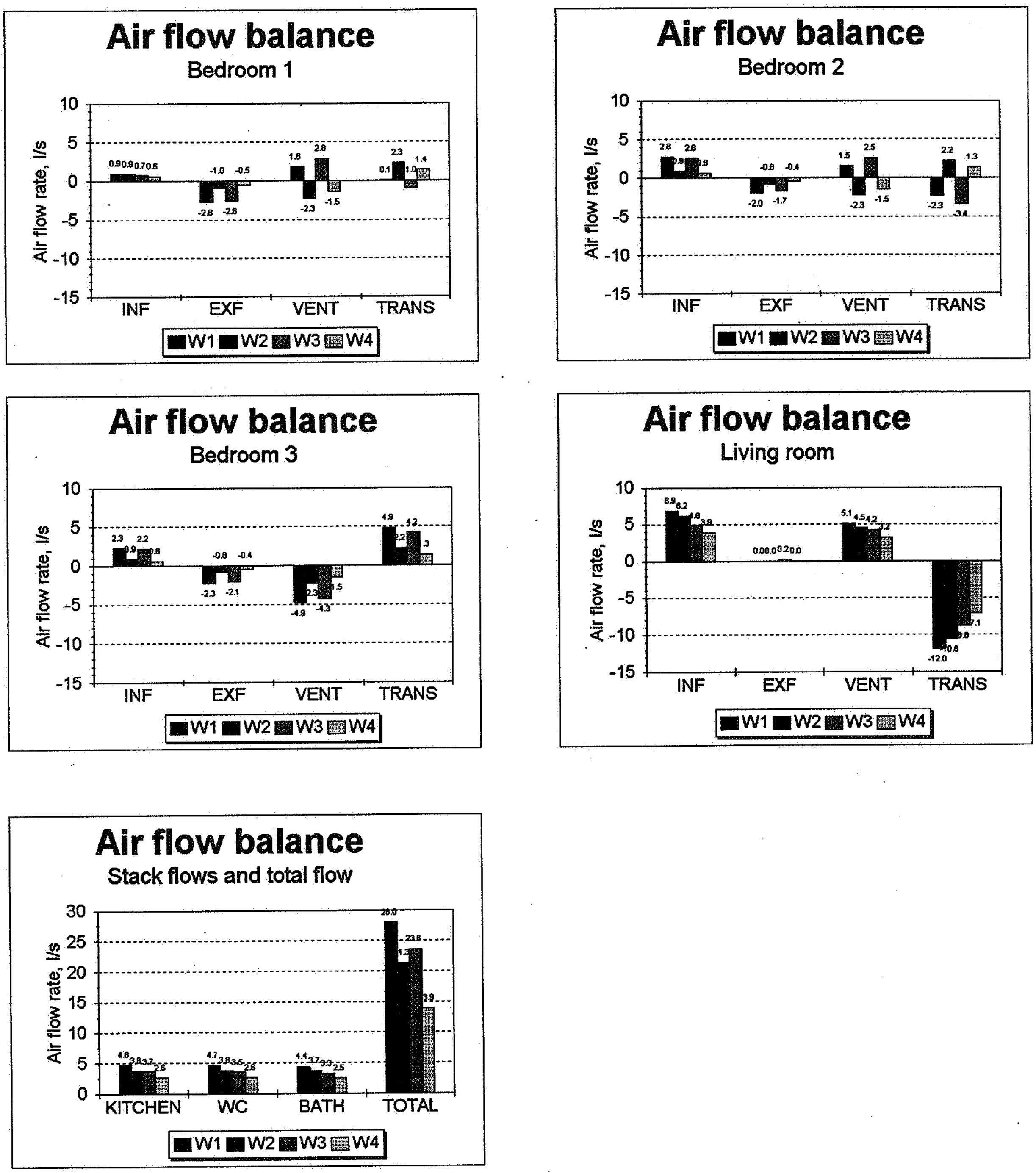

Figure 3 The air flow balances for the four habitable rooms, shaft flows and total flow.

The following comments refer to the simulation results for the different rooms, the shaft flows and the total flows.

Bedroom 1 - first floor

The room has its facade on the windward side, and the side-wall on the leeward side of the house. For all four weather conditions the bedroom is under-ventilated. In the best case, the sum of infiltrated air and ventilation air (i.e. air flowing through a supply air device in the facade) is 2.8 l/s (W3). The flow direction in the supply air inlet is reversed in the two cases when there is no wind. This indicates internal over-pressure at the supply air device level.

Bedroom 2 - first floor

The room has both its facade and side-wall on the windward side of the house. The principal ventilation behaviour is very similar to that of bedroom 1, though the infiltration rates are somewhat higher.

Bedroom 3 - first floor

The room has its facade on the leeward side, and side-wall on the windward side of the house. The fact that the supply air device is placed on the leeward side of the house has certain consequences - the air flow is reversed in the supply air device for all four weather conditions. Except for some infiltrated air, the only air flow into the room arises from transferred air from the upper hall. The outdoor air supply is limited to values below 2.3 l/s and this occurs due to infiltration through the west-facing wall of the room.

Living room - ground floor

The room has its facade and one side-wall on the windward side of the house, and one side-wall on the leeward side. For all four weather conditions, the ventilation behaviour is "favourable", i.e. the flow balance is according to optimum conditions for a ventilation system with supply air to be introduced in the house through purpose-provided ventilation openings in the facade. The outdoor air flow rate is of the order of 0.3 to 0.5 $l/s,m^2$.

Habitable rooms - general

It is concluded that, during typical winter and spring/fall conditions, a passive shaft ventilation system could create acceptable ventilation conditions on the ground floor of a two storey house in a cold climate. On the first floor, however, the ventilation performance is generally poor.

Shaft flows and total flow

The total air exchange of the house ranges from 13.9 l/s (0.23 ach) during calm spring/fall conditions, up to 28 l/s (0.46 ach) under windy winter conditions. These values correspond well to many field measurements of ventilation in houses of this type in different countries. The sum of the flows in the three shafts equals approx. half of the total air exchange in the house. If the house had been more airtight the shafts′ fraction of the total would have been higher. The individual exhaust flow rates are considerably lower (2.5 - 4.8 l/s) than those prescribed in the building regulations of most countries (approx. 10 l/s). In many passive stack ventilated houses however, there are local extract fans which can be operated occasionally, on demand.

Parametric study

As mentioned under "Simulation Assumptions" the parametric study was aimed at investigating how sensitive the ventilation performance is to different input parameter values regarding envelope leakage and area of supply air devices in facades.

The main results are shown in Figures 4 and 5, with a number of air flow rates reported under "lower quartile" and "median". The results in the figures should be interpreted as flow rates corresponding to percentages of the heating season (5400 h), i.e. 1 350 and 2 700 hours, respectively. The air flow rates (l/s) given under each percentage originate from the cumulative frequency distribution. This means that if the flow given under "lower quartile", i.e. 25 % is q, the probability of air flow rates less than q during the heating season is 25 %. This is easily seen in cumulative frequency diagrams. Some examples of such ones, for a "average" case are shown in Figure 6. **The air flow rates in figures 4 and 5 refer to the sum of infiltration flows and flow through purpose-provided openings in facades.**

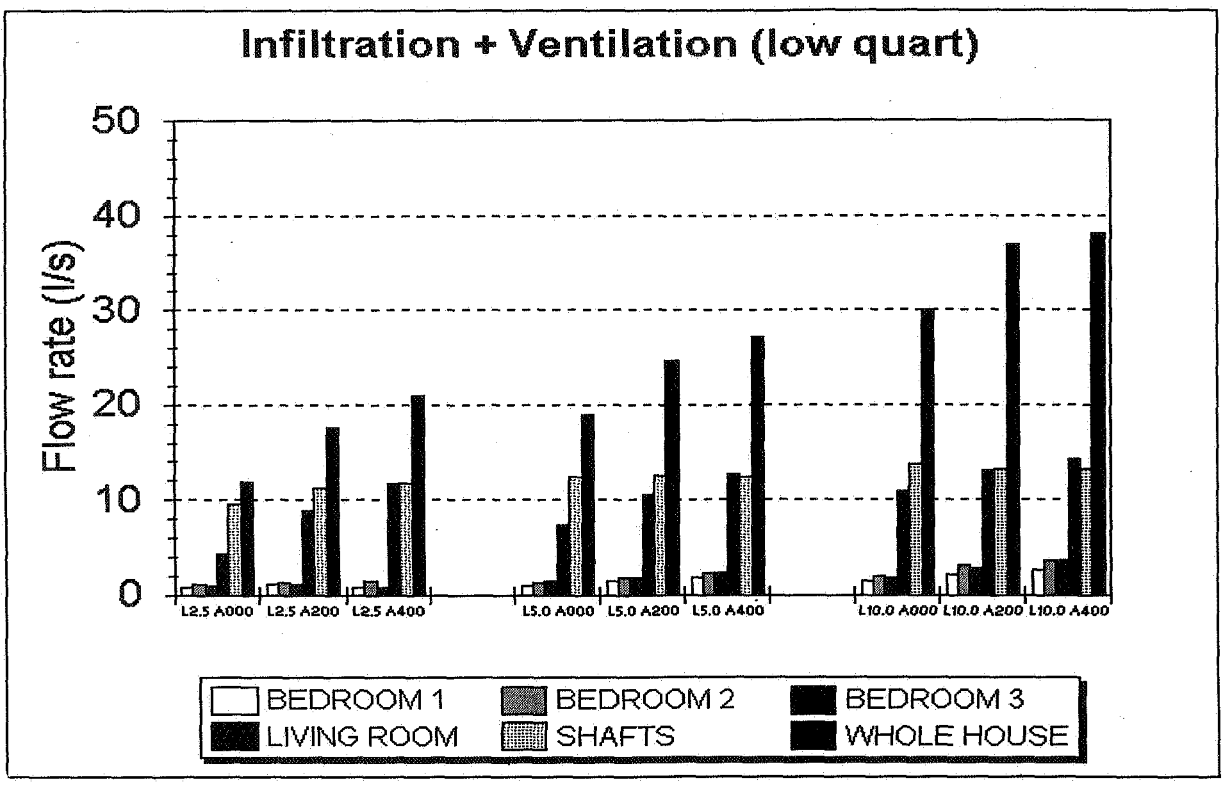

Figure 4 Infiltration + ventilation flows (lower quartile).

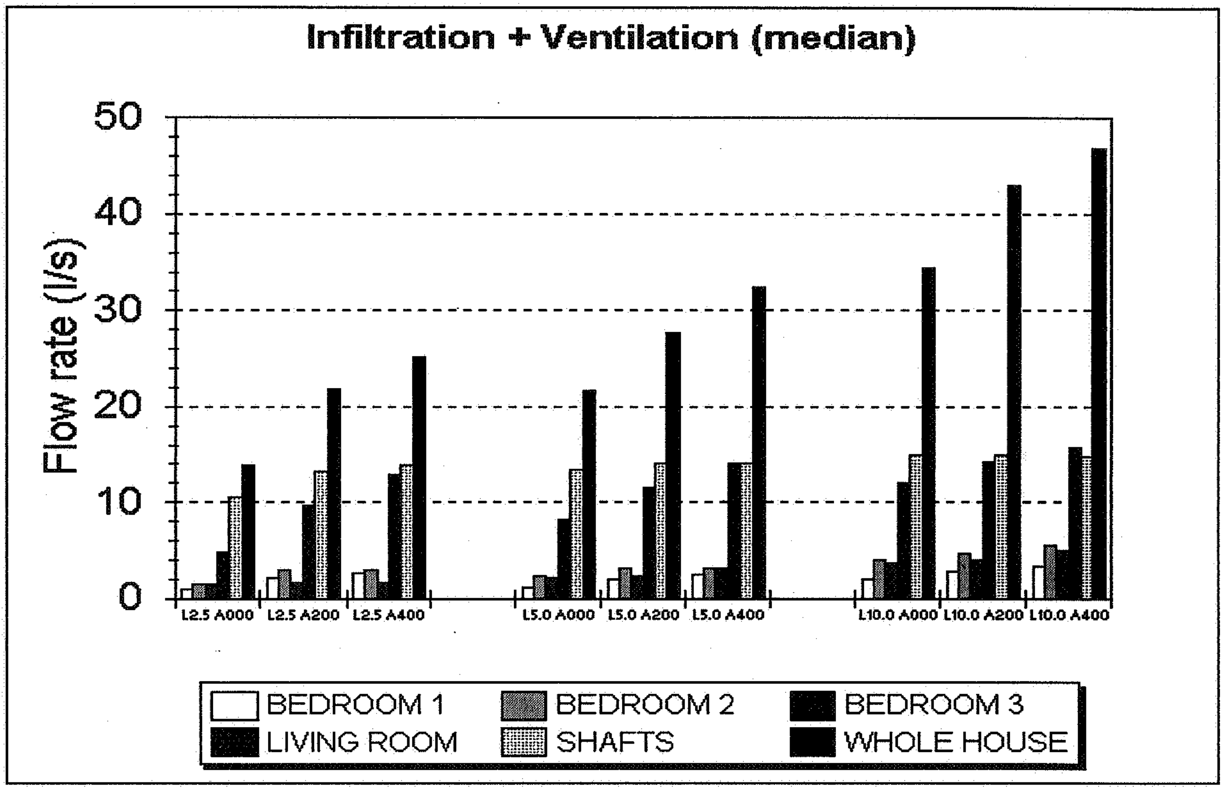

Figure 5 Infiltration + ventilation flows (median).

It could be concluded that, by using a passive stack ventilation system in a two-storey house in a cold climate (as described in the simulation assumptions) :

1 it is possible - during at least 75 % of the heating season - to achieve a ventilation rate in the whole house of at least 0.5 ach or approx. 30 l/s only if the house has a leakage rate above approx. 10 m3/m2,h@50 Pa or has purpose-provided supply air devices in the facade with a total area (far) greater than 400 cm^2,

2 the flow rates in the vertical shafts from kitchen, WC and bathroom are on average small but quite stable in the range of approx. 3-4 l/s,

3 all bedrooms (on the first floor) are under-ventilated as far as outdoor air is concerned,

4 the living room (on the ground floor) is the only room in the house with - in most cases - adequate ventilation.

Contemplating the results, it would perhaps be possible to improve the performance of the passive stack ventilation, especially in the bedrooms, if the air supply devices in the facade were placed lower than in the simulations (2.1 m above floor level) and/or each bedroom was equipped with an individual exhaust shaft combined with a more or less airtight door. In order to increase the shaft flows it would, of course, also be possible to increase the height of the shafts above roof level and/or use a cowl of a special design.

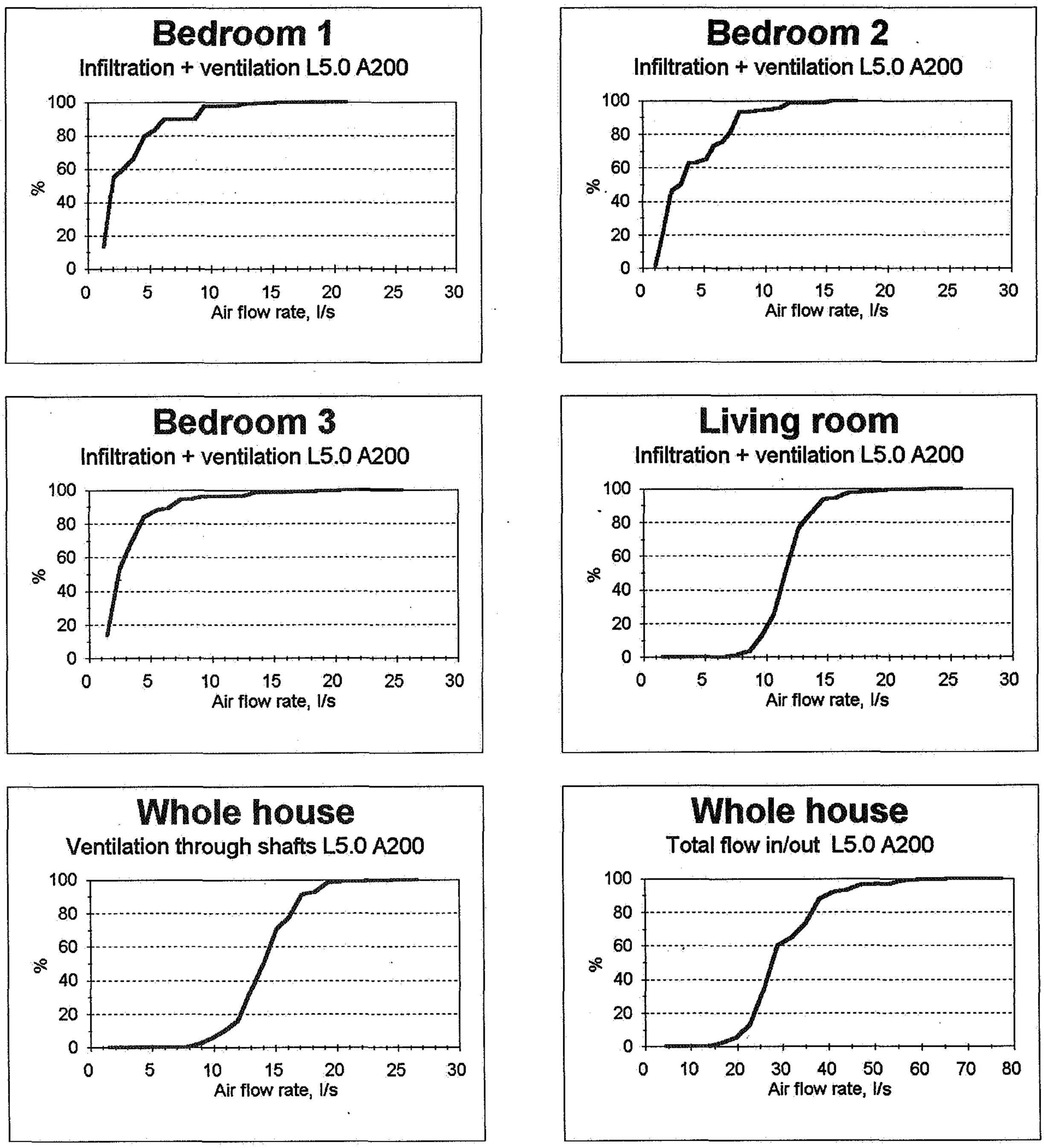

Figure 6 Infiltration + Ventilation flow rates. Cumulative frequencies.

Future work

The simulations will continue, taking into account other, warmer climates and other types of dwellings, e.g. apartments in blocks of flats.

Acknowledgements

This work was supported by the Swedish Council for Building Research. Thanks for good assistance during the coarse of this work go to Dr. Helmut E. Feustel, LBL Indoor Environment, Berkeley, US and to Mr. Roger Hagstad J&W Bygg&Anläggning, Consulting Engineers, Lund, Sweden.

References

FEUSTEL, H. & SMITH, B., ***COMIS 1.3 - User Guide***, LBL, Berkeley, 1992.

FEUSTEL, H. & RAYNOR-HOOSEN, A., (ed.), ***COMIS - Fundamentals***, LBL, Berkeley, 1990.

de GIDS, W., Personal communication. 1995.

ORME, M., ***AIVC Technical Note 44***, AIVC, Coventry, UK, 1995.

MÅNSSON, L.-G., (ed.), ***Annex 27 State of the Art Report***, to be published 1995.

Δ

Implementing the Results of Ventilation Research
16th AIVC Conference, Palm Springs, USA
19-22 September, 1995

Energy Demand for the Conditioning of the Supply Air in Ventilation

Prof.Dr.Ing.Fritz Steimle

Institut fuer Angewandte Thermodynamik und Klimatechnik, Universitaet Essen, Universitaetstr.15, 45141 Essen, Germany

ENERGY DEMAND FOR THE CONDITIONING OF THE SUPPLY AIR IN VENTILATION

PROF. DR.-ING. F. STEIMLE,
Institut für Angewandte Thermodynamik und Klimatechnik
Universität Essen
Universitätsstr. 15, 45141 Essen, Federal Republic of Germany

1. Main tasks of Air Conditioning

The main tasks on A/C-plants are:

1. The transport of air in order to be able to decrease the air contamination in the rooms.
2. The transport of water in order to control the humidity-level of the air in the rooms.
3. The transport of thermal energy in order to control the temperature-level of the air in the rooms.

The transport mechanism of No. 1 and No. 2 is only possible by moving air to the rooms and back. But No. 3 can be achieved also by circulation of heat carriers in liquid stage.

To compare the enthalpy-transport by air volume with the enthalpy-transport by water circulation it is necessary to calculate not only the transportation energy but also the carried heat:

Transportation Energy: $$P = \frac{\dot{V} \cdot \Delta p}{\eta}$$

Carried Heat: $$\dot{Q} = \dot{V} \cdot \rho \cdot c_p \cdot \Delta t$$

The ratio of $\dot{Q}$ and P gives an idea of the carried heat by one unit of transportation energy.

Typical values for air and water cooling are given in table 1.

As we can see it is possible to transport nearly 450 times as much heat by water than by air with the same energy supply to pump or fan, respectively.

The air systems themselves also have great differences in this value because of the high range of pressure drop.

Therefore a lot of systems are bivalent, using air and water. The ammount of air is calculated for the air renewal to reach the desired indoor air quality. The heat transport which can not be done by this air volume is done by a water system in induction units or free convective cooling using heat exchangers at the walls or cooled ceilings.

There are large differences in the demand between comfort A/C and industrial application. Industrial applications ask mostly for special conditions either in temperature or in humidity and mostly for air renewal. Therefore it is fairly difficult to give a general overview. But in the comfort A/C-area some trends can be shown clearly.

	Unit	Air	Water
Density ρ	kg/m³	1,2	1000
specific heat capacity c_p	J/kg K	1000	4200
temperature difference Δt	*K*	8	10
Power efficiency η of fan/pump	-	0,8	0,8
pressure drop	*Pa*	1000	10000
$\dot{Q}/P$	-	7,6	3360

Table 1: Typical values for air and water cooling.

2. Heat load from human bodies

The different heat transmission mechanisms take over different parts of the total heat load. The ratio is depending on various parameters. With rising air-temperature the convection is decreasing meanwhile the latent heat by evaporation is increasing. In fig. 1 the influence of

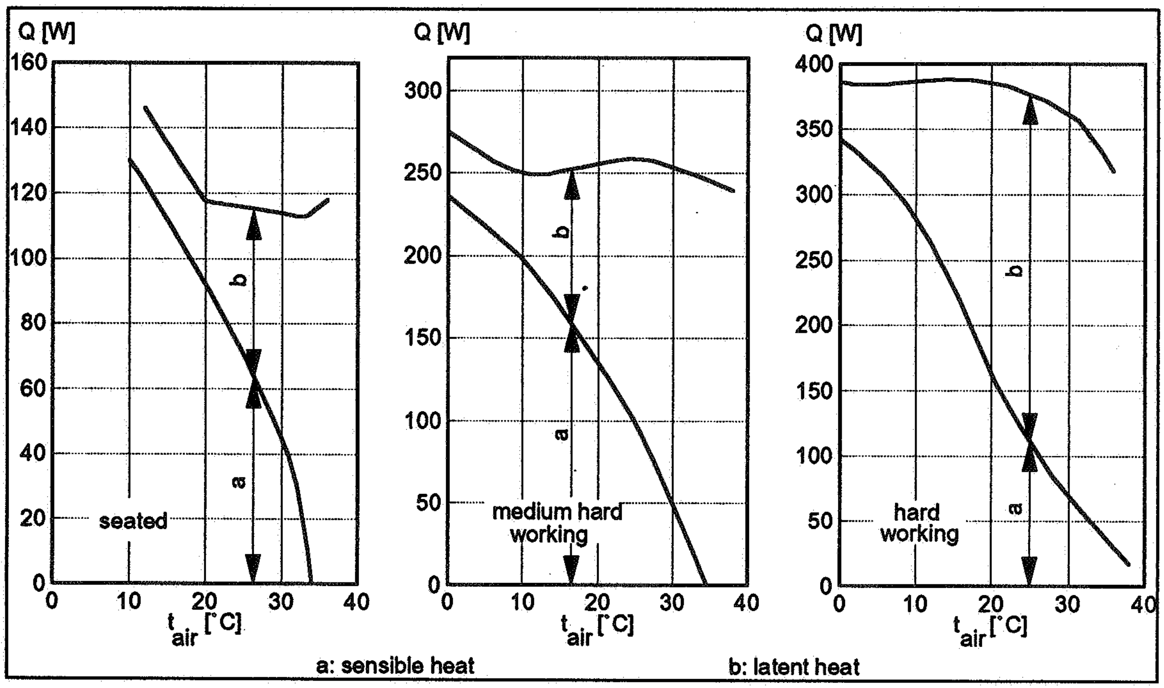

Figure 1: Heat-transmission of persons in normal clothing /1/

the activity level on the different ratios is shown. The total heat losses with an activity level related to 120 W (left part of Fig. 1) is fairly constant over a wide range of temperature. But the ratio between the latent heat and the sensible heat is very different at various air temperatures.

Higher activity level related to 250 W (middle part of Fig. 1) or to 350 W (right part of Fig. 1) shows the same tendency. The sensible heat is always the sum of convection and radiation.

At higher temperatures the evaporation must take over sometimes incomming radiation. In cars e.g. the incoming solar radiation must be considered already at lower room-temperatures. This solar radiation meets the human body and transports heat to the body which must be bilanced by additional evaporation. That is the reason why a large amount of water vapour ist transported to the air.

Main standards and regulations are done for offices with fairly the same activity level for all persons in the room. But also in these rooms a different heat transmission to the room can be seen in comparing the different individuals. /2/

Because the parameters of the heat convection are fairly stable, and because of the constant body temperature and a fixed clothing the control mechanism of the body temperature by changing the heat losses can only be done in the latent heat range. The rise of the temperature of the body surface can only be shifted in very small limits and the room air temperature and the air-velocity can not be ajusted individually. A change in the radiation is also not possible at a fixed wall temperature and given room configuration.

Fairly often different activity levels can be found in the same room. Some examples are shown with the following values (Tab. 2).

activity	range of heat transmission	mean value
1. seated	90 W - 150 W	120 W
2. typewriting	120 W - 170 W	150 W
3. speaker	160 W - 250 W	200 W
4. waiter	200 W - 300 W	250 W
5. dancing	200 W - 400 W	300 W

Table 2: Activity levels.

These activity levels are very different but we can find them in the same room at the same time and with the same clothing. As it was shown in fig. 1 the total metabolic rate is nearly independent of the temperature. However, the distribution of the heat transmission to radiation, convection and evaporation therefore depends also on the room temperature. Calculated values on the bases on some measurements are shown in the next table (Tab. 3).

3. Humidity and comfort

If we regarde a ball-room we will have seated persons, speaker, waiter and dancing groups which have only a small difference in radiation and convection. To be able to meet the heat balance the human body sends water to the surface to reach evaporation cooling. The related amount of water will be at 20°C between 45 g/h and 220 g/h. The relative values at 26°C are 90 g/h and 300 g/h.

This amount of water must be transfered to the air. This can be reached by a high mass transfer coefficient or by a big difference between the absolut humidity at skin level and in the room air. An increase of the mass transfer coefficient will also give an increase of the heat transfer coefficient. This correlation is given in the Lewis law.

When we use the same values of the absolut humidity as in normal office buildings we will get no common comfort in rooms with very different activity levels.

	20°C					26°C			
	Heat	**Radiation**	**Convection**	**Evaporation**	**Water**	**Radiation**	**Convection**	**Evaporation**	**Water**
Seated	120 W	45 W	45 W	30 W	45 g/h	30 W	30 W	60 W	90 g/h
Typewriting	150 W	50 W	50 W	50 W	72 g/h	33 W	33 W	85 W	125 g/h
Speaker	200 W	60 W	55 W	85 W	125 g/h	40 W	37 W	123 W	180 g/h
Waiter	250 W	65 W	70 W	115 W	170 g/h	43 W	45 W	162 W	230 g/h
Dancing	300 W	65 W	80 W	155 W	220 g/h	43 W	50 W	207 W	300 g/h

Table 3: Heat distribution with the same clothing and different activity levels.

In table 3 we see that at 20°C a seated person will have a convective heat transfer of about 30 W and an evaporation heat of about 60 W. A dancing person, however, will have about 50 W of convective heat and more than 200 W by evaporation. If this will be done by a higher mass transfer coefficient the convective heat losses of a sitting person will increase too and will cause the feeling of draft.

To be able to avoid this the high water mass transfer must be reached with a big difference of absolut humidity instead of an increased transfer coefficient. This means a temperature of 20°C and a low absolut humidity in the air with the standard air velocity will meet the comfort conditions for both groups of the population in the same room. The small temperature difference and a normal heat transfer coefficient will not give any draft for sitting persons and also give enough evaporation potential for people with higher activity level like speakers, waiters and dancers.

The relative humidity in the rooms should not be lower than 30 %. Below this level the nose and the throat can dry out and this must be avoided. In a lot of different materials which are used in buildings a low humidity can also give a high electrostatic load which also cause discomfort /3/.

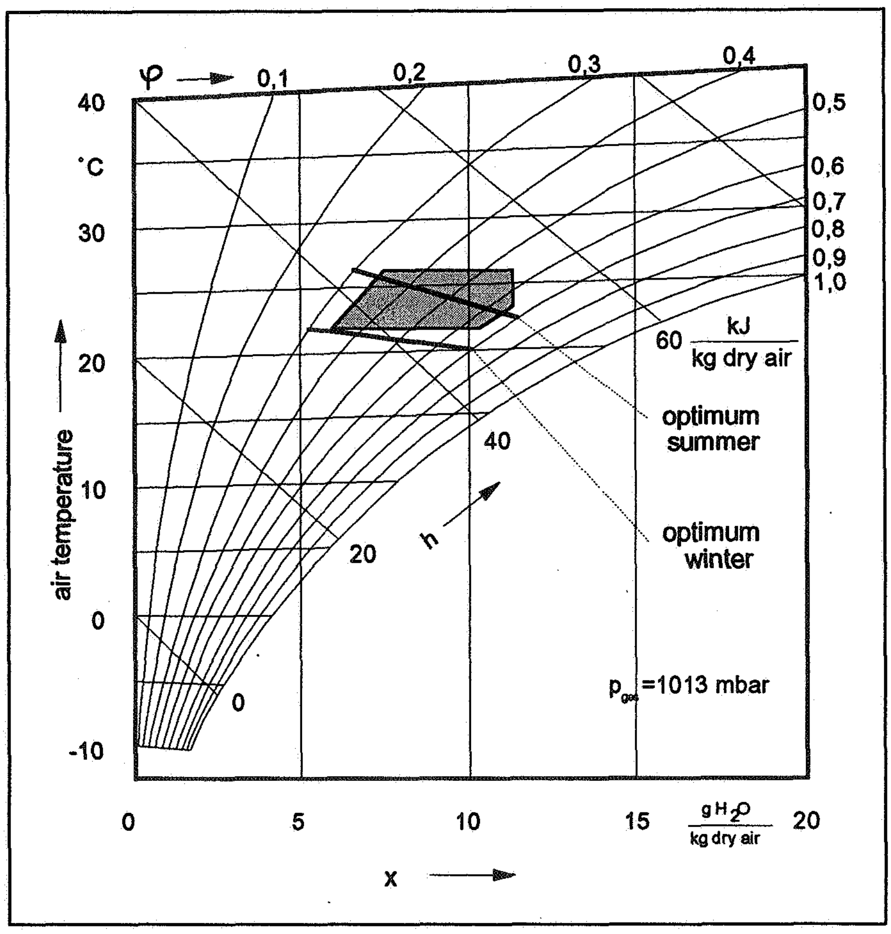

Figure 2: Comfort zone DIN 1946 pt 2.

The investigations of O. Fanger /4/ about the thermal comfort shows a much smaller influence of the humidity, but these values are only valuable for office buildings. The reason of these results is the very small change of activity level, a very simular clothing and a fairly stable air temperature. As shown the activity level is of great influence. It is not possible, therefore, to use the values for office buildings in a much broader scale. In figure 2 the optimal conditions are shown compared with the comfort zone of DIN 1946 part 2. These results can also be shown by experiments. /5/.

In air conditioned testrooms a group of about 30 people had to find out which rooms seems to be colder compared with the other one.

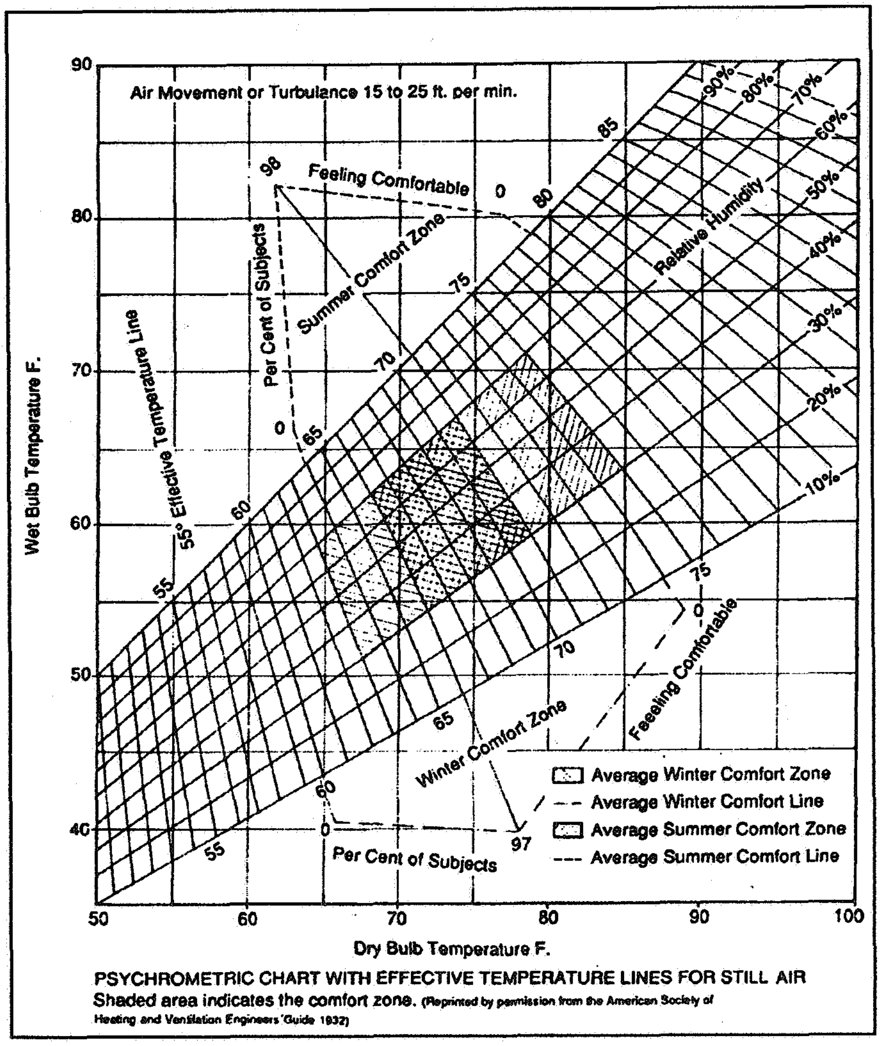

Figure 3: Psychrometric chart by Samuel Lewis 1932 /6/.

Unanimously they stated that a room with 26°C and 30% humidity is definetly cooler than a room with 24°C and 60 % humidity. These tests give the line of optimum conditions for summer (see figure 2). A very similar result can be derived from psychometric chart by Samuel Lewis from 1932 (see figure 3) Additionally Lewis also gives an optimum line for winter which is also shown in figure 2.

4. Influence of the humidity on the refrigeration capacity

The cooling load is not enough to discribe the refrigeration capacity because it is also necessary to consider the air changes. The air change rate cause especially in summertime a different dehumidification load which effects the refrigeration capacity. The minimum air changes are influenced strongly by the material which is used in the interial design. This can be shown in table 4 /7/. This example shows how great the influence of the material can be to the total energy consumption offer building. This influence is somewhat higher than the influence of the insulation.

	ventilation [m³/m² h]	air changes [ach]	energy demat for heating [W/m²]
marble floor	0,1	0,04	1
carpet floor	2 up to 8	0,8 up to 3,2	25 up to 100

Table 4: Ventilation rates.

In summer everybody is speaking about cooling in air conditioning plants when he is going to decrease the air temperature. For the dehumidification we have to calculate in central Europe a difference between the highest outdoor enthalpy and the enthalpy at the dew point of the supply air of about 25 kJ/kg dry air. It is very important to know that the highest enthalpy is not in the area of the highest temperature.

5. Refrigeration systems for A/C

Mainly refrigeration systems for air conditioning are running with a temperature range of 6°C up to 12°C. Nearly all water chillers are designed for this temperature. The 6°C as supply temperature is necessary to reach the dehumidification of the outdoor air used for air renewal.

Normally the same system temperature is used to transport heat from inner heat gains to the central system. In chilled ceiling systems the temperature a the surface must be about 20°C in summertime to avoid condensing water at the surface.

chilled water temperatures supply/ return	cooling capacity	electrical power input	C.O.P	relative C.O.P
5°C / 10°C	198 kW	42,5	4,6	1
6°C / 12°C	208 kW	43,1	4,82	1,048
10°C / 15°C	250 kW	45	5,55	1,21
15°C / 20°C	298 kW	47	6,34	1,38

Table 5: C.O.P.´s for different chiller temperatures.

If there is used the same water chiller either for the dehumiditation and for the cooled ceilings the 5°C or 6°C chiller water will be mixed with return water to reach the higher supply temperature of about 15°C. If the water chiller will be devided in two parts working on a different temperature level a lot of energy can be saved. In table 5 the C.O.P. for different chiller temperatures are shown. They are measured in a water cooled condenser with 30°C/35°C. Compared with the supply temperature of 5°C the chiller has 38 % increase in C.O.P. at 15°C water supply temperature. If the COP of a chiller is increasing, the energy used by the cooling tower is lower at the same cooling capacity. This is a very high energy saving which must be considered in new system design.

These figures show a big influence of the temperature. Therefore the refrigeration systems for the A/C -plants will be devided in future. One part takes the dehumidification loads from the handling of the outdoor air with a supply water temperature of 5°C or 6°C and the other part is taking the inner load at temperatures between 15°C and 20°C. This needs quite a different design but saves a substantial part of the power input.

6. Conclusion

A/C -technology is changing especially in the comfort part by considering the influence of the humidity. A main development in energy savings is the seperation of dehumidification and transport of sensible heat gains.

LITERATURE

/1/ Schweizer Kühllastregeln, 1969, Schweizer Verein für Heizung und Lüftung

/2/ Steimle, F., Klimakursus, C.F. Müller-Verlag Karlsruhe, 1969

/3/ Steimle, F., Spegele, H., Die Behaglichkeit in klimatisierten Räumen, Kältetechnik-Klimakursus 22 (1970) S. 81/82

/4/ Fanger, O., On thermal comfort, McGraw Hill, 1972

/5/ Steimle, F., Feuchte als Behaglichkeitskomponente, KI 2/1994, S. 66-68

/6/ Lewis, S.R., Air conditioning for Comfort Engineering Publications, Inc, Chicago 1932

/7/ Steimle, F., Internationale Konferenz der IEA über neue Energietechniken, April 1992, Dortmund

Implementing the Results of Ventilation Research
16th AIVC Conference, Palm Springs, USA
19-22 September, 1995

Short Term and Long Term Measurements of Ventilation in Dwellings

**Ake Blomsterberg*, Thomas Carlsson*,
Johnny Kronvall****

*** Swedish National Testing & Research Institute,
Box 857, S 501 15 Boras, Sweden
** J & W Bygg&Anlaggning AB, Slagthuset, S 211 20
Malmo, Sweden**

Synopsis

A study of the reliability of systems by considering the ability of different systems to maintain a required air flow rate over time is included in a subtask of IEA Annex 27 "Evaluation and Demonstration of Domestic Ventilation Systems". Measurements were performed to determine the variation in ventilation rates due to variation in climate and variation in performance of the ventilation system. The monitoring was carried out in one-family houses and apartment buildings, which are representative of the Swedish housing stock. Three different ventilation systems were examined; passive stack, mechanical exhaust and mechanical exhaust-supply.

The monitoring period was started with diagnostic tests to discover if the installed ventilation system was functioning as designed and to determine certain values. The airtightness was tested. The air flows in mechanical ventilation were measured.

The actual monitoring phase included measurements in dwellings of overall and local (individual rooms) ventilation rates and boundary conditions. High cost and inconvenience prevent the use of continuous monitoring of these ventilation rates. A good compromise was found to be a combination of short-term continuous and long-term averaging tracer gas measurements. The main results were:
- passive stack ventilation varies over time and is at times too low
- exhaust ventilation is reasonably constant over time if the dwelling is not leaky, but is at times too low in individual rooms
- balanced ventilation is almost constant over time if the dwelling is airtight.

The paper presents and discusses the measurement techniques and the results from the measurements carried out during 1995.

1. INTRODUCTION

IEA Annex 27 "Evaluation and Demonstration of Domestic Ventilation Systems" was started last year. The overall scope of the work in this annex is to establish a general evaluation tool, which makes it possible to pre-evaluate the overall performance of different ventilation systems for domestic buildings in different climates. A number of performance criteria are dealt with within the annex. They include e. g. air quality, thermal comfort, energy, noise, life-cycle costs, moisture and reliability. The Swedish part of the research in the annex covers the reliability aspect of domestic ventilation i. e. the ability of different systems to maintain a required flow rate over time. This study is funded by the Swedish Council for Building Research. The work is divided into:
- numerical simulation of ventilation in typical dwellings
- measurements in representative dwellings
- numerical simulation of measured dwellings and comparison with the measurements
- development of a design tool for determining the reliabilty of a ventilation system
- application of the developed design tool on typical dwellings.

This paper presents results from phase 2, measurements in representative dwellings, which were carried out during the winter of 1995.

2. THE DWELLINGS TESTED

The dwellings which were examined in this project represent typical Swedish buildings. They are representative as to building technology, size of the building and ventilation system (see table 2.1 and 2.2).

Year of construction	Number, thousands	Natural, %	Exhaust, %	Balanced, %
0-1940	578	99	0,5	0,5
1941-1960	330	99	0,5	0,5
1961-1975	509	87	9	4
1976-1988	361	20	47	33
1989-1992	96	0	45	55
	1874			

Table 2.1. Year of construction and ventilation system for the Swedish one-family housing stock (Tolstoy 1993).

Year of construction	Number, thousands	Natural, %	Exhaust, %	Balanced, %
0-1940	365	64	34	2
1941-1960	770	62	34	4
1961-1975	686	19	66	15
1976-1988	192	3	36	61
1989-1992	137	0		
	2150			

Table 2.2. Year of construction and ventilation system for the Swedish multi-family housing stock (Tolstoy 1993).

The dwellings with passive stack ventilation have exhaust air terminal devices in rooms such as bathrooms, kitchens and laundryrooms and sometimes outdoor air supply to the other rooms through outdoor air vents near windows. The exhaust air terminal devices are attached to a vertical shaft to the outside. Space heating in most of the houses is provided for by radiators located below windows.

The dwellings with exhaust fan ventilation have exhaust air terminal devices in rooms such as bathrooms, kitchens and laundry-rooms and outdoor air supply to the other rooms through outdoor air vents near windows. Space heating in most of the houses is provided for by radiators located below windows.

All of the dwellings with balanced ventilation have exhaust and supply ventilation. Air is exhausted from rooms such as bathrooms, kitchens and laundryrooms and air is mainly blown into bedrooms and living-rooms. Most of the houses are equipped with radiators for space heating and with some kind of heat recovery.

The dwellings were chosen randomly. Important criteria were, however, type of ventilation, year of construction, and number of storeys (see table 2.3).

Ventilation system	Year of construction	No of storeys	Floor area, m²	Remark
Apartment building				
Balanced	1988	3	120, 120	Unoccupied
Exhaust	1990	3	58, 50	
Passive stack	1955	3	56, 55	Cross ventilation, unoccupied
One-family house				
Balanced	1991	1½	128	Crawl-space
Exhaust	1976	1½	160	Slab on grade
Passive stack	1958	1	114	Basement

Table 2.3 The tested buildings.

3. METHODS

3.1 Introduction

The measurements were started with diagnostic tests to discover if the installed systems were functioning as designed and to determine certain values:
- pressurization in order to determine airtightness of building envelope and ducts
- measurements in order to determine air flows in ducts of mechnical ventilation systems

The actual monitoring phase was began with short-term monitoring (during a winter, spring/fall and summer period):
- constant concentration tracer gas during 1 - 7 days to determine hourly variations in ventilation rates.

After each short-term monitoring long-term monitoring were carried out:
- passive tracer gas in order to determine monthly averages of ventilation rates.

During the long-term monitoring the boundary conditions were determined as follows:
- the outdoor temperature at the site was measured
- the indoor temperature was measured in at least two rooms
- the wind speed and direction was measured at a nearby weather station
- the occupants made a daily diary regarding airing and kitchen fan use.

3.2 Airtightness

The standard method for finding the leakage function of a building is fan pressurization. According to the Swedish standard for fan pressurization (SS 02 15 51) all openings in the exterior envelope intended for ventilation purposes must be sealed before the test is performed. Other openings are kept closed. For the purpose of modelling air infiltration and exfiltration, a second test was also made, with open supply vents in the dwellings with exhaust ventilation and with open vertical shafts in the dwellings with passive stack ventilation. Rooms with separate ventilation such as boiler rooms and garages are disregarded.

3.3 Ventilation

The most straightforward method of measuring the total ventilation rate i.e. the combined effect of mechanical ventilation and natural ventilation or natural ventilation only is to measure it directly. There are many ways of measuring total ventilation, and almost all of them involve a tracer gas, which permits the indoor air to be labelled so that the outdoor air ventilation can be traced (Charlesworth 1988). If the ventilation is mechanical with ducts, then in most cases the air flow in the ducts should first be measured using techniques for volume and mass flow rate measurements, without a tracer gas (ASHRAE Fundamentals 1993, NVG 1995).

The short-term measurements in the houses tested were carried out using the constant concentration technique in order to evaluate hourly variations in the total and individual room ventilation rates. The outdoor air ventilation is obtained directly. The supply of outdoor air to several individual rooms simultaneously is monitored continuously, i.e. outdoor air which enters an individual room directly instead of first passing through an adjacent room. The estimated inaccuracy in the measured outdoor air ventilation rate is ± 10 %.

A passive tracer gas technique was used to perform the long-term averaging of ventilation rates. The technique can be described as a constant flow technique with pen-sized tracer gas sources and samplers. Two different tracer gases were employed in order to be able to determine the ventilation rates for the entire dwelling and at least one bedroom. A homogeneous emission technique was used (Stymne 1994). Tracer gas was continuously injected into each room apart from bathrooms and kitchens. The tracer gas sources are adjusted to predetermined injection rates, which are proportional to the volumes of the rooms. The estimated inaccuracy in the measured outdoor air ventilation rate is ± 15 %.

3.4 Temperature

The indoor and outdoor temperatures were recorded using thermistors connected to one-channel dataloggers. Each logger stores 1800 values. The duration of the measurements can be varied from 15 minutes to 360 days. The estimated inaccuaracy is ± 0.5 °C.

4. RESULTS

4.1 Airtightness

The average airtightness of the tested apartments is 2.3 ach, compared with 6.0 for the tested one-family houses. In a previous study the airtightness as a function of year (-1940, 1941-60, 1961-75, 1976-88) of construction was presented (Kronvall 1993). Most of the tested buildings are fairly representative for their year of construction, with the exception for the apartments with passive stack and exhaust ventilation. The tested apartments with passive stack ventilation are much tighter and the ones with exhaust ventilation leakier.

Building	Number of storeys	Tested storey	Ventilation system	Volume, m³	Airtightness at 50 Pa, ach	"Typical" value, ach
Apartment	3	1	Passive stack		2.2	6.0
Apartment	3	3	Passive stack		1.8	6.0
Apartment	3	1	Exhaust		2.7	1.4
Apartment	3	3	Exhaust		5.1	1.4
Apartment	3	1	Balanced		1.3	1.4
Apartment	3	3	Balanced		0.9	1.4
Detached one-family house	1 1/2	-	Balanced		3.1	4.4
Detached one-family house	1 1/2	-	Exhaust		6.7	5.7
Detached one family house	1	-	Passive stack		8.3	6.0

Table 4.1 Measured airtightness of tested buildings compared with estimates for the Swedish housing stock ("Typical").

4.2 Ventilation rates

4.2.1 Passive stack ventilation

The hourly averages show that the overall ventilation rate varies over time. This is especially true for the apartment on the first floor, where the total outdoor air ventilation varies between 90 m³/h (0.6 ach) and 190 m³ (1.4 ach) (see figure 4.1 and 4.2). The measuring period was too short in the one-family house to see any variation. The average ventilation rate in this house was 80 m³/h (0.3 ach) during a period of 6 hours.

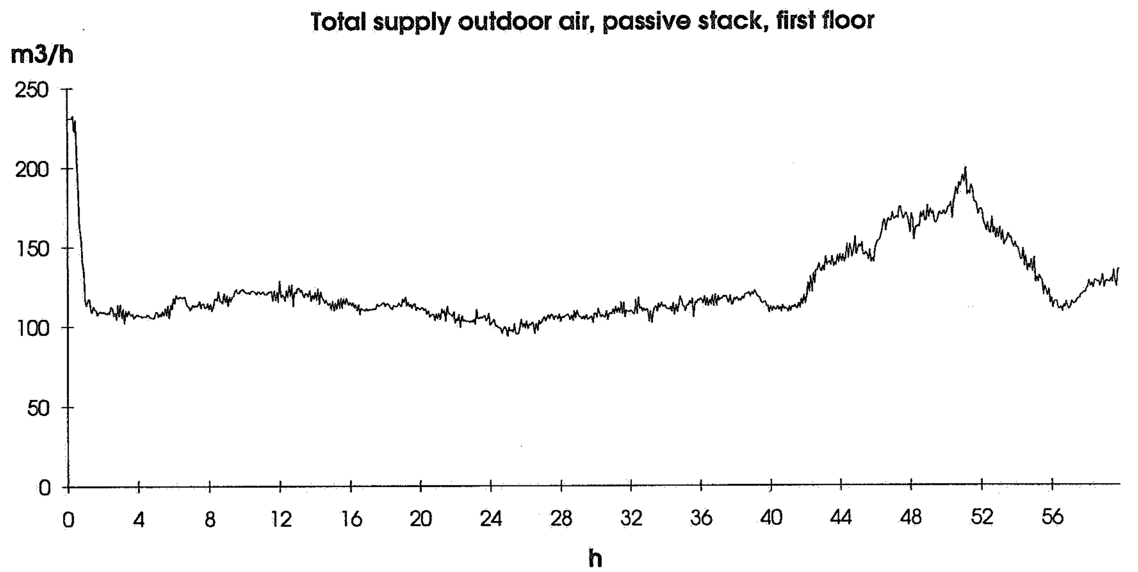

Fig 4.1 Total supply of outdoor air for the apartment on the first floor with passive stack ventilation, during a period of 60 hours. Average outdoor temperature -0.9°C (min - 8 °C, max 5 °C), average wind speed 2.9 m/s.

The outdoor air ventilation rates are very different for different rooms (see table 4.1 and 4.2) and is e g too low in the bedrooms of the one-family house.

Apartment 1st floor	**Living-room**	**Bedroom**	**Kitchen**	**Hall**	**Total**
Outdoor air, m^3/h	48	22	14	40	122
Temperature °C	19	19	19	19	
Apartment 3rd floor					
Outdoor air, m^3/h	35	17	27	6	85
Temperature °C	20	19	19	-	

Table 4.1 Average outdoor air ventilation rates for individual rooms in the passive stack apartments. For boundary conditions see figure 4.1. Apartment 3rd floor: average outdoor temperature 3 °C (min 1 °, max 5 °C), measuring period 45 hours.

	First floor				**Basement**				
	Living room	Bed-room	Bed-room	Kit-chen	Game room	Garage	Hall	Base-ment	Total
Outdoor air, m^3/h	16	4	4	5	17	17	8	9	79
Temperature °C	20	-	18	-	16	-	-	-	

Table 4.2 Average outdoor air ventilation rates for individual rooms in the passive stack one-family house. Average outdoor temperature 0 °C (min - 0.5, max 1.5 °C), measuring period 6 hours.

The long-term (monthly averages) measurements in the apartments give values similar to the short-term (hourly averages) measurements (see table 4.1 and 4.3). In the one-family house the long-term average (34 days) is much higher than the short-term average (6 hours) (see table 4.2 and 4.4). This is probably due to differences in airing, use of range hood fan and weather. During the short-term measurements the house was unoccupied.

	Living room	**Bedroom**	**Kitchen**	**Hall**	**Total**
Outdoor air, m^3/h	49	27	20	15	111
Temperature °C	-	-	-	21	

Table 4.3 Average outdoor air ventilation rates for individual rooms in the passive stack apartment on the first floor. Measuring period 25 days. Average outdoor temperature 1.2 °C (min -8 °C, max 8 °C), average wind speed 2.3 m/s.

	First floor				**Basement**				
	Living room	Bed-room	Bed-room	Kitchen	Game room	Gar age	Hall	Base-ment	Total
Outdoor air, m^3/h	19	9	13	9	13	33	8	17	141
Temperature °C	-	-	20	-	-	-	-	-	

Table 4.4 Average outdoor air ventilation rates for individual rooms in the passive stack one-family house. Average outdoor temperature 0.8 °C (-8.0, 11.5 °C), average wind speed 2.3 m/s, measuring period 34 days.

4.2.2 Balanced ventilation

Both apartments have an almost constant outdoor air ventilation due to a high level of airtightness (see figure 4.2). The measuring period was too short in the one-family house to see any variation. The average ventilation rate in this house was 155 m³/h (0.5 ach) during 6 hours. The ventilation rates of individual rooms, in the dwellings with balanced ventilation, agreed well with the measurements of the air flows through the supply air terminal devices.

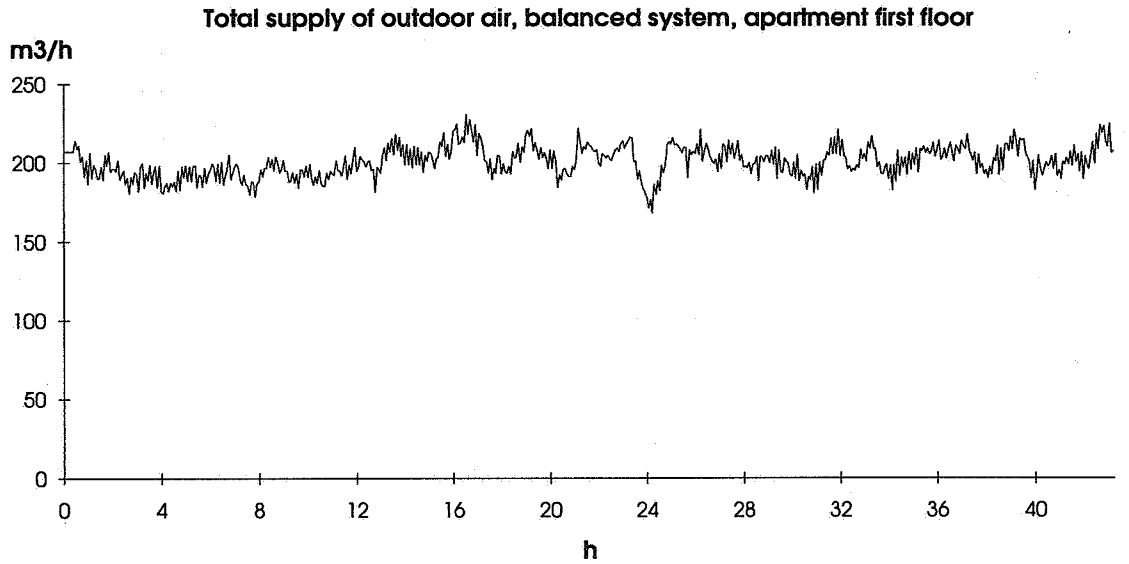

Figure 4.2 Total supply of outdoor air for the apartment (1st floor) with balanced ventilation, during 44 hours. Average outdoor temperature 3 °C (min 0.5 °, max 16 °C), wind 2.8 m/s.

4.2.3 Exhaust ventilation

The continuous measurements of the overall outdoor air ventilation in two apartments show some variation over time in the ventilation rate (see figure 4.3). For the apartment shown this is due to fairly leaky exterior walls. The average ventilation rate was 97 m³/h (0.75 ach).

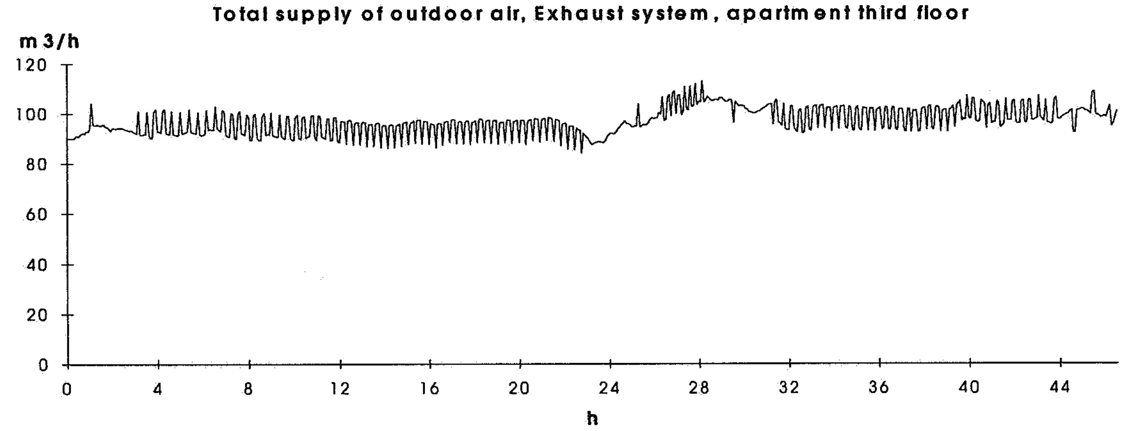

Figure 4.3 Total supply outdoor air to the on third floor with exhaust ventilation during 46 hours. Average outdoor temperature 3°C (min - 0.5 °C, max 6.5 °C), wind speed 2.3 m/s.

The outdoor air ventilation rates of individual rooms show some rooms to have too low a ventilation rate e. g. bedroom 15 and 16 in the one-family house and some rooms to have too high a ventilation rate e.g the kitchen in the apartment on the third floor (see table 4.5 - 4.6).

Apartment 1st floor	**Bedroom**	**Living room**	**Kitchen**	**Total**	**Measuring period**
Outdoor air, m^3/h	23	35	32	91	6 hours
Apartment 3rd floor					
Outdoor air, m^3/h	74	23	-	97	46 hours

Table 4.5 Average outdoor air ventilation rates for individual rooms in the exhaust ventilated apartments. Indoor temperature 21 °C. 1st floor: outdoor temperature 6 °C (min 5.5 °C, 9 °C). 3rd floor: see figure 4.3.

	Upstairs			**Downstairs**						
	Living room 14	Bed-room 15	Bed-room 16	Hall	Bed-room 9	Kit-chen	Laun-dry	Living room 6	Bed-room 7	Total
Outdoor air, m^3/h	36	8	6	33	9	6	37	3	24	163
Temp., °C	20	20	-	-	-	19	19	18	-	

Table 4.6 Average outdoor air ventilation rates for individual rooms in the exhaust ventilated one-family house. Average outdoor temperature 1 °C (min 0 °C, max 2.5 °C), measuring period 6 hours.

The long-term measurements show results similar to the short-term measurements (see table 4.7 - 4.8). There are some exceptions, the long-term average ventilation is higher for the living room in the apartment on the first floor, the same is true for one of the living rooms in the one-family house.

Apartment 1st floor	**Bedroom**	**Living room**	**Kitchen**	**Total**	**Measuring period**
Outdoor air, m^3/h	31	65	24	111	29 days
Temperature °C	-	21	-		
Apartment 3rd floor					
Outdoor air, m^3/h	73	27	-	119	29 days
Temperature °C	-	23	-		

Table 4.7 Average outdoor air ventilation rates for individual rooms in the exhaust ventilated apartments. Average outdoor temperature 1.3 °C (min - 8 °C, max 8 °C), average wind speed 2.3 m/s.

	Upstairs			**Downstairs**						
	Living room 14	Bed-room 15	Bed-room 16	Hall	Bed-room 9	Kit-chen	Laun-dry	Living room 6	Bed-room 7	Total
Outdoor air, m^3/h	41	10	10	16	14	15	-	25	12	167
Temperature, °C	20	-	-	-	-	-	-	-	-	

Table 4.8 Average outdoor air ventilation rates for individual rooms in the exhaust ventilated one-family house. Average outdoor temperature 0.7 °C, (min -8 °C, max 8 °C), average wind speed 2.3 m/s, measuring period 32 days.

5. CONCLUSIONS

5.1 Measuring techniques

Ideally the total ventilation should be monitored continuously during an entire year. There are several techniques for this purpose, but high cost and inconvenience prevent their use. A compromise is then to use short-term (1 - 7 days) continuous measurements, long-term averaging measurements and an estimation technique. The best approach is to adjust a ventilation model to fit measured ventilation values. This will improve the accuracy of the determination of ventilation. Numerical simulations of tested dwellings and comparisons with the measurements will be performed in this project. The measurements will be repeated for a summer month and a fall month.

The most straightforward approach to measurement of the total ventilation rate is to measure it directly using a tracer gas. If the ventilation system is mechanical, then the air flows in the ducts should first be measured using techniques for volume and mass flow rate measurements. There are three different tracer gas techniques: decay, constant concentration, and constant flow of a tracer gas. The constant concentration and the constant flow technique were employed as being the most accurate methods of determining the overall and the local (individual rooms) outdoor air ventilation rate. The following comments can be made:

Method	Comments
Constant concentration:	insensitive to effective volume problems
	unstable constant concentration can occur
	used in multichamber mode to determine supply of outdoor air
	complicated and expensive equipment
	not very practical in an occupied building
	useful for continuous long-term automated measurements
	inaccuracy in total flow rates ± 5 - 10 %
Constant flow:	relatively insensitive to effective volume problems
(passive technique)	less complicated equipment than for constant concentration
	useful for long-term averaging
	inaccuracy in total flow rates ± 15 %;
	the purging air flow can be determined
	can easily be used in an occupied building

5.2 Ventilation rates

The outdoor air ventilation rates in the dwellings with passive stack ventilation varied over time, as could be expected. Some of the individual rooms had an outdoor air ventilation rate, which at times were too low.

The exhaust ventilated dwellings had a reasonably constant outdoor air ventilation rate over time. The ventilation rate would have more constant, if the dwellings had fullfilled e g the airtightness requirements of the Swedish Building Code. Individual rooms sometimes had too low an outdoor air ventilation rate. This was especially true for the leaky one-family house, which had no outdoor air vents. If the house had fullfilled e g the airtightness requirements of the Swedish Building Code and had had outdoor air vents, then the distribution of outdoor air to individual rooms would have been better.

The dwellings with balanced ventilation had an over time almost constant outdoor air ventilation rate. This was due to the fact that the air leakage of the dwellings was very low. The dwellings fullfilled the requirements on airtightness as given in the Swedish Building Code. The ventilation systems in these dwellings were well adjusted, which meant that the individual rooms were supplied with a reasonable amount of outdoor air.

The ventilation rates will be further evaluated using a multi-zone network modell.

7. REFERENCES

ASHRAE, 1993, Handbook of Fundamentals. American Society of Refrigerating and Air-conditioning Engineers, Atlanta, Georgia, USA.

Blomsterberg, Å., 1990. Ventilation and airtightness in low-rise residential buildings - Analyses and full-scale measurements. Swedish Council for Building Research, D10:1990, Ph. d. thesis, Stockholm, Sweden.

Blomsterberg, Å., 1991. Ventilation control within exhaust fan ventilated houses. Proceedings the 12th AIVC Conference, Ottawa, Canada.

Charlesworth, P., 1988. Air exchange rate and airtightness measurement techniques - an application guide. AIVC, Coventry, Great Britain.

Kronvall, J., Boman C.-A., 1993, Ventilation rates and airtightness in the Swedish housing stock. Proceedings the 14th AIVC Conference, Copenhagen, Denmark.

NVG (Nordic Ventilation Group), 1995, Metoder for mätning av luftflöden i ventilationsinstallationer (Methods of Measuring Air Flows in Ventilation Systems). Meyer Information Förlag AB, Gävle, Sweden (in Swedish).

Stymne, H., Boman, C.-A., 1994. Measurement of ventilation and air distribution, using the homogeneous emission technique - a validation. Proceedings of Healthy Buildings ´94, Budapest, Hungary.

Stymne, H., Blomquist, C., Sandberg, M., 1994. Determination of local mean ages of air by the homogeneous injection tracer gas technique. Proceedings of the 15th AIVC Conference, Buxton, Great Britain.

SS 02 15 56, 1988, Swedish Standard for Buildings - Determination of the Total Outdoor Air Inflow. SIS (The Standardization Commission in Sweden), Stockholm, Sweden.

Tolstoy, N., Borgström, M., Högberg, H., Nilsson, J., 1993. Technical properties of the Swedish housing stock. Swedish Institute for Building Research, TN:29, ELIB-rapport 6, Gävle, Sweden (in Swedish).

Implementing the Results of Ventilation Research
16th AIVC Conference, Palm Springs, USA
19-22 September, 1995

Temperature and Velocity Distribution for Air Slot Devices

Ulf Kruger

Dept of Building Services Engineering, Chalmers University of Technology, S 412 96 Gothenburg, Sweden

Temperature and velocity distributions for air slot devices

Ulf Krüger

SYNOPSIS

Depending on the demands regarding the size and location of the occupation zone and the need for outdoor air flow rates, different ventilation systems and air supply devices have to be used in different kinds of buildings. The occupation zone in a residential building can be difficult to define, as many different activities can take place. Furthermore the furnishings of the room can change with time.

The highest air velocities and the lowest air temperatures in the occupation zone will often occur close to inlet air devices. The importance of the location and selection of inlet air devices is exemplified by studying an air slot device for mainly residential use. The slot device was placed over a window at a height of 2.0 m above floor level. Both measurements and calculations of air velocity and temperatures are presented in the paper. From a thermal comfort point of view the device tested seem to give satisfactory performance only for air flow rates less than 4 l/s. The draught problem will increase with lower inlet temperatures.

It is also shown that the internal heating in a device can be important with regard to thermal comfort. The factors that influence the relationship between outdoor and supply temperature are also discussed.

LIST OF SYMBOLS

A_o	effective area of the supply opening (m^2)
b	width of device (m)
d	characteristic length (m)
d_h	hydraulic diameter (m)
h	height of device (m)
L_i	distance to fully established velocity distribution (m)
PD	percentage dissatisfied people due to draught (%)
Re	Reynolds number
t_a	air temperature (°C)
t_{out}	outdoor temperature (°C)
T_m	minimum (or maximum) air temperature across an air jet (K)
T_o	temperature of the supply air (K)
T_r	air temperature (reference temperature) of the room (K)
Tu	turbulence intensity (%)
U	average air velocity in the device (m/s)
$\bar{u}$	mean air velocity at a point in a room (m/s)

x distance (m)
υ kinetic viscosity (m^2/s)
θ_m non-dimensional temperature decay ratio

1. INTRODUCTION

In ventilated spaces people often complain about draught. When draught problems in an apartment or an office are discussed, it often suffices just to look at the occupied zone. The area near the ceiling, for example, is usually not so important from a thermal comfort point of view. The demands regarding the size and location of the occupied zone must be strongly connected to the kind of building in question and the activities going on in the building. This means that occupation zones can be defined in many different ways.

In an office building, the occupants often have the same positions in the rooms throughout the working day. Often they sit at their desks at a predetermined place. In this case, the occupied zone is just a small part of the room. The choice of ventilation system in office buildings depends mainly on the thermal load and the thermal loads also determine the air flow rates. The conditions are completely different in residential buildings.

In residential buildings, many different activities take place. Furthermore, the furnishings of the rooms are not known before moving in and can also change with time. Thus, it is important that the whole area of the room can be used. Here the thermal loads are not the most significant factor for the choice of air flow rates, but rather the air quality.

2. DEFINITIONS OF OCCUPATION ZONE IN RESIDENTIAL BUILDINGS

The demands for thermal comfort are similar in most comfort standards [1, 2]. The standards are often based on the equations originally derived by Fanger [3]. Consequently the choice of ventilation system can depend more on how the occupied zone is defined in a particular case. In Figure 1, different occupied zones are shown. Common for all these occupied zones is a horizontal plane located above head height, approximately 1.8 m above floor level. Below this plane, the occupied zones differ as regards the positions of the vertical limitation planes.

The ANSI/ASHRAE 55-1992 Standard has general vertical limitation planes 0.6 m from walls or fixed air conditioning equipment. However this general definition is not acceptable when discussing residential buildings. If such a definition was to be acceptable, this would mean very strong restrictions on what part of a room that could be defined as the occupation zone. Moreover, only the area comprising the middle of a room could be used. When looking at offices the normal occupied zone is small and here the zone definition should be different for each room. Thus, it should also be possible to move the workplace to another part of the room.

When discussing occupied zones in residential buildings, the near zones of supply air devices, radiators and windows are the critical parts of the room, especially the near zone of supply devices. This is because the air is mainly supplied to the room through small outlet areas. A step in the right direction could be to change the position of the vertical plane limitations to 0.5 m from outdoor walls or fixed air conditioning equipment and to 0.1 m from indoor walls when defining the occupation zone for residential buildings [4].

From the point of view of apartment owners, it goes without saying that the whole room should be possible to use, as that is what they pay for.

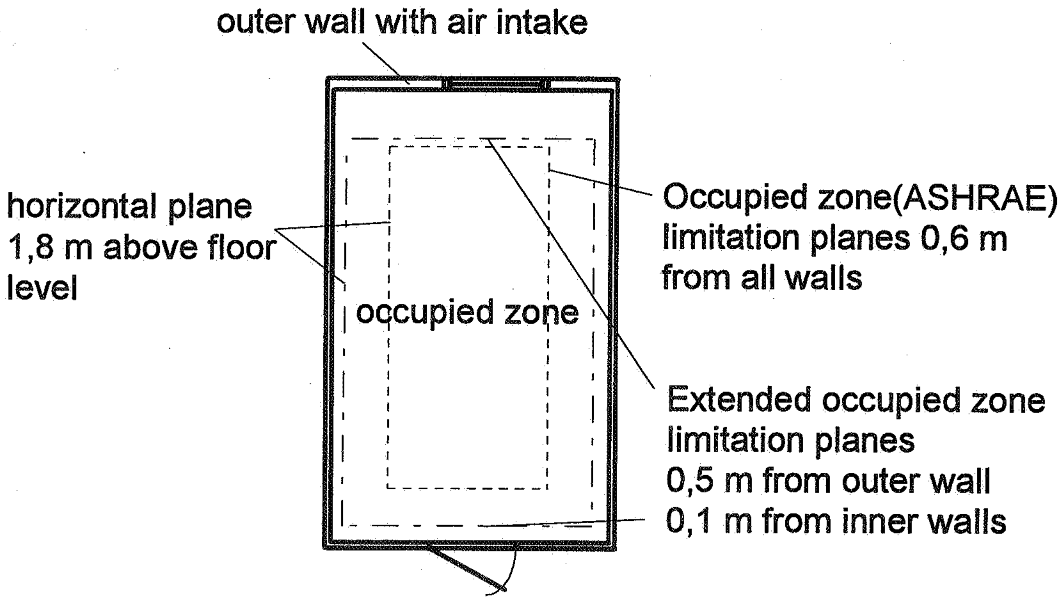

Fig 1. Room with different occupation zones.

To evalute the thermal comfort indoors due to draught risk, the PD-index (percentage people dissatisfied due to draught) can be used [5]. Draught can be defined as an unwanted cooling of the human body caused by air movements. The risk of draught depends on air velocity, turbulence intensity and air temperature according to equation (1).

$$PD = (34 - t_a)(\bar{u} - 0.05)^{0.62}(0.37\bar{u}Tu + 3.14) \qquad (1)$$

If an air flow of 10 l/s with an air temperature of 21°C is to be supplied to a room, an inlet area larger than 0.07 m^2 is needed to provide a good thermal climate. In this case, assumptions have been made that the velocity is equal over the whole inlet area of the device and that the whole room volume is regarded as the occupied zone. The calculations are also based on a measured turbulence intensity of 40% for an air slot device [4]. Higher air velocity than 0.14 m/s, lower air temperature than 21°C or higher turbulence intensity will result in more than 15% being dissatisfied due to draft (see equation (1)). If the inlet area is smaller than 0.07 m^2, the PD-index will become higher. On the other hand, if the air is supplied through a device placed above head height, problems with high velocities will not necessarily exist during summer time but in the cold season the air jet will bend down in the occupation zone and cause discomfort [4].

When the outdoor air is supplied with a mechanical exhaust system, the air entering the room in the winter season is colder than the room air. This means that a larger inlet area is needed during winter to get the same thermal comfort as in the summer.

3. INTERNAL PRE-HEATING OF THE OUTDOOR AIR IN SLOT DEVICES

The thermal comfort in the near-zones of supply devices is not particularly affected by the location of the exhaust devices in mechanically ventilated buildings. The air stream from the supply devices can, on the other hand, be noticeable at large distances from the devices. Several factors influence the way the air is distributed at different distances from a supply device.

- the design and location of the supply device
- the air flow rate and supply air temperature
- the dimension of the room and air obstructions such as furnishings
- air movements in the room such as convection streams from radiators, machines, people and other warm or cold surfaces

It is important to know the inlet temperature when calculating the trajectory of the air stream in the room or the air temperature in the stream at different positions. If the device is placed above head height, an unpreheated air stream gets into the occupation zone faster, the larger the temperature difference is between the air stream and the room. The inlet temperature of a supply device depends on the outdoor temperature and the air flow rate through the device.

A common and cheap supply device for an exhaust ventilation system for residential buildings is the air slot device. Such air devices are normally placed over windows. Air slot devices for mechanical exhaust systems have been found to allow a maximum air flow rate of 4 l/s if a satisfactory thermal climate is to be maintained [4,6].

In Figure 2, the results of an investigation of the internal heating in a slot device is illustrated at an air flow rate of 4 l/s. The air slot device has an inlet area of 300 x 11 mm. The device, which is completely made of plastic, consists of five sections placed lengthways. Moreover, the device has a damper in the outlet part. The measurements were made when the device was placed in a window frame with a thickness of 60 mm.

The measurements were carried out at each lengthways position at 3 minute periods and in three different positions to get average air temperatures values. To be able to verify that all the measurements had been done under the same conditions (constant air flow rate in the device), a reference sensor was placed at the outlet of the device.

The shapes of the three air temperature curves in Figure 2 are quite similar. The air temperature increases very slowly in the first part of the device and more rapidly in the second part. In the outlet part of the device where the damper is located, the temperature increase is small. Factors that have an influence on the temperature increase are discussed below.

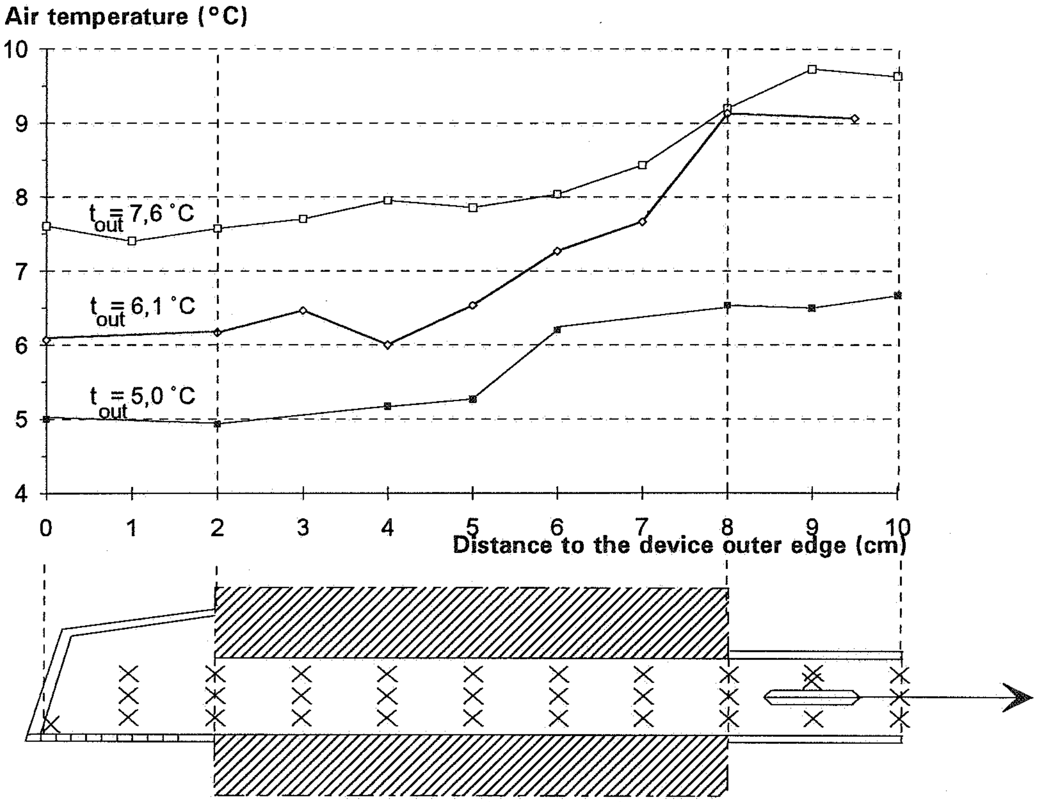

Fig 2. Temperature profile in a slot device at different outdoor temperatures, t_{out}.

- The thermal force is stronger further downstream inside the device where the temperature difference is larger between the air and the surfaces of the device that are located in the window frame. This is only partly an explanation why the temperature increase is larger at the end of the device.

- The heat transfer from the surfaces of the device to the air is affected by the heat transfer coefficient. The heat transfer coefficient is considerably higher for turbulent flows than for laminar flows. The type of flow that exists can be determined by calculation of the Reynolds number. The Reynolds number can in this case be estimated to 940 according to equation (2). In long ducts, the air flow is laminar when the Reynolds number is below 2100 [7]. However, this does not mean that the flow in the device is mainly laminar because the equation does not take into account the part of the device where the velocity profile is not completely developed.

$$Re = \left(\frac{Ud}{\upsilon}\right) \qquad (2)$$

-The velocity profile is not fully developed at the entrance of the device. Theoretically the velocity profile should have an almost rectangular shape, but in this case the air stream does not fall in perpendicular to the inlet of the device. As a rough estimate of the entrance length where the velocity profile is not completely developed, equation (3) can be used [8]. The entrance length, L_i, is defined as the distance from the inlet to the position where the centre velocity has reach 99% of the velocity that appears in a fully developed velocity profile. According to equation (3), the entrance length becomes much longer than the device. Thus, an accurate value of the heat transfer coefficient can not be determined in a simple way as the velocity and temperature profiles will affect the heat transfer considerably.

$$\frac{L_i}{d_h} = 0.0575 \cdot Re_{d_h} \tag{3}$$

- Another explanation for the higher temperature increase at the end of the device could be that room air was ejected or leaked into the device. This possibility was examined by filling the room with tracer gas. However, no tracer gas concentration could be measured in this case inside the device.

- A possible explanation for the low temperature increase in the outer part of the device could be that an air whirl establishes there so that a part of the outdoor air escapes from the device again.

4. TEMPERATURE AND VELOCITY DISTRIBUTIONS

The discussion below is based on the assumption of a free jet, thus, limitations of room walls, backward air streams or internal heat sources will not be taken into account.

The jet from a slot device could be treated as a plane jet or as a three-dimensional jet. In practice, jets issuing from openings of aspect ratios of $1 < b/h < 40$ should be treated as three-dimensional [9]. This slot device has an aspect ratio of 27. Air jets can be classified downstreams into four different velocity or temperature decay regions, where different equations should be used to estimate the profiles. However, the extents of these regions are different. A non-dimensional jet temperature decay ratio, θ_m, can be defined by:

$$\theta_m = \left(\frac{T_m - T_r}{T_o - T_r} \right) \tag{4}$$

Measurements of the air temperature in the air jet from the slot device [4] have been carried out at a distance, x, of 0.23 m after a slot device outlet. The lowest temperature in the air stream at this distance was 17.4°C at an outdoor temperature of 6.1°C. The air temperature at this distance has increased by approximately 8°C compared to the air temperature at the device outlet (see Figure 2). The result can be compared to the calculated decay of the maximum temperature for free jets. Figure 3 gives $\theta_m = 0.41$ for a device with an opening b/h ratio of 27 and an effective area of the supply opening, A_0 of 33 cm^2. With the measured room temperature of 22°C equation (4) gives $T_m \approx 17$°C, which is in close agreement with the measured value.

In the same way, an air velocity analysis for an air jet can be made by comparing measured and calculated air velocities. The centre velocity at different distances from the device for different openings of rectangular shapes can be estimated from [9] when the velocity in the device and the dimensions of the device are known. Estimated velocity maximum for the mentioned slot device at a distance of 0.83 m from the device is 0.32 m/s with an air flow rate of 3.5 l/s. This can be compared with the measured velocity which was 0.28 m/s at the same distance from the device [4].

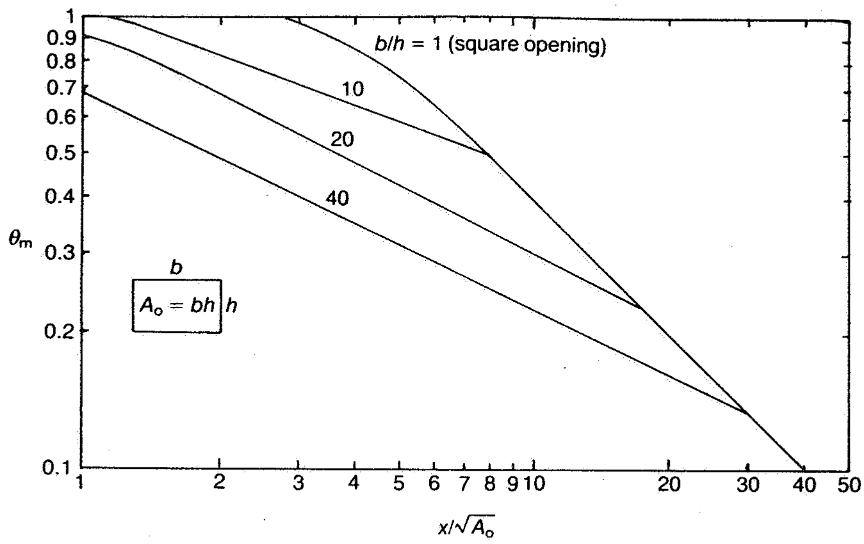

Fig 3. Decay of the maximum temperature for free jets of different aspect ratios [9].

5. DISCUSSION

The demands of outdoor air flow rates in residential buildings vary in different standards. For example ASHRAE Standard 62-1989 [10] recommends an air flow rate of at least 7.5 l/s, person.

The air velocity at different distances from the air slot device has been calculated [4, 9] for an air flow rate of 4 l/s and is shown in Figure 4. Assumptions have been made that it is a free jet that is not influenced by any air movements in the room (no air backflow or convection flows). It is obvious that the slot device system is not to be recommended for residential buildings as not even 4 l/s can be supplied without causing draught (see also [4]).

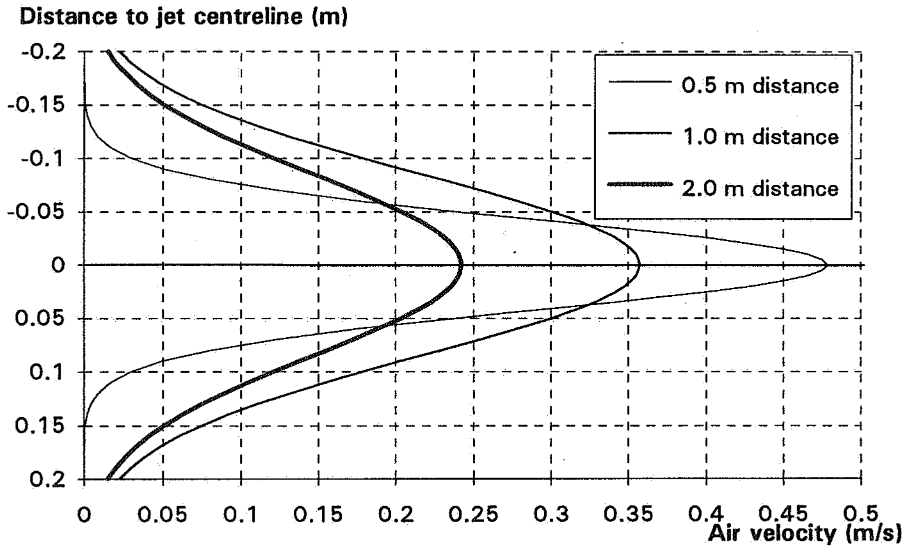

Fig 4. Velocity profiles at different distances from an air slot device for a flow rate of 4 l/s.

6. CONCLUSIONS

Air slot devices can not be recomended as inlet devices when supplying outdoor air to residential buildings. However, the demands on the size of occupation zone influence the possible selections of ventilation systems and air supply devices. It is, thus, of importance to define different occupation zones in different kinds of buildings. The following facts should be kept in mind when planning new or modifying old ventilation systems:

- Different ventilation systems have to be used depending on the demands on the size and location of occupation zone.
- The occupation zone in residential buildings should include all room-space except the near zones of fixed air conditioning equipment, radiators and windows.
- The air temperature increase in a supply device can be of importance for the thermal comfort indoors.
- Investigations of the thermal comfort in rooms with outdoor air supplied through devices with non pre-heated air should be carried out at low inlet temperatures corresponding to the lowest outdoor temperatures during the year.

REFERENCES

[1] International Standard ISO 7730, Moderate thermal environments- Determination of the PMV and PPD indices and specification of the conditions for thermal comfort, (1990).

[2] ANSI/ASHRAE Standard 55-1992, Thermal Environmental Conditions for Human Occupancy, *American Society of Heating, Refrigerating, and Air-Conditioning Engineers*, Atlanta, USA.

[3] Fanger, P O, Thermal Comfort, *Danish technical press*, Copenhagen (1970).

[4] Krüger, U. Ventilation och termiskt klimat i bostadsrum. Laboratorie- och fältmätningar. *Department of Building Services Engineering, Chalmers University of Technology*, Göteborg, Sweden (1993), (In Swedish).

[5] Fanger, P O, Melikov, A K, Hanzawa, H, Ring, J, Turbulence and draft, *ASHRAE Journal*, No 4 (1989).

[6] Krüger, U, Laboratory Tests and Field Measurements of Air Velocities and Temperature Gradients in Residential Buildings, *Proceedings of the Roomvent '92 Conference*, Aalborg, Vol 3, p 323-339 (1992).

[7] Frank Kreith, Principles of Heat Transfer. *University of Colorado, Intext Educational Publisher*, New York (1976).

[8] Sundén, B, Kompendium i värmeöverföring, *Inst. för Tillämpad termodynamik och strömningslära, Chalmers tekniska högskola*, Nr 88/7, Göteborg, Sweden (In Swedish).

[9] Awbi, H B, Ventilation of Buildings, *E & FN SPON*, London (1991).

[10] ASHRAE Standard 62-1989, Ventilation for Acceptable Indoor Air Quality. *American Society of Heating, Refrigerating, and Air-Conditioning Engineers*, Atlanta, USA.

The Southampton Survey on Asthma and Ventilation: Humidity Measurements During Winter

D A McIntyre, F R Stephen

E A Technology, Capenhurst, Chester, CH1 6ES, UK

The Southampton survey on asthma and ventilation: humidity measurements during winter

Synopsis

As part of a collaborative trial on the effects of ventilation on house dust mites and asthma, 20 mechanical ventilation units were installed in houses in the Southampton area in southern England. The hypothesis is that continuous ventilation over winter months can maintain humidity below a mixing ratio of 7 g/kg, with a consequent reduction in house dust mite numbers. The systems served upstairs only, extracting from bathroom and landing and supplying fresh air to bedrooms. Temperature and humidity in the experimental houses and 20 control houses were recorded in the patients' bedrooms at carpet level. Over the 4 months from December to March the mechanically ventilated houses had significantly lower absolute humidities. Of the 20 MV houses, 15 had a mean mixing ratio below 7 g/kg, compared with only 3/20 of the non-MV houses.

1 Introduction

Much asthma is caused by an allergic reaction to the house dust mite and many approaches are under investigation for the control of mites[1]. It is known that increased levels of humidity provide a favourable environment for the growth of mites and there is strong evidence to indicate that dust mites may be controlled by maintaining a reduced indoor humidity during winter months[2]. During cold weather, indoor humidity may be reduced by ventilation with outside air to remove internally generated moisture. The use of mechanical ventilation with heat recovery (MVHR) enables this to be done efficiently, with neither draughts nor excessive heat loss.

EA Technology is collaborating in a major clinical trial on the effects of mechanical ventilation on humidity and asthma. The trial is under the overall direction of the Department of Child Health at Southampton University and the Building Research Establishment is undertaking the dust mite analysis together with IAQ measurements and householder surveys. The study covers asthma patients in 40 houses in the Southampton area and mechanical ventilation was installed in 20 houses in time for the 1994/95 heating season, after which monitoring continued for a year. In addition, half the houses have been supplied with a high efficiency vacuum cleaner to test whether it is effective in reducing ambient levels of houses dust mites and associated allergen. This report analyses the measurements of bedroom temperatures and humidities in the 40 houses covering a period up until the end of the 94/95 heating season, relating them to outside weather and the presence of mechanical ventilation.

2 Selection of houses

Southampton University recruited patients from among people attending the Southampton asthma clinic and those willing to participate completed a questionnaire about their home. Houses were rejected for the study if they were unsuitable for mechanical ventilation installation or were likely to have excessive background ventilation.

Houses were assigned to 4 experimental groups.

Group	Intervention	Number
1	Ventilation & vacuum cleaner	10
2	Ventilation	10
3	Vacuum cleaner	10
4	Monitoring alone	10

Groups 1 & 2 have mechanical ventilation, 3 & 4 do not. Allocation of houses to groups was done after preliminary observations of bedroom humidity became available. Houses were divided into 4 humidity bands and assigned randomly to groups within bands. Pressurisation tests were later carried out by the Building Research Establishment and analysis showed no significant difference in house leakage between experimental groups. The leakage results will be reported separately.

3 Ventilation equipment

To provide the benefits of mechanical ventilation without the disruption associated with retrofitting a whole house ventilation system, an 'upstairs' system was installed, complemented by an extract fan in the kitchen. The main MVHR unit containing fans and heat exchanger is mounted in the loft space, supplying tempered fresh air to bedrooms and extracting moist air from the bathroom. An additional extract point is fitted in the landing; this avoids excessive extraction rates through the bathroom terminal and intercepts moist air moving up the stair well. The system therefore only requires access to the loft space for installation and no ductwork within the house has been needed. An EU4 grade filter was mounted in the main air intake duct, capable of intercepting pollen grains.

On commissioning, the system was set to provide an air supply of 8 l/s for a double and 6 l/s for a single bedroom. Air extract in the bathroom was set at twice that in the landing, to avoid spillage of moist air out of the bathroom. The system was balanced between total extract and supply rates. After commissioning, the system was switched off. All systems were switched on at the start of the measurement period in Week 45 beginning 9th November 1994. Householders in Groups 1&2 were advised on the use of the mechanical ventilation and asked to run the system continuously.

4 Data logging

A short experimental programme was undertaken to explore the effect of logger position within a room. Data from the carpet or the floor of the room was found to be a very reliable source of information and was less susceptible to rapid variations in humidity. A 10 minutes scan period provided an accurate record of events within the room.

Small independent loggers were used, mounted in a perforated aluminium case. The case rests on the bedroom floor and can be moved and replaced by the householder when cleaning. Two further loggers were mounted on the north facing side of two dwellings within the survey area. Data was collected from the loggers using a portable computer during a visit to the subject's house. All loggers were checked before despatch and found to give satisfactory accuracy. There were some problems with the outdoor humidity sensors when exposed to lengthy periods at an RH above 90%. This caused the reading to drift upwards to give some readings above 100% RH, with a long recovery time afterwards when the humidity fell again. Discussions with the manufacturer of the sensor revealed that this problem is common and that it is possible to precondition sensors which will be used in humid environments. The troublesome loggers were replaced. Weather data has also been obtained for the Southampton region from the Southampton Weather Centre.

5 Analysis

5.1 Measurement periods

A standard week numbering nomenclature is used. A week runs from Monday to Sunday. Week 1, 1994 commences 3rd January and Week 1, 1995 starts on 2nd January 1995. Data loggers were installed in the houses between March and May 1994. All loggers were operational by Week 27. Installation of ventilation systems took place during October and November 1994; after installation the systems were commissioned and then left switched off. All ventilation systems were turned on together at the start of the heating season in Week 45, 1994.

The hypothesis to be tested in the analysis of the logger readings is that absolute humidities measured in the bedrooms of the ventilated houses (Groups 1&2) are lower than those measured in the control houses (Group 3&4). The WHO working party[5] proposed that dust mite growth is inhibited below an absolute humidity of 7 g/kg when expressed as a mixing ratio. The analysis in this paper uses 7 g/kg as a reference level. Analysis of weather records[3,4] shows that the four winter months of December to March inclusive consistently have a lower mean absolute humidity than the remainder of the year and the 18 weeks from Week 48, 1994 to Week 13, 1995 were selected for the main analysis. In addition several descriptive statistics are presented for the total available measurements from Week 27, 1994 to Week 21, 1995.

5.2 Weather

Figure 1 compares the monthly mean temperatures and humidities recorded on the roof of the Southampton Weather Centre during the total experimental period with records of other years. Thirty year mean air temperature data for Southampton was obtained

Figure 1 The weather during the measurement period was warmer and more humid than usual

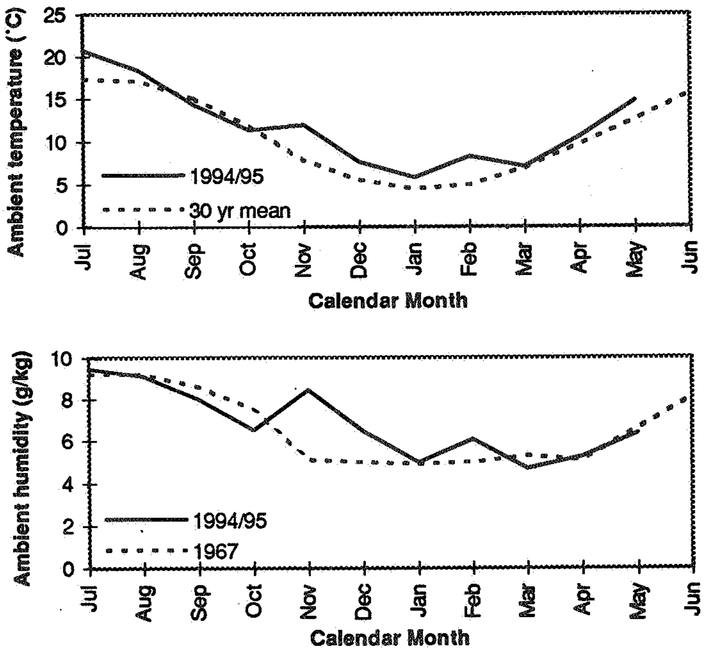

from[6], but no comparable humidity data was to hand. Measured humidities were compared with those of the standard year 1967, used by environmental engineers to represent typical conditions. It can be seen that the test period was in general warmer and more humid than average. Southampton, being on the south coast of England, tends to be warmer and more humid than many other parts of the UK. In general, the UK can be assumed to be similar to or drier than Southampton, with the exception of the extreme South West region, typified by Plymouth, which is markedly moister.

5.3 Weekly mean bedroom temperatures

	All houses	Groups 1&2	Groups 3&4
Mean	17.29	17.51	17.08
Standard deviation	2.05	1.91	2.18
Median	17.52	17.74	17.25
Upper quartile	18.47	18.56	18.38
Lower quartile	16.19	16.55	16.03
n	713	359	354

Difference between group means: $t = 2.81$, $df = 711$. $P < 0.01$

Table 1 Analysis of weekly mean bedroom temperatures over the 18 week test period

Table 1 summarises the measurements of weekly mean bedroom temperatures during the test period for all houses. The bedrooms in Groups 1&2 are 0.4 K warmer than those in Groups 3&4 and the difference is statistically significant. However, it was not hypothesised as an effect of MVHR and is not large enough to be of practical significance. Weekly mean bedroom temperatures are shown plotted against weekly mean outdoor temperature in Figure 2. Both experimental and control groups show a

Figure 2 Bedroom temperatures in Groups 1&2 were slightly warmer than those in Group 3&4

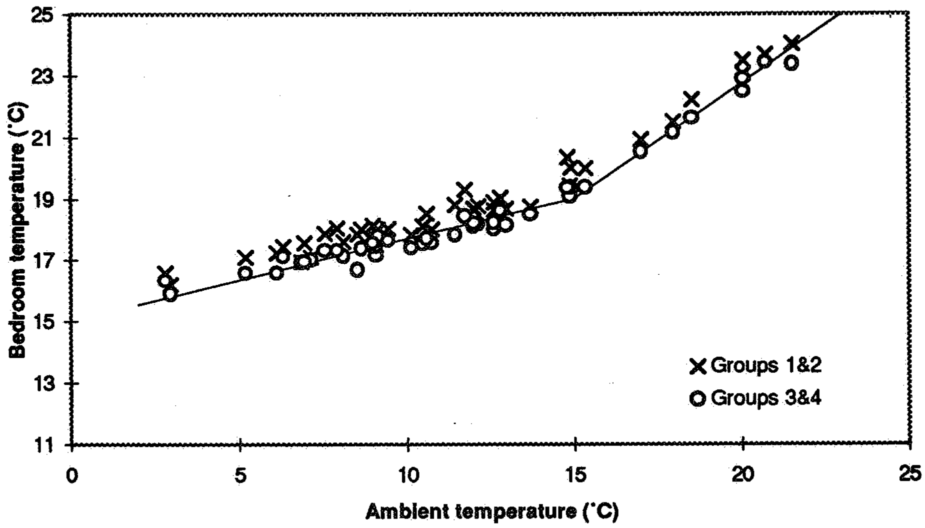

similar behaviour. Above about 15°C ambient temperature, the bedroom temperature rises with increasing outdoor temperature, with a slope only a little below unity. Below 15°C, bedroom temperature falls only slowly with decreasing ambient temperature. A straight line has been fitted by eye to the points. The temperature behaviour is typical of dwellings, implying that no heating is used above 15°C outdoor temperature. Below this, heating is used to maintain comfort.

5.4 Bedroom humidities

Table 2 summarises the measurements of weekly mean bedroom humidities for the test period. Groups 1&2 have a significantly lower humidity than the Groups 3&4, with a difference between means of 0.75 g/kg.

	All houses	Groups 1&2	Groups 3&4
Mean (g/kg)	7.13	6.75	7.53
Standard deviation	1.02	0.82	1.06
Median	7.03	6.69	7.42
Upper quartile	7.73	7.27	8.18
Lower quartile	6.36	6.14	6.77
n	713	359	354
Values < 7.0	49%	65%	32%

Difference between group means: $t = 10.56$, $df = 711$. $P<0.001$

Table 2 Analysis of mean weekly bedroom humidities for all houses during the 18 week test period

Weekly mean bedroom humidities are shown plotted against outdoor humidity in Figure 3 for the entire 48 week measurement period. The points are well fitted by linear regression. The difference in slopes is significant at better than the 1% level. The implication of the graphs is that ventilation is restricted in cold weather in both groups of houses and significantly more so in the in the non MV houses compared with the test group.

Figure 3 Regression lines of bedroom vs. outdoor weekly mean humidity were significantly different for the two groups:

1&2 $g = 2.33 + 0.81\ g_o$ $r^2 = 0.95$

3&4 $g = 3.63 + 0.69\ g_o$ $r^2 = 0.94$

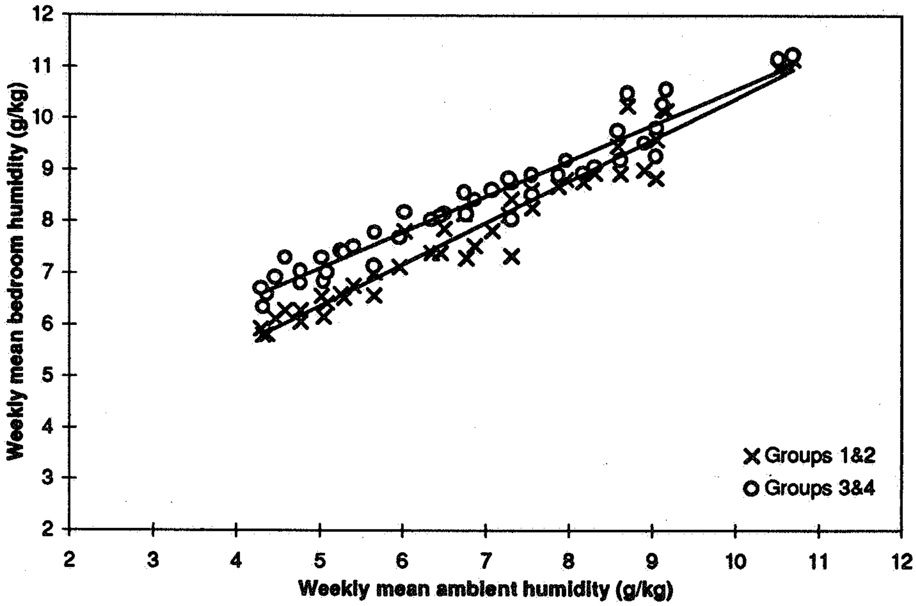

6 Discussion

6.1 Bedroom temperatures

There was a small but significant difference between the temperatures of the MV and non-MV groups, with the MV houses being on average 0.4 K warmer. This difference was not hypothesised. The use of mechanical ventilation ensures a constant supply of tempered air into the bedroom whose temperature depends on the efficiency of the heat exchanger and the temperature of the air being extracted from bathroom and landing. The air will therefore be below the general indoor air temperature and would be expected to have some cooling effect in the ventilated bedroom. The measurements show no support for unacceptably cool bedrooms associated with mechanical ventilation.

6.2 Humidity

The difference in bedroom humidity between the MV and non-MV groups is highly significant and we may conclude that the use of mechanical ventilation has indeed resulted in a reduction of indoor humidity. The difference in mean mixing ratios is 0.75 g/kg over the 18 week test period. Figure 3 shows that the difference in humidity between the groups increases at lower outdoor temperatures. This may be interpreted

Figure 4 15/20 MV houses had a winter mean humidity below 7 g/kg, compared with 3/20 non-MV houses

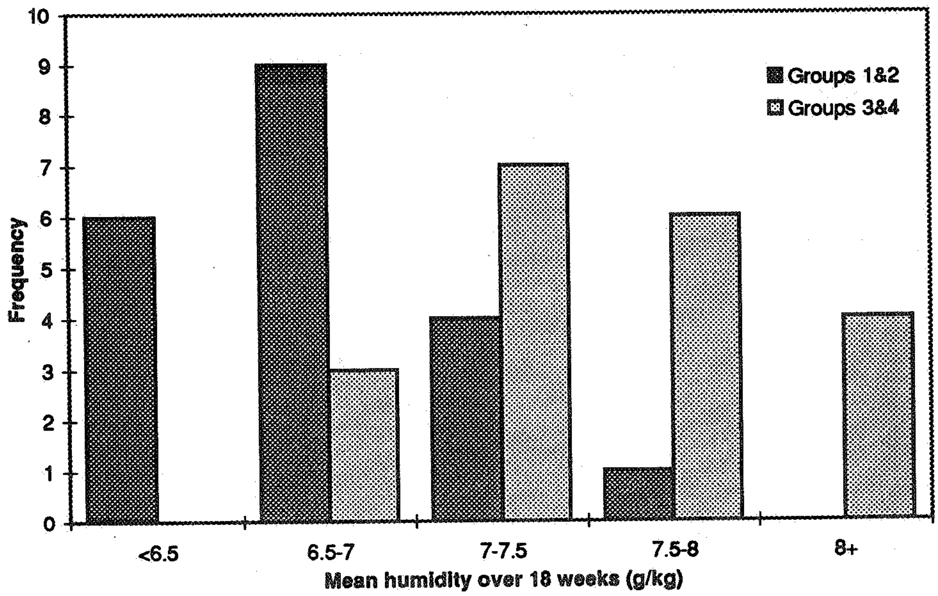

that ventilation is better maintained in the MV houses, with the non-MV houses reducing ventilation in cold weather to conserve heat.

At the level of individual houses, Figure 4 shows that the groups are well separated, with three quarters of the MV houses having a mean over the test period of less than 7 g/kg, while only 3/20 of the non-MV houses do so. This paper analyses the results in terms of a critical mixing ratio of 7 g/kg, below which it may be supposed that house dust mites do not thrive; this figure is derived from[5]. In practice, of course, we cannot suppose that there is a sharp threshold. Many factors remain to be properly resolved: the interaction temperature and humidity, the influence of local micro climate in carpet or mattress and the effect of the variation of humidity may all have an important influence. If so, the mean mixing ratio over the winter period would not be a sufficient indicator to explain variation in house dust mite numbers or activity.

The experiment was conducted over the winter of 1994/95, which was milder than average, and took place on the South Coast of England. Only the extreme South West of the UK has generally higher humidities than Southampton; the consequence is that a successful result achieved in Southampton can only be strengthened in locations either north and west.

7 Conclusions

The use of mechanical ventilation with heat recovery reduced the measured bedroom humidities in a sample of 20 houses, compared with a group of 20 houses without

MVHR. The mean reduction in mixing ratio measured over the 4 winter months November 1994 to March 1995 was 0.75 g/kg. ($P<0.001$)

Fifteen of the 20 houses with MVHR had a mean bedroom humidity of under 7 g/kg over the winter four months, compared with 3/20 of the houses without.

There was little difference in mean winter bedroom temperature between the two groups. The MV group was 0.4 K warmer ($P<0.05$)

8 Acknowledgements

The EA Technology programme is funded as part of the EA Technology Members' Core Research programme and is a contribution to the study being carried out jointly by the Department of Child Health, Southampton University, the Building Research Establishment and EA Technology. Dr Jill Warner of Southampton University has been awarded a Senior Research Fellowship by the National Asthma Campaign Research Committee and the British Lung Foundation.

This report describes only part of a larger study, and would not have been possible without the collaboration of all other parties involved. Particular acknowledgement is made to Jeanette Frederick and her colleagues, who were the prime contact with the households and who retrieved data from the loggers.

9 References

[1] COLLOFF, M J et al
"The control of allergens of dust mites and domestic pets: a position paper"
Clinical and Experimental Allergy 22 (2), 1992, pp1- 28.

[2] MCINTYRE, D A
"The control of house dust mites by ventilation: a pilot study"
13th AIVC Conference, Nice. Coventry, UK. 1992, pp497 - 507.

[3] LACY, R E
"Climate and building in Britain"
HMSO, London, 1977.

[4] MCINTYRE, D A
"Ventilation and Humidity: Weather Data for the United Kingdom"
R3000/T, EA Technology, 1993.

[5] PLATTS-MILLS, T A E and DE WECK, A L
"Dust mite allergens and asthma - A world wide problem"
J Allergy Clin Immunol 83 1989, pp416- 427.

[6] "Averages of temperature for the United Kingdom 1941-70"
Met O 883, HMSO, London, 1976.

**Implementing the Results of Ventilation Research
16th AIVC Conference, Palm Springs, USA
19-22 September, 1995**

A Low Cost Technique for the Measurement of High Ventilation Rates

D K Alexander, S Lannon

**Welsh School of Architecture, UWCC, Bute Building,
King Edward VII Ave, Cardiff, CF1 3AP, UK**

Synopsis

A recent investigation into the thermal environment of tropical housing required a low cost method for the measurement of high ventilation rates. As a result a simple measurement system, using the detection of the decay of smoke density, was developed. The sensor, based on an infrared LED emitter and a silicon diode receiver, was easily portable, highly robust and could be constructed for less than £50. It was found to be suitable for the measurement of decay rates in excess of 20 air changes per hour. The visible smoke tracer required for the system was easily generated by a number of methods, including smouldering coir matting, smoke bombs and theatrical smoke generators.

1 Introduction

In support of a recent investigation into the thermal comfort of tropical housing [1], the need arose to measure the ventilation rates occurring in those buildings. In tropical climates the building envelope can be highly porous, and the large leakage areas have the potential to produce very high ventilation rates under windy conditions. Thermal modelling of the conditions in these types of houses indicated that comfort conditions could change significantly between different assumed ventilation rates, even at the levels of 50 - 100 air changes per hour [2].

Little information was found to be available as to the actual ventilation rates to be encountered in such dwellings; few field trials had been made where ventilation was a measured parameter. Within the scope of a doctoral investigation is was decided to attempt to measure the ventilation rates of such dwellings, to determine if the large rates assumed in the thermal modelling actually occurred in practice.

2 Traditional Methods

In developing the methodology for these measurements, it was considered that tracer decay techniques were the most appropriate. However there appeared to be three key drawbacks in the equipment then available, which were based on the measurement of the commonly used tracer gases N_20, SF_6, and CO_2;

- the ventilation rates were expected to be high, for instance >20 ac/h. It was considered that the lower cost gas analysers had long time constants, and that this could affect their ability to accurately measure large ventilation rates.
- gas analysis equipment with low time constants were too costly for the funding available. There were none available to commit to a long term project abroad, it was not feasible to transport regularly from the U.K. to S.E. Asia, and it was not within the project budget to purchase new equipment at that scale.
- the reliable and regular supply of tracer gas in large amounts to remote rural locations would be difficult or impossible to achieve.

3 The effect of instrument time constant

The time constant of a gas analyser can theoretically have a significant effect on the accuracy of the estimation of high ventilation rates. This instrument time constant will depend largely on the flow rate and purging effectiveness through the detecting equipment. In Infrared Gas Analysers (IRGAs) this time constant can be short (on the order of seconds) but is apparently inversely proportional to the equipment cost. High quality fast IRGAs may cost in excess of £10000, while simpler lower cost instruments in the range of £1000 can have response time in the order of 10's of seconds. Gas chromatography equipment have significantly longer response times than that.

Figure 1 shows the calculated effect of instrument time constant on the estimate of ventilation rates by measured tracer decay. Imposed "true" ventilation rates of 50 and 100 air changes per hour were used. It can be seen that significant errors may be made for time constants >30 sec for the very high rates assumed. Note that 100 ac/h in a dwelling room may seem extraordinary but equates to a mean air flow across a typical room of only 0.3 m/s or less. High air velocities in rooms or tropical housing are in fact desirable for achieving comfort conditions, and recent field measurements by Rahman [3] have confirmed that air movements of this order are common.

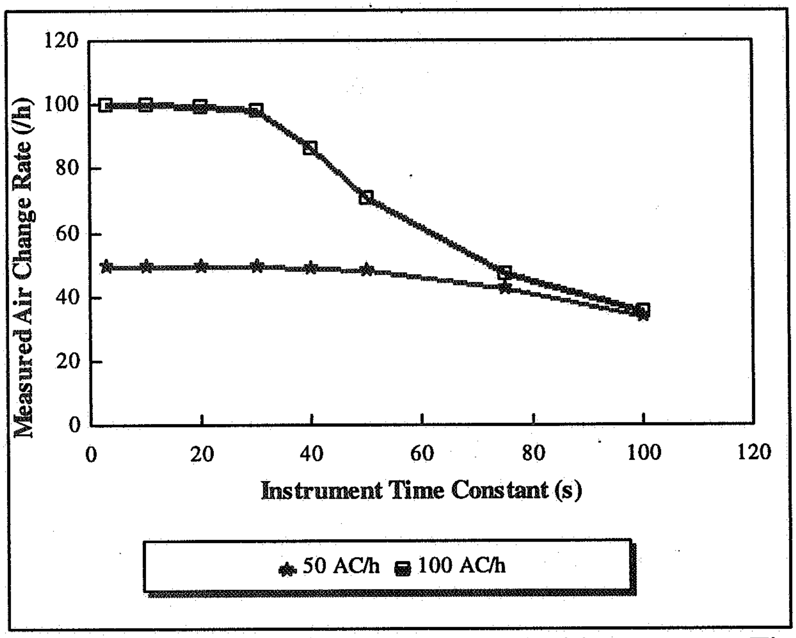

Figure 1 Theoretical Measurement Errors Associated with Instrument Time Constants

3 The smoke detector

To circumvent the cost and time constant restrictions discussed above, an alternative instrument or technique was sought. Etheridge and Nolan [4] described the measurement of ventilation in wind tunnel models using smoke as a tracer substance and an optical detector. We considered that this approach was appropriate to adapt for use in full scale buildings, as it was potentially fast, cheap, portable and robust.

The decay of smoke, as long as the condensation of the smoke matter was not significant, should be commensurate with the decay of a tracer gas, and so could be used to estimate ventilation rates. Since large ventilation rates were expected in our applications, condensation was not felt to be a problem. Smoke of various forms have been used widely in building science to visualise air movement, detecting leaks, and as a qualitative indication of ventilation. We are not aware of previous use in a quantitative measure of ventilation in full scale buildings.

The instrument described by Etheridge and Nolan is based on the optical detection of smoke in air, using an infrared LED emitter and silicon diode detector pair. The detection of smoke is by optical scattering caused by the particles present in the smoke. In a properly aligned system, figure 2, the detector will be illuminated only by the light scatter off the smoke. Etheridge and Nolan determined that the response of such a system was linear to smoke concentration. Since ventilation measurement by tracer decay relies on the differences in concentration over time, linearity of the measurement system is a crucial requirement. Fortunately for a low cost system, the ability to produce an absolute calibration is not a requirement for the analysis of the decay data.

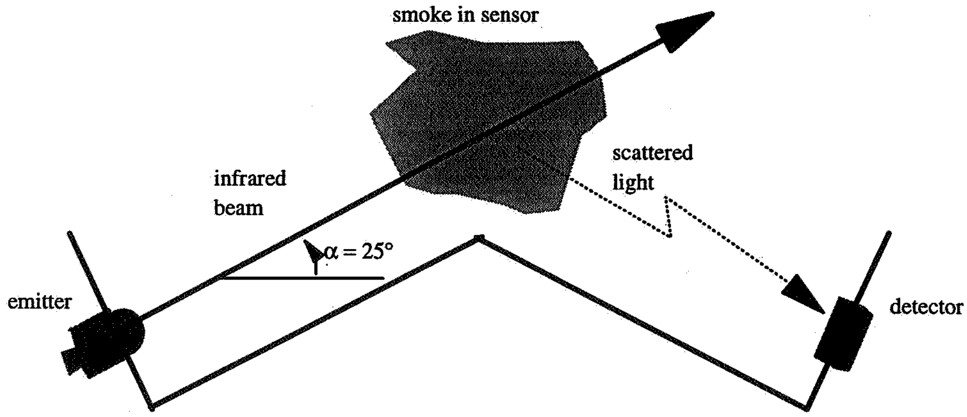

Figure 2 Optical Smoke Sensor Geometry

The sensor head produced by us is shown in figure 3. The emitter/detector pair are enclosed in a small opaque box, through which room air is drawn by a small fan. The box is highly baffled to exclude light, and its interior is painted matt black. Using the parts listed in table 1, the instrument costs less than £50 in 1995, and produces a signal of between 5 and 75 mV dc output according to the density and type of smoke to which it is subjected. The higher output quoted corresponds to a distinct, but not unacceptable (for short periods) haze in room air, equivalent to a visibility of approximately 50m. The dark signal of 5 mV has been found to be stable over long periods and changing light conditions. The response time of the sensor is virtually instantaneous (τ <1 s).

Component	Description	R.S. number	Approximate Cost , £
LED emitter	High power Infrared, Narrow Beam	195-344	1
Detector	5mm^2 silicon diode with integral amplifier.	308-067	16
Fan	miniature 5 V.dc fan, 40x40x12 mm	498-126	20
Case	ABS box, 150x80x50mm	508-936	2
Miscellaneous	Brackets, paint etc.		5

Table 1 Components of Sensor Head

The voltage signal produced by the sensor head is intended to be recorded by a portable data logger or chart recorder. We have used logging equipment produced by Grant and by Campbell. These data recorders are not inexpensive (in the region £500-£1000) but are general purpose and multi-channel. Simpler single input data recorders are now readily available in the region of £100 each. The entire system, sensor and recorder, could potentially be powered by rechargeable battery, making it suited for use in remote areas.

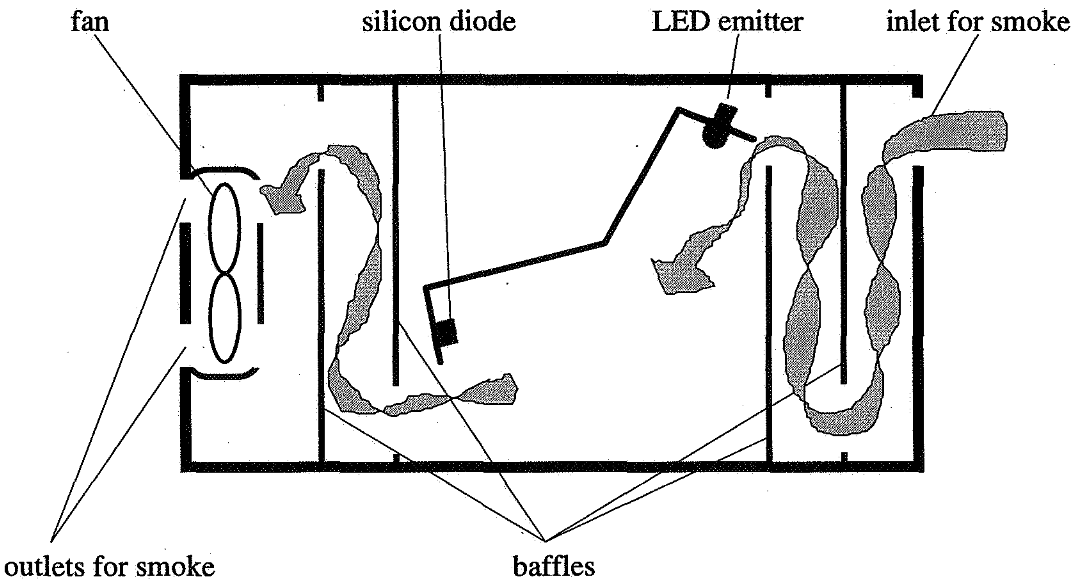

Figure 3 Drawing of Sensor Head

4 Testing in Laboratory Conditions

Tests were made to compare the results achieved with this instrument against known flow rates and against more traditional tracer gas methods. These tests were made in a room of approximately 60 m^3. A controlled, known ventilation flow was produced by a large fan installed in the door way of the test room; external windows across the room from the door were open. Several mixing fans were introduced into the room, but at the flows imposed by the door fan, these were probably unnecessary. The door fan, a building envelope pressurisation fan ("blower door"), was capable of generating between 0.1 - 2.5 m^3/s flows through the room, equivalent to air change rates of 5 to 150 air changes per hour; the fan flow rate was measured by orifice pressure drop during each test. In some trials, CO_2 was injected in the test room, as well as smoke and CO_2 levels measured by a Horiba IRGA.

Figure 4 shows a comparison of the decays of both smoke and CO_2 concentration during a single test. Figure 5 shows comparisons of the measurement method against the "known" rates as determined from the fan flow rate.

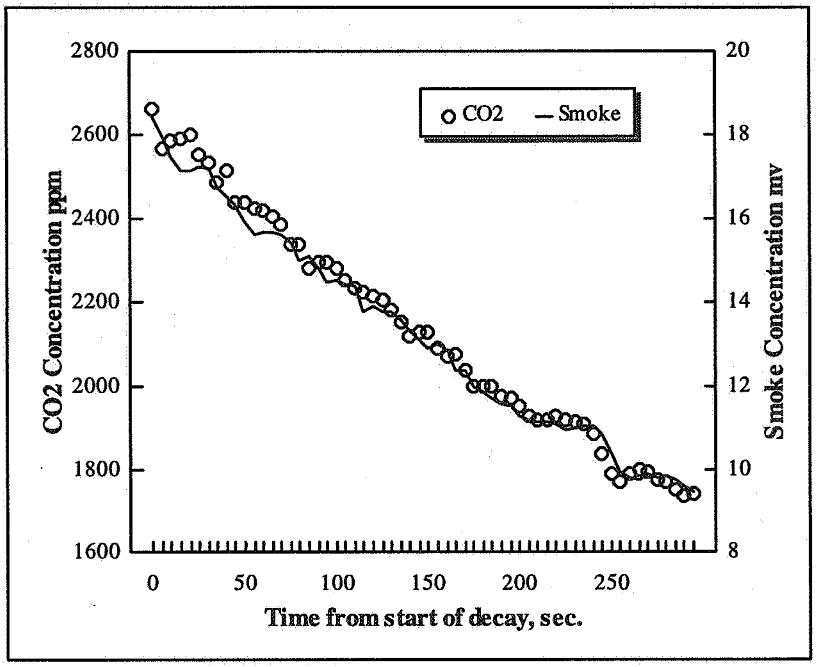

Figure 4 Example of Recorded CO_2 and Smoke Decay Curves

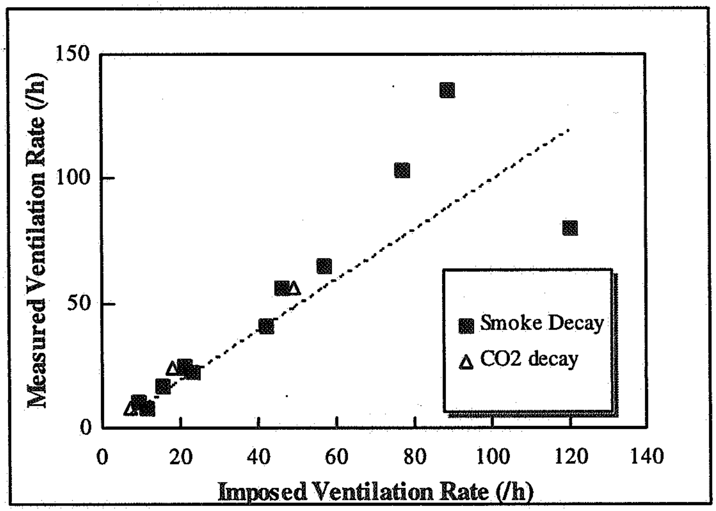

Figure 5 Comparison of Smoke Decay Results

The smoke and CO_2 methods were felt to be comparable, agreeing to within 12% for rates under 50 air changes per hour. The agreement at high rates (~100 ac/h) was not as satisfactory, but it is not at this time known if this was a characteristic of the smoke decay, the smoke sensor, or of the errors associated in calculating a ventilation rate from a (very high) flow rate. For the latter a ventilation effectiveness must be assumed and this may been in error. Thus at the higher flow rates, the estimate of the "true" ventilation rate could equally be in error as the measurement method. Additional work is planned to test the sensor further.

Given that CO_2 is itself not an ideal tracer gas to use for ventilation measurements, due to the naturally present background level, it can be concluded that the smoke decay method is at least as accurate as the CO_2 decay method, and potentially more accurate at high flows due to its' faster response time. For a low cost instrument this level of accuracy is felt to be suitable for its intended purpose. Potentially, accuracy and sensitivity could be increased by further development, but undoubtedly this would come only as a result of higher costs.

In the development of the system other smoke detector systems were also investigated. Notably, those found in fire detection systems are considerably more sensitive to low concentrations of smoke than the sensor described here. Unfortunately the component sensors of such systems are optimised for that particular use and provide only a binary output; e.g. above or below a threshold concentration. As such they are not directly suited for ventilation measurements, nor can they be modified for such.

Smoke from various sources were also tested for suitability. The tests described were made with a commercial oil based smoke generator; this smoke could be objectionable after exposure for a long time. Other sources of smoke have been tried; all were detectable by the instrument, though some were more pleasant than others to use. Those that have been tested are theatrical smoke generators (more acceptable to occupants, pleasantly scented, but low dispersion fluid should be used), joke shop smoke bombs (foul persistent smell), sewer leak-detection smoke pellets (copious coloured smoke but strong smell), cigarettes (socially unacceptable in many locations), incense (powerful odour if enough density of smoke produced), and even smouldering coir matting (a readily available local source for the target application).

It is accepted that this smoke decay technique is not a method readily applicable to buildings in use, due to the rather alarming appearance during the tests. However, there are equally many claims made about the acceptability of many of the tracer gases commonly used in ventilation research. The advantage of the system described here is that due to its' low cost, it may be usable in situations were other techniques would not be available or appropriate, and therefore may provide hard data where otherwise there would be none. It is notable and paradoxical that a secondary advantage of the system lies in the visibility of the tracer gas used; air flow visualisation may be done concurrently with the ventilation tests, supplementing the information gained.

A further advantage to be gained from the low cost of the instrument is that multiple monitoring points may be easily used in large spaces, without the need for pneumatic multiplexing. This can decrease the need for artificial mixing during measurements and lead to more natural measurement results, and possible greater accuracy at higher ventilation rates.

5 Testing in Field Conditions

The use of the instrument in the field went well, ventilation rates from 10 to 30 ac/h were measured in examples of modern housing in rural areas of Malaysia [3]. Measurement in examples of the traditional, very porous, housing was however less successful, in that there was an inability to generate sufficient initial smoke density, due to the high rates encountered. To account for this, it is considered that rates greatly in excess of 30 were being encountered. A more energetic smoke generator may have been able to overcome this problem, and provide more robust data.

6 Conclusion

To summarise, a smoke sensor has been developed to allow the measurement of ventilation rates in buildings, using smoke as a tracer. The sensor is low cost, and of comparable accuracy to the use of CO_2 as a tracer gas. The sensor is small and robust, suitable for sustained field work, and capable of monitoring high ventilation rates. The smoke may be generated by local materials or simple equipment. It is hoped that such an instrument may provide measurements where more traditional methods may unavailable or inappropriate.

References

1) Jones,P.J., Alexander,D.K., Rahman,A.M.
"The Thermal Performance of New Low Cost Housing in Malaysia"
Proceedings of Symposium and Exhibition on Low Cost Housing, University Sains Malaysia, Penang, 9-11 Dec. 1993, Volume II pp 32-38.

2) Hanafi, Z.
"Environmental Design in Hot Humid Countries with Special Reference to Malaysia"
PhD Thesis, UWCC, September 1991.

3) Rahman, A.M.
"Design for Natural Ventilation in Low Cost Housing for Hot Humid Climate of Malaysia"
PhD Thesis, UWCC, 1994.

4) Etheridge,D.W, Nolan, J.A.
"An Optical Technique for Measurement of Ventilation Rates in Models"
Building and Environment, Vol 14, pp 65-68, 1979.

Implementing the Results of Ventilation Research
16th AIVC Conference, Palm Springs, USA
19-22 September, 1995

Quantification of Radon Migration From a Uranium Mine Through the Soil into Buildings by the Use of Tracer Technique

Willigert Raatschen*, Richard A Grot**, Walfried Lobner***

*Dornier GmbH, Friedrichshafen, Germany
** Lagus Applied Technology, Inc., San Diego, CA, USA
***WISMUT GmbH, Chemnitz, Germany

QUANTIFICATION OF RADON MIGRATION FROM A URANIUM MINE THROUGH THE SOIL INTO BUILDINGS BY THE USE OF TRACER TECHNIQUES

Willigert Raatschen[1] , Richard A. Grot[2] and Walfried Löbner[3]

[1]Dornier GmbH, Friedrichshafen, Germany
[2]Lagus Applied Technology, San Diego, USA
[3]WISMUT GmbH, Chemnitz, Germany

ABSTRACT:

This paper describes the results of a series of tracer gas tests performed in the mining community of Schlema in eastern Germany. The purpose of these tests was to determine the influence of various mechanisms and subterranean features on the radon levels in the ambient air and in the buildings of the community. Under the former Democratic Republic of Germany (the DDR regime), the mines in and near Schlema and in the ore mountains in Sachsen were an importance source of uranium. These mines have now been closed down and the area is currently under remediation. The remedial measures being applied are varied and consist of, for example: flooding the lower levels of the mine with water, filling the upper tunnels under the community with rock aggregate and blocking their entrances and applying impermeable layers and vegetation over the tilling dump piles near the community. The subterranean complex under the community is extensive due to the many centuries of mining activity. It is currently under depressurization due to the operation of huge mine exhaust fans whose primary function is to provide adequate ventilation air and environmental control for the miners working underground. The mining company WISMUT has undertaken several projects to study the effects of the remediation and the closing down of the mine on the nearby communities.

The project described here is one of these projects which was designed to determine the importance of air currents emulating from the mine complex on the radon levels in the community and to determine the influence of the flooding of the mine and the importance of the depressurization caused by the mine exhaust fans on the radon levels in the community. The purpose of this project was to quantify the component of the radon flux into the buildings from the uranium mine caused by the flow of air currents from the mine both when the mine was depressurized by the operation of the mine exhaust fans and when the mine exhaust fans were shut off.

Tracer gas measurements were carried out in two phases: with the main exhaust fan of the mine turned off and then with the exhaust fans on. By seeding the tunnels of the mine with a tracer gas, SF_6, the transport of air from tunnels in the mine through the soil above and then through the foundation of the buildings into the cellar was determined. Simultaneously the air change rate in the cellar was measured by the use of PDCB (Perfluorodicyclobutane) as a tracer gas to allow a complete mass balance of tracer for the cellar. A simple mass balance using the air flows calculated from the tracer gas measurements and the measured radon concentrations in ambient air and the mine was used to predict the radon level in the building due

to the air flows from the mine into the buildings. These predicted radon levels were compared to measured radon levels in the buildings. Fifteen (15) buildings in different areas of the community were examined. Some buildings exhibited almost immediate classical exponential tracer build-up response curves which indicated a strong communication with the mine tunnel complex. The calculated radon concentrations in the buildings based on the tracer measurements were in good agreement with the measured radon concentrations in the buildings, i.e. the buildings' radon concentration could be well predicted using the air flows from the mine into the buildings and the radon concentrations in the mine tunnels. Additional preliminary measurements of tracer migration from mine complex into radon dumps and more distant subterranean parts of the complex for which there was no direct flow paths indicated that the tracer technique used would be very well suited for also studying underground movement of contaminants including the determination of contaminant egress from radon dump piles in the area.

Introduction

The small mining town Schlema is located in the south of Saxonia, 15 km south-west of Chemnitz and 10 km north of the Czechoslovakian border.

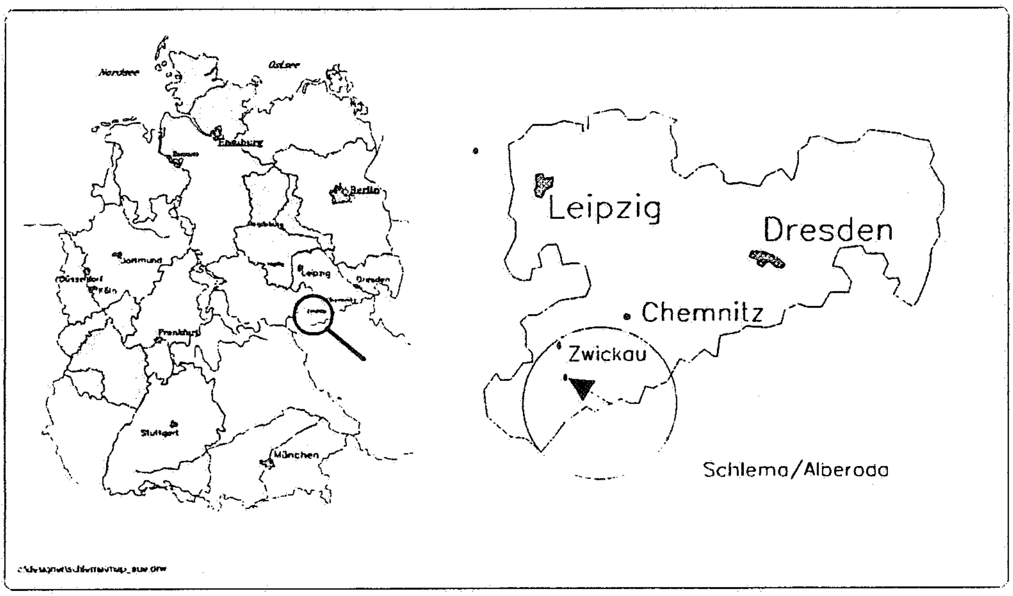

Figure 1. Map of Germany (left) and Saxonia (right) with the location of Schlema/Alberoda

After World War II the Russians started to extract uranium ore from the mines near Schlema. However, the region had been an active mining area for several centuries. The area around Schlema was very well known for the diversity of the ores and minerals found there. The neighboring village of Schneeberg was famous for its silver mines which were first exploited by the region's first silver miners in the 16th century. The silver miners from Schneeberg dug a tunnel, which is called the Markus-Semmler-Stollen (MSS tunnel) from Schneeberg through the Schlema valley. The tunnel ends at the river 'Mulde' in Schlema. The MSS tunnel was built to drain the silver mine in earlier times. It is 15 - 35 m beneath the surface, approximately 1 m wide and 2 m high. The uranium ore beneath the Schlema valley was extensively exploited during the last four decades. The mining activity created a complex of tunnels, cracks, fissures, cave-in areas and unknown flow paths. In the 1970's and 80's the mining activities moved deeper into areas below the Schlema valley, eventually reaching depths of more than 2000 m. Remedial flooding of the lower levels of the mine has filled the lower levels to a depth of about 1000 m below the surface. Since the radon exhalation is still very strong, it was necessary to keep the old mining area in the valley of Schlema depressurized to keep the radon concentration at tolerable levels.

Fig. 2 shows a map of Schlema. The thick line shows the underground mining area, the dashed line marks the MSS tunnel with its entrance at the river 'Mulde'. The main air supply and exhaust shaft of the mine are 3.5 km north east of Schlema. The reasons for elevated radon concentrations in this area are potentially multiple.

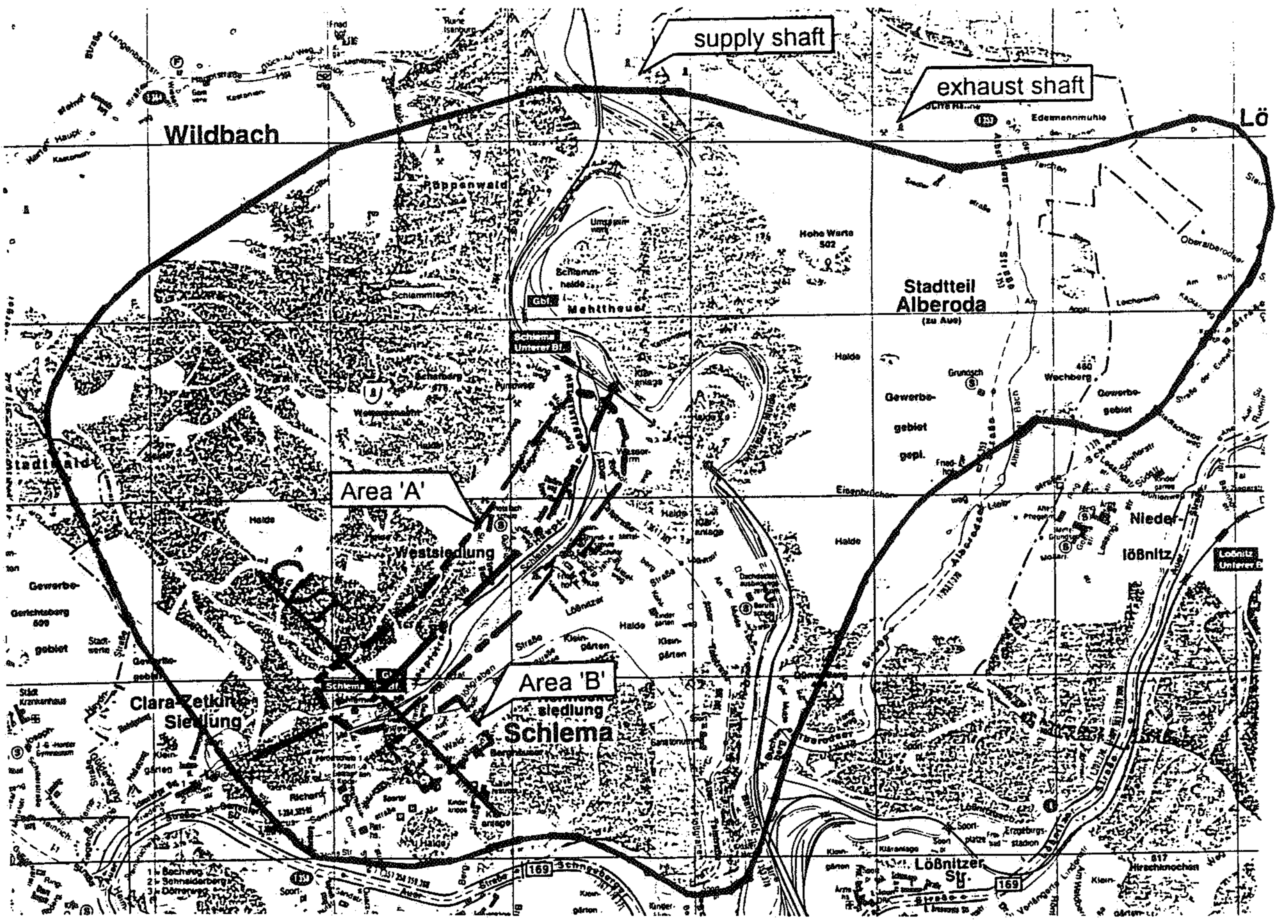

Figure 2. Map of the Schlema valley with the MSS tunnel, Area 'A' and 'B' and main exhaust and supply shafts

Fig. 3 shows the most important potential radon paths. These possible paths include: the traditional near field flow of ambient air into the soil and then into the building due to the natural driving forces which the building causes by depressurization produced to the "stack" and wind effects; the movement of air from the mine directly into the buildings; the movement of air from the mine into the exterior ambient through fissures and cracks in the soil; the exhalation of air from the mine shafts into the ambient; the exhalation of air from the tilling dump piles which could be a combination of air movements caused by wind and thermal variations of the ambient or by air currents from the mine through the dump piles; and also the possible contamination of the valleys near the exhaust fans from the mine.

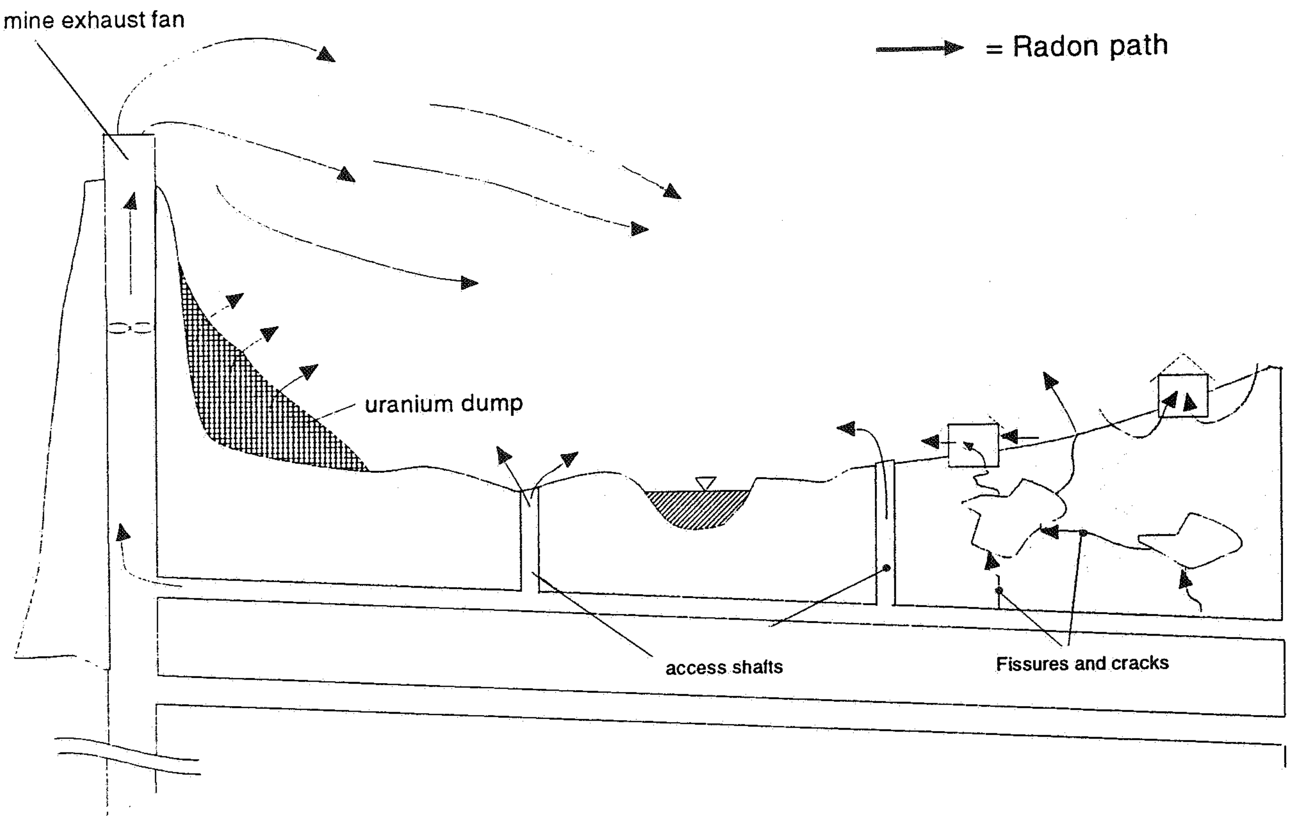

Figure 3. Sketch of the potential radon sources and paths in the Schlema valley

Since the radon levels in the dwellings could be caused by different sources and flow paths and each influence the others in a very complex manner, it is currently not possible

- to quantify the radon emissions through the soil by measuring the radon concentration alone
- to predict the radon exposure to the people due to a change in the mine ventilation.

One way of approach to answer these questions is the use of tracer technology in which separate parts of the subterranean complex are seeded with a tracer gas and the migration of the gas monitored over a period of time.

3. THE EFFECT OF THE VENTILATION OF THE MINE

3.1 Forced ventilation with exhaust fans in operation

Fig. 4 shows a schematic of the main airflow paths and directions of the mine. It can be seen, that the mine exhaust fans draw one part of air through the main supply shaft and the other part through the MSS tunnel and from other diffuse openings and paths to the surface. This depressurizes the underground of the Schlema valley and keeps radon concentrations in the houses low.

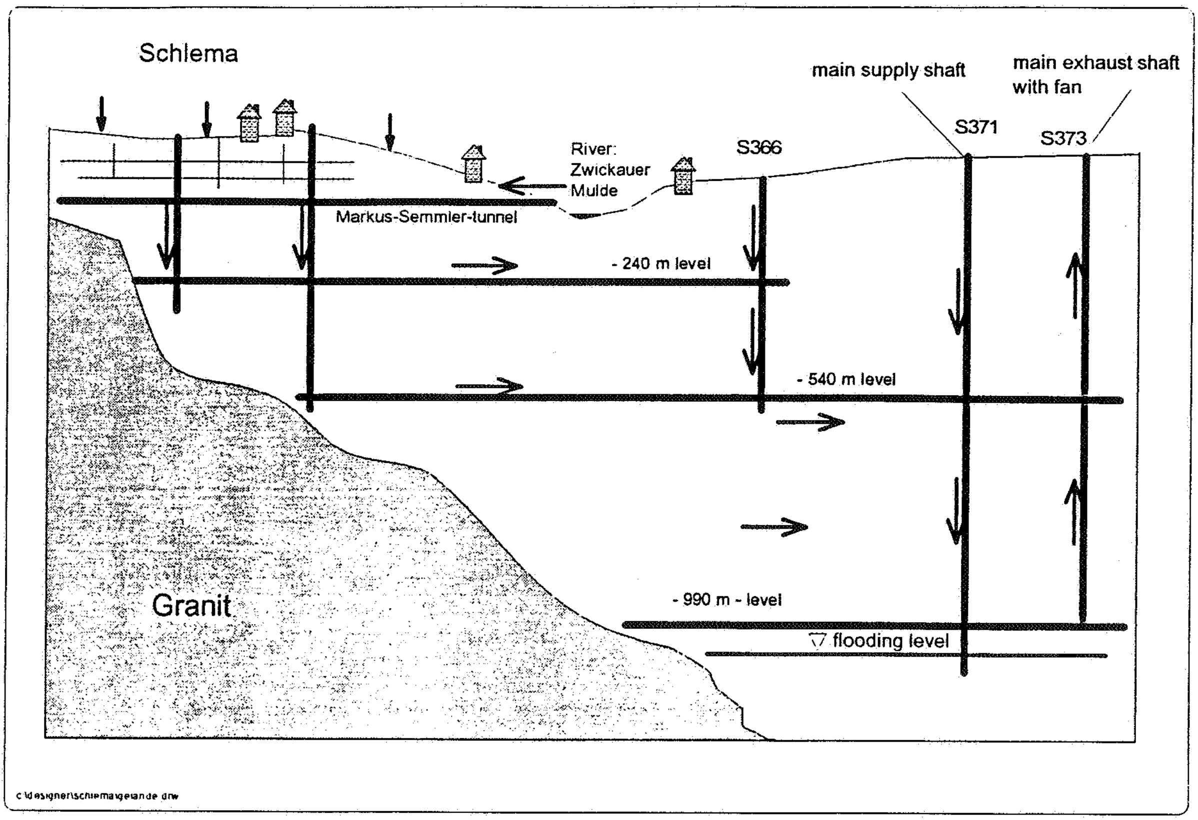

Figure 4. Schematic of airflow paths in the mine with mine fans operating

3.2 Natural mine ventilation with main fan off

The airflow in the mine under natural ventilating conditions are shown in Fig. 5. The airflows from the MSS tunnel into the mine are reversed from those with the exhaust mine fans operating. The area in the Schlema valley is no longer depressurized, i.e. radon concentrations, which can built up in the mine to levels of 450 kBq/m^3, now can flow into MSS tunnel and from there through shafts and other flow paths into the ambient atmosphere and the buildings. Whereas the volume flows in the mine with fans operating could be measured and were fairly well known, there was little knowledge about these flows under natural ventilating conditions. This uncertainty caused a risk in the set-up of the measurement procedure, since there was only one week for the tracer test. During this time, where the fan was off, the whole mine was closed; so it was not possible to enter the mine to adjust the measurement set-up if a mistake was made. Luckly, this did not happen.

4. SELECTION OF BUILDINGS

The buidlings were divided into two groups. The first group of 10 buildings, Area 'A', was located in the Schlema valley, see Fig. 2. There, it was known from previous radon level measurements that a change in the mine ventilating system would have a direct impact on the radon concentration in the houses. All buildings were above or close to the MSS tunnel.

The second group contained 5 buildings, Area 'B', approximately 600 m uphill of the MSS tunnel. There was no known underground connection to the main mine, only one small exploration tunnel of 300 m length, 30 m below the surface. It was expected that the mine ventilation system would only have a minor or no impact on the radon concentration in these houses.

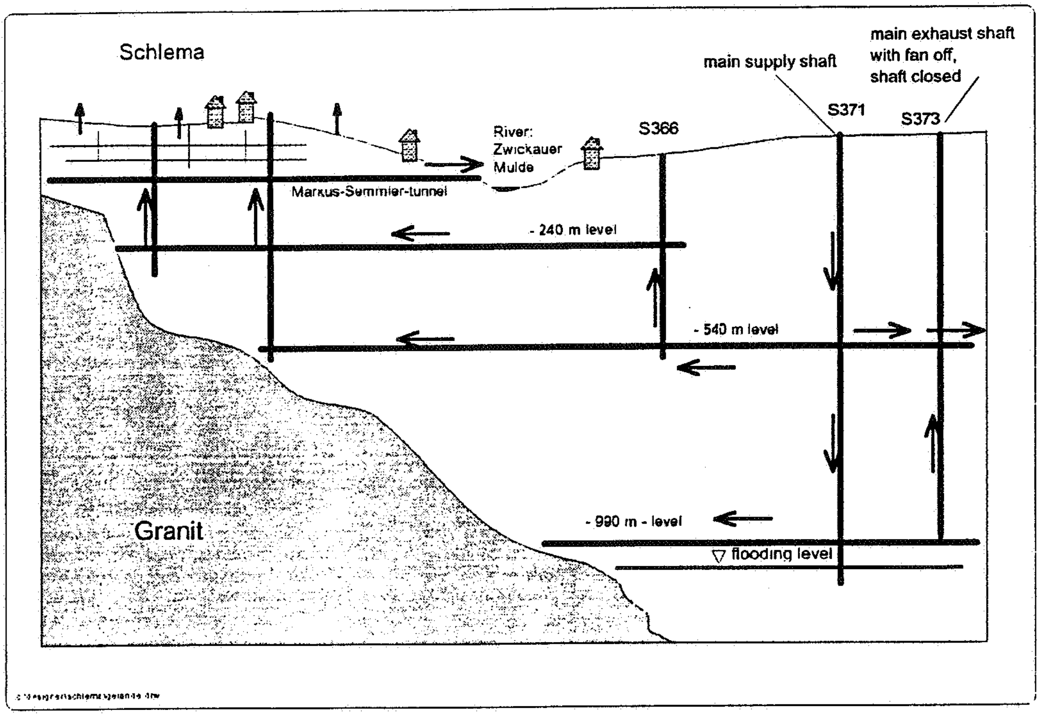

Figure 5. Schematic of airflow paths in the mine with the main fan off

5. TEST PROCEDURE

5.1 Tracer injection into the mine

There were two test phases: phase I under natural ventilating conditions and phase II under normal mechanical ventilation. It was planned to inject a constant rate of SF_6 tracer into the MSS tunnel to achieve an almost constant concentration in the mine. The target concentration was ~ 10 ppm, though it was felt that, given the sensitivity of the tracer monitors, a level of 100 ppb would suffice. The injection flow rate was set at a value considered sufficient to produce 10 ppm due to the lack of precise information on the extent of the underground complex and the porosity and permeability of the soil.

All injection and sampling tubes were installed two weeks before the tests since the mine was closed with the main fan off due to the high radon concentrations. Polyethylene tubing (6 mm inner diameter for sampling and 4 mm i. d. for dosing) was used. Air samples were drawn from various locations in the MSS using dual-head pumps. Syringes were drawn from the pump exhausts for later analyses.

Pure SF_6 was injected via a pressure regulator and a mass flow meter through dosing tubes into the MSS tunnel.

5.2 Sample locations and concentration measurements

From all the buildings, air samples were sequentially drawn at approximately 4 hour intervals and analyzed for the arrival of tracer molecules. Additionally, ambient air samples up wind of each building were also taken using syringes and the syringes were analyzed for SF_6. The radon concentration in the mine, inside the buildings and outside the buildings were measured. To allow a complete mass balance for each building, air exchange rate measurements were

made using the tracer-decay method with a second tracer gas, Perfluorodicyclobutane(PDCB)
.

Fig. 6 visualizes the mass balance of SF_6 for a cellar.

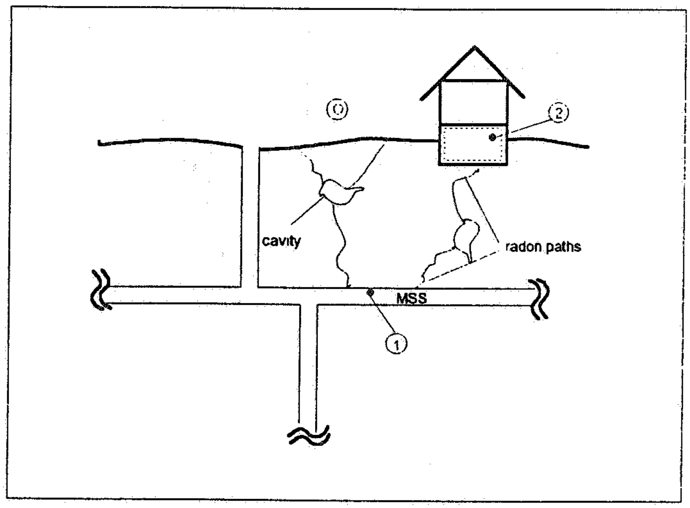

$$Q_{12} = Q_{20} \frac{C_{S,2} - C_{S,0}}{C_{S,1} - C_{S,0}} \quad (1)$$

$$C^*_{Ra,2} = \frac{Q_{12}}{Q_{20}} (C_{Ra,1} - C_{Ra,0}) + C_{Ra,0} \quad (2)$$

Figure 6. Schematic of SF_6 mass balance in a cellar of a building

Q_{12} = volume flow rate of air from the MSS tunnel (zone 1) through the soil into the cellar of a building (zone 2)

Q_{20} = volume flow rate of air from the cellar (zone 2) into the ambient (zone 0)

C_{SO}, C_{S1}, C_{S2} = SF_6 concentration by volume for zones 0, 1 and 2

$C^*_{Ra,2}$ = predicted Radon concentration in the cellar of the house due to airflow from the MSS tunnel.

$C_{Ra,1}$; $C_{Ra,0}$ = measured Radon concentration in the MSS tunnel (zone 1) and in the ambient air outside the house (zone 0)

To calculate the airflow Q_{12} from the MSS tunnel through the soil into the cellar, the exfiltration airflow Q_{20} of each house must be known. Q_{20} was obtained by an air exchange rate measurement (see section 5.4) using the decay of the PDCB tracer.

5.3 Tracer gas equipment

SF_6 and PDCB were detected by gas chromatography with an electron capture detector (GC-ECD). The detection limit, range and accuracy of the equipment used are shown in table 1.

	Tracer Gas	
	SF_6	PDCB
Accuracy	3% of reading	3% of reading
Detection Limit	< 50 ppt	< 50 ppt
Detection Range	0.050-50ppb	0.1-40 ppb

Table 2. Technical Specifications of ECD gas chromatograph AUTOTRAC Used for the Measurements. Samples above the upper detection limit were diluted with a tracer free gas before analysis.

5.4 Air exchange rate measurement

To clearly distinguish between ambient air and soil gas entry into the cellar of the house, a SF_6 mass balance of the cellar volume had to be made. Fig. 7 shows the flow paths of air

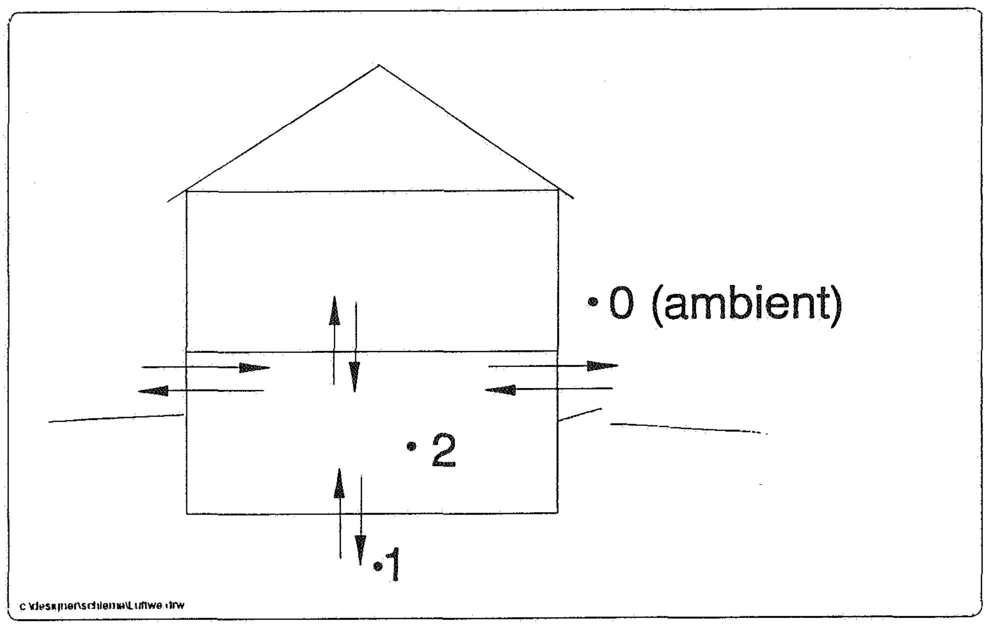

Figure 7. Flow paths into and out of the cellar zone

and SF_6 inside and outside of the cellar. To measure these airflows, the air in the cellar was tagged with PDCB. The decay of the tracer with time after stopping injection is a measure of the air change rate. If the tracer concentration is plotted on a logarithmic scale versus time, the slope of this curve is equivalent to the air change rate, n. For this part of the tests, the tracer monitor AUTOTRAC automatically analyzed the tracer data from each building and calculated the air change rate.using a regression method. The data were also entered into a specially designed spread sheet template which checked the analysis.

A 2 l bottle of 0.2 % PDCB in N_2 was used for injection by releasing the mixture for 5 to 10 minutes injected at a flow rate of 0.2 l/min. The advantage of the small bottle was that one could walk with it through the cellar area slowly injecting the tracer in all parts of the cellar. This improved the mixing process of PDCB with the room air considerably. The initial concentrations were between 100 to 300 ppb. Fifteen (15) minutes after the end of injection, the first air sample was drawn by a 50 ml syringe. The advantage of a syringe is also that you can walk through the cellar rooms while slowly drawing air into the syringe to obtain a local mean concentration. At intervals of approximately 15 minutes, 4 additional air samples were taken. Fig. 8 gives an example of an air change rate tracer decay in building B2.

If the room volume V_R of the cellar is known, the exfiltration rate, n (air change rate) can be obtained from the equation:

$$Q_{20} = n \cdot V_R$$

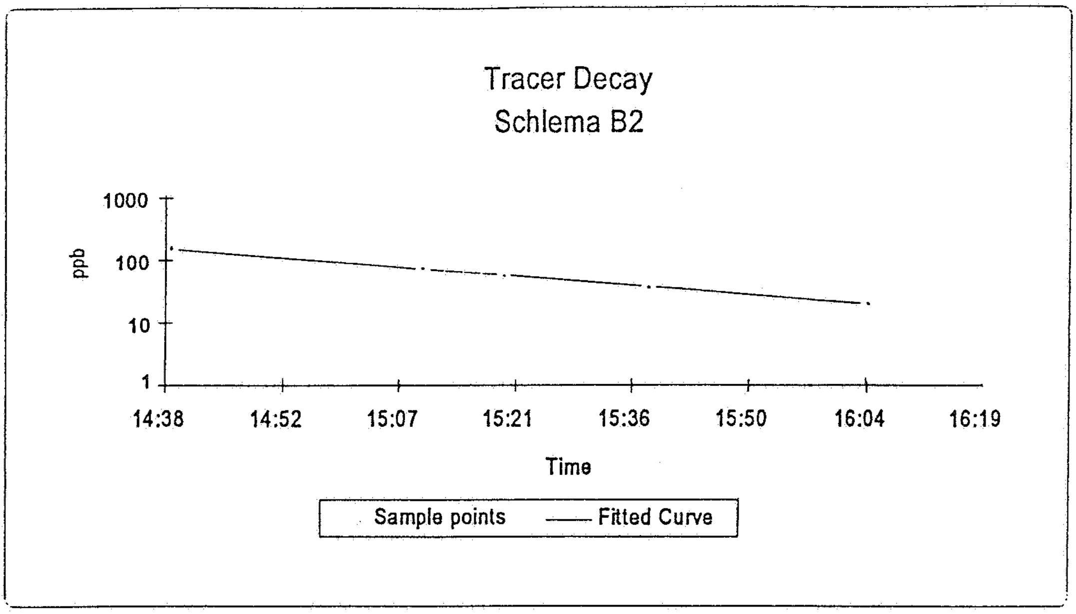

Figure 8. PDCB tracer decay curve used to determine the air change rate in building, B2

6. MEASUREMENT RESULTS OF PHASE I - MINE EXHAUST FAN OFF

6.1 Buildings in the Schlema valley, area A

The tracer test phase I was performed between Christmas and new year 1993. Ambient temperatures varied between -2 to - 12°C at night with weak winds from west parallel to the Schlema valley. A constant tracer gas flow was injected at diverse underground locations to insure an almost constant concentration of SF_6 in the mine. Fig. 9 gives a detailed sketch on the flow in the main tunnels and shafts. UG 113 and UG 91 were 2 x 2 m shafts for the miners to have direct access to the MSS tunnel to do remediation work.

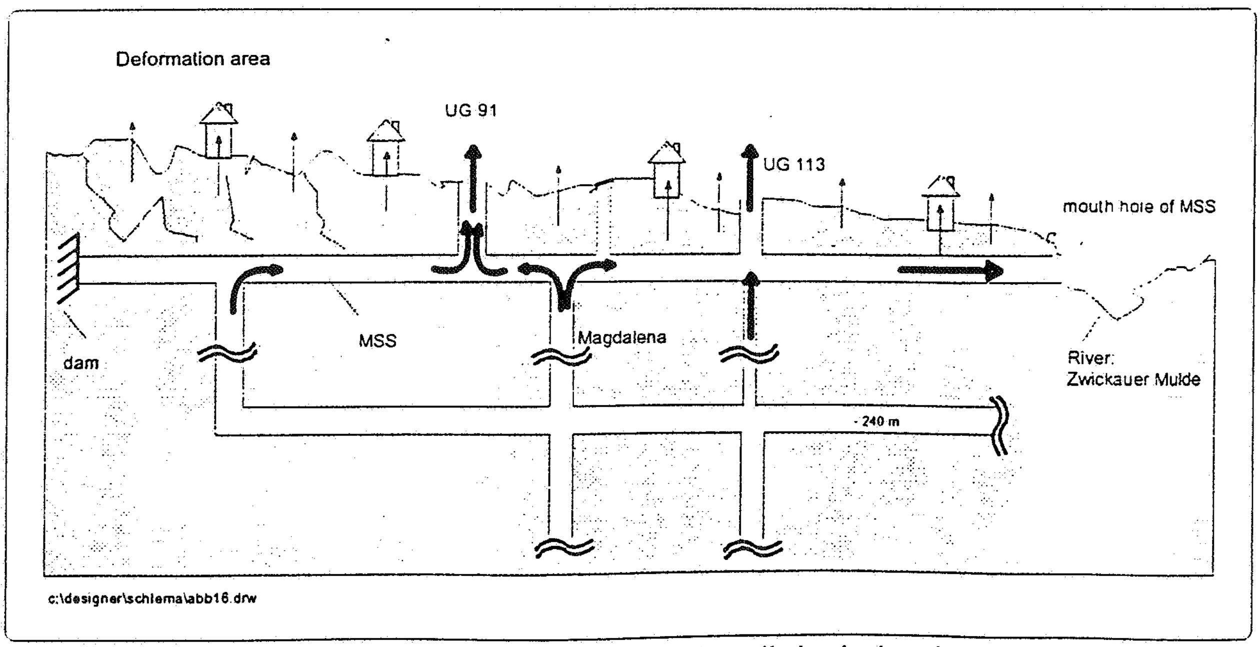

Figure 9. Main flow paths around the MSS under natural ventilation in the mine

Fig. 10 displays the measurement results for building B 2. On Dec. 28 at 14:36 the dosing in the MSS tunnel section below B 2 was started. At 16:45 the equilibrium concentration of ≈ 7 ppm war reached. The first SF_6 molecules in the cellar of B2 were

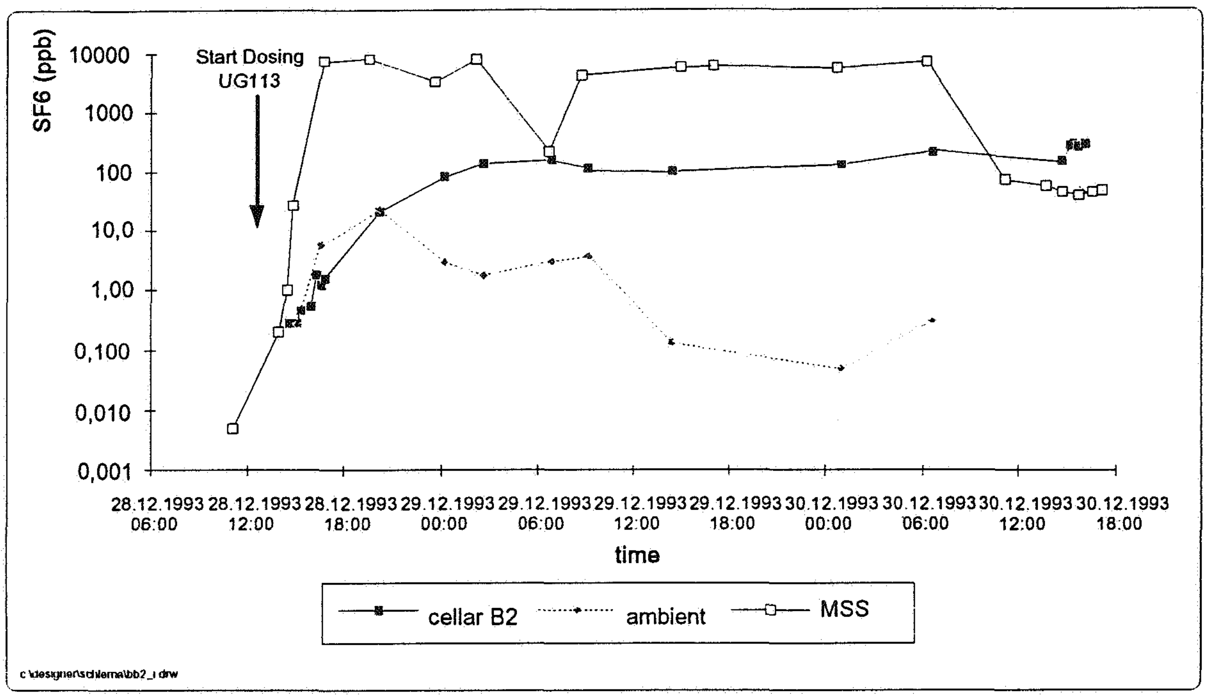

Figure 10. Tracer Response for Building B2.

detected only 45 minutes after dosing start at 15:20 with concentration of 450 ppt. With a direct path length of approximately 15 m through the soil to the building foundation, the data indicate that the mean velocity of the flow from the tunnel to the building was 0.33 m/min.

The air change rate of the building B2 was measured as $n = 1.43h^{-1} \pm 0.04$, see Fig. 8. Applying equation 1, the airflow through the soil into the cellar was calculated to be 11 m^3/h. In building B2 the radon concentration was measured twice, once as a 3 day mean concentration with passive E-Perm samplers and also continuously with Alpha GUARD devices. Fig. 11 shows the measured and predicted radon concentration in B 2 during a time span of 3 hours. Due to random oscillations in the mine it was not possible to keep the underground tracer concentration constant. Therefore data uncertainties were in some cases significant.

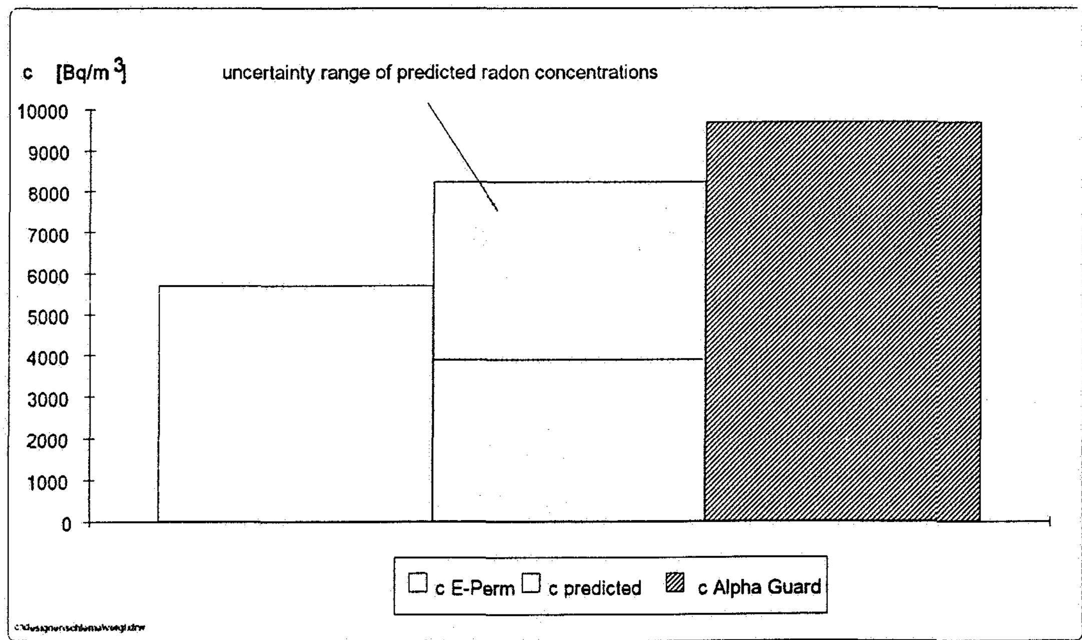

Figure 11. Measured and predicted radon concentrations in building B2

The soil gas flows of six buildings out of ten in the area Schlema valley are summarized in Fig. 12. Fig. 13 shows the measured and predicted radon concentrations according to equation 2. Only in B4 was the agreement between measured and calculated radon concentration poor.

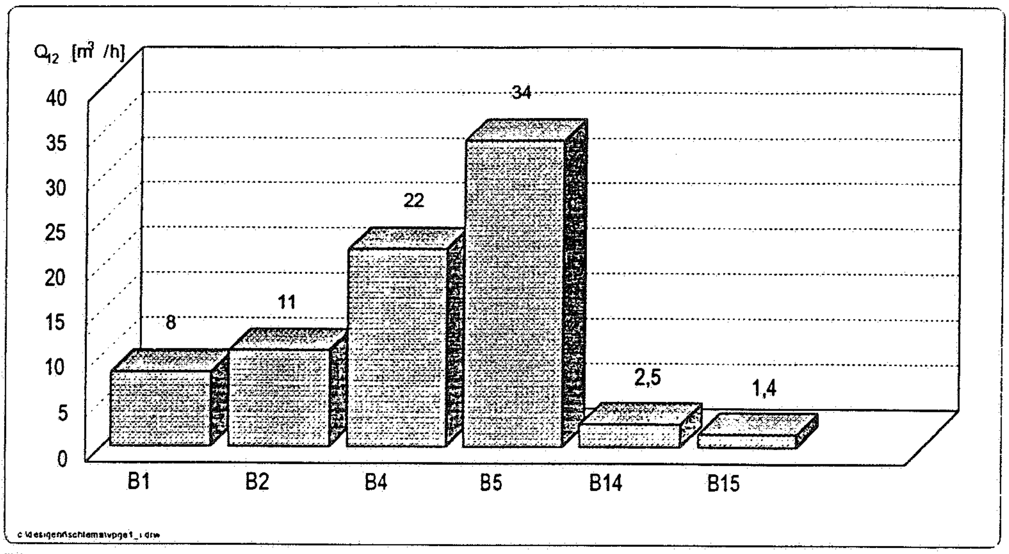

Figure 12. Measured airflows from MSS into buildings of the Schlema valley during measurement phase I, main fan off

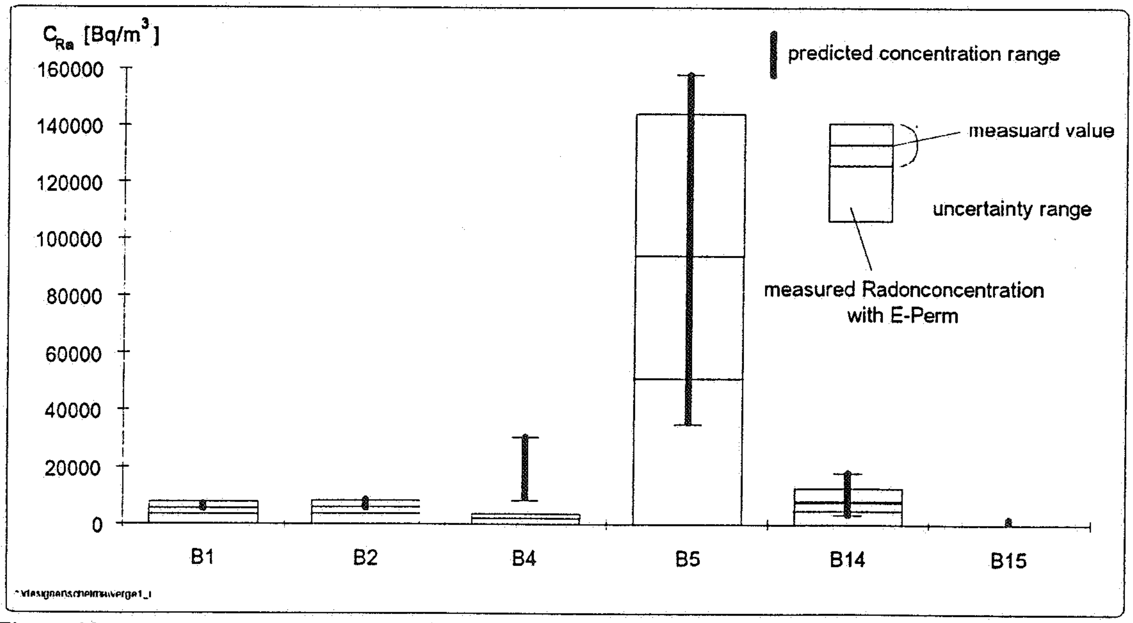

Figure 13. Measured versus predicted radon concentrations in buildings of the Schlema valley during measurement phase I, main fan off

Looking at building B 5, the highest mean radon concentration of 98000 Bq/m³ was measured. Although the uncertainty is high, the predicted mean value is in excellent agreement with the measured value. In this case, the airflow through the soil contributed to 21 % to the infiltrated air in the cellar. The data from this phase indicate that the air flow from the mine into the buildings was the principal mechanism which caused the excessive radon levels in the buildings when the mine exhaust fans were shut down.

6.2 Buildings in area 'B', 60 m uphill from the MSS tunnel.

As mentioned above, there was no direct connection known between the main mine and the small tunnel (LL2-ST3) for reconstruction work below the 5 selected buildings of area 'B'.

Fig. 14 shows a vertical cut through MSS area 'A' and area 'B'.

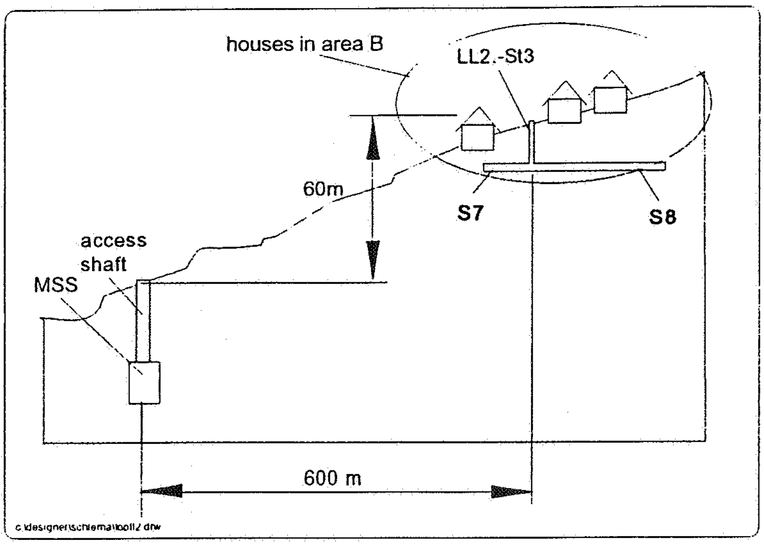

Figure 14. Topography between area 'A' and 'B'

The dosing of SF_6 into LL2-ST3 started one day later than in the MSS tunnel. This was to check if SF_6 tracer molecules arrive in area 'B' from the tracer injection in area 'A'. Fig. 15 clearly indicates that 6 hours after injection start in MSS the first SF_6 molecules arrived in the left part (S 7) of tunnel LL2-ST3.

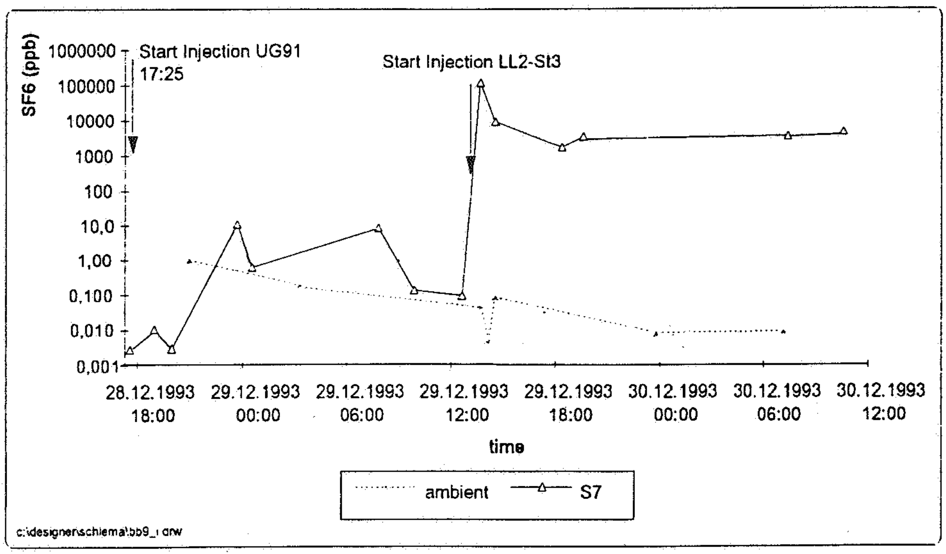

Figure 15. SF_6 arrival from MSS in tunnel LL2-ST3 at sample point S7

It is assumed that there exists an uphill convection flow through fissures, porous soil and cracks to the 60 m higher area 'B'. The very low ambient temperatures ≈ - 10°C enhanced the stack effect and this convection flow.

7. MEASUREMENT RESULTS OF PHASE II - MINE EXHAUST FANS ON

During Jan. 24 - 28, 1994, with the mine exhaust fans with a capacity of 226 m^3/s operating (note: the operation of these fan can require up to 4 megawatts of electrical generating capacity), the second measurement phase was conducted. The ambient temperatures were with + 2 to + 7°C about 10 K higher than during phase I. The wind speed was a little higher, but had the same direction west-east through the Schlema valley.

The results of phase II are summarized in Fig. 16 and 17.

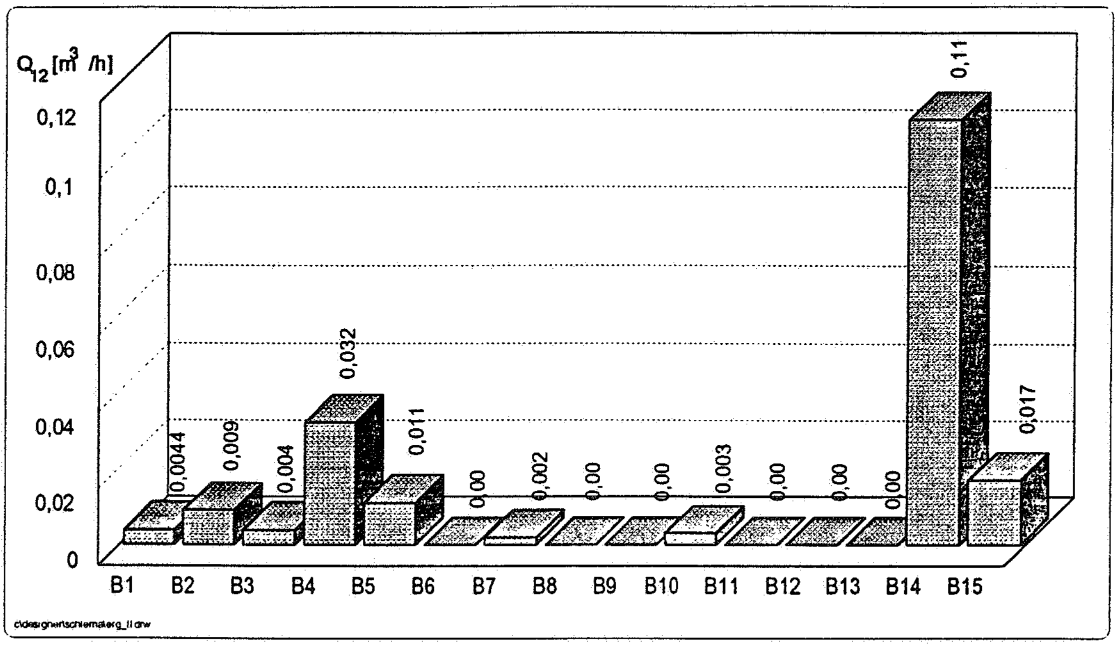

Figure 16. Measured airflows from MSS into buildings of the Schlema valley during measurement phase II, when mine exhaust fans were in operation

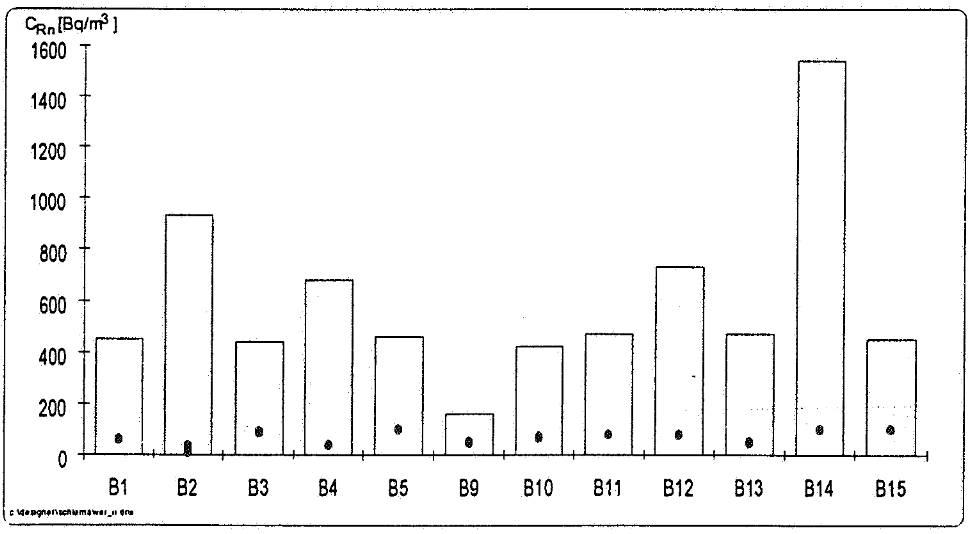

Figure 17. Measured (bars) versus predicted (points) radon concentrations in buildings of the Schlema valley during measurement phase II, when mine exhaust fan was in operation. The bars indicate the predicted concentrations.

If we compare the airflows through the soil of phase I and II, a reduction by a factor of 700 to 3000 had taken place. In Fig. 17 we see that the measured radon concentration is underestimated by concentration predicted by using only the radon transported by air movement from the MSS tunnel. This would indicate that in contrast to the situation with the fan off the airflow from the mine is not the main source of radon in the dwellings when the main mine exhaust fan is operating. Fig. 18 tries to explain the reason for this discrepancy.

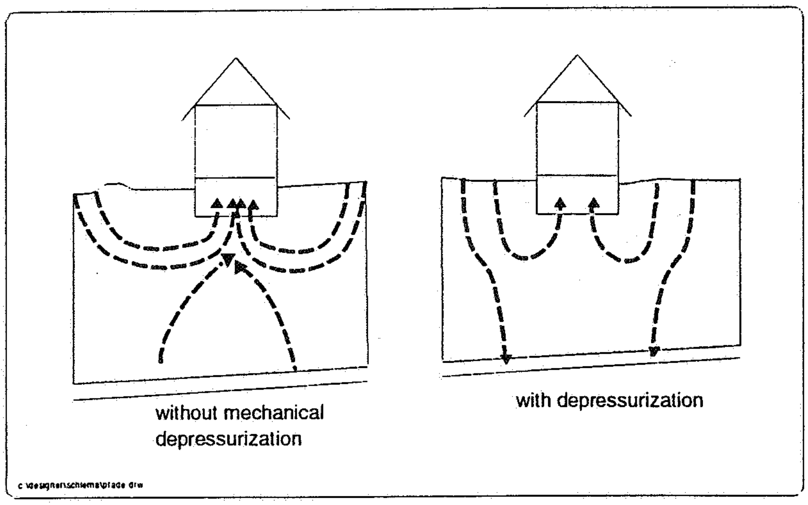

Figure 18. Flow paths of radon and air with and without mechanical ventilation

With no mechanical depressurization of the mine, air with around 450 kBq/m^3 moves from the very deep tunnels in the mine into the MSS tunnel and a small portion of this flow enters the buildings through cracks in the soil. There may be a further enrichment with radon of the air from MSS into the building as the uranium rocks near the surface also emit radon. This effect is not accounted for in the calculation and mass balance in equations 1 & 2. For phase I the results prove that a possible enrichment of the airflow from MSS into the cellar was negligibly small. The typical building induced natural radon path, where ambient air moves into the soil around the building and enters the building due to pressure differences caused by the stack effect of the building, had also a very small impact during phase I. The good agreement of the results supports this assumption.

But with mechanical depressurization, the flow from the MSS tunnel into the buildings was very effectively reduced. What still remains is the natural pathway of air from the surface around the building, into the soil, and then into the cellar. The magnitude of these volume flows may be much smaller - but with a continuous generation rate of radon in the soil, the radon concentration of the soil air is higher and produces still significant high radon concentrations in the buildings.

The depressurization of the mine and the change of the pressure field around the building may also effect the natural pathways of radon in such a way, that air from the surface, which, without depressurization would enter the building, would now be directed into the mine (see Fig. 18). This would cause an even lower radon level in the buildings then if there were a not depressurized mine beneath the buildings.

8. ADDITIONAL SUPPLEMENTARY TEST RESULTS

One day before the phase I tracer test in the mine was conducted, a pulse test into the main supply shaft of the mine was made to

- estimate the air velocity from the supply shaft to MSS
- check if there is an air path between the mine and a uranium dump, which was above the mine.

8.1 Air velocity in the mine

Fig. 5 shows the airflows in the mine under natural ventilating conditions. At Dec. 27, 1993 at 14:20 a 10 l bottle of pure SF_6 was emptied in 5 minutes into the main supply shaft. The shortest way of the SF_6-tagged supply air to reach the MSS tunnel was to go down to the -540 m level, then 3.5 km horizontally, then go up again to the -240 m level and then arrive at MSS. As shown in Fig. 19, at measurement point S6 in the MSS tunnel

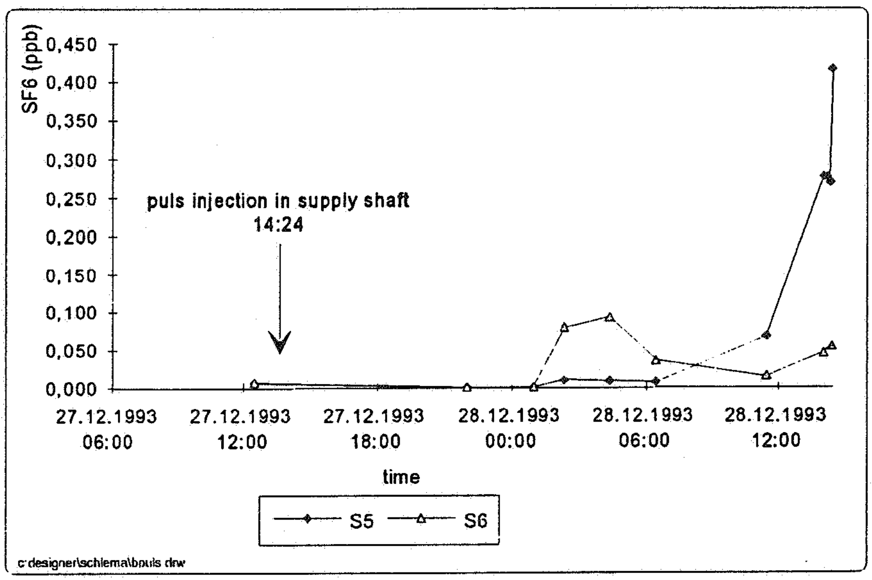

Figure 19. Concentration histories in MSS tunnel after the pulse injection

the arrival of the first SF_6 molecules was on Dec. 28 at 2:20 (12 hours after injection). At sample point S5, the pulse arrived on Dec., 28, at 11:28 (21 hours after injection). With a total flow path length of approximately 4 km, the maximum air velocity was estimated at 2.8 m/min.

8.2 Check of communication between the mine and an uranium dump

Fig. 20 shows a scheme of the mine and an uranium dump on top of it.

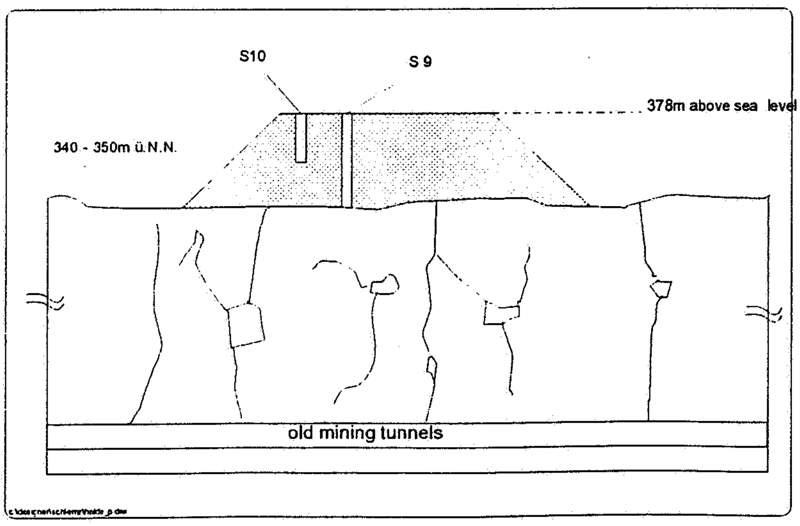

Figure 20. Schematic of mine and uranium dump with air paths

The dump has an oval form with a length of ~ 900 m, a width of 300 m with a top height of ~ 30 m above the ground level. There was one bore hole which passed down to the dump sole (S 9) and the other bore hole which was only 6 m deep (S 10). After the pulse injection, air samples were also taken at these two sampling locations. It should be noted, that the ambient temperature was -12°C at night, very low. This led to a strong stack flow from the bottom of the dump to the top surface. On Dec. 29, at 0:22 the first SF_6 molecules arrived on top of the dump as can be seen in Fig. 21

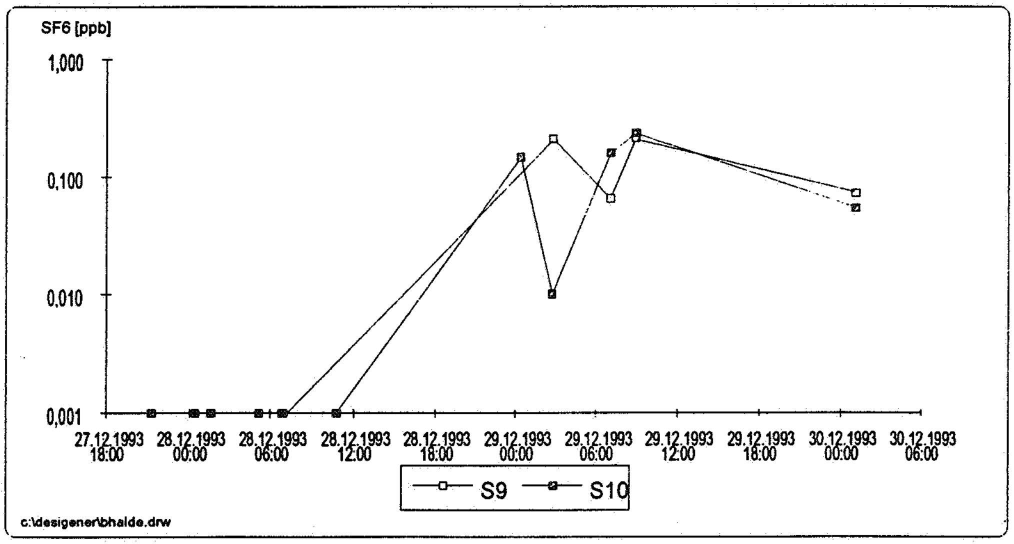

Figure 21. Measured SF_6 concentrations on top of the uranium dump after the pulse test

9. CONCLUSIONS

The tests reported here showed that tracer technology is capable of precisely measuring airflows in mines and through the soil and can be a powerful tool for determining the importance of various mechanism on the radon levels in buildings (and potentially, the movement of other contaminants through the soil). The tests clearly demonstrated the effect of the operation of the mine exhaust fans on the radon levels in the ambient atmosphere and in the dwellings in the community of Schlema located over the mining complex. The tests also showed that air for the mine flows through the soil even if direct tunnel connections do not exist and can cause exhalation of radon, for example, at the top of the tilling dump piles over the mine. The importance of these flows on the ambient radon levels in the valleys near the dumps will require further testing. Essential for these kind of measurements is the choice of a good tracer and sensitive analyzing equipment (ppt level sensitivity). SF_6 proved to be a very good and inexpensive tracer for this purpose. Due to the high sensitivity and automated features of the AUTOTRAC GC-ECD used, it was possible to analyze and process a large number of samples and obtain reliable results even in the ppt range, minimizing the quantity of tracer required.

Implementing the Results of Ventilation Research
16th AIVC Conference, Palm Springs, USA
19-22 September, 1995

The Effect of Ventilation & Pressure Differences on Concentrations of Radon at Workplaces

Pirjo Korhonen, Hekmi Kokotti, Pentti Kalliokoski

Department of Environmental Sciences,
University of Kuopio, Finland

SYNOPSIS

The workplaces located in southern (18 places) and central Finland (8). The total amount of workrooms measured was 87. The mean concentration of radon was 254 Bq/m^3 (range from 12 to 1647 Bq/m^3) during working hours. The calculated radon entry rates varied from 2 to 4780 kBq/h. The measured air exchange rates varied from 0.1 to 13.3 1/h and calculated ventilation flow rates varied from 30 to 55200 m^3/h. Radon concentration was found to depend on the type of foundation, whereas types of ventilation or the ventilation flow rates did not correlate significantly with the concentrations of radon. The highest concentrations of radon were detected when the negative pressure differences were between 1 Pa to 6 Pa.

INTRODUCTION

Radon is a radioactive gas, which enters a building mainly from soil below the building. Radon could also be exhalated from tap water or building materials; however, those are generally only minor sources in Finland. /1,2/. In addition, indoor concentration of radon depends on meteorological factors, subgrade structures, air exchange rate, and pressure conditions /3/.

The negative pressure indoors tends to increase the intake of radon from soil through walls or floors. Kokotti et al. /4/ have found that pressure difference is the most important single factor of influencing radon entry rate. Hintenlang et al. /5/ have, however, found that the dependency of pressure difference is a complicated one having a maximum at the low negative pressure region. Balanced ventilation, when it operated at full effectiveness, has been found to decrease concentrations of radon in underground and partly underground workplaces in southern Finland /6/. Radon is a serious problem in the Finnish buildings. Radon levels exceeding 400 Bq/m^3 are commonly detected in homes, especially in the southern part of the country, with many areas of weathered granite and eskers /7/. In this area, as many as 30 % of the workplaces investigated by the Finnish Centre for Radiation and Nuclear Safety (STUK) had radon levels above 300

Bq/m^3. Finnish occupational exposure limit for radon is 400 Bq/m^3, which corresponds to effective equivalent dose of 2.5 mSv. The level of 300 Bq/m^3 is used as an action limit requiring more detailed investigations /8/.

The aim of this study was to investigate how concentrations of radon and radon entry rates depend on different type of ventilation and pressure difference at workplaces locating underground or partly underground.

MATERIAL AND METHODS

Measured workplaces

The workplaces in this study were located in southern (18 places) and in middle Finland (8 places). They included different kinds of offices and servicing rooms in schools, office buildings, telecommunication centers and rooms of the military forces. The total number of workers using the rooms was about 250. The volumes of the spaces studied varied from small office rooms of 20 m^3 to large research laboratories of 17 200 m^3.

Measurement techniques

Data concerning volumes, foundation, depth, working hours, number of employees and types and operation times of ventilation were collected by questionnaire. Radon levels were analyzed continuously near the workers' breathing zone by using the Lucas cell method /9/ with a Pylon AB-5 assembly, which includes a detector, a photomultiplier and a system of data collection based on a microprocessor. The output data of the Pylon detector were processed with SP-55 software run on a PC. The flow rate of the pump was 0.4 l/min. The interval of continuous measurements was 30 minutes (averaged to one hour). Concentrations were measured during periods ranging from two hours to several days. The integrated long-term radon levels were determined by alpha track etch films and analyzed by STUK /10/. Alpha films revealed the average radon level during one month, with integrated concentration of radon also determined at night and weekends, when the ventilation was not used at full capacity. The pressure differences across the wall, either separating or external, were monitored by an electronic manometer together with a datataker. The pressure differences were averaged from three-minute to one-hour intervals in the same way as the periods of radon levels were measured. During daytime working hours, air exchange rates were measured by the tracer gas technique and by the dilution method using difluorodichloromethane and nitrous oxide as the tracer gases and an infrared spectrophotometer, Miran 1A, as the analyzer. Ventilation flow rates were calculated by multiplying air exchange rates by volume of the workroom. The radon entry rates were calculated by multiplying the concentration of indoor radon by the measured air exchange rate and by the volume of the workroom.

RESULTS

The arithmetic mean concentration of radon during working hours was 254 Bq/m^3, and the range was from 12 to 1647 Bq/m^3. In 15 workrooms measured (17 % of the all workrooms), the concentrations of radon exeeded 400 Bq/m^3. All the violations of the exposure limit were found in the high risk area in southern Finland, where the violation percentage was 22 %. The mean concentrations measured during working hours were approximately on the same level than the local average concentrations detected earlier inhomes by Arvela et al. 1994 /7/ (table 1).

	Central Finland	Southern Finland
Homes	< 100	> 300
Workplaces		
* during working hours	90	300
* alpha film	140	550

Table 1. Measured radon levels (Bq/m^3) at workplaces (in this study) and corresponding levels at home (Arvela et al. 1994 /7/) in southern and in central Finland.

The radon levels integrated with alpha etch track film were higher than the levels measured during working hours. These integrated levels included nights and weekends, when the ventilation systems were usually operated at a lower capacity or not at all.

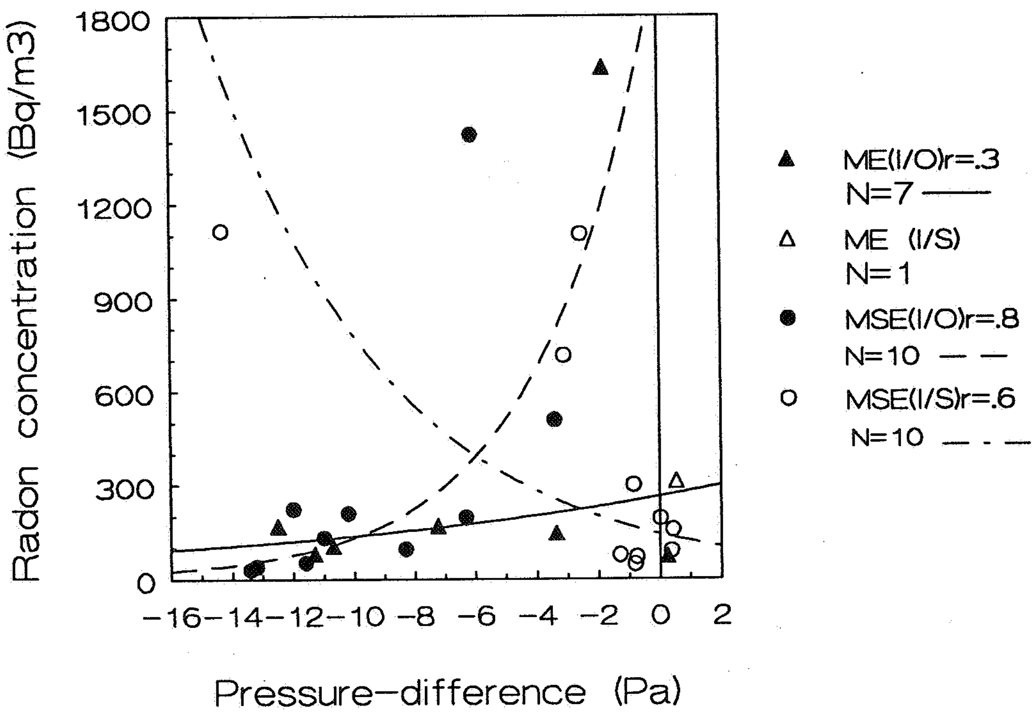

Figure 1. The radon levels (Bq/m^3) with the pressure differences (Pa) during working hours.

Pressure differences were measured either across an outdoor wall (I/O) or across a separating wall (I/S). There were 28 workrooms where pressure differences could be measured. When negative pressure differences were between 1 Pa and 6 Pa, exceptionally high radon levels (figure 1) were detected in four places ventilated with mechanical supply and exhaust and in one place ventilated with mechanical exhaust. The concentrations of radon seemed to increase exponentially (r=0.8) when the pressure difference (I/O) approached zero in spaces ventilated with mechanical supply and exhaust. On the other hand, when the pressure differences were measured across the separating wall (I/S) the concentrations of radon were found to decrease when the pressure differences approached zero (r=0.6). Radon entry rates followed the same pattern as concentrations of radon in the rooms with mechanical supply and exhaust ventilation.

The negative pressure below ten Pascals also seemed to induce high radon entry rates (figure 2). Generally, negative pressure in rooms having mechanical exhaust ventilation seemed not to effect significantly radon levels or entry rates (figure 1 and 2). The ventilation flow rates varied from 30 m^3/h to 55200 m^3/h (arithmetic mean of 1970 m^3/h). Ventilation flow rates in workrooms with the ventilation of mechanical exhaust and with the ventilation of mechanical supply and exhaust decreased exponentially with negative pressure approaching zero (figure 3). The radon entry rates varied from 2 kBq/h to 4780 kBq/h and the arithmetic mean was 480 kBq/h. The radon entry rates and the concentrations of radon did not have significant linear correlation (r=0.42) (figure 4).

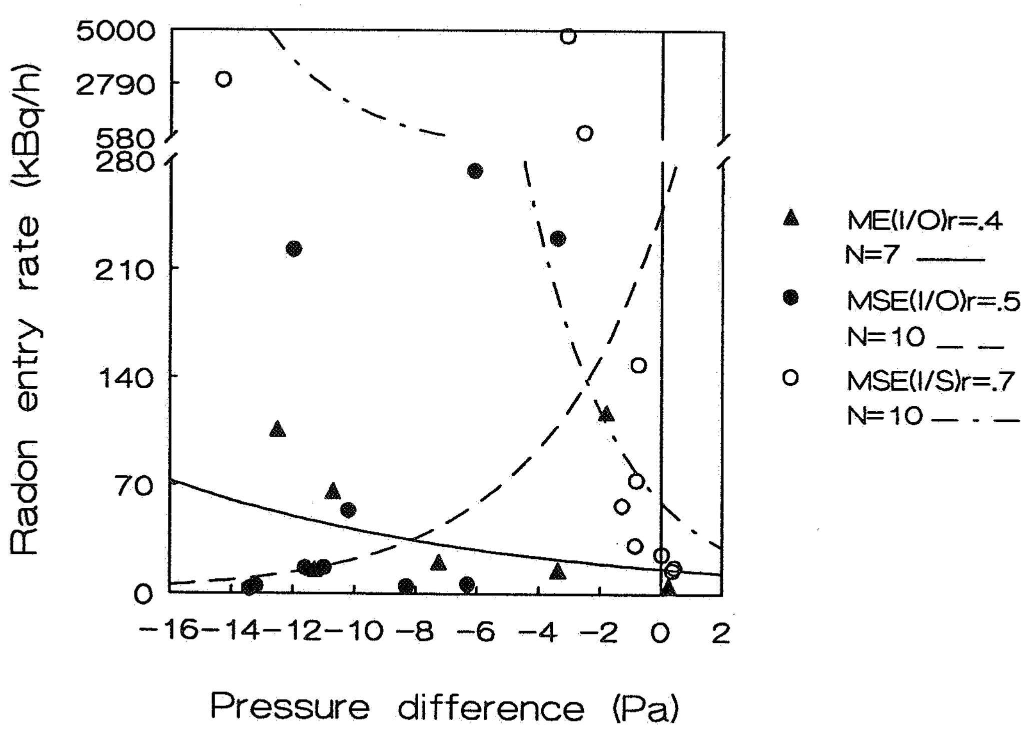

Figure 2. The radon entry rates (kBq/h) with the pressure differences (Pa) during working hours.

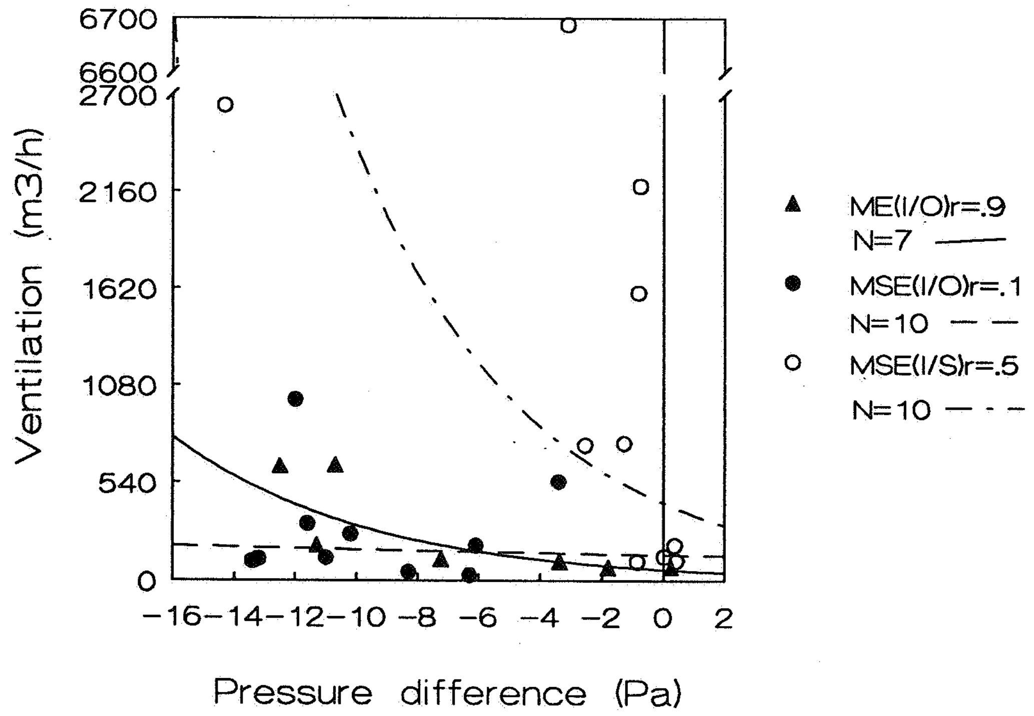

Figure 3. The ventilation flow rates (m^3/h) with the pressure differences (Pa) during working hours.

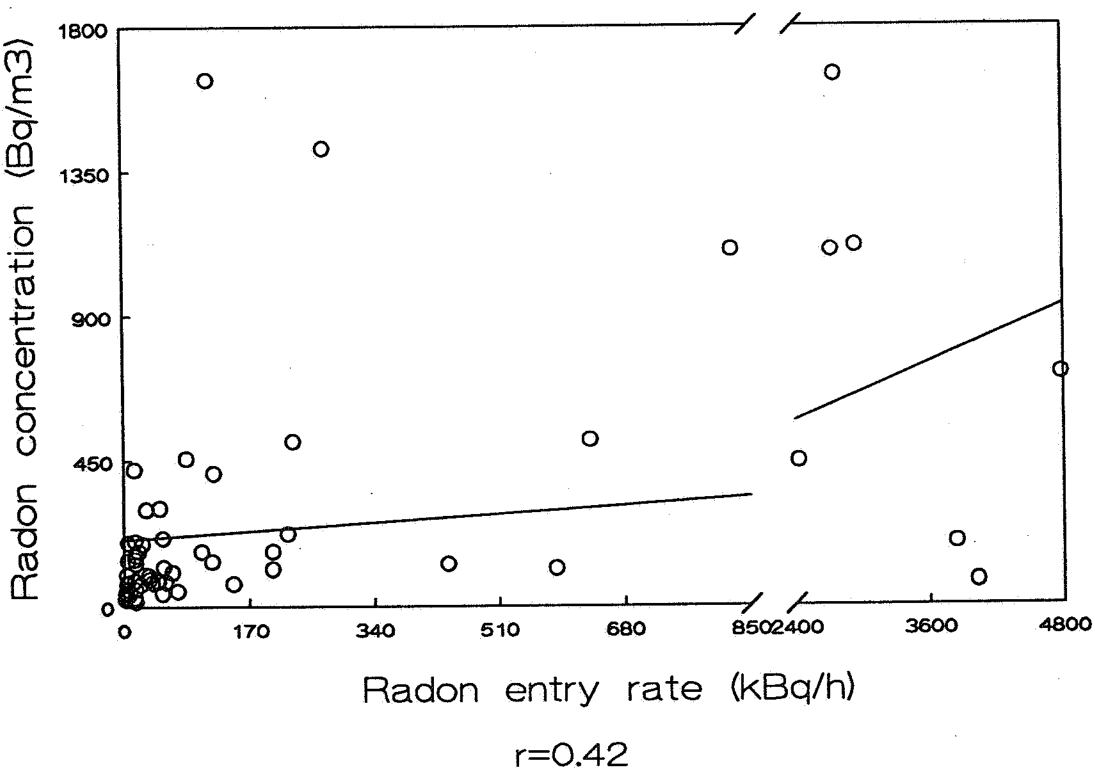

Figure 4. The radon levels (Bq/m^3) with the radon entry rates (kBq/h) during working hours.

Statistical test (Kruskal-Wallis) revealed quite significant correlation with the concentrations of radon and the type of foundations (p=0.06), but no correlation between type or flow rate of ventilation, when the whole data were considered.

CONCLUSIONS

Radon levels varied a lot due to differencies between the buildings, the ventilation systems, the foundations and the locations of places. In a high risk area, southern Finland, the radon levels at work were observed to be clearly higher than in central Finland and to be approximately at the same level as detected earlier by Arvela et al. 1994 /7/ in homes in the same area. Negative pressure differences (ranging from 1 Pa to 6 Pa) seemed to rise exponentially the radon levels and the radon entry rates in spaces ventilated with mechanical supply and exhaust. The low pressure differences (below 10 Pa) were also found to increase radon entry rates. The negative pressure (measured across the separating wall) decreased exponentially when the ventilation flow rate was decrease in rooms with mechanical ventilation.

REFERENCES

1. ASIKAINEN, M and KAHLOS, H.
"Natural Radioactivity of Drinking Water in Finland"
Health Physics, Vol 39, 1980, pp 77-83.

2. MUSTONEN, R.
"Natural Radioactivity in and Radon Exhalation from Finnish Building Materials"
Health Physics, Vol 46, No 6, 1984, pp 1195-1203.

3. SHERMAN, M.
"Superposition in Infiltration Modeling"
Indoor Air, 2, 1992, pp 101-114.

4. KOKOTTI H., KALLIOKOSKI P. and JANTUNEN M.
"Dependency of Radon Entry on Pressure Difference.
Atmospheric Environment, 1992, 26A,12, pp 2247-2250.
5. HINTENLANG D.E. and AL-AHMADY K.K.
"Pressure Differentials for Radon Entry Coupled to Periodic Atmospheric Pressure Variations.
Indoor Air, 1992, 2, pp 208-215.
6. KOKOTTI H., KORHONEN P., KESKIKURU T. and KALLIOKOSKI P.
"Effect of ventilation on radon levels in underground workplaces"
Occupational Hygiene, 1995, 1, pp 305-315.
7. ARVELA, H. and CASTRÉN O.
"The need and expences of radon mitigation at single-family house in Finland" (Pientalojen radonkorjauksen tarve ja kustannukset Suomessa), The Report of Indoor Air Seminar (Sisäilmastoseminaari), Helsinki, Finland, 14.2.1994. Seppänen O., Tuomela P. (edit), 1994. 2, pp 123-128. (In Finnish).
8. ANNANMÄKI, M., OKSANEN, E. and MARKKANEN, M.
"Radon at workplaces - control and preliminaty summary" (Radon työpaikoilla - valvonta ja alustava yhteenveto tuloksista), The Report of Indoor Air Seminar (Sisäilmastoseminaari), Helsinki, Finland, 14.2.1994. Seppänen O., Tuomela P. (edit), 1994; 2:129-134. (In Finnish).
9. LUCAS, H.
"Improved Low Level Alpha Scintillation Counter for Radon"
Rev. Sci. Instr, 1957; 28, pp 680-683.
10. MÄKELAINEN, I.
"Experiences with Track Etch Detectors for Radon Measurements"
Nuclear Tracks, 1986; 12:717-720.

Implementing the Results of Ventilation Research
16th AIVC Conference, Palm Springs, USA
19-22 September, 1995

Ventilation Effectiveness Measurements in Selected New Zealand Office Buildings

M R Bassett*, N Isaacs**

*Building Research Association of New Zealand
**Centre for Building Performance Research, Victoria University of Wellington

1. Synopsis

Office workers continue to complain about air quality problems, and a significant industry has developed to measure pollutants and environmental conditions such as temperatures and humidity. The effectiveness of the ventilation system is often ignored because it is a difficult measurement to carry out and interpret. The results contained in this paper make a start towards understanding the performance of mechanical ventilation in New Zealand office buildings.

A common ventilation approach in New Zealand office buildings involves supplying non-recirculated fresh air to the vicinity of unit air handlers in the plenum. This fresh air is mixed with exhaust air, and directed through ceiling registers to work stations below. Exhaust air returns through ceiling grills directly into the plenum and thence eventually to an in-plenum extract. In these cases some fresh air may be lost directly to the exhaust and the air change effectiveness of the system may fall short of the dilution ventilation description.

In this project the local mean age of the air was determined at a matrix of locations in four buildings in both open plan and partitioned working areas and in the plenums. Measurements were made using a pulse tracer approach with sulphur hexafluoride (SF_6) and a gas chromatograph with an electron capture detector.

The importance of planning the ventilation system around the floor layout has been illustrated by local mean age-of-air results. Air change effective results have shown that within a diverse range of air handling systems, most can be described by the dilution ventilation model.

2. Experimental approach

The tracer gas-detection system used in this study consists of a gas chromatograph (GC) and electron-capture detector with a tracer delivery and sampling system automated to step through a sequence of up to eight independent LMA (local mean age-of-air) measurements [1]. In the buildings examined in this study, dosing the fresh air inlet with tracer gas was achieved with a system that released discrete shots of tracer into the fresh air supply. The time taken to dose the inlet was typically 5 seconds and the volume of pure SF_6 delivered in each shot was $50cm^3$.

For LMA measurements it is important that the calibration of the detection equipment is well established. For this electron-capture detector and peak-area integration software, it is known that the calibration depends on the carrier gas pressure but that the response is linear over the normal working range of 1 to 100ppb [1]. Certified reference tracer gases at 5 and 20 ppb were used to fit a linear relationship between the integrated output from the gas chromatograph and tracer concentration. This calibration process was carried out each time the equipment was moved.

The parameters measured in this study were the LMA and the air change effectiveness. The local mean age-of-air was determined by the pulse method with integration of local tracer concentrations and extrapolation to infinite time by fitting an exponential decay equation to the tail of the data [2]. The LMA was calculated from equation 1 as follows:

$$\bar{\tau}_p = \frac{\int_0^{t'} t\, C_p(t)\,dt + \frac{C_0}{n} e^{-nt'}\left[t' + \frac{1}{n}\right]}{\int_0^{t'} C_p(t)\,dt + \frac{C_0}{n} e^{-nt'}} \qquad (1)$$

Where $C_p(t)$ = The concentration of tracer gas at point p at time t (ppb).
$\bar{\tau}_p$ = The local mean age-of-air in units of t (hours).
n = The exponent in a fitted exponential decay curve.
C_0 = A constant in the fitted exponential equation (ppb).
t' = The time at which measurements terminated (hours).

A similar procedure can be used to compensate for data taking over a finite time when the room mean age-of-air is determined from tracer concentrations measured in the exhaust duct. This is described in more detail in [2] where it was concluded that truncation errors could be as high as 30%. Compensation for finite data taking times in local mean age-of-air measurements, in contrast, were mostly in the range 2% to 7% for measurement times between 2 and 4 hours.

3. Building and mechanical system descriptions

The ventilation performance measurements described here were carried out in four buildings (labelled A to D) located in the central business district of Wellington New Zealand. Buildings A and B are the same as A and B in an earlier paper [2] and buildings C and D provide new data. All were office buildings with varying degrees of internal partitioning ranging from open plan to individual offices.

Building A was originally designed and constructed in 1967 as the city base for a national airline. It consists of office spaces (the top floor) and freight handling areas (middle floor). The air handling systems for each floor are independent but in practice there was found to be some interaction between zones because the fresh air and exhaust air flow rates are not balanced.

Building B is a 7-floor office building constructed in the early 80's. Each floor is supplied with fresh air from a central duct and exhaust air is removed from the plenum area into a central extract shaft. Fresh air is delivered into the breathing zones by plenum-mounted fan coil units which are cooled by a central chilled water plant. Each unit recirculates a proportion of exhaust air from the plenum area but there is no significant mixing of air between floors. Floor 3 is mostly open plan but with about one third of the floor area partitioned into offices. Floor 2 is mostly open plan but does contain one small office.

Building C was built in the early 80's but with significant expansion in the late 80's. It provides 7 floors of open plan office space with fresh air supplied to each floor. In common with building B, fresh air is delivered to the vicinity of plenum-mounted fan coil units which deliver air to the breathing zones below. There is a single exhaust point in the plenum as in building B, but in this case it serves a floor plan which is three times larger.

Building D was built in the commercial building boom of the mid 80's and therefore contains the most recently specified air handling system in the four buildings. In common with buildings B and C, fresh air is supplied to each floor and distributed to the breathing zones by plenum-mounted unit air handlers. The main differences in this buildings are the high level of internal partitioning and the reliance on exfiltration through the envelope and services shafts for exhaust losses.

The important floor plan and air handling system details are presented in Table 1.

Building A Top Floor	
Floor area (effective test space) 1,526 m^2	**Volume** (including plenum) 4,731 m^3
Air handling - Two roof air handlers delivering heated fresh air, return air ducted through the plenum.	
Fresh air delivery - Not able to be measured	**Exhaust air removal** - Not able to be measured
Building A Middle Floor	
Floor area (effective test space) 521 m^2	**Volume** (including plenum) 2,553 m^3
Air handling - Internal air handler with exposed duct running centrally at ceiling level. Internal extract from exposed duct following the external wall at ceiling level.	
Fresh air delivery - 1,826 m^3/h	**Exhaust air removal** - 3,219 m^3/h
Building B Second Floor	
Floor area (effective test space) 454 m^2	**Volume** (including plenum) 1,438 m^3
Air handling - Fresh air ducted to local heat pump air conditioners in the plenum area. Exhaust carried from plenum area into an extract shaft exhausting at roof top.	
Fresh air delivery - 1,750 m^3/h	**Exhaust air removal** - Not able to be measured
Building B Third Floor	
Floor area (effective test space) 469 m^2	**Volume** (including plenum) 1,486 m^3
Air handling - Fresh air ducted to local heat pump air conditioners in the plenum area. Exhaust carried from plenum area into an extract shaft exhausting at roof top.	
Fresh air delivery - 1,573 m^3/h	**Exhaust air removal** - Not able to be measured
Building C Fifth Floor	
Floor area (effective test space) 1,476 m^2	**Volume** (including plenum) 4,723 m^3
Air handling - Fresh air ducted to local heat pump air conditioners in the plenum area. Exhaust carried from a central point in the plenum into an extract shaft exhausting at roof top.	
Fresh air delivery - 3,563 m^3/h	**Exhaust air removal** - 2,600 m^3/h
Building C Sixth Floor	
Floor area (effective test space) 1,476 m^2	**Volume** (including plenum) 4,723 m^3
Air handling - Fresh air ducted to local heat pump air conditioners in the plenum area. Exhaust carried from a central point in the plenum into an extract shaft exhausting at roof top.	
Fresh air delivery - 4,183 m^3/h	**Exhaust air removal** - 2,540 m^3/h
Building D Seventh Floor	
Floor area (effective test space) 499 m^2	**Volume** (including plenum) 1,536 m^3
Air handling - Fresh air ducted to local heat pump air conditioners in the plenum area. No exhaust ducted from the floor. Exhaust by exfiltration through envelope.	
Fresh air delivery - 1,092 m^3/h	**Exhaust air removal** - No mechanical extract

Table 1: Building descriptions and air handling system capacities.

Fresh air delivery to occupied spaces

The approach to ventilating buildings B, C and D is common in New Zealand. It involves supplying fresh air to the vicinity of unit air handlers in the plenum which filter and condition the air as it is delivered to the breathing zones below. The extent to which this fresh air mixes with exhaust air in the plenum, and the extent to which fresh air is lost directly to exhaust, are the two main questions asked of this project. Within the buildings in this study there are significant differences in the approaches to ducting fresh air to the unit air handlers. Three approaches are illustrated in Figures 1,2 and 3. The approaches illustrated in these figures were considered by the design engineers to allow recirculated air from the plenum to be entrained and conditioned along with fresh air from the connected duct.

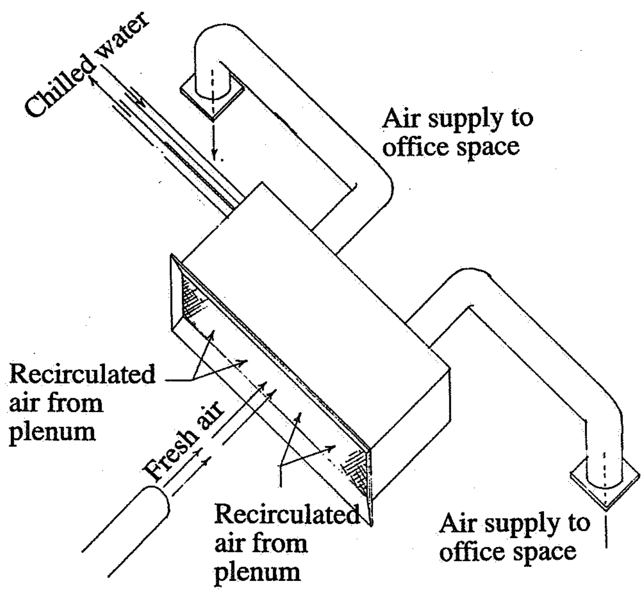

Figure 1: Air discharged in the general direction of the unit air handlers in buildings C and D, permitting recirculation of exhaust air from the plenum. In building D the distance between the closest fresh air delivery point and the unit air handler ranged between 0.5 and 10 meters.

On level 3 of building B there is a further development of the fresh air supply to unit air handler connection, as shown in Figure 2. In building B the fresh air was originally only released from the central air supply duct directly into the plenum. After an indoor air quality survey the approach shown in Figure 3 was adopted. This variation was also found on floor 5 of building C.

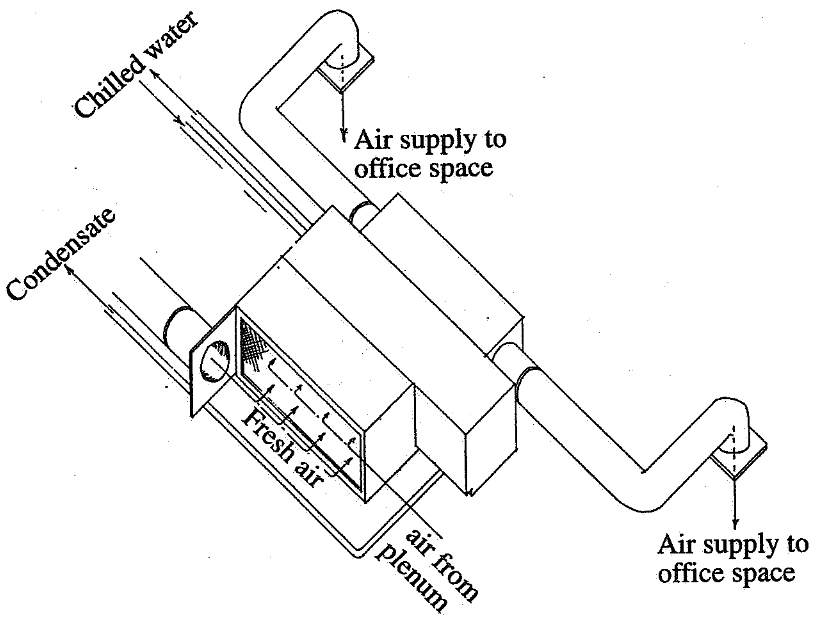

Figure 2: Direct ducting of fresh air to the face of the air handlers in building B.

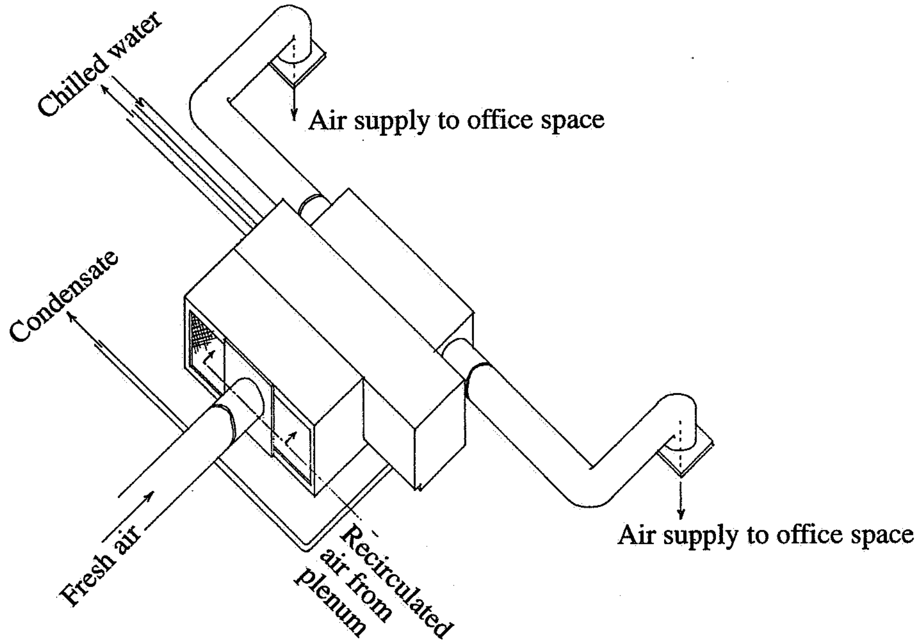

Figure 3: Direct ducting of fresh air to the air entry point of unit air handlers on floor 2 of building C.

4. Effectiveness of air distribution

The local mean age-of-air 1.5 m above floor level (in hours) has been measured and marked out on floor plans for all four buildings. Detailed data for buildings A and B can be found in [2] and local mean age data for buildings C and D are presented here in Figures 4, 5 and 6. A measure of the repeatability of these results has been determined from measurements carried out in five locations on the middle floor of building A. Lumped into this uncertainty will be experimental errors as well as the effect of infiltration changes and supply air temperature fluctuations. The pooled relative standard deviation of this data is 4%. There are, of course, systematic errors and errors in interpretation that add further to the overall uncertainty. The systematic error has been estimated to be 20%, which is similar to the 95% confidence interval suggested by Fisk [3] for breathing-level air-exchange effectiveness and air diffusion effectiveness measurements.

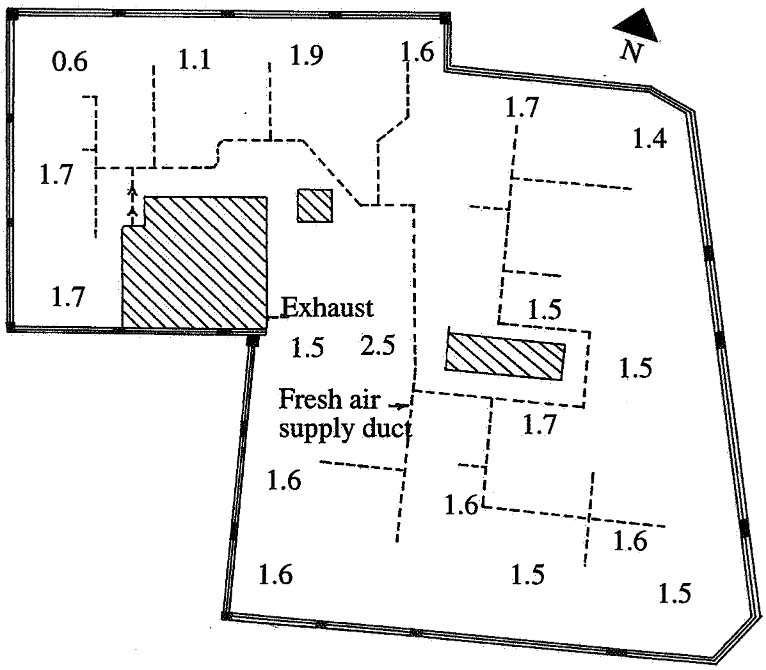

Figure 4: Local mean age-of-air (in hours) for floor 5 of building C in the breathing zone.

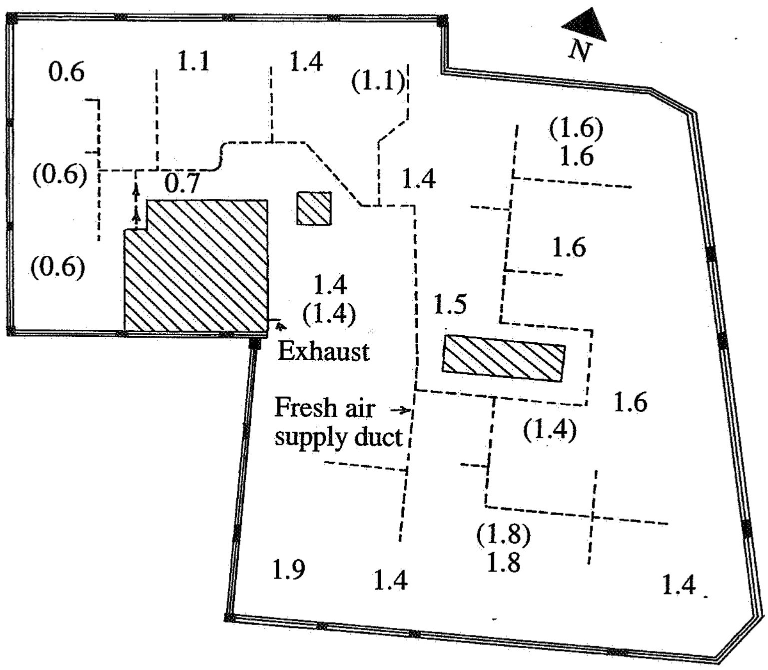

Figure 5: Local mean age-of-air (in hours) for floor 6 of building C in the breathing zone and [in brackets] measured in the plenum.

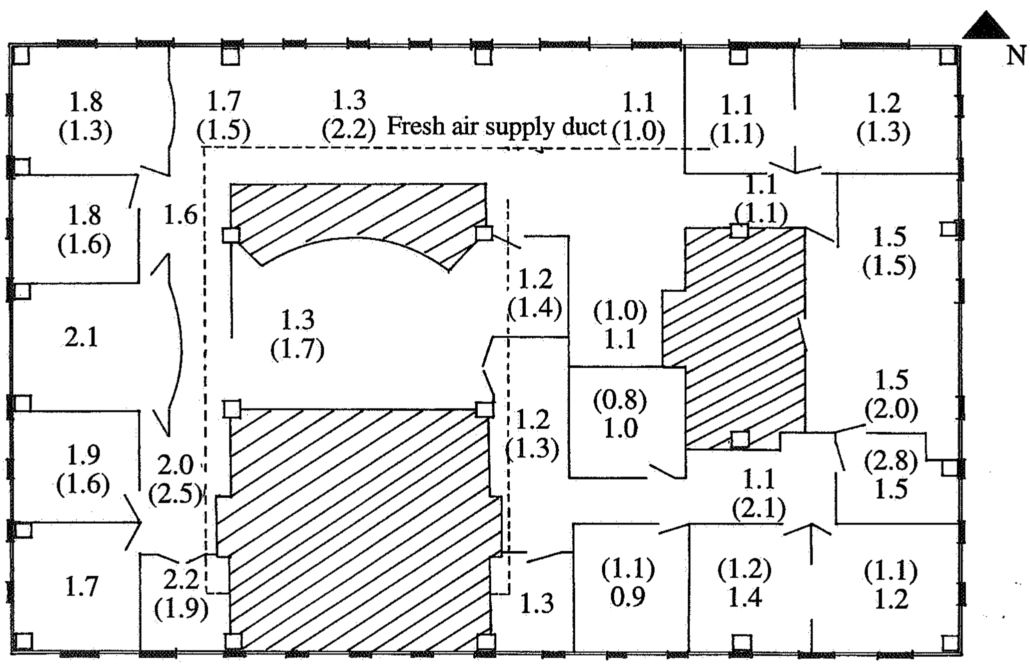

Figure 6: Local mean age-of-air (in hours) for floor 7 of building D in the breathing zone with all doors open and (in brackets) measured with all doors closed.

The nominal time constants for the fresh air supplied by the ventilation systems were measured using an electronic air velocity probe and a pitot static tube, and found to exceed or come close to the fresh air deliveries specified by NZS 4303 [3] for office buildings. In all cases they exceed the ventilation requirements in force when the buildings were constructed.

Variations in the LMA over the floor plan give an insight into the effectiveness of air distribution systems. In buildings C and D, in particular, there are clearly defined areas of the building with relatively long mean ages. In building D the mean age-of-air is 1.2h along the north-south axis of the building following the fresh air ducting path and at the east and west ends of the building the mean age-of-air is appreciably longer at 1.7h. This difference can be attributed to relative isolation from the fresh air supply of unit air handlers in the east and west ends of the building.

A similar lengthening of local mean age with distance from fresh air supply points was noted on the top floor of building A [2]. In the open plan areas of buildings B, C and D the local mean age-of-air is generally more uniform throughout the space than is the case for partitioned areas in these buildings. The only exception to this is one end of building C floor 6 where air-handling commissioning notes show fresh air delivery rates to exceed design requirements even with the dampers fully closed. Here the LMA is 0.6h where in the remainder of the floor it is 1.5h.

An indication of the variation in LMA has been given in Table 2 in the form of the standard deviation of the mean age-of-air measured 1.5m above floor level divided by the average mean age-of-air. The normalised standard deviation in LMA is shown to more than double in partitioned areas, illustrating the importance of floor space design considerations in the planning of air conditioning systems.

Building /floor	B/2	B/3	C/5	C/6	D/7
Entire floor	6%	27%	10%	12%	34%
Partitioned areas	-	31%	-	-	34%
Open plan areas	6%	12%	10%	12%	-

Table 2: The normalised standard deviation in local mean age-of-air measured in buildings B, C and D.

In some individual rooms on floor 3 of building B and floor 7 of building D the local mean age-of-air was found to change when doors were opened or closed, but over many rooms the average mean age-of-air remained unaffected. The average mean age in the partitioned areas of floor 7 of building D was 1.5 hours with the doors closed and 1.4 hours with the doors open. In the partitioned part of floor 3, building B, the average mean age with doors closed was 0.44 hours and with doors open 0.49 hours. These differences are considered to be insignificant.

Most rooms in the partitioned areas of buildings B and D contained both fresh air diffusers and an exhaust path to the plenum. There were two exceptions to this. One room on the east side of building D lacked a fresh air supply and the only separate room on the second floor of building B lacked an exhaust return to the plenum. In these two cases, the LMA with doors closed was about twice that of adjacent areas.

5. Ventilation effectiveness

The breathing-zone local mean age-of-air data has been averaged to give an estimate of the room mean age of air. These averages, along with the nominal time constants and the room mean age of air determined using exhaust air analysis where possible, are given in Table 3.

Building/floor Ventilation parameter	A/2	A/3	B/2	B/3	C/5	C/6	D/7
Room mean age of air (space averaged) in hours	0.75	0.60	0.76	0.64	1.65	1.31	1.41
Room mean age of air (analysed at exhaust duct) in hours	0.76	-	0.79	0.60	-	-	-
Nominal time constant (hours)	0.79	-	0.82	0.95	1.33	1.13	1.40
Space averaged air change efficiency %	53%	-	54%	74%	40%	43%	50%

Table 2: Ventilation effectiveness parameters measured in seven building ventilation zones.

Where it was possible to measure the nominal time constant, the air change efficiency measured in the breathing zones was between 40% and 75%. There was no obvious link between these results and the connection between fresh air supply and the unit air handlers. Indeed, local mean age-of-air measurements in the plenum of building C showed that, in this case, the plenum and the occupied areas were effectively one zone.

In five cases the air change efficiency ranged between 40% and 53%, indicating that the ducted fresh air performed a dilution ventilation role. In floor 3 of building B, the air change efficiency was 75% and apparently closer to the displacement flow description. It must be remembered that the LMA was measured 1.5m above floor level and in highly partitioned areas this might not always be representative of the entire room volume. Other workers, e.g. Fisk and Faulkner [4], have measured ventilation-effectiveness parameters in mechanically ventilated buildings and developed a picture of the effectiveness of systems in a range of buildings. In their data, similar conclusions are reached concerning the description of mechanical ventilation in office buildings as dilution ventilation systems. It is too early to form secure conclusions about the effectiveness of ventilation systems in New Zealand office spaces, but further measurements are planned.

6. Conclusions

This study has measured the local mean age-of-air in the breathing zones of four mechanically ventilated buildings in New Zealand. Three of the buildings used a common approach, of ducting fresh air to unit air handlers in the plenum space where it is directed to the occupied spaces below. In some cases the fresh air supply was tightly coupled to the unit air handler while, in others, fresh air was discharged more generally into the plenum. The following key points concerning the performance of these ventilation systems were established:

- The floor-averaged nominal time constants for the ventilation systems studied in four buildings ranged between 0.79 to 1.4 hours. These exceed or come close to the fresh air deliveries specified by NZS 4303 [3] for office buildings, and in all cases exceed the requirements in force when the buildings were constructed. The floor-averaged mean age-of-air in the breathing zones of the four buildings ranged between 0.6 and 1.65 hours, which in most cases came close to the nominal time constant for the space.

- The air change effectiveness in three buildings employing unit air handlers fell in the range of 40% to 54%, with a further result at 74%. There was no obvious link between these results and the connection between fresh air supply and the unit air handlers. Indeed, measured local mean age-of-air measurements in the plenum of building C showed that the plenum and the occupied areas were effectively one zone.

- Variation in the local mean age-of-air in the breathing zones of the four buildings has depended on the coverage of the fresh air distribution system as well as on the extent of internal partitioning. The normalised standard deviation of the local mean age-of-air expressed as a percentage of the room average mean age was about twice as high in partitioned areas as it was within large open plan areas. In ventilation performance terms, however, this was not considered to be significant. Far more important were two cases of rooms missing either a fresh air supply or an exhaust return to the plenum. Here the local mean age-of-air was twice that of adjacent areas.

Further measurements are planned in order to develop a wider understanding of ventilation effectiveness achieved in New Zealand buildings.

7. Acknowledgments

This work was funded by the Building Research Levy and the Foundation for Research, Science and Technology. The assistance of the building owners for access to the buildings, and the staff of BRANZ and the Centre for Building Performance Research for conducting the measurements, are also greatfully acknowledged.

8. References

1 Bassett, M.R. and Beckert, H. M., 1989. *Automated tracer equipment for air-flow studies in buildings*. Proceedings of the 10th AIVC Conference, "Progress and Trends in Air Infiltration and Ventilation Research". Depoli, Finland.

2 Bassett, M.R. and Isaacs, N., 1994. *Preliminary ventilation effectiveness measurements by a pulse tracer method.* Proceedings of the 15th AIVC Conference, Buxton, England.

3 Standards New Zealand., 1990. NZS 4303, *Ventilation for acceptable indoor air quality.* Wellington. This is an adaptation of ASHRAE Standard 62-1989, *Ventilation for acceptable indoor air quality*. New York.

4 Fisk, W. J. and Faulkner, D., 1992. *Air change effectiveness in office buildings: Measurement techniques and results*. Proceedings of the International Symposium on Room Air Convection and Ventilation Effectiveness, pp282-294. Tokyo.

Implementing the Results of Ventilation Research
16th AIVC Conference, Palm Springs, USA
19-22 September, 1995

Natural Ventilation Design at the Welsh School of Architecture

P J Jones, D K Alexander, J Jenkins

Welsh School of Architecture, UWCC, Bute Building,
Kind Edward VII Ave, Cardiff, CF1 3AP, UK

ABSTRACT FOR 16TH AIVC CONFERENCE

Title: **Natural Ventilation Design at the Welsh School of Architecture**

Author(s) **P J Jones, D K Alexander, H Jenkins**
Welsh School of Architecture, Cardiff, UK

As a result of an emphasis on the assessment of the environmental performance of building design, student project work at the Welsh School of Architecture has been significantly influenced by the prediction techniques available there. The techniques and tools on offer include multicell and CFD mathematical modelling, and wind tunnel physical modelling.

As well as becoming a part of the overall design assessment made by the students, these methods are becoming visible in their effect the development of the design itself. As in the earlier response to the introduction of CAD facilities, interest in the use of these tools is increasing and sparking off an overall increase in interest in natural ventilation design.

This paper presents recent student work which incorporates aspects of natural ventilation design, and illustrates the contributions made by the assessment tools available.

Implementing the Results of Ventilation Research
16th AIVC Conference, Palm Springs, USA
19-22 September, 1995

Application of Air Flow Models to Aircraft Hangars with Very Large Openings

J van der Maas*, A Schaelin**

* LESO-PB, Ecole Polytechnique Federale de Lausanne (EPFL), CH-1015 Lausanne, Switzerland
** Energy Systems Laboratory (LES) Swiss Federal Institute of Technology, ETH-Zentrum, CH-8092 Zurich, Switzerland

Application of Air Flow Models to Aircraft Hangars with Very Large Openings

J. van der Maas, LESO-PB, École Polytechnique Fédérale de Lausanne (EPFL), CH-1015 Lausanne, Switzerland

A. Schälin, Energy Systems Laboratory (LES), Swiss Federal Institute of Technology, ETH-Zentrum, CH-8092 Zurich, Switzerland

Synopsis

In line maintenance hangars, air planes stay about 2 hours, usually at night-time. The cooling-down of the inside air during the opening time of the hangar gates (up to 5 times per night, lasting 15 to 30 minutes each) has a considerable impact on the comfort conditions for the workers, and on the energy required for reheating.

The time-dependent air flow rates and associated heat loss rates during the door opening and closing cycles is assessed by simple transient thermal models and CFD (Computational Fluid Dynamics) calculations. The results obtained by these models agree well with the experimental data of the transient temperature response during the opening and closing of the door of a real full-scale hangar.

The effect of using huge air curtains (up to a height of 20 m, a width of 80 m, and moving air volumes at rates of 400 m^3/s) to prevent heat loss was studied numerically by CFD in two- and three-dimensional models for time-dependent conditions. The study covers also transient effects when an aircraft is actually crossing the air curtain, and shows the feasibility of assessing the energy saving potential of such air curtains using CFD.

1. Introduction

In line maintenance hangars for small repairs, air planes stay about 2 hours, usually at night-time. Such hangars can hold several planes, so 5 door openings lasting up to half an hour each occur frequently. The cooling-down of the inside air during the opening time of the hangar gates has a considerable impact on the comfort conditions for the workers, and on the energy required for reheating

In order to assess the energy loss during the opening time, measurements have been carried out in a real full-size hangar by Sulzer Energy Consulting, Winterthur, Switzerland. The time-dependent air flow rates and associated heat loss rates during the door opening and closing cycles is assessed by simple transient thermal models and CFD (Computational Fluid Dynamics) calculations, and compared to the available measurement data.

Therefore the possibility of installing a huge air curtain across the hall hangar opening (full-width, about 80 m long and 20 m high) was investigated by a computational fluid dynamics (CFD) simulation within a project request intitiated by Swissair Real-Estate, Zurich Airport, Switzerland.

Some of the modeling techniques have been developed already earlier for the modeling of bidirectional air flow through open windows and doors [Schälin et al. 1992], where "large" has been used for openings of the order 1-3 m, as opposed to the width of cracks. In this paper "very large" is used for door sizes of the order 15-30 m.

This paper reports some of the most interesting measurement results and comparisons with different models for the air flow in a hangar through the open door, plus some results for different configurations of an air curtain.

Several studies of the dynamics of gravitational flows occurring during door opening can be found in the literature [Linden and Simpson, 1985; Kiel and Wilson 1986]. However these studies were concerned with the adiabatic case where heat transfer is not playing a role. By combining a single zone thermal model with the gravitational flow model, [Van der Maas and Roulet, 1989; 1990] were successful in predicting the dynamic energy losses through open doors and windows. A extension of this cooling model to several zones ventilated in series [Van der Maas and Roulet, 1993] was shown to be able to estimate the temperature stratification after opening a window or door for the case of single-sided ventilation.

2. Measurements in an Aircraft Hangar

Measurements in a hangar have been performed by Sulzer Energy Consulting, Winterthur, Switzerland. The aim of the measurements was to investigate the cooling-out of the hangar during the opening-time when an airplane enters or leaves the hangar. An important design issue, motivating the measurments is the temperature recovery time after closing of the door, in relation with the type of heating system (floor heating or air heating systems). The issue is crucial for the design of hangars with frequent opening times (several times an hour) related to the short maintenance periods of modern aircraft. The problem is characterized by time-dependent flow and time dependent boundary conditions whereas static concepts as the U-value of the envelope are of no use when describing the indoor temperature variation with time.

2.1. Hangar description and measurement set-up

The investigated hangar is 150m wide, 90m in depth and the distance from floor to roof is 33m. The rolling doors comprise 8 segments, 18 m wide and 27m high. The roof is well insulated with a U-value better than 0.4. The 13'500m^2 concrete floor slab contains floor heating pipes at a depth of 15cm.

The floor heating system has a power of 1.7MW, which corresponds to 130W/m^2. The space setpoint temperature for the floor heating system is 18°C, with a maximum surface temperature of 26°C. Twenty auxiliary hot air blowing systems are installed above the doors and along the walls with a total power of 3.3MW.

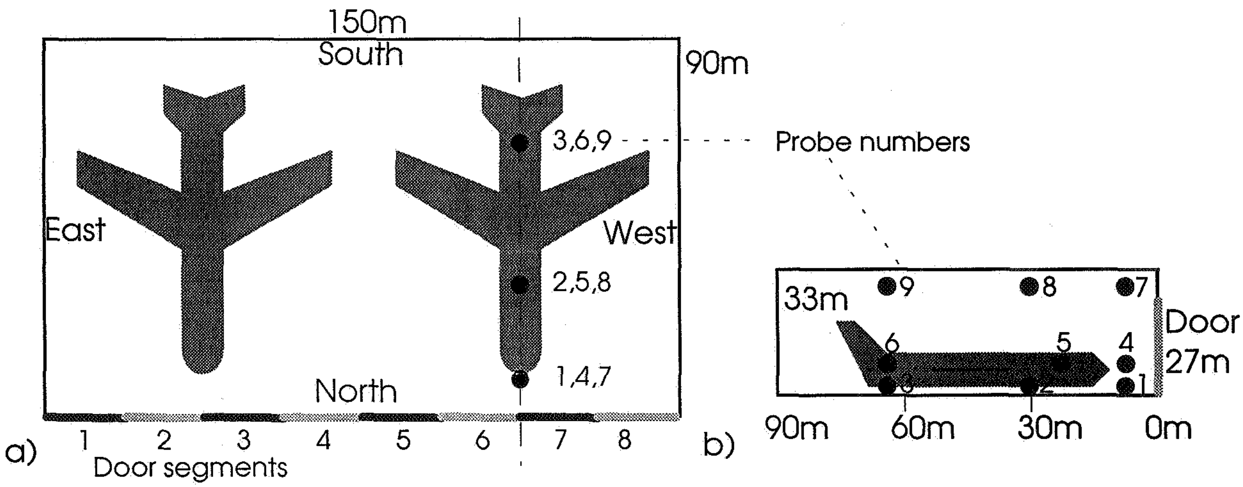

Figure 1. Measurement positions in the 90x150x33m hangar. a) top view with cross section of Figure b) indicated. b) cross section between door segments 6 and 7.

Figure 1 shows the configuration of the hangar and the temperature measurement positions. Small temperature loggers were installed using as a support the maintenance structure around the airplane. Data were logged every 10s before and during the door opening, and during and after the door closing. In a plane normal to the door plane, 9 temperature measurement points have been chosen (see also Table 1)

-3 near to the floor : 1-front, 2-middle, 3-back

-3 in the middle : 4-front, 5-middle, 6-back

-3 just above the top of the door level : 7-front, 8-middle, 9-back

The probes 2 and 5 were mounted on the maintenance structure around the plane and only probes 1 and 4 are fully exposed to the cold air gravity current. Probes 3 and 6 were placed at the back of the plane external from the structure.

Of the three data series which are available, one has been chosen for presentation. The data concern the measurements during a winter night, where two door segments were opened (maximum opening width 37m).

Probe	Placement	distance from door	height above floor
1	bottom door	10	0.5
2	bottom center	32	0.3
3	bottom back	64	0.3
4	center door	9	5
5	center center	19	7
6	center back	63	5
7	top door	6	30
8	top center	29	30
9	top back	66	30

Table 1: Measurement probe positions (see also Figure 1).

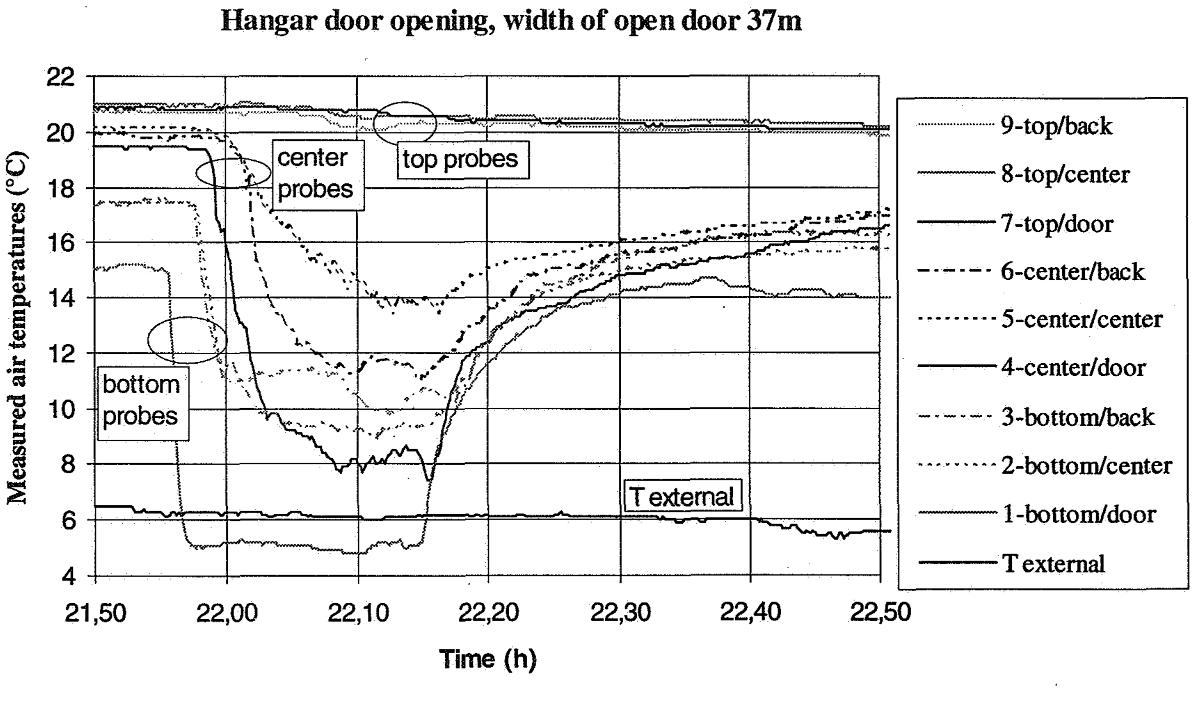

Figure 2. The measured air temperatures at nine positions in a center plane normal to the hangar door opening (Table 1, probes 1 to 9) during the opening and closing of 2 hangar door segments (door opening 2 in Table 2).

2.2. Experimental results

In Figure 2, the temperatures of probes 1 to 9 are given during and after the door opening. It took about 5 minutes for the doors to roll aside, and during this opening phase the temperatures at floor and middle level dropped rapidly, while above the top of the door the temperatures did not change remaining nearly constant at 20.5°C. During the closing phase of about 6 minutes, a rapid temperature rise near floor is observed.

The following can be observed on Figure 2. Probe 1 is coolest and drops to 5°C, which is two degrees below the outdoor temperature. From this it can be concluded that the measurement of the outdoor air temperature is not correct; indeed afterwards it was concluded that this probe was mounted too close to the structure of the building. Probes 2 and 3 are shown to have a delay of 2.5min, and are 5 to 6K higher in temperature than Probe 1. Probe 4 (middle door) is delayed by 3.5min. and is 1K colder than probe 2. Probe 5 (middle middle) is delayed by 6min and is 6K warmer than the middle door. This probe was mounted on the maintenance structure and was not directly exposed to the cold air current. Probe 6 (the middle back) is delayed by 6min and 2K warmer than Probe 4. During temperature recovery, the probes remain colder than before opening by about 2K. The top probes, steady decrease with outdoor temperature, but not influenced by door opening.

3. Application of Thermal Zonal Models

The model described in [Van der Maas and Roulet 1993], applies when a single air flow path can be defined. A partial validation of the model with details of the used algorithms can be found in this reference. The principle of the model is to couple for each zone airflow and heat transfer by requiring a heat balance and conservation of mass. The definition of a single air flow path implies that the zones must be placed in series of one another.

In Figure 2, the multizone cooling model is given schematically for three zones. The algorithm for the cooling model includes a recurrence relation which allows to calculate the air temperature in the last zone, from knowledge of the inlet temperature of the first zone. The ventilation flow rate is the same for all zones and depends on these air temperatures. A few iterations are sufficient to obtain the air temperatures for which the heat balance is satisfied for all the zones. The input parameters for each zone are: (i) the heat transfer surface area and the heat transfer coefficient, (ii) a material parameter characterizing the dynamic thermal response of the surface temperature, called thermal effusivity, and (iii) the initial wall surface temperature.

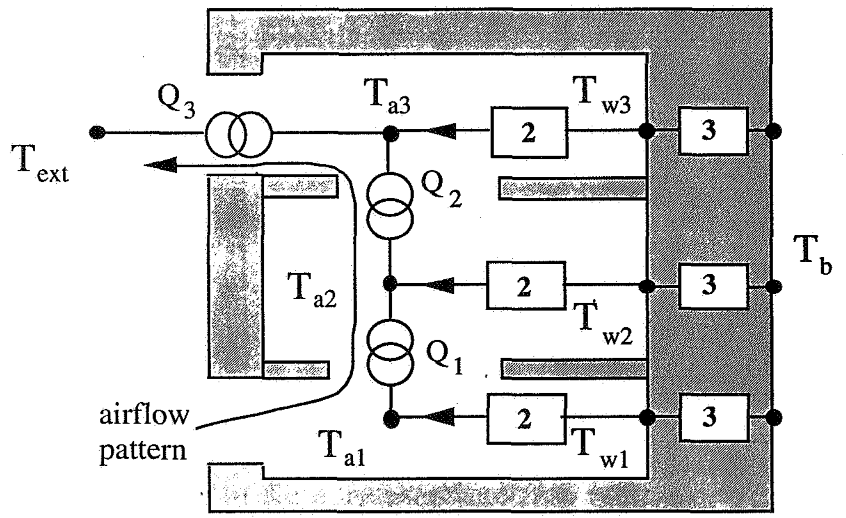

Figure 3. Multi zone cooling model with three zones. (2) are the heat transfer resistances and (3) is the dynamic wall resistance. The heat sources Q_i, represent the combined effect of internal heat gain and ventilation heat loss. For each zone the principles of mass and energy conservation apply assuming that in the dynamic regime the zones are only coupled through the air temperature nodes.

The (time dependent) output parameters for each zone are calculated from the external air temperature variation and are: (i) the air temperature, (ii) the surface temperature, and (iii) the ventilative cooling load.

The airflow pattern without wind is quite well defined by the nature of the gravity wave. After opening the door, the gravity current enters, flattens and spreads out over the floor and flows to the back, where it is relected back and the hangar starts to fill up with cold air (warm air is escaping through the top of the door) like a displacement ventilation system. This is confirmed from the delays with which the several probes react to the cold air entering the hangar (see Figure 2). First probe 1, near the door; then the other bottom probes, next the second layer probes. Unfortunately there are no temperature readings between heights 5 and 27m, so that the dynamics cannot be followed in detail.

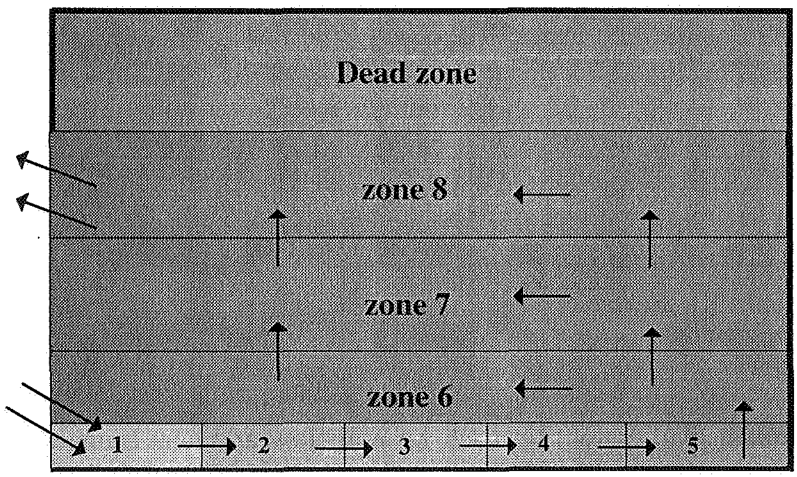

Figure 4. The 8-zone geometry representing the gravity current air flow pattern with open hangar door.

The zones have been defined following this gravity current air flow pattern (Table 1, Figure 3). The height of the first zones should correspond ideally to the height of the gravity wave. The height is half the door height close to the door, but when it spreads out over the floor, it flattens [Lane-Serff et al. 1987]. From Figure 2 it can be seen that Probe 4 which is close to the door senses the cold wave a full two minutes later than the lower probe 1. Because of the positioning of the measurement probes, the zones in contact with the floor were taken to be three meter high and included probes 1, 2 and 3. Zone 6 reaches from 3 to 5m, including probes 4, 5 and 6.

Because the flow pattern is only approximately described by these zones, the choice of the zones is not unique.

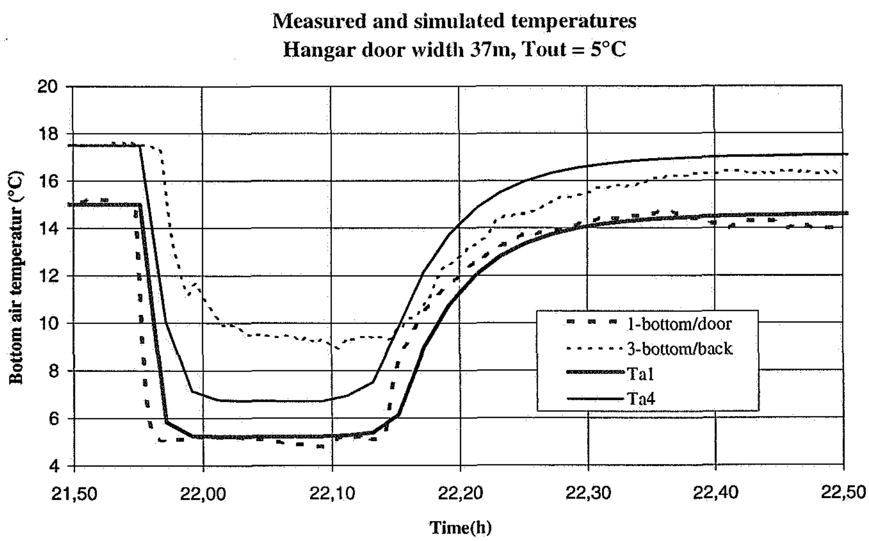

Figure 5. Comparison between measured and simulated air temperatures in zone 1 (bottom door, Ta1) and zone 4 (bottom back and Ta4).

In Figure 5, the predicted temperatures of zones 1 and 4 have been compared with the measured temperatures of probes 1 and 3. It is seen that near to the door and to the floor, the temperature falls rapidly to close to the outdoor temperature. The probe 3 temperature is higher than this simple model predicts. (It is difficult to understand how important the role is of the structure surrounding the airplane).

It is interesting to consider the effect of the opening width on the cooling. Indeed the heat loss rate is expected to be proportional with the opening width. In Figure 6, the mean temperature at ground level was calculated for three doorwidths. It is seen that a reduction of the door width from 37 to 5m width, is not sufficient to avoid a substantial lowering in air tempeature. This implies that even when the heat loss rate is reduced by more than a factor 7, the indoor temperature continues to drop substantially.

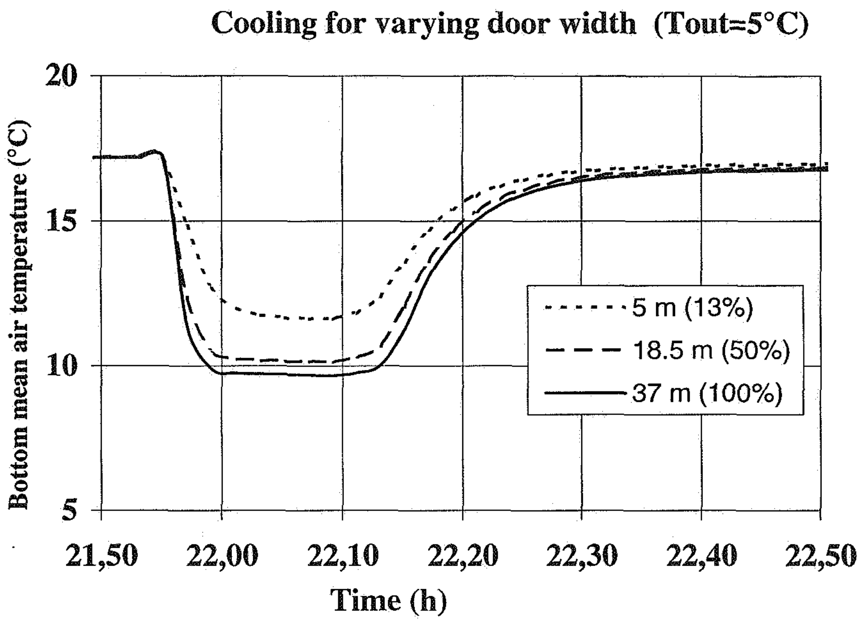

Figure 6. The simulated air temperature averaged over zones 1 to 5, for different opening widths. A 5m wide door opening still causes substantial cooling.

This effect is related to an important factor in the model described in Figure 3, which is the ratio between the heat transfer resistance between the air and the wall, and the equivalent ventilation resistance of the door. As long as the ventilation resistance is relatively small, the indoor temperature will drop to close the outdoor temperature.

Discussion of energy losses. It can be concluded that the overall features of the cooling of the hangar are reproduced. It appears that the energy losses during the opening are mainly due to the replacement of warm indoor air by cold outdoor air, the cooling of the floor and structure is relatively small.

Without air curtain, the heat loss rate as a function of opening time decreases rapidly : once the warm air (T_2) has been replaced by colder air (T_1) the heat loss rate by convection is considerably reduced, the residual heat loss being governed by the cooling of the wall surfaces.

In the extreme case of adiabatic walls, the energy loss stops after a few minutes and equals $E=(T_2-T_1)\rho\ Cp\ V$. The recovery time is shortened when the wall surface temperature remains high (massive surfaces). However the heating power which can be provided by the warm wall surfaces is limited. To reduce the recovery time hot air blowing systems can be used with advantage. Hot air blowers have a low inertia and can function efficiently for short periods of time. Because hot air rises, the warm air should be distributed at ground level which means that the hot air should be blown downward and reach the floor.

The heating power Φ, can be calculated as a function of desired recovery time τ_R :

$$\Phi\ \tau_R = E \qquad \text{or} \qquad \Phi = (T_2-T_1)\ \rho\ Cp\ V/\ \tau_R \qquad (1)$$

For a volume of $364'000\ m^3$, the power in MW and a recovery time of 5 min this estimate yields: $\Phi = 1.5\ (T_2\text{-}T_1)$ MW. For a fixed hot air heating system of 10 MW for example, the recovery time depends on the difference between the outdoor temperature and the desired indoor temperature :

$$\tau_R\ (\text{min}) = (T_2\text{-}T_1)\ \rho\ Cp\ V/\ \Phi/60 = 0.7\ (T_2\text{-}T_1) \qquad (2)$$

and to increase the temperature by 10K would require 7 minutes or a burst of energy totalling about 1000kWh.

4. CFD Calculations for an Aircraft Hangar

The CFD calculations have been performed using the commercial code FLOVENT, a CFD program designed for ventilation purposes. It can be used for simple cartesian grid systems and is based on the SIMPLE algorithm [e.g. Patankar 1980]. The standard k-ε-turbulence model is included. Following quite different situations have been studied:

- Investigation of mass flow through door and air flow pattern inside a hangar, when a hangar door is opened suddenly: transient 2-dimensional simulation.
- Parameter study for air curtain in the door plane to prevent heat loss during door opening: steady-state 2-dimensional simulation.
- Preliminary heat loss study for air curtain: transient 2-dimensional simulation.
- Detailed heat loss study: transient 3-dimensional simulation.

4.1 Hangar with free flow through open door

In a previous study [Schälin et al. 1992] the bidirectional air flow through a large opening (a normal door of a height of 2.2 m) in a room, which is closed apart from the door and not ventilated, was investigated in some details. The velocity profiles obtained by CFD show good agreement with experimental data and prove the ability of the CFD modeling technique for this flow type at this moderate height.

In this study the CFD modeling technique was applied to very large openings. In order to save computation time, the hangar as described in section 2.1 was modeled in two dimensions only (see Figure 7). Boundary and initial conditions were taken as much from the experimental values as possible. Initial conditions assumed were 20°C inside the hangar and 5°C outside. These conditions and the resulting velocity and temperature distribution are not known in sufficient details; therefore it cannot be expected that the curves in Figure 2 could be represented in full detail and an expensive three-dimensional calculation was not carried out. The main purpose of this study was the demonstration of the ability to predict the main flow features by CFD. The size of the grid used was 57x42 cells; it is shown partly in Figure 9.

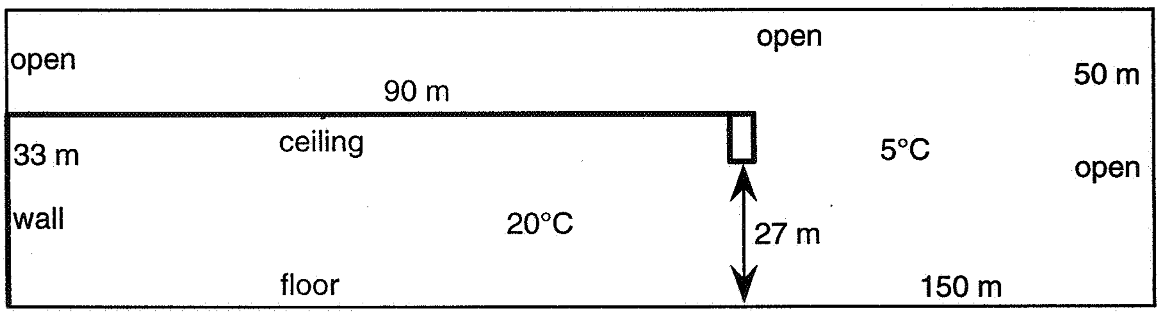

Figure 7: Geometry used for two-dimensional air flow simulation in the hangar described in section 2.1.

At the beginning of the calculation time (t=0) the door was suddenly removed and a bidirectional flow starts to establish through the door. Figure 8 shows the temperature distribution at several instances in the first 60 s. It can be seen quite easily that after 60 s the cold air has reached the end of the hangar along the floor. After that the cold air starts to empty the hangar from the back; the behaviour is like a gravity wave which is reflected at the back wall.

The velocities in the door plane are in the beginning about 1.5 m/s near the floor and 2.5 m/s near the top of the door, and will fall to 0.6 m/s after 3 minutes (200 s) and to about 0.2 m/s after 10 minutes (600 s). The observed velocities in a real hangar are of the same order, but no measurement values are available. A calculation for the maximum velocity in the beginning,

$$v_{max} = C_d \sqrt{\frac{g H \left(T_a - T_{ext}\right)}{T_{ext}}} \quad (3)$$

and C_d=0.63 [Van der Maas et al. 1989], gives 2.4 m/s in very good agreement.

After about 5 minutes most warm air in the hangar has been replaced by cold air, except for that part near the ceiling which is at a larger height than the door height (i.e. above 27 m). That air part remains unaffected for a longer time (see Figure 2, experimental results). Figure 9 shows the temperature distribution in the hangar after a calculation time of 20 minutes (1200 s). This feature (stagnant warm air in the upper part of the hangar) cannot be obtained by using the k-ε-turbulence model, as that model assumes a fully turbulent flow which is not the case in the upper part of the hangar. Without low-Reynolds-number corrections, it will overpredict the amount of turbulence in those stiller parts [Chikamoto et al. 1992] of the flow which leads to a higher mixing and a total sweep-out of warm air even in these higher parts. As it is not possible to include user-defined model corrections in the CFD program used, the results in Figure 8 have been obtained in a laminar calculation; the flow characteristics in the beginning are similar to those obtained by using the k-ε-turbulence model.

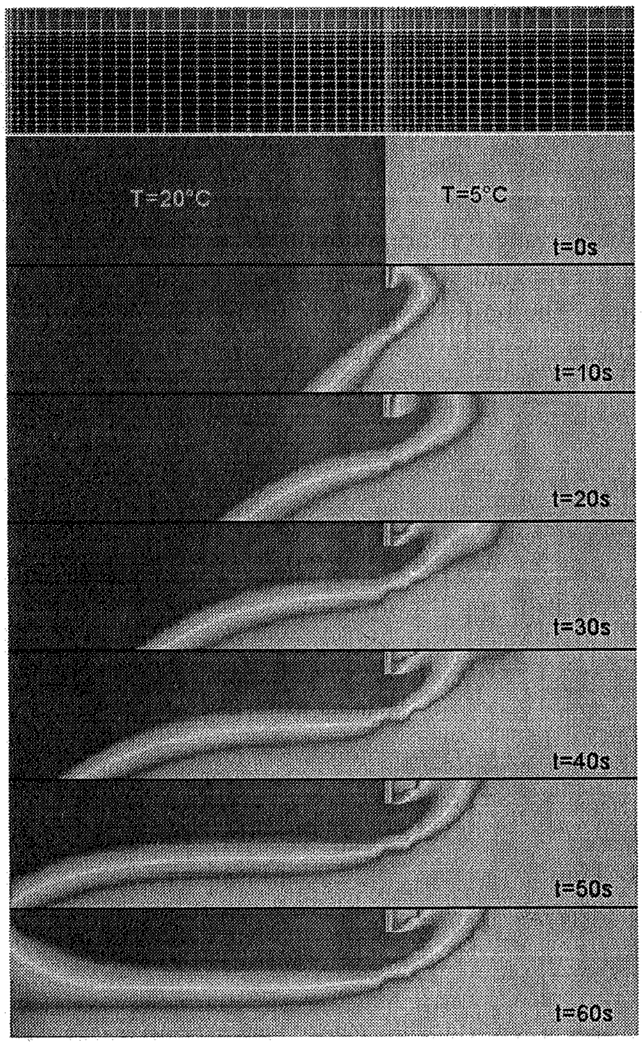

The described feature can be seen in the experimental curve in Figure 2, where the bottom position probes show a fast decrease in temperature, the probes at the medium level exhibit a slower decrease and the top probes at a height of 30 m remain unaffected by the door opening. The probes at a height of about 5 m (probes 4-6) show a delayed temperature decrease by 1 minute; this feature cannot be seen in the CFD calculation because in the measurement situation the air flow is entering a door which is open only one quarter of the hangar width; the cold air flow distributes at decreasing height.

Figure 8 (left): Time sequence of temperature distribution after opening of hangar door.

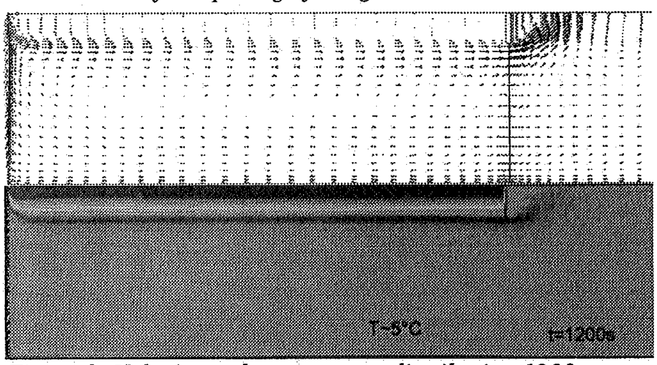

Figure 9: Velocity and temperature distribution 1200 s (20 min.) after opening of the door.

The spreading out of the 2D gravity wave and the lowering of its height with the distance from the door was observed and explained briefly in [Linden and Simpson, 1985; Lane-Serff et al. 1987].

Figure 10 shows the velocity profile across the door height after 30 s. The neutral level is slightly above mid-height, and higher velocites are found near the top of the door. The profiles are not parabolic due to the viscous forces which are not taken into account by the simple Bernoulli theory (Equation 1). [Wilson and Kiel, 1990] discuss the shearing at the neutral level (zero velocity, at about mid-hight) and the mixing of counterflows, which modifies the velocity profile from pure parabolic.

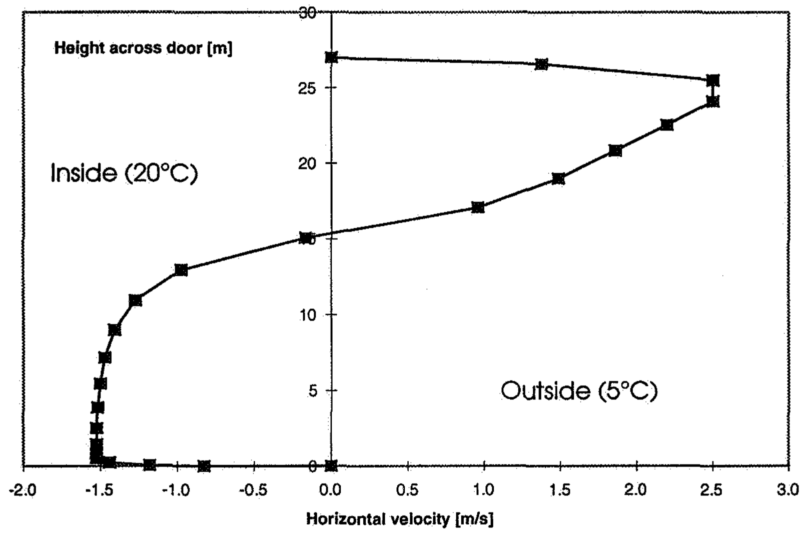

Figure 10. Velocity profile across door height after 30 s.

4.2 Hangar with air curtain

In a student's diploma thesis several questions around the feasibility and energy savings effectivity of an air curtain for the whole hangar door opening of a planned new Swissair hangar were investigated. The CFD calculations have been done for the geometrical dimensions of the projected hangar. Figure 11 shows the layout of the hangar. The dimensions are 90 m x 110 m x 22 m; the central part of the hangar is 31 m high. The hall is large enough to hold 4 medium-size planes or a very large one. The door height is 14 m on the sides and 22 m in the central part, and the total width 83.8 m.

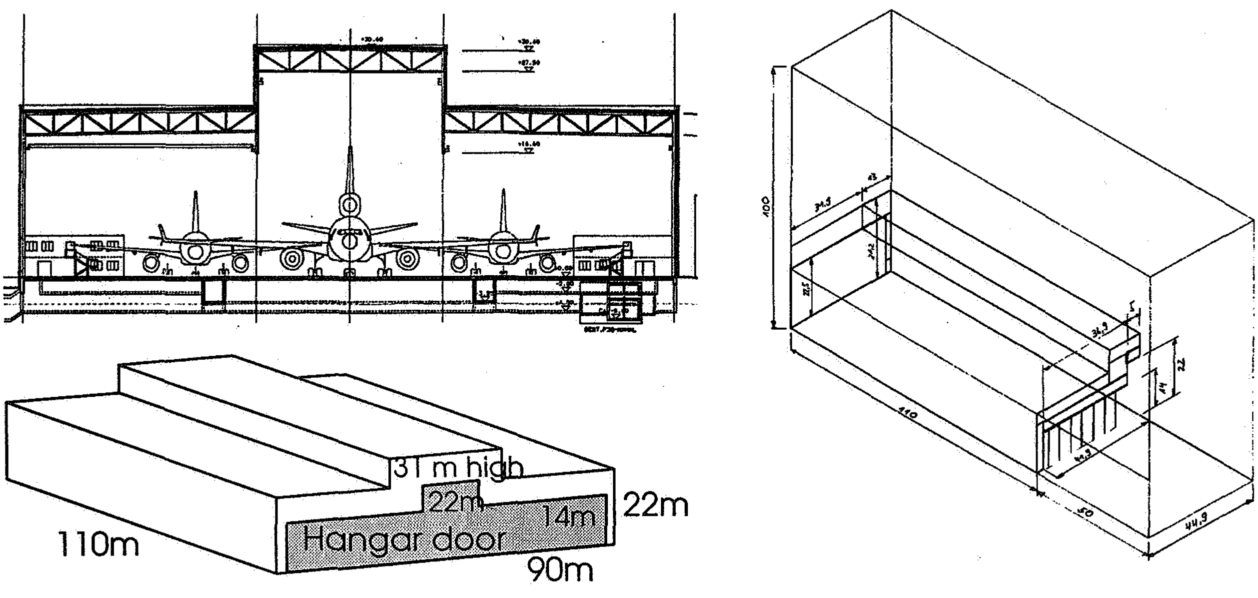

Figure 11: Projected new Swissair hangar. Top: front view with air planes. Below: sketch in perspectiv view. Right: Model for 3-dimensional calculation.

4.2.1 Parameter variation for stable air curtain

A large parameter variation was done in 2-dimensional steady-state calculations to find out favourable conditions for a stable air curtain. Out of different possible jet configurations like blowing from above and sucking from below, a quite simple jet blowing from above was chosen in order to avoid complicated installation work. Such a simple jet would be also suited to be installed in an existing hangar. The jet was assumed to be a plane jet along the whole door width (as opposed to an array of single jets). Figure 12 shows the data used for this study.

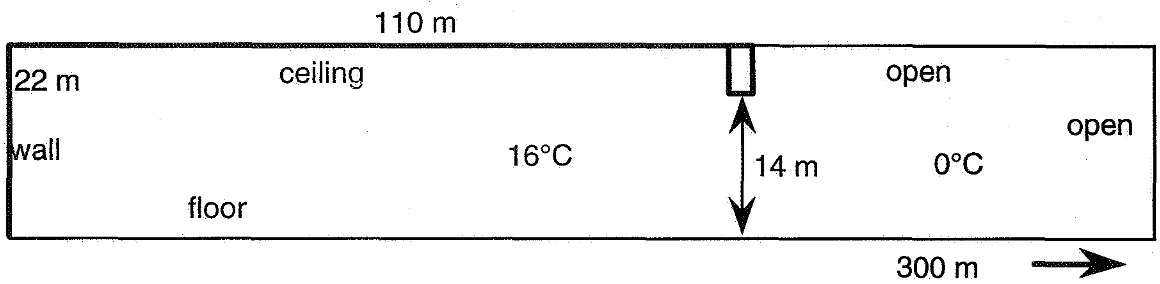

Figure 12: Geometry used for the 2-dimensional calculation for the Swissair hangar project.

Varied parameters were: jet angle (-15°, 0°, 15° to the vertical direction), jet width (0.1 m, 0.3 m), air velocity (5 to 20 m/s), jet heating (ΔT=0 to 2.5 K, if air is taken from inside, ΔT=0, 10 K, if air is taken from outside), presence of wind (0, 3, 6 m/s). The outside temperature was always assumed to be 0°C, and the inside design condition was around 16°C. It is not possible to report on all these cases, but as a main result, the optimum condition in the presence of wind was found to be in the range of: jet angle 15° towards outside, jet velocities around 10-15 m/s, and a width of 0.3 m. For a velocity of 14 m/s, a width of 0.3 m and a length of 83.8 m, the volume flow rate equals 352 m^3/s, and the mass flow rate about 410 kg/s, using a density of 1.17 kg/m^3.

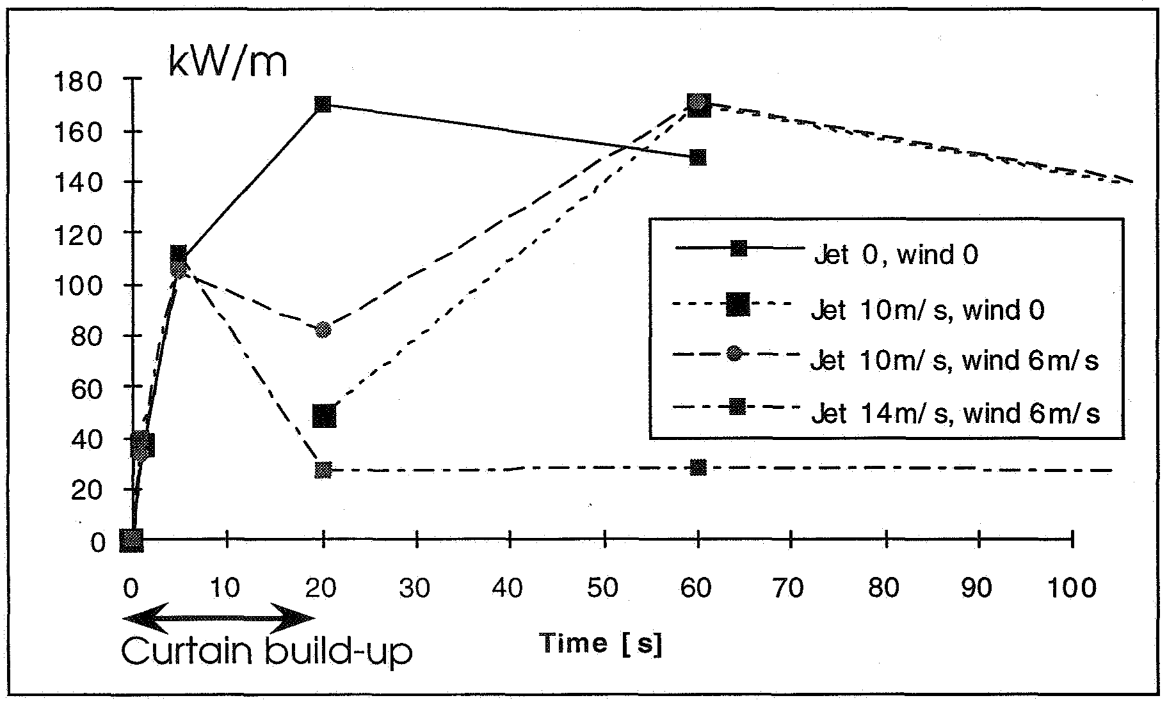

Figure 13: Heat loss in kW/m (per m of open hangar door width) for different combinations of air curtain velocities and wind speed. The curtain build-up time applies only to the 3 cases with air curtain.

4.2.2 Heat loss investigation in 2 dimensions

Preliminary energy loss calculations were done for the optimum jet configuration. In the transient CFD study the starting condition was 16°C inside and 0°C outside. At t=0 the door is open and the jet starts blowing. In this study it takes some time until the air curtain is established. The strong loss during the first 20 s can be avoided by turning on the fans earlier before the door opening.

For a velocity of 14 m/s the build-up time of the air curtain is about 20 s, much better than for a velocity of 10 m/s with a build-up time of 60 s. In the case of a jet of 14 m/s, also a better shielding between inside and outside is achieved. The inside temperature after 5 min is still around 14°C. Velocities inside the hangar along the floor are around 2 m/s.

Figure 13 shows the heat loss in kW/m through the door plane for different jet configurations, the best performance being achieved for the 15 m/s jet. The peak loss for the whole hangar width would be about 14 MW, assuming that the door would be suddenly opened completely. The power effort for the jet across the hall hangar is much smaller than the heat loss reduction; the kinetic energy of the air is about $mv^2/2=410$ kg/s * $14^2/2$ m^2/s^2 = 40 kW, and the electric power consumption of the fans would be 60 kW at a fan efficiency of about 0.7.

However these 2-dimensional calculations can only be considered as preliminary, as effects related to the real door opening process are not contained.

4.2.3 Heat loss investigation in 3 dimensions

Therefore a 3-dimensional calculation was set up for a hangar. The calculation was done for just half the hangar; a symmetry plane was assumed in the middle, see Figure 11. The size of the grid used was 50x33x23 = 37950 cells.

The calculations were performed in the presence of a wind of 6 m/s at frontal incidence for a hangar which is air-tight apart from the open front door. The door was opened step by step until it was totally open (full width of 83.8 m) after 1 minute. In the second minute of the transient calculation an air plane of the dimensions of an Airbus A320 was moved successively into the hangar. The times were chosen that short in order to save computation time. Observations in a real hangar have shown, that these times are realistic, but they represent an ideal case of optimum timing. In real practice, hangar doors stay open 10-20 minutes or more to let an airplane in or out. Consequently losses will be larger.

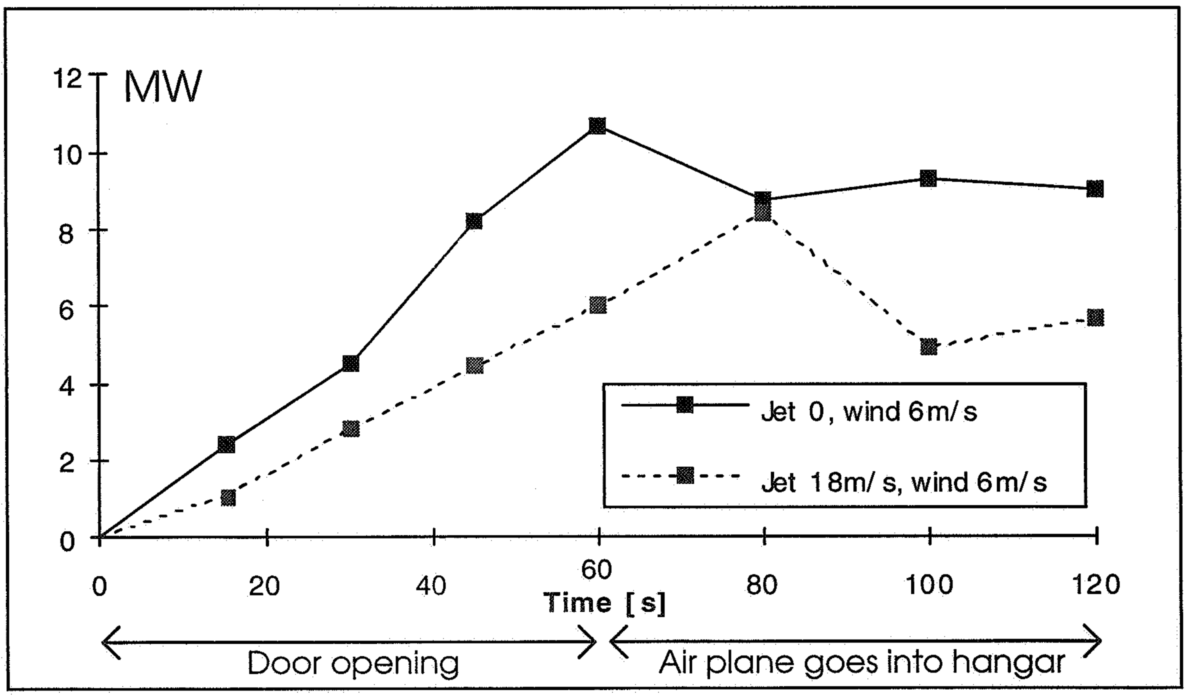

Figure 14: Heat loss rate during opening of hangar and pulling in the air plane into the hangar, obtained by numerical calculation of 3-dimensional cases, one with and one without air curtain. The MW values are for the whole hangar with full door width.

Figure 14 shows the total heat loss through the door plane with an air curtain, in comparison with a case without curtain. As the door opens linearly during the first 60 s until it is totally open, the loss also increases linearly in time. The jet used was at a somewhat higher velocity of 18 m/s than in the 2-dimensional case, as the door height in the center is also higher (22m instead of 14m).

The result shows a energy loss lower by about 40%, as compared to the case without air curtain (integrals of curves in Figure 14). In reality, this loss is even lower because the air curtain can be turned on when the door is still closed, but no more detailed calculations have been done yet. The loss is comparable in size with what is reported in the air curtain literature.

In these studies the influence of the low air plane temperature (it can be considerably below 0°C after a flight) and the radiative cooling has not been considered. It is more important when considering the overall heating power but less important when comparing situations with and without air curtain.

Figure 15 shows the temperature distribution in the door plane when the air plane of the size of an Airbus A320 is moved through the air curtain. The function of the air curtain is only slightly influenced. Below the wings some cold air can enter the hangar but this is negligible as compared to the energy balance over the whole calculation time.

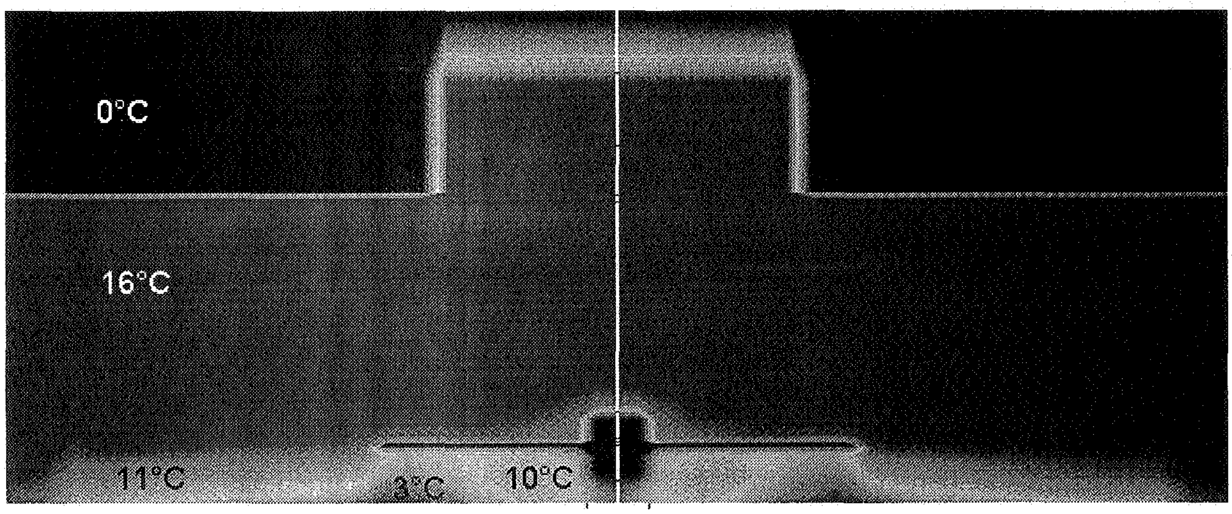

Figure 15: Air plane crossing air curtain in 3-dimensional case with air jet velocity of 18 m/s and external wind of 6 m/s. The calculation was done for only one half of the hangar. Some cold air can enter the hangar below the wings during the actual crossing, but the shielding effect over the whole calculation time is good.

The studies have shown the feasibility of air curtains and the potential for energy saving for such large doors. Whether the pay-back time is short enough to make the investment attractive from the purely economical point of view or not, depends very much on the the practical use of the fans (and on the energy cost). If the fans are used only for very short door openings as discussed here (in the order of 3 minutes), then they are not used a very long time (assuming 10 openings per night lasting 3 minutes each, during 120 nights, equals only 60 hours of use); if one door opening process lasts 15 minutes, the fans are used 300 hours, and the investment is more favourable. It is the practical experience of Swissair, that a door opening process is lasting 10-20 minutes. The actual energy saving for such a long door opening process must be investigated separately, because the energy saving, as compared to the case without air curtain, tends to decrease. The loss without air curtain decrease after some minutes when the hangar is filled with cold air, whereas the loss with air curtain remains constant.

5. Conclusions

Simple thermal zonal models and CFD models have been applied successfully to the prediction of air flow through very large openings in aircraft hangars.

- The thermal zonal model combined with the gravity wave concept allows the prediction of the inside air cooling after opening of a hangar door. The agreement with the experimental curves is very good in view of the simplicity of the model.
- The temperature recovery time after closing depends on the opening time, the time constant for heat transfer and the auxiliary air heating power.
- The recovery time can be shortened by using high power hot air blowers for a short period of time; the hot air stream should reach floor level. A floor heating system cannot deliver the required power and has a time constant which is too long.
- The CFD calculation yields velocities in the door planes which agree well with the the velocities obtained by the gravity wave concept.
- The CFD results using laminar flow (i.e. no turbulence model) agree well with the observation that the warm air in the volume above the door level is kept inside the hangar. This feature was not obtained using the wide-spread k-ε turbulence model.
- A parameter study was performed to obtain feasible design parameters for huge air curtains in the door plane to reduce heat losses when air planes are entering or leaving the hangar. The 3-dimensional study allows an estimation of the energy saving potential of such air curtains.

Acknowledgements

The work is performed in the framework of the IEA-ECB Annex 26 project "Energy-efficient ventilation in large enclosures" and is financially supported by the Swiss Federal Office of Energy (KWH/OFEN, Hangar project EF CO(93) 006).

We express our thanks to H. Boksberger, Swissair Real-Estate, Zurich Airport, Switzerland, for using the hangar measurement data and we acknowledge the help of F. Florentzou who implemented the zonal model in a simulation tool (LESOCOOL) and made the comparison with the measurements.

References

FLOVENT, 1994. Reference Manual 1.4. Flomerics Ltd., Kingston-Upon-Thames, Surrey, England.

Kiel, D.E., Wilson, D.J., 1986. "Gravity driven flows through open doors". Proc. 7th AIVC Conference, Stratford-upon-Avon, UK, paper 15, 1986.

Lane-Serff, G.F., Linden, P.F., Simpson, J.E., 1987. "Transient flow through doorways produced by temperature differences". ROOMVENT '87, session 2a.

Linden, P.F., Simpson, J.E., 1985. "Buoyancy driven flow through an open door", Air Infiltration Review, Vol. 6, No. 4, 1985.

Chikamoto, T., Murakami, S., Kato, S., 1992. "Numerical simulation of velocity and temperature fields within atrium based on modofied k-ε-model incorporating damping effect due to thermal stratification". Proc. Int. Symp. Room Air Convection and Vent. Effectiveness, Tokyo, 22-24 July, pp. 501-509, 1992.

Patankar, V.S., 1980. "Numerical Heat Transfer and Fluid Flow". Hemisphere Publ., Washington, 1980.

Schaelin, A., Van der Maas, J., Moser, A., 1992. "Simulation of airflow through large openings in buildings". ASHRAE Tr., BA-92-2-4, 1992.

Van der Maas J., Roulet C.-A., Hertig J.-A., 1989. "Some aspects of gravity driven airflow through large openings in buildings". ASHRAE Transactions, Vol. 95(2), pp. 573-583, 1989.

Van der Maas J., Roulet C.-A., 1990. "Ventilation and energy loss rates after opening a window". Air Infiltration Review, Vol. 11, No. 4, pp. 12–15, 1990.

Van der Maas, J., Roulet, C.-A., 1993. "Multizone cooling model for calculating the potential of night time ventilation". Proc. 14th AIVC Conference, Copenhagen, Denmark, 21-24 September, 1993.

Wilson, D.J., Kiel, D.E., 1990. "Gravity driven counterflow through an open door in a sealed room". Bldg. and Environment, Vol. 23, No. 4, pp. 379-388, 1990.

Implementing the Results of Ventilation Research
16th AIVC Conference, Palm Springs, USA
19-22 September, 1995

Ventilation and Air Movement within Factories. A Comparison of CFD Predictions with Measured Data

P J Jones*, R Waters **, G Powell*, C Byabagambi***

* The Welsh School of Architecture, University of Wales, Cardiff, UK
** Design Flow Solutions Ltd, UK
*** British Gas Plc, UK

Ventilation and Air Movement within Factories. A Comparison of CFD Predictions with Measured Data.

P. J. Jones[1], R Waters[2], G Powell[1] and C Byabagambi[3].

In the UK, factory design and construction has undergone significant improvements in the last few years, achieving improved energy efficiency for space heating through reductions in U-values and air leakage. One of the consequences of higher thermal insulation requirements has been an improvement in design detailing which has lead to lower air infiltration rates than previously expected. As air infiltration rates are reduced it becomes increasingly important that fresh air is delivered to the places that it is required, i.e. at occupancy level.

Internal air movement patterns within two modern factories have been investigated using a CFD model (DFS-AIR) during winter time conditions. The air movement patterns have been predicted for a warm air heating system and also a radiant heating system. The pattern of air movement of the factories with the loading door open was also investigated.

The results from the CFD investigation were then compared with measured data obtained from a recent research project that investigated the performance of insulated cladding systems for the same buildings. For the warm air heated factory, air speed and air temperature data was available to produce contour plots of the air stream. For the radiant heated factory the air temperature profile was measured to determine both horizontal and vertical air temperature gradients. Ventilation rate measurements were available for both factories with the loading door closed (constant concentration) and also loading door open (tracer decay).

The work was funded by The Welsh Development Agency, Rockwool Ltd and British Gas plc.

[1] The Welsh School of Architecture, University of Wales, Cardiff.
[2] Design Flow Solutions Ltd.
[3] British Gas plc.

Contact.: G. Powell
The Welsh School of Architecture
University of Wales
Bute Building
King Edward VII Avenue
Cathays Park
Cardiff.
CF1 3AP

Tel: 01222 874000 Ext. 5496
Fax: 01222 874926

Implementing the Results of Ventilation Research
16th AIVC Conference, Palm Springs, USA
19-22 September, 1995

Predicting Indoor Air Flow by Combining Network Approach, CFD and Thermal Simulation

J A Clarke*, J L M Hensen*, C O R Negrao**

*** University of Strathclyde, Montrose St., Glasgow G1 1XJ, Scotland, UK**
**** ESRU PhD Student associated with CNPq-Brasilia, Brazil**

SYNOPSIS

This paper describes a method which aims to generate an overall view of multizone building air flow by integrating methods for bulk air flow analysis, air flow field analysis, and building thermal analysis.
This has been achieved by implementing a computational fluid dynamics approach within the ESP-r building energy simulation environment which already incorporated a nodal air flow network approach.

The current state of the method is demonstrated by a case study. The main conclusion from this is that the integrated method is very promising. Other preliminary conclusions concern the difficulty of finding suitable boundary conditions and numerical values for input parameters.

1 INTRODUCTION

In building energy simulation it is still common practice to assume a uniform distribution of air temperature inside a thermal zone. Thus a room - or other type of building space - is considered to be completely mixed.
From this simplification follows that there is neither information on the spatial distribution of air velocities nor on distribution of air temperature and contaminants within a zone.

Although uniform zone air might be a reasonable assumption for many problems where the focus is on (long-term) energy matters, this simplification is not valid for cases involving relatively strong couplings between heat and air flow or involving relatively strong temperature gradients. The former typically occurs when the strategy to avoid overheating in the summer is to increase natural ventilation. A displacement ventilation system is a typical example of the latter.

Given the increased practical importance of such applications, there is a growing interest in practice and academia to establish prediction methods which are able to integrate air flow prediction and building thermal simulation.

Building energy/environmental prediction based on computational modelling is receiving much attention at the present time: mathematical models, discretisation techniques and numerical methods are being refined, and application know-how is maturing. Building energy simulation (BES), in which the building's distributed capacity and air volumes are discretised (the latter relatively crudely), and computational fluid dynamics (CFD), in which some fluid domain is finely discretised, are two significant development fields.

After outlining some other approaches to predicting zonal air flow, this paper describes the method employed in the current research, which is to combine BES and CFD.

2 PREDICTING ZONAL AIR FLOW

There are several approaches for the prediction of zonal air flows:

Empirical

These approaches use jet, plume and other flow theories to predict certain aspects (typically penetration depth, jet dimensions, etc) of intra zonal air flows. As such they have a limited application area, and there are for instance almost no theories which deal with dynamic aspects nor with buoyancy driven flows (except for some specific cases such as drafts from cold windows (Kriegel 1973)).

Nodal network

In this approach (see eg Inard and Buty 1991) a building space is represented by a number of linked nodes, where the interconnections represent certain flowrate vs pressure relationships (usually based on the empirical approaches above). Obviously this approach can not provide detailed results of the temperature and flow fields. It is hoped however that the results will be sufficient - in terms of energy matters - to describe the bulk flows and the main temperature gradients. The main problems associated with this approach are related to nodal distribution, the pressure flowrate relationships, establishing boundary conditions, and the parameter values.

Computational fluid dynamics

CFD approximates an enclosed space by a series of control volumes. Air flow, turbulence, and energy propagation are represented in each of the control volumes by a series of discretised conservation equations. In principle this is an 'ideal' approach, however there are a number of practical problems such as huge computational burden, theoretical limitations of the turbulence models (especially for the type of low Reynolds flow encountered in buildings), etc.

Table 1 Air flow modelling approaches on offer in the ESP-r virtual building energy modelling laboratory

scheduled infiltration and ventilation rates
high frequency measured infiltration and ventilation rates
nodal network air flow method in stand-alone mode
nodal network air flow method integrated with thermal solver
CFD (2D or 3D, steady-state or dynamic) with fixed boundary conditions
CFD with boundary conditions generated by network and thermal solvers

Despite the associated practical problems, it is felt that CFD is the way forward for predicting intra zonal air flows in a building energy context. In order to enable future research in this area, ESP-r was recently extended to include a CFD algorithm. This is in line with the objective for ESP-r to be a virtual laboratory for building energy modelling issues. In terms of air flow modelling features, the system now offers the possibilities as outlined in Table 1.

3 COMBINING BES, NETWORK APPROACH, AND CFD

Elaborate descriptions of the internal workings of the ESP-r building simulation environment in terms of energy simulation in general can be found in (Clarke 1985) and in terms of simultaneous heat and mass flow simulation in (Hensen 1991). The current paper focusses on an approach for combining building energy simulation, with both nodal network and a CFD approaches to air flow prediction.

At the core of the approach is a method which allows ESP-r's existing network flow model (see eg Clarke and Hensen 1991). to operate in tandem with a CFD algorithm which is fully integrated at the source code level. As explained in another paper (Hensen 1995) ESP-r uses partitioning to couple building heat flow and air flow - and building moisture flow and plant heat flow and plant fluid flow(s) and lighting and electric power and ....- because of the advantages which accrue from problem partitioning.

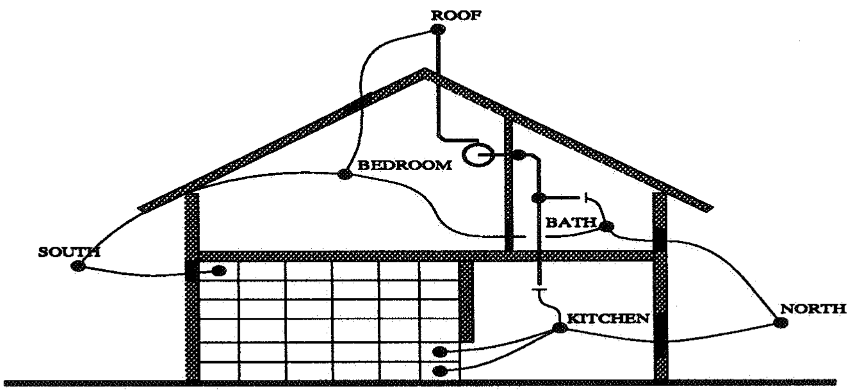

Figure 1: A connected flow network and CFD domain

The integration and implementation details of the CFD algorithm are the subject of another publication (Clarke et al. 1995).
The CFD algorithm is based on the 2D, steady state TEACH system (Gosman and Ideriah 1976), with extensions to enable 3D, transient operation and buoyancy effect. These extensions are reported elsewhere (Negrão 1994).
The implementation of CFD within ESP-r has been enabled at two levels of granularity in order to allow researchers to explore the conflation issue. At the first level, the CFD domain is essentially decoupled with the building/^plant solver (with fully integrated network air flow) passing the intgernal surface temperatures to the CFD solver, which passes back the surface convection coefficients. At the second level, one or more network nodes are replaced by a gridded CFD domain, with the 'snipped' network reconnected to one or more of the CFD cells as illustrated in Figure 1.
The actual coupling details are as illustrated in Figure 2a which shows two possible scenarios: a one-to-one coupling to represent a window crack and a one-to-many coupling to represent a doorway.

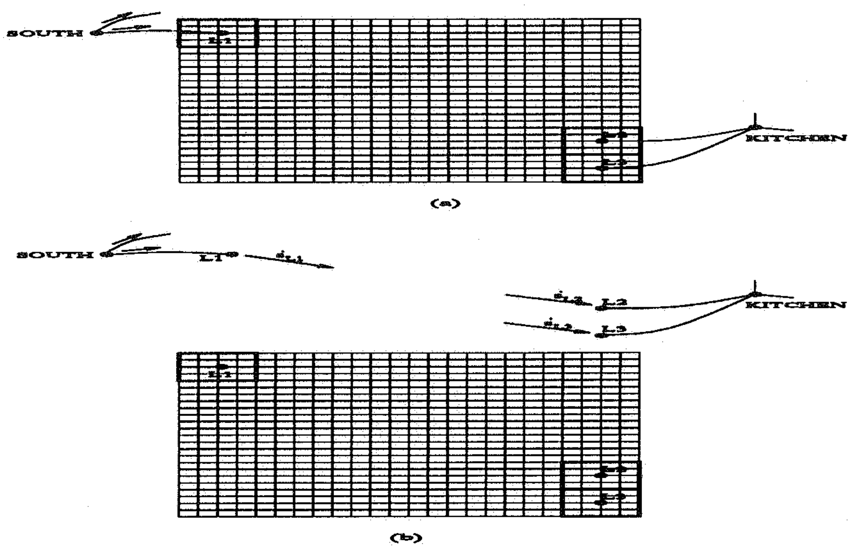

Figure 2: Node-to-grid cell coupling strategies

The nodes L1, L2 and L3 represent the effect of the CFD domain on the network model. To allow each domain solution to be performed separately, the flow network must be decoupled from the CFD domain. Figure 2b shows how the domains are detached from each other. The sources or sink of mass ($\dot{s}_{L1}$, $\dot{s}_{L2}$ and $\dot{s}_{L3}$) on the decoupled network represent the air flow entering or leaving the finely discretised domain. If these sources or sinks of mass are considered known values, the flow network can then be solved. Pressures at the network nodes, including nodes L1, L2 and L3, and flow rates through the network, including the branches SOUTH-L1, L2-KITCHEN, L3-KITCHEN are then determined.

The $\dot{s}_{L1}$, $\dot{s}_{L2}$ and $\dot{s}_{L3}$ quantities which are indicated in Figure 2b are generated by the CFD algorithm. These quantities are the product of the velocity components crossing the interface of the cell, densities and interface cell areas. The source/sink terms are thus computed by the following expression:

$$\dot{s}_k = \sum_j^m \sum_i^n (\rho VA)_{i,j,k}; \quad k = L1,\ L2,\ L3 \tag{1}$$

where m is the number of cells which are connected to a mass flow network node, n is the number of interfaces of each cell (the interfaces at the opening boundary are not included), ρ is the air density, V is the velocity component at the cell interface and A is the interface area. If the flow is entering a cell it is considered positive while if it is exiting it is negative. a +ve $\dot{s}_k$ is therefore a source of mass and -ve a sink.

Operating separately, but in tandem, the solution of the CFD domain is carried out using the BES-side generated boundary conditions: imposed velocities (momentum) within the coupling branches (SOUTH-L1, L2-KITCHEN and L3-KITCHEN). This requires knowledge of flow direction in order to determine the correct coupling point. In the current case the velocity is determined from the network-side flows (as computed for SOUTH-L1, L2-KITCHEN and L3-KITCHEN) divided by the product of sending node density and branch area.

Since the air flow between the coupling points is CFD-side dependent, while the pressures or momentum are network-side dependent, the two solvers must iterate until convergence is reached. Since the number of CFD-side equations for a single zone will usually be considerably greater than the number of equations for the building/plant flow network, the CFD-side controls the iteration - i.e. the network solution is initiated and completed for each CFD iteration.

3 CASE STUDY

The following example is intended to indicate the potential of the new method and demonstrate the expected magnitude of the differences in predictions between the combined approach and the network-only approach. The case studied is the house problem of Figure 1 with only relative simple models and coarse grids applied to allow investigation of the CFD network connection strategies. The two cells located at the openings are connected to two flow network nodes, one external (south) and one located within the kitchen. Initially, buoyancy effects are not considered. The wind induced pressures at the external node are evaluated by means of pressure coefficients which differ with surface location. A non-linear relationship between mass flow rate and pressure difference is defined to represent the connection between flow network nodes and CFD cells:

$$\dot{m} = 0.65\ A\ \sqrt{2\ \Delta P}. \qquad (2)$$

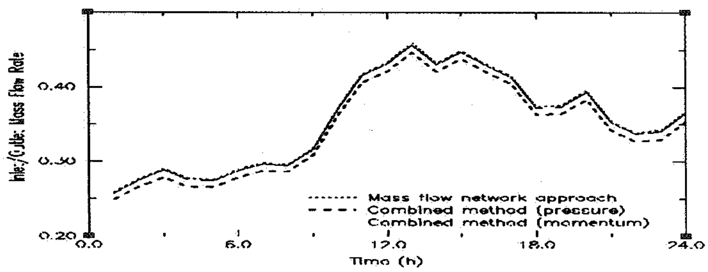

Figure 3: Mass flow rates - buoyancy not included.

Convergence of the CFD domain is only possible if the convergence criteria of the network domain is of the same order of magnitude. Low linear under-relaxation factors for the CFD momentum equations ($\alpha = 0.1$) were necessary to avoid boundary condition oscillations (when pressures and momentum as evaluated by the flow network). Approximately 600 iterations were necessary for a simulation which required approximately 200 iterations for a CFD only model.

In order to compare the combined model with the network flow approach, the flow network as shown in Figure 1 was simulated. A simulation was performed for a day in which the wind vector would induce a pressure at node SOUTH which was higher than that at node KITCHEN, giving a west to east air flow. The two boundary nodes (SOUTH AND KITCHEN) considered above are now connected to node LIVING.

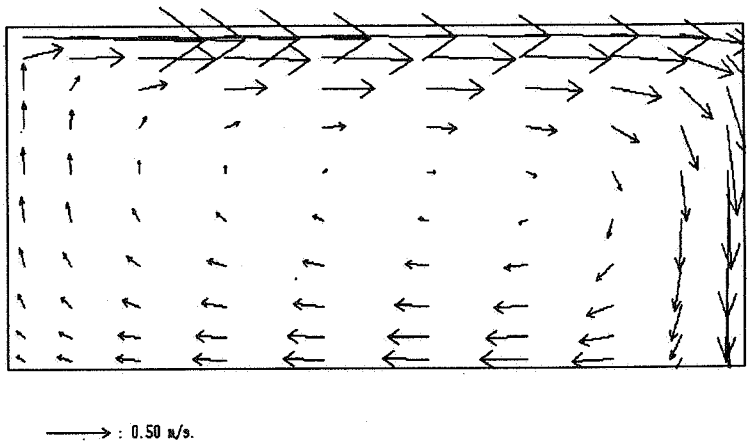

Figure 4: Velocity field - buoyancy not included

The LIVING node then represents the entire pressure field of the zone and no stack effect is considered. Figure 3 shows the differences between the air flows evaluated by the network method and by the combined method. As can be seen the results are similar.
Figure 3 shows two sets of results for the combined approach, representing two boundary condition types: imposed pressure and imposed momentum. Only the latter is considered in the current paper.

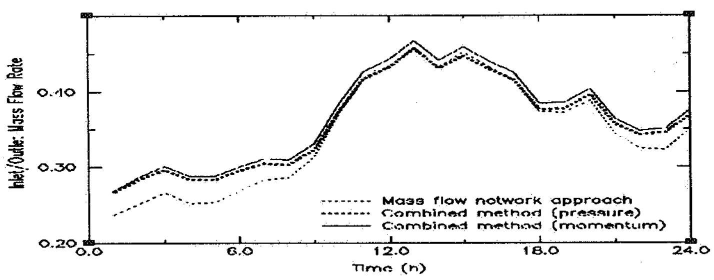

Figure 5: Mass flow rate - buoyancy included

Buoyancy effects are now introduced in order to investigate the effect of natural convection on the flow. The difference in height between nodes SOUTH and KITCHEN induce stack pressures at nodes L1, L2 and L3. As expected, the flow is affected by natural convection. The inlet fresh air produces a recirculating flow inside the zone for either kind of boundary condition. This promotes a higher inlet air flow to the room as evident in a comparison of the flow rates of Figures 3 and 5: in the latter case the differences are more pronounced at the beginning and end of the day. At these times, the outside temperature is lower than the wall surface temperatures and natural convection is more significant. During other periods, the ambient temperature approximates to the wall surface temperatures and the buoyancy effect disappears.

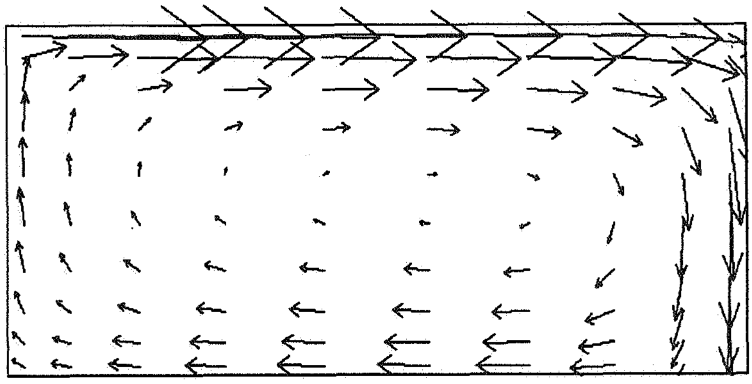

Figure 6: Velocity field - buoyancy included

Figure 6 shows the predicted velocity field. The buoyancy induced flow recirculation is not so evident, although the velocity is higher when buoyancy taken into account. For 3-D transient cases, convergence was not obtained for the case when buoyancy effects are included. The reason for this is the subject of further investigation.

4 CONCLUSIONS

A method has been implemented within ESP-r by which BES and CFD techniques are coupled. Preliminary studies indicate the advantages of this combined approach when compared with the network approach, even with relatively simple CFD models. It should be stressed that currently the main focus is on enabling future research (as opposed to achieving high accuracy now).

The results obtained thus far indicate that conflation of the two modelling approaches can be satisfactorily achieved by maintaining each method's separate solution algorithm. The two modelling approaches are connected via regions which each approach considers as its boundary condition. The overall system balance is achieved through an iterative procedure. Careful consideration has to be given to how the boundary conditions are implemented, especially for the CFD solution which is sensitive to the specifications of the inlet conditions.

It is felt that inclusion of the CFD approach in ESP-r is again a step further towards a fully integral building appraisal system.

References

Clarke, J.A. 1985. *Energy simulation in building design,* Adam Hilger Ltd, Bristol (UK).

Clarke, J.A. and J.L.M. Hensen 1991. "An approach to the simulation of coupled heat and mass flow in buildings," in *Proc. 11th AIVC Conf. Ventilation System*

Performance held at Belgirate (I) 1990, vol. 2, pp. 339-354, IEA Air Infiltration and Ventilation Centre, Coventry (UK).

Clarke, J.A., W.M. Dempster, and C.O.R. Negrao 1995. "The implementation of a computational fluid dynamics algorithm within the ESP-r system," in *Proc. 4th IBPSA World Congress "Building Simulation '95", Madison, Aug 1995*, pp. ??-??, Int. Building Performance Simulation Association, Madison, WI.

Gosman, A.D. and F.J.K. Ideriah 1976. *TEACH-2E A general computer program for two-dimensional, turbulent, recirculating flows*, Imperial College, London.

Hensen, J.L.M. 1991. "On the thermal interaction of building structure and heating and ventilating system," Doctoral dissertation Eindhoven University of Technology (FAGO).

Inard, C. and D. Buty 1991. "Simulation of thermal coupling between a radiator and a room with zonal models," in *Proc. 12th AIVC Conf. "Air Movement and Ventilation Control within Buildings", Ottawa*, IEA Air Infiltration and Ventilation Centre, Coventry (UK).

Kriegel, B. 1973. "Fallstromungen vor Abkuhlungsflachen in Gebauden und mogliche Schutzmassnahmen," Doctoral dissertation Technical University Berlin.

Negrao, C.O.R. 1994. "Combining mass flow network and CFD approaches," PhD Progress Report, University of Strathclyde, Glasgow.

Implementing the Results of Ventilation Research
16th AIVC Conference, Palm Springs, USA
19-22 September, 1995

Experimental Validation of ASHRAE SPC-129 Standard Method of Measuring Air Change Effectiveness

Francis (Bud) Offermann III, Martin T O'Flaherty, Marc A Waz, Nathan B Erlin

Indoor Environmental Engineering, 1448 Pine St, Suite 103, San Francisco, CA 94109, USA

IMPLEMENTING THE RESULTS OF
VENTILATION RESEARCH

16th AIVC Conference, Palm Springs, USA,
19-22 September, 1995

Experimental Validation of ASHRAE SPC-129 Standard Method of Measuring Air Change Effectiveness

Francis (Bud) J. Offermann III PE CIH
Martin T. O'Flaherty, Marc A. Waz, and Nathan B. Erlin

Indoor Environmental Engineering
1448 Pine street, Suite 103
San Francisco, CA 94109
(415)-567-7700

SYNOPSIS. ASHRAE has developed a draft of a measurement standard, Standard 129, entitled "Standard Method of Measuring Air Change Effectiveness." This standard defines a method of measurement for measuring air change effectiveness in mechanically ventilated spaces, and provides a discussion of how the values of air change effectiveness may be used to demonstrate compliance with ASHRAE 62-1989.

Since Standard 129 defines relatively complicated tracer gas procedures for measuring air change effectiveness, the Standard Project Committee 129P and the cognizant technical committee (TC 5.3) have recommended an experimental evaluation of the measurement procedure. The objectives of the proposed work are to obtain information on the practicality of the measurement procedures and to quantify the precision of measured values of air change effectiveness.

The experimental test plan involves measuring the air change effectiveness at ten workstations in an 800 ft^2 office space mock up. Tests will be repeated under fixed temperature and airflow rate conditions ten times for the step up and ten times for the step down (decay) measurement methods. Sulfur hexafluoride will be used as the tracer gas and three different sample collection techniques will be used simultaneously; line sampling, grab sampling, and integrated bag sampling.

This paper presents our experimental protocol to evaluate this proposed new standard. Preliminary results will be presented at the meeting and the complete set of data will be published as an ASHRAE technical paper at an upcoming ASHRAE meeting.

1.0 INTRODUCTION. Today there is an increased interest in ventilation effectiveness being stimulated by the tremendous increase in the interest of indoor air quality and the general lack of information regarding the impact of ventilation effectiveness upon indoor air quality.

An early ventilation effectiveness parameter called "the mixing factor" was used to describe the mixing of outside air in a space as early as 1958 in the United States (ACGIH). This mixing factor was defined as the ratio of the effective air changes to the theoretical or nominal air changes. A 1960 article by Richard Brief suggested that the mixing factor "may vary from 1/3 to 1/10." He further cautioned that a mixing factor of 1/10 be used by individuals "not particularly familiar with the efficiency of air mixing within enclosed spaces." An early tracer gas study by Peter Drivas, reported mixing factors of 0.3 to 0.7. Following these early recommendations and experimental studies many researchers have cited values in this range when discussing outside air mixing factors.

However, it should be noted that the rather low mixing factor values reported in the Drivas study were obtained in laboratory test spaces with very high air exchange rates (e.g. 13-15 air changes per hour) where we would expect there to be difficulties in achieving good mixing conditions. Yoshiaki Ishizu noted in a 1980 paper that when the outside air flow rate "divided by the volume of the room increases, the mixing factor becomes smaller."

While we now have considerably much more experimental data regarding mixing of outside air in buildings, it is still just a drop in the bucket with perhaps less than a dozen building studies under very specific operating conditions and done using different measurement protocols. The little data available today suggests that for office systems operating at minimum outside percentages the mixing of outside air <u>in rooms</u> gives rise to ventilation rates not substantially different from that if there was perfect mixing (e.g. within 10-30%). Rather less data are available regarding mixing of outside air at the air handler although there have been reports of differences of as much as 30% as compared to perfect mixing. Some measurements of European non-recirculating displacement ventilation systems have reported air exchange rates in the occupied zone up to 30% higher than those predicted by perfect mixing.

Thus, while the impact of mixing upon the distribution of outside air may not be as significant as previously held (e.g. mixing factors of just 1/10 to 1/3), the possibilities of actual air exchange rates being even 20-30% less than that calculated assuming perfect mixing is sufficient to inspire the development of models to predict performance. The development of these models should be an exciting dance between the empirical researchers who provide the test data upon which the theoretical researchers may validate and improve their models. A standard measurement protocol for collecting field or laboratory data is desirable since it will provide a larger and more reliable data set for model validation and thus expedite the progress of the model development process.

Further driving the increased interest in ventilation effectiveness is the fact that this concept is connected to minimum outside air requirements set forth in the current ASHRAE Standard 62-1989, "Ventilation for Acceptable Indoor Air Quality." The minimum ventilation rates contained within Table 2 of Standard 62-1989, are based upon an assumption that the outdoor air being delivered to the space is perfectly mixed with the indoor air.

To this end, ASHRAE has developed a draft of a measurement standard, Standard 129, entitled "Standard Method of Measuring Air Change Effectiveness." This proposed standard defines a standard method of measurement for measuring air change effectiveness in mechanically ventilated spaces, and in Appendix B provides a discussion of how the values of air change effectiveness may be used to demonstrate compliance with ASHRAE 62-1989.

Since Standard 129 defines relatively complicated tracer gas procedures for measuring air change effectiveness, and is based upon the experience of a small number of researchers, the

Standard Project Committee 129P and the cognizant technical committee (TC 5.3) have recommended an experimental evaluation of the measurement procedure as defined in the RFP "Validation of Standard 129 - Standard Method of Measuring Air Change Effectiveness." The project being described here is in response to this RFP.

2.0 STUDY OBJECTIVES. The objectives of the proposed work are:

1.) to obtain information on the practicality of the measurement procedures in the draft of Standard 129 and to obtain recommendations that can be used to improve future versions of the standard; and

2.) to quantify the precision of measured values of air change effectiveness, when the measurement procedures specified in the draft of Standard 129 P are utilized.

3.0 TEST PROTOCOL. The following is our technical plan to conduct the work requested in 891-TRP. The following is a description of each of the tasks together with a description of our test facilities and instrumentation we propose to dedicate to this research project.

3.1 Task 1. Test Space Preparation. We will use a specially prepared test room that meets the criteria stipulated in Section 4 of the draft Standard 129. In addition the test space will be prepared to meet the following additional requirements:

a.) furnished with typical office furniture including desks, tables, chairs, and partitions.
b.) contain functional lighting and office equipment.
c.) contain 10 workstations and a floor area of at least 800 ft^2.
d.) have at least one adjoining indoor space.
e.) equipped with a typical air distribution system with multiple supply outlets and return grilles at or near ceiling height.

<u>3.1.1 Test Space Description</u>. The test space is located on the second floor of a three story office building. Indoor Environmental Engineering's offices and laboratory are located on the first floor. The floor area of the test space is 800 ft^2 and has a slab-to-slab ceiling height of 10.9 feet. A suspended ceiling is positioned 29 inches below the ceiling slab and holds the fluorescent lighting fixtures and supply air diffusers and return air grilles. The test space is adjoined on three sides by other indoor spaces and an exterior wall on one side. The test space has been pressurized to identify any leaks between the space and adjacent spaces and these leaks have been sealed. An instrument room for the tracer gas equipment and data acquisition system are located in the adjoining space immediately to the north of the test space.

<u>3.1.2 Test Space Furnishings</u>. The test space is furnished with 10 workstations as depicted in Figure 1. Each work station is equipped with a desk, chair, and partitions. In addition to these requested furnishings we propose to add simulated heat loads in place of real occupants and computer equipment. We propose to add two 100 watt heat loads, each contained within separate cubicle enclosures at each work station. This controlled approach will add a heat load similar to that of occupants and computers, but in a more repeatable and controlled manner. The test space is furnished with six fluorescent fixtures four bulb (four 34 watt bulbs per fixture) which are mounted in the suspended ceiling.

<u>3.1.3 HVAC Equipment.</u> The test space is equipped with a dedicated constant volume air handler which serves only the test space. The air handling unit is a basic fan coil unit suspended from the ceiling. Outside air is delivered to the mixing box where it mixes with return air which is drawn up through the return air grilles in the suspended ceiling. Outdoor air is delivered in a controlled manner by a separate forced air supply. Exhaust air is removed from the space also in a controlled manner by a separate forced air exhaust. Both exhaust and

outside air flow rates are adjustable and the flow rates are monitored by orifice plate flow measuring stations.

Space temperature and supply/return air temperature difference is controlled by a proportional controller which controls an electric re-heat coil in the air handling unit. The supply and return air temperature difference is maintained within 1 °C. This temperature control is important since buoyancy effects are an important factor influencing the mixing of the supply air in the space.

3.1.4 Ventilation System Configuration for Tests. The repeat measurements of air change effectiveness requires that all airstrip flow rates be constant for the entire series of tests. This requirement is important, since one of the objectives of the series of repeat test is to determine the precision of the measurement method, and the flow rates of the air streams is an important variable in determining the air change effectiveness.

For these tests we propose to set the outside air delivery rate to the test space to 200 cfm. This corresponds to the minimum rate of 20 cfm/occupant (i.e. 10 workstations x 20 cfm/occupant) proposed by ASHRAE Standard 62-1989. We have selected this rate since it is under the minimum prescribed rates proposed by Standard 62-1989 that air change effectiveness becomes critical to meeting the minimum ventilation requirements.

We also plan to set the total supply air flow rate to the test space to 600 cfm. This corresponds to a moderate supply air circulation rate of 0.75 cfm/ft^2 and a relatively high outside air percentage in the supply air stream of 33%. A high air circulation rate with a low outside air percentage is not desirable for these tests since it will tend to create a well mixed space. Under well mixed conditions the repeated tests of air change effectiveness will predominantly be just a measure of the precision of the tracer gas sampling and analysis. In order for some of the more stochastic variables related to air mixing to come in to play, it is desirable to create a ventilation scenario where there is less than perfect mixing.

Thus, the relatively high nominal outside air exchange rate in combination with the relatively high outside air percentage proposed for these tests will insure a ventilation scenario that is not atypical of office spaces and is likely to create an air change effectiveness of less than unity.

3.2 Task 2. Instrumentation and Equipment Preparation. We propose to use sulfur hexafluoride (SF_6) gas as a tracer gas for all tests conducted in this study. SF_6 meets all of the criteria stipulated in Section 5.1 of the draft Standard 129. The following is a description of the analytical, sampling and injection equipment proposed for this study.

3.2.1 Tracer Gas Analysis Equipment. We propose to use a pair of gas chromatographs equipped with electron capture detectors. These instruments are highly sensitive and reliable gas analyzers which are microprocessor controlled. The linear measurement range of the instrument is 0.02 ppb to 20 ppb with a precision of ± 3 % of the measured value. We propose to calibrate the analyzer using specially prepared calibration gasses together with a precision gas divider. These calibrations span the range of concentrations (i.e. 0.05 ppb to 20 ppb) we are planning for the tests. All calibration gasses will be prepared to a tolerance of ± 2%.

3.2.2 Tracer Gas Sampling Equipment. As required in Parts 4 and 5 of the RFP Scope of Work, three different air sampling methods are required:

- direct sampling into the analyzer
- grab sampling followed by subsequent analyses and
- time integrated sampling with sample bags followed by subsequent analyses

The following describes the equipment we propose to use for each of these three sampling techniques.

• Direct sampling into the analyzer. We propose to use the microprocessor controlled multi-port sampling manifold built into each of the two chromatographs. Each chromatograph is capable of sequentially sampling from up to 9 different locations. We are proposing a total of twelve sample locations (i.e. breathing level at 10 workstations, in the single exhaust air stream at one location, and in the outside air stream). The simultaneous use of two gas chromatographs will allow for a sample analysis frequency of one sample every 45 seconds. We propose to use special 4mm OD, 3mm ID nylon tubing for transport of tracer gas samples to the chromatograph. This type of tubing, unlike Teflon tubing, is not prone to adsorbing or desorbing tracer gas from the sample.

• Grab sampling followed by subsequent analyses. We propose to collect grab samples using a 60 cc polypropylene slip-tip syringes. As with the direct sampling method, we propose to use special 4mm OD, 3mm ID nylon tubing for pump assisted transport of tracer gas samples to the syringe samplers. Samples will be withdrawn from the sample lines through a gas tight needle septa using a custom built 12 syringe sampling unit. The syringe samples will then be analyzed by installing the sample bags directly onto the inlet ports of chromatograph, which will sequentially transfer the samples for analysis.

• Time integrated sampling with sample bags followed by subsequent analyses. We propose to use 1 Liter Tedlar (2 mil) bags to collect time integrated samples. Air samples will be transported into the bags at a constant rate using 33 RPM peristaltic pumps fitted with Norprene tubing. The sample flow rates of the peristaltic pumps will be set for a constant sampling rate in the range of 3 to 5 cc/min.

<u>3.2.3 Tracer Gas Sampling Locations.</u> We are proposing to measure the tracer gas concentration at seated breathing height (i.e. 4 feet above the floor) at each of the ten workstations. The 4 mm OD nylon sampling lines and integrated bag samplers will be attached to a guide wire strung between the floor and sealing at each workstation seat. We will also measure the tracer gas concentration in the exhaust air stream at a position downstream of the orifice plate (i.e. to insure good mixing) and upstream of the exhaust fan (i.e. to avoid effects from any air leakage). The 4 mm OD nylon sampling lines and integrated bag samplers will be attached to a multipoint air sampling manifold installed in the exhaust duct in a manner to insure a representative sample of the tracer gas concentration as required in Section 5.4.4 of the draft Standard 129. The use of sealed PVC pipe will insure that the exhaust air concentration is not effected by air leakage.

<u>3.2.4 Tracer Gas Injection Equipment</u> . We propose to use a mass flow meter to provide a constant injection rate of tracer gas. The mass flow controller has a measurement precision of 0.2% full scale which exceeds the requirements set forth in Section 5.3.1 of the draft Standard 129. The inlet to the mass flow controller will be connected directly via 1/4 OD copper tubing to a pressure regulated supply of tracer gas from a compressed tank of tracer gas (i.e. 0.1% pure SF_6 balance air). The outlet of the mass flow controller will be connected directly via 1/4 OD copper tubing to a multipoint tracer gas injection manifold installed in the outside air upstream of both the outside air fan and orifice plate flow monitoring station in a manner to insure a uniform concentration of the tracer gas in the outside air stream. The data acquisition system will read the analog output of the mass flow controller once per minute in order to provide a detailed record of the tracer gas injection rate into the test space. We will validate the calibration of the mass flow controller using a bubble meter once before and once after the series of tests.

<u>3.2.5 Air Flow Rate Measurement Equipment</u>. We will measure the outside, exhaust, supply, and return air flow rates using methods described in ASHRAE 111-1988, ASHRAE 41.7-

1984, and ASHRAE 41.2-1987. We will monitor the exhaust and outside air flow rates with orifice plate flow measuring stations. The outside air and exhaust air ducts are six inch PVC pipe which has been specially sealed to be air tight. Orifice plate differential pressures will be monitored with electronic pressure transducers with analog outputs connected to the data acquisition system. We will measure the supply and return air flow rates as required in Section 6.3 of the draft Standard 129 using velocity traverses of the ducts. We will measure the supply air flow rate from each of the supply air diffusers and return air grilles using an electronic airflow capture hood. The airflow capture hood will be calibrated once before and once after the series of tests using an orifice plate flow measuring station.

3.2.6 Air Temperature Measurement Equipment. We will monitor the temperature in the supply and return air streams using resistance temperature detectors (RTD's) positioned in the air streams to provide a representative measurement of the air temperature.

3.2.7 Data Acquisition System. We will use an 12-bit 8-channel A/D converter (Strawberry Tree) connected to a Macintosh personal computer. As described in the above sections this data acquisition system will be used to collect once per minute the tracer gas injection rate, the outside air, exhaust air, and supply air flow rates, and the supply and return air temperatures. The accuracy of the data logger is ± 0.2 % of reading. Data will be backed up on hard disc as well as displayed in real time on the computer screen to facilitate monitoring of the test data during the tests. Tracer gas data will be collected by a separate personal computer connected to the chromatographs.

3.3 Task 3. QA/QC Measurements.

The QA/QC checks of the measurement system performance described in Sections 5.2.2 through 5.4.4.2 of the draft Standard 129. These QA/QC tests include the following tests:

- 5.2.2 Tracer Gas Analyzer Precision and Stability
- 5.2.3 Tracer Gas Analyzer Calibration
- 5.3.1 Tracer Gas Injection Rate Stability
- 5.3.2 Tracer Gas Injection System Leak Check
- 5.4.1 Sample Tubing Check
- 5.4.2 Grab Sampling Check
- 5.4.3 Time Integrated Sampling with Sample Bags Check
- 5.4.4 Representative Sampling from Airstreams Check

These QA/QC tests will be conducted once prior to any of the test space air change effectiveness measurements and once following the test space air change effectiveness measurements.

3.4 Task 4. Well Mixed Chamber Tests.

We propose to conduct the well mixed chamber tests as described in Section 5.7 of the draft Standard 129 four times as required in the RFP (Scope Item #3). We propose for these tests to use a small cubicle chamber with an air volume of 2 m^3. The size of this chamber will insure that the air samples withdrawn from the test chamber must not exceed 0.01 chamber volumes per hour as required in Section 5.7 of the draft Standard 129. The chamber is fabricated from plywood and is lined on this inside with 6 mil polyethylene which is sealed with an adhesive to the plywood to form an air tight enclosure.

We propose to supply the chamber with 1.0 air changes per hour of tracer free air at a constant rate. The outside air and exhaust air ducts are three inch PVC pipe which has been specially sealed to be air tight. Orifice plate differential pressures will be monitored with electronic pressure transducers with analog outputs connected to the data acquisition system. The data acquisition system will read the orifice plate pressure drops once per minute in order to provide a detailed record of the air flow rates into and out of the test chamber. A pair of mixing fans in the chamber will be used to insure complete mixing of the tracer gas in the chamber. As required in Section 5.7 of the draft Standard 129 the concentration of tracer gas will be monitored at eight locations in the chamber selected to be in the centroids of eight equal volumes of air. The tracer gas concentration will also be monitored in the exhaust air stream using a multipoint air sampling manifold installed in the exhaust duct in a manner to insure a representative sample of the tracer gas concentration as required in Section 5.4.4 of the draft Standard 129.

All three sampling methods (i.e. direct, grab, and integrated bag samples) will be performed simultaneously during the four repeated measurements of a tracer step up test and the four repeated measurements of a tracer decay test. These tests will be completed prior to any of the test space air change effectiveness measurements.

3.5 Task 5. Ten Repeated Step Up and Decay Tests.

We propose to conduct ten repeated step up and step down tests as described in Scope Items #4 and #5 of the RFP. The test space and instrumentation/equipment will be configured as proposed in Tasks 1 and 2. All three sampling methods (i.e. direct, grab, and integrated bag samples) will be performed simultaneously during these repeated tests. Internal heat loads, all air stream flow rates, and supply and return air temperatures will be kept constant for the entire series of tests within the limits specified in the draft standard.

4.0 REFERENCES

1. ACGIH
"Industrial Ventilation"
American Council of Governmental Industrial Hygienists, 5th ed,1958, pp 2-2.

2. Brief, R.
"Air Engineering"
April, 1960, pp 39-41

3. Drivas, P.
Environmental Science and Technology, V6, No. 7, July, 1972.

4. Ishizu, Y.
Environmental Science and Technology, V14, No. 10, July, 1980.

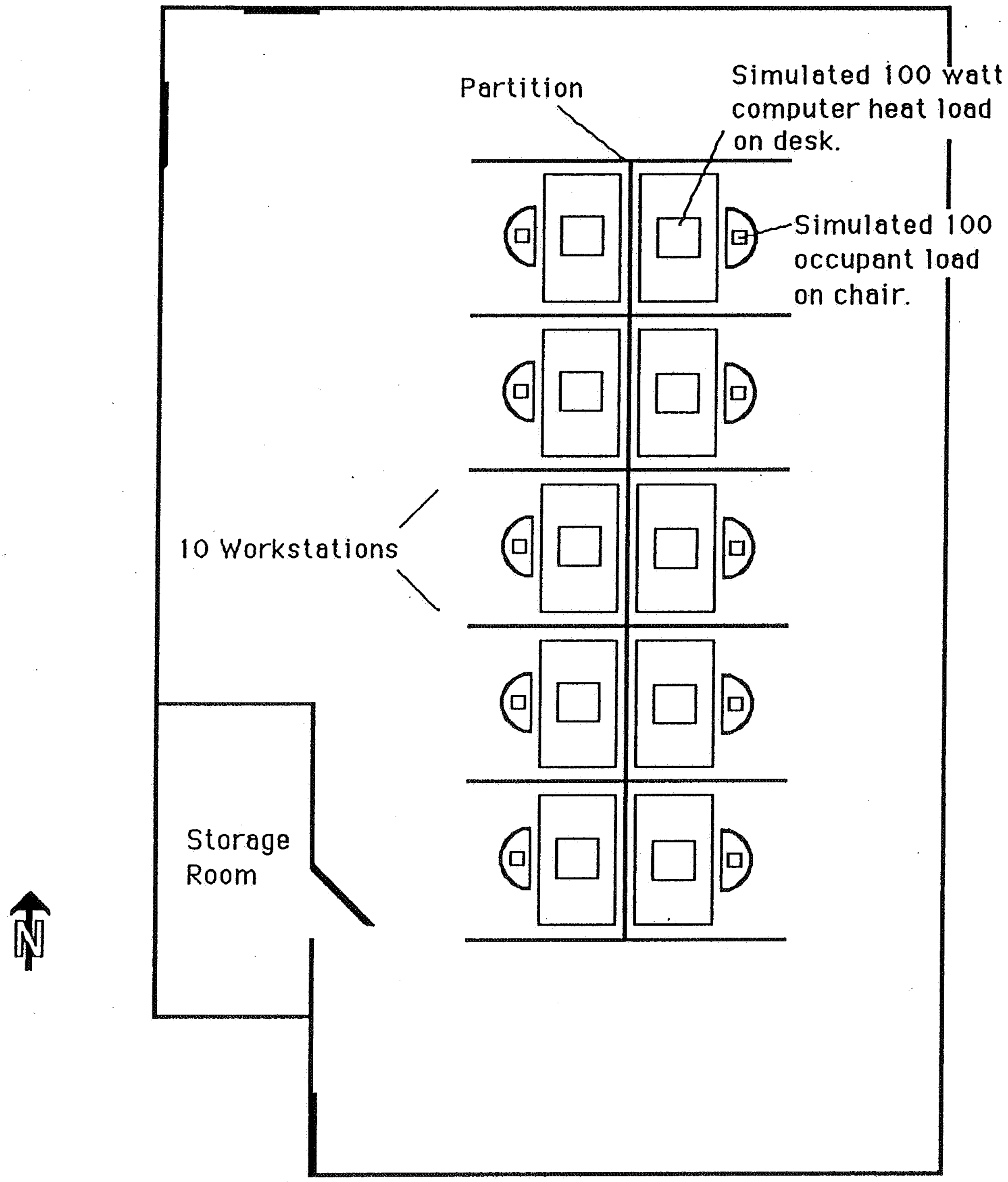

Figure 1. Floor plan of test space depicting the location of ten workstations with simulated people and computer heat loads.

Implementing the Results of Ventilation Research
16th AIVC Conference, Palm Springs, USA
19-22 September, 1995

Fan Pressurization Measurements by Four Protocols

Stephen N Flanders

US Army Cold Regions Research and Engineering Laboratory, 72 Lyme Road, Hanover, New Hampshire, 03755-1290 USA

FAN PRESSURIZATION MEASUREMENTS BY FOUR PROTOCOLS

SYNOPSIS

Thirty-one independent fan pressurization measurement series were performed on seven apartments in three family housing buildings at Fort Riley, Kansas, using four protocols (Table 2). The tests followed procedures in new or revised fan pressurization standards by the International Standards Organization (ISO), American Society for Testing and Materials (ASTM) and Canadian General Standards Board (CGSB). In addition, the effect of interzonal flow was considered.

The three standards gave similar results. The tests during windy and calm conditions demonstrated that basic uncertainty calculations give a comparative indication of the quality of the results. The tests addressing interzonal flow did not show a strong influence on airtightness results, based on whether the adjacent units were open, closed, or pressurized at the same level.

LIST OF SYMBOLS

Table 1 Explanation of symbols.

Symbol	Explanation
ACH_{50}	Air flow rate at P_{ref} = 50 Pa per unit of zone volume(1/h)
C	Flow coefficient ($m^3/s\ Pa^n$)
L	Leakage area (m^2)
n	Flow exponent (dimensionless)
P	Pressure difference across the building envelope (Pa)
P_{ref}	Reference pressure difference across the building envelope (Pa)
Q	Air flow rate (m^3/s)
Q_{ref}	Air flow rate at P_{ref} (m^3/s)
Q_4	Air flow rate at P_{ref} = 4 Pa (m^3/s)
Q_{10}	Air flow rate at P_{ref} = 10 Pa (m^3/s)
Q_{30}	Air flow rate at P_{ref} = 30 Pa (m^3/s)
ρ_e	Air density passing through the leaks in the building envelope (kg/m^3)

1.0 INTRODUCTION

1.1 Fan Pressurization Standards

Fan pressurization measurements of building air leakage have long been in use. ASTM [1] first published E-779 in 1981. Canada published CAN/CGSB-149.10 [2] in 1986. Now there are proposed revisions or supplements to each. Recently ISO adopted the soon-to-be-published ISO 9972 [3].

This paper investigates new protocols proposed for CAN/CGSB-149.10 [4] and a proposed blower-door-based standard that supplements E-779, here designated ASTM E-X [5]. These are compared with ISO 9972. In addition this paper touches on protocols for multizone tests.

1.2 Goals of the Experiment

The experiment reported in this paper had two goals: to compare test protocols and to ascertain the airtightness of the buildings tested. The comparison of test protocols was to determine differences in measured values and their statistical uncertainties, as calculated by each protocol. The question of airtightness of the buildings tested is of importance to the Corps of Engineers [6], which specified that they should have no greater than seven air changes per hour, when tested at a 50-Pa pressure difference.

2.0 PROCEDURES

2.1 Fan Pressurization Protocols

Fan pressurization measurements of airtightness may have a variety of different goals. Testing the airtightness of the building envelope requires that all intentional openings be closed. Testing to characterize a building's probable behavior under natural forces influencing air exchange requires that intentional openings be set to their normal positions.

Each of the protocols tested uses fan-induced air pressure differences across the building envelope to cause a measurable air leakage rate through the envelope. With the information on pressures and air flows, each offers a number of measures of airtightness. ISO 9972 permits pressurization and depressurization; ASTM E-X allows both but encourages depressurization; CGSB requires depressurization.

2.1.1 *Measured Quantities* – All three standards require measurement of air pressure and air flow. All require adjustment of the measured air flow with a density correction to become the corrected air flow at the fan, and a dynamic viscosity correction in the case of ASTM E-X, to adjust the envelope flow to a reference condition. ISO 9972 corrects for dynamic viscosity and density in the airtightness calculation.

ISO and CGSB require a series of pressure-flow measurements at differences in pressure that range between 10 and 60 Pa (ISO) or 15 and 50 Pa (CGSB). CGSB also offers a single-point measurement at 30 Pa. ASTM E-X offers two options, a single-point measurement at 50 Pa or a two-point measurement with 50 and 12.5-Pa pressure stations.

2.1.2 *Airtightness Calculations* – All three standards offer a calculation of a leakage area (L in m^2) which corresponds to the area of an orifice that would result in a corresponding flow at a reference pressure. ISO 9972 cites 4 Pa as a conventional reference pressure, but allows other values. ASTM E-X makes no requirement, but cites 4 Pa as one advocated by ASHRAE [7]. The CGSB calculates Equivalent Leakage Area (*ELA* in cm^2) which is L times 11.57, taken at a reference pressure of 30 Pa.

The leakage area is based on a fit of data for induced pressure differences across the envelope, P in Pa, to measured airflows through the building envelope, Q in m^3/s, to a power law, as follows:

$$Q = C \cdot P^n \tag{1}$$

where C and n are constants determined by performing a linear regression on Eq 1, in the natural logarithm domain. ASTM E-X is designed to diminish the uncertainty of estimating L at P_{ref}=4 Pa. It focuses on a high and a low point that are each the means of multiple data. Under either protocol the leakage area (m^2) is:

$$L = C \cdot P_{ref}^{(n-0.5)} \cdot \left(\frac{\rho_e}{2}\right)^{0.5} \tag{2}$$

where ρ_e is the density of the air coming through the leaks in the building envelope.

Only ASTM E-X offers an index based directly on flow, ACH_{50}, in air changes per hour (1/h), calculated as the corrected flow at 50 Pa divided by the volume of the zone. This is the criterion cited by the Corps of Engineers in its specifications for airtightness.

2.1.3 *Uncertainty Calculations* – The CGSB and ISO documents rely on standard calculations of variance and confidence intervals about a regression. These calculations do not incorporate estimates of bias. Bias is difficult to estimate in field measurements in the absence of independent standards. ASTM E-X uses uncertainty[1] calculations based on estimates of precision and bias, expressed in quadrature, adapted from Sherman and Palmiter [8]

2.1.4 *Multiple Zones* – ISO 9972 and the CGSB document pertain strictly to a single zone. They allow for the opening of interior doors and other impediments to uniform pressure within the zone to create a single zone. Flanders [9] has tried testing interzonal airtightness by a protocol that measured the change in air flow in a zone that maintained a constant pressure while the pressure was varied in the adjacent zone. Such a technique potentially has high uncertainty due to the small flow values obtained and the bias inherent from not being able to assure that all the observed flow passes between the two zones.

Moffat [10] suggested that closing doors and other operable connections between zones, and at the same time opening doors and windows to the outdoors in the adjacent zones, would create a practical measurement of building envelope airtightness in buildings with multiple zones. Such a technique does not by itself account for interzonal flow. In most buildings interzonal flow is as undesirable as air leakage across the envelope's exterior, because it represents paths for fire, sound, and indoor air pollution. ASTM E-X defines the test zone to be "a building or a portion of a building that is configured as a single zone for the purpose of this test method." This is consistent with Moffat's suggestion.

2.2 Test Sites

The fan pressurization tests were performed on three buildings at Fort Riley, Kansas that were under construction, but near completion, as family housing. The tests were conducted in cooperation with the design and contracting agency, the Missouri River Division

---

[1] Defined as the estimate of error from precision and bias errors.

of the U.S. Army Corps of Engineers. Similar buildings were tested previously and found to have ACH_{50} values of less than seven, with an unknown treatment of ventilation openings.

2.2.1 *Building Descriptions* – Each building was of light metal-frame construction with adjacent two-story residential units. There were three types of unit, end units of 276 m^3, middle units of 304 m^3, and a handicap-accessible unit of 287 m^3. Building 44671 was a triplex with one unit of each type. Building 44673 was a duplex with two end units. Building 44675 (Figure 1) was a four-plex with two end units and two middle units.

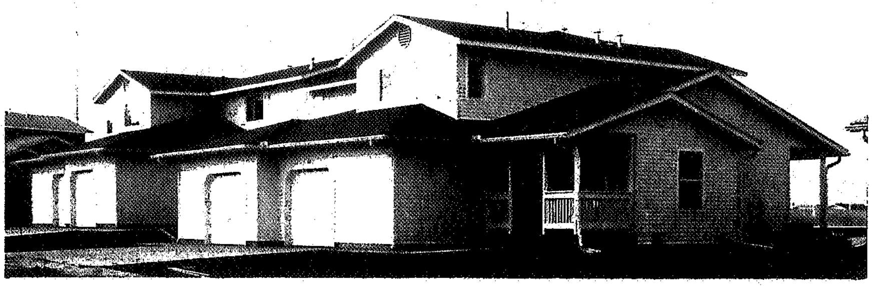

Figure 1. Four-plex family housing unit, Building 44675.

2.2.2 *Test Configuration of the Buildings* – Because of constraints placed on us by the building owner, the dryer vent was taped closed (no dryer was installed) for the tests, but the bathroom and kitchen vent fans were uncovered. This represents the building configured for use, but not a measure of construction airtightness. All doors and windows were latched closed. There was no fireplace. The gas-fired hot water heater was left in operation.

2.3 The Test Cases

The primary factors considered in the study were the differences between protocols, the differences between and within building types, and the effects of wind on precision and bias.

2.3.1 *The Protocols Tested* – In this study the following protocols were tried (Table 2):

Table 2. Summary of protocols use in this study.

Source	Protocol
ISO 9972, CGSB	Regression of P and Q data to calculate L.
ASTM E-X	Two-point measurements of P and Q to calculate L.
CGSB, ASTM E-X	Single-point measurements at 50 or 30 Pa.
ASTM E-X	Adjacent zone open, closed or at equal pressure.

This paper compares the values and uncertainties of L calculated for traditional reference pressure values of P_{ref} = 4, 10, and 30 Pa, using both regression and two-point techniques. For the single-point techniques, the comparison is of ACH_{50} values for different wind and building conditions. For interzonal flow, a comparison is made among ACH_{50} values when the adjacent zone was pressurized at an equal level, when its doors and windows were simply closed, and when its doors and windows were open.

2.3.2 *End or Middle Units* – Testing multiple examples of similar building types allows characterization how consistently the units were built. Comparing different types of units of similar construction allows comparing effects of the different configurations. Only one handicap-accessible unit was tested, so most comparisons were between and among the end and middle units.

2.3.3 *Calm or Windy Conditions* – The tests occurred on two consecutive days. On the first day the wind was at 4.5 m/s with gusts of 6.7 m/s. On the second day the wind was light and variable. Wind has potential to cause bias by shifting the neutral plane caused by wind across the building in such a way that it changes the relative roles of leakage sites during the fan pressurization tests. Wind has the potential to increase measurement imprecision due to the effects of gusts and eddies during the test.

2.4 The Apparatus

The fan pressurization apparatuses were two blower door units. The plug filling the door opening was a steel frame with a urethane-coated membrane sealed against the door jamb with an inflatable tube. The fans mounted facing in or out to conduct pressurization or depressurization. The control units were digital and offered the following level of imprecision in monitoring air pressure and air flow (Table 3), as stated by the manufacturer:

Table 3. Imprecision of instruments.

Measurement	Imprecision
Air flow – Percentage of flow at the test pressure	±3
Pressure difference – Percentage of the mean value of at least five samples.	±1

3.0 RESULTS

3.1 Tests Performed

The following tests were performed, as shown in Table 4. All but four were under depressurization.

Table 4. Number of tests performed by test condition.

	End Units		Middle Units	
Test Condition	Calm	Windy	Calm	Windy
Multipoint, open-adjacent (O)	9	4	2	3
Multipoint, guarded-adjacent (G)	2	—	2	—
Single-point, closed-adjacent (C)	3	2	1	3

In addition, two tests were performed under calm conditions in the handicap-accessible unit.

To obtain data for use in all four protocols, we performed fan depressurization tests with multiple readings at 10, 30, and 50 Pa. Those single-point tests with the adjacent apartment closed were at 50 Pa only.

3.1 Calculated Airtightness

This paper uses ACH_{50} as a means to compare airtightness values as flows at 50 Pa normalized to the volume of the zone tested. This is one means of normalization. Another means, to normalize by unit of exterior envelope area, was not tried. This paper uses L as a means to compare the two-point protocol of ASTM E-X and the traditional multipoint regression protocols of ISO 9972 and CGSB.

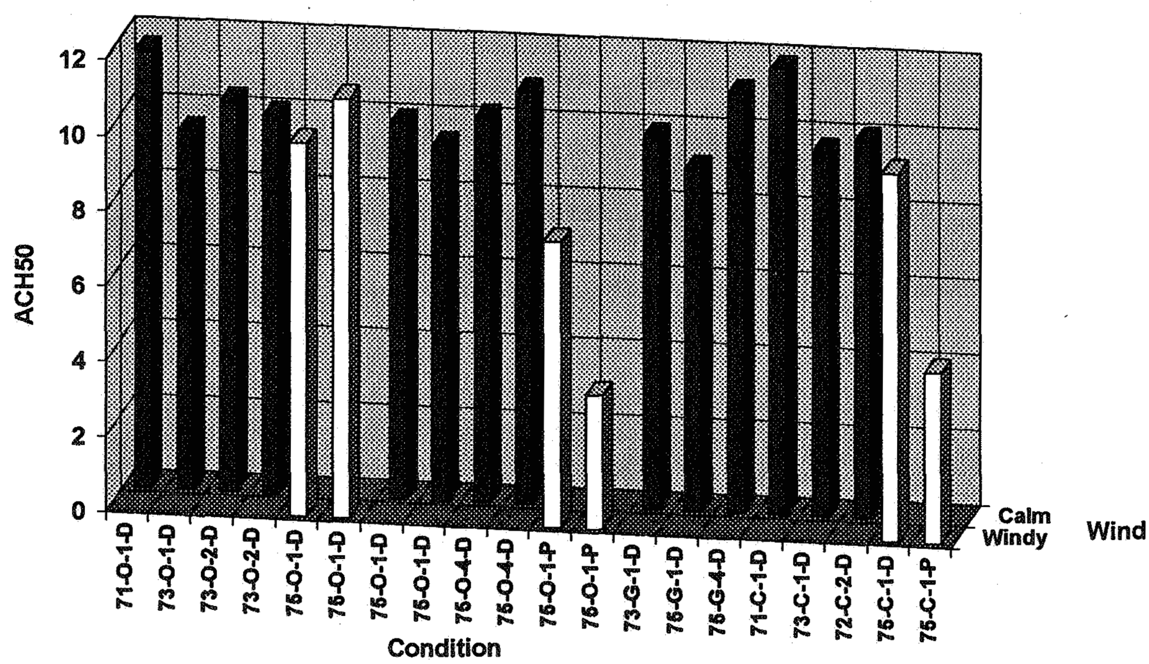

Figure 2. ACH_{50} for all end units measured and all test conditions.

Key: ##-(**O**, **C**, **G**)-#-(**D**, **P**) = Building 446##-(Condition)-Apartment #-(**D**epressurize, **P**ressurize), where Condition is: **O** = multipoint, **open**-adjacent, **C** = single-point, **closed**-adjacent, **G** = multipoint, **guarded**-adjacent.

3.1.1 *ACH_{50} Comparisons* – The greatest bulk of data pertains to the end units tested. Figure 2 illustrates the consistency of the ACH_{50} values obtained in each of the test conditions described in Table 4. These had a coefficient of variation[2] of 18% for the open-adjacent conditions across all units, including replicates. For the closed-adjacent conditions, the coefficient of variation was 10%. Those obtained under windy conditions were the least consistent. The data for the middle apartments show similar consistencies.

[2] Standard deviation divided by the mean, expressed as a percentage.

The median ACH_{50} values for depressurization and ratios between the closed-adjacent and the open-adjacent conditions (C/O) and between the guarded-adjacent and the open-adjacent conditions (G/O) are summarized in Table 5.

Table 5. ACH_{50} median values (1/hr).

	Values			Ratios	
Test Condition	O	C	G	C/O	G/O
End apartment	**10.4**	**10.0**	**10.5**	**1.0**	**1.0**
Middle apartment	**13.8**	**10.1**	**12.5**	**0.73**	**0.95**
Handicap-access	**12.8**	**12.7**	—	**0.99**	—

3.1.2 *Leakage Area* – In calculating the values of n and C from Eq 1 by the two methods, using two points or a multipoint regression analysis and then computing L from Eq 2 for each method, the values for each were in agreement by one digit in the second significant digit. In summary, the median of the ASTM two-point L-values were 99% of the ISO 9972 values for end apartments and 102% for middle apartments.

The median values for the flow exponent n was 0.59±0.00 for the end apartments, as calculated by either ASTM E-X or by ISO 9972. For the middle apartments, the median value for the flow exponent n was 0.56±0.01 for the end apartments, as calculated by either method.

3.2 Uncertainties

Wind was an important factor in the uncertainty calculations of Q_{ref}, C, and n, as illustrated in Table 6. The uncertainties, recommended by Sherman and Palmiter [8], are based on the individual uncertainties of the high and low measurements of P and Q; they are applicable both to the two-point and multipoint protocols. The predicted air flow rates Q_4, Q_{10}, and Q_{30} at P_{ref} = 4, 10, and 30 Pa have much higher uncertainties under the windy conditions observed than under the calm conditions observed.

Table 6. Median uncertainties of Q_{ref}, C, and n for end apartments.

	Uncertainty (%)	
Calculation	Calm	Windy
Q_4	**29**	**110**
Q_{10}	**18**	**72**
Q_{30}	**6**	**26**
C	**28**	**129**
n	**18**	**26**

The coefficient of variation for ACH_{50} in end units was 38% on the windy day and 5%, or less, on the calm day.

3.3 Discussion of Results

3.3.1 *Calculated Airtightness* – The end apartments were studied in statistically significant numbers. The resulting airtightness measurements, whether ACH_{50} or L, were more consistent than would have been predicted for all protocols and wind conditions. Clearly, one would have to take many more independent measurements under windy conditions than under calm in order to achieve reasonable certainty of the result.

Calculations based on data about a single P and an assumed value of $n = 0.65$ would have been wide of the mark, since the actual values varied between $0.59 \geq n \geq 0.55$.

On the windy days the ACH_{50} and flow exponent values were markedly different between pressurization and depressurization for two tests. Furthermore, the regression fit was poor for pressurization tests.

3.3.2 *Uncertainties* – The two-point protocol of ASTM E-X and the traditional multipoint regression protocols of ISO 9972 and CGSB closely agreed about the values of C and n, on which Eqs 1 and 2 are based. Even when the wind conditions were calm, the uncertainty of Q_4 was almost 30%, based on the median percentage values of measurement uncertainties for P and Q in all end apartments tested. This suggests that modeled flows, based on values of P_{ref} in the 4-Pa range, will be approximate. Measurements of ACH_{50} require calm conditions when coefficients of variation of 5% or better can be expected.

3.3.3 *Interzonal Flow* – One expects to see the largest ACH_{50} when the adjacent apartment is open (O), the next largest ACH_{50} when the adjacent apartment is closed (C), and the lowest ACH_{50} when the adjacent apartment has the same pressure (G). The summary in Table 5 does not agree with this hypothesis, nor do individual measurements of the same apartment. However, there are too few data, spanning both windy and calm conditions, to clearly demonstrate meaningful differences among the test conditions.

3.3.4 *ACH_{50} Criterion* – The criterion value of $ACH_{50} = 7$ or less, as specified by the Corps of Engineers [6], was not observed. The specified testing protocol was not specific enough to assure consistent results from different testers. In these tests the openings for the kitchen and bathroom vent fans were not sealed. Under depressurization, back-draft dampers should have minimized the effects of kitchen and bathroom vent openings. Tests of unintentional leakage sites in the construction should occur with such openings sealed.

4.0 CONCLUSIONS

- Protocols from all three standards give similar C and n results. The results are reliable when the data are obtained under calm conditions.
- Tests of similar apartments gave similar ACH_{50} results.
- Tests of multifamily apartment units should be made with adjacent units open to the outdoors to demonstrate the integrity of the construction between units.
- Calculated uncertainties may be optimistic due to autocorrelation of data obtained by current standard protocols.
- Calculations based on extrapolations to 4 Pa will be sketchy even with good data.
- Standards should include an airtightness index like ACH_{50}.

ACKNOWLEDGMENTS

The author thanks Steven Rumbaugh of the Missouri River Division of the U.S. Army Corps of Engineers who helped arrange for the test. He further thanks Greg Krajeski and Erika Peterson who performed the tests.

REFERENCES

1. AMERICAN SOCIETY FOR TESTING AND MATERIALS
"Standard test method for determining air leakage rate by fan pressurization"
E 779-87, 1987, Philadelphia.

2. CANADIAN GENERAL STANDARDS BOARD
"Determination of the airtightness of building envelopes by the fan depressurization method"
CAN/CGSB-149.10-M86, 1986, Ottawa.

3. International Standards Organization
"Thermal insulation – Determination of building airtightness – Fan pressurization method"
ISO 9972, 1995, Geneva.

4. CANADIAN GENERAL STANDARDS BOARD
"Determination of the airtightness of building envelopes by the fan depressurization method"
CAN/CGSB-149.10-M86, Draft 2, July 1994, Ottawa.

5. AMERICAN SOCIETY FOR TESTING AND MATERIALS
"Standard test method for determining airtightness of buildings by blower-door pressurization techniques"
Draft Standard, June, 1995, Point of Contact: Stephen N. Flanders, Hanover, New Hampshire.

6. CORPS OF ENGINEERS
"Air leakage testing," Specification, Fort Riley 226 - Section 13100,
US Army Corps of Engineers, Missouri River Division, 1993, Omaha.

7. ASHRAE
ASHRAE Handbook 1994 Fundamentals
American Society of Heating, Refrigerating and Air-Conditioning Engineers, 1994, Atlanta.

8. SHERMAN, M. and PALMITER, L.
"Uncertainties in fan pressurization measurements"
LBL-32115, Lawrence Berkeley Laboratory, 1993, Berkeley.

9. FLANDERS, S.
"Airtightness Measurement for Multiplex Housing"
CRREL Report 92-2, US Army Cold Regions Research and Engineering Laboratory, 1992, Hanover, New Hampshire.

10. MOFFAT, S.
"Methods for airtightness testing of multi-unit R2000 housing"
Sheltair Scientific Ltd., 1987, Vancouver.

Implementing the Results of Ventilation Research
16th AIVC Conference, Palm Springs, USA
19-22 September, 1995

The Combined Use of CFD and Zonal Modelling Techniques to Aid the Prediction and Measurement of Ventilation Effectiveness Parameters

M W Simons, J R Waters, J Leppard

School of the Built Environment, Coventry University,
Priory Street, Coventry, UK

1 Synopsis

In order that sampling points may be strategically located, it is desirable to have knowledge of the spatial variation of ventilation effectiveness parameters prior to measuring them using tracer gas sampling techniques. The research described in this paper is being carried out to establish a tracer gas sampling strategy as well as to facilitate the prediction of ventilation effectiveness parameters.

The procedure developed requires the division of the internal space into a large number of cells and, by the application of CFD, the mass flow rates between adjacent cells to be established. Software developed at the University to predict interzonal flows has now been interfaced with the CFD software allowing the ventilation effectiveness parameters within each cell of the CFD model to be established.

Investigation of the computed values of the parameters reveals that the characteristics of many adjacent zones are almost identical. A method has been developed to combine small adjacent zones possessing similar characteristics thus allowing the model to be reduced to one of a small number of zones each possessing significantly different properties.

It is demonstrated in this paper that, in the simple mechanically ventilated buildings to which the research has at present been restricted, it is possible to produce reliable contour diagrams of ventilation parameter variations from a small number of properly defined large zones. The large zones found in this way may be used both as a guide to the location of tracer gas sampling points and as the basis of a simplified model for design calculations.

2 List of Symbols

Symbol		**Units**
ε^c	contaminant removal effectiveness	
ε_p	local air change index at point p	
ε_p^c	local air quality index at point p	
$\bar{\tau}_p$	local mean age of air at point p	s
τ_n	nominal time constant	s

3 Introduction

The measurement of ventilation effectiveness parameters requires the injection of tracer gas followed by sampling of the air at various points within the space. However, physical limitations imposed by the equipment used for this work restricts measurement to a relatively small number of points. It is essential therefore that sampling points are selected carefully in order that when the ventilation parameters are measured, they reflect the air movement characteristics of the whole of the space under consideration. This work represents a development of that reported by MW Simons etal [1].

4 Ventilation Effectiveness Parameters

4.1 The most commonly used measures of ventilation, air change rate, and its reciprocal the nominal time constant, τ_n, share the disadvantage of relating to the whole space and not reflecting the variability of air movement within the space. This may be overcome by the use of Ventilation Effectiveness Parameters which may be categorised as follows:

Air change efficiency, which is a measure of how effectively the air present in the room is replaced by fresh air from the ventilation system, and

contaminant removal effectiveness, which is a measure of how quickly a contaminant is removed from a room.

The above parameters are described in detail in the AIVC Technical Reports 28,[2] and 28.2,[3] respectively. A brief explanation of the parameters relevant to this report follows.

4.2 Air Change Efficiency

(I) Local Mean Age of Air, $\bar{\tau}_p$

Local mean age is defined as the average time it takes for air to travel from the inlet to any point p in the room, and may be written as:

$$\bar{\tau}_p = \int_0^\infty t.A_p(t).dt$$

where $A_p(t)$ represents the age distribution curve for air arriving at point p. The local mean age of the air is different for all points, p within the room.

(ii) Local Air Change Index, ε_p

This index characterises the age of air at a point relative to the overall supply rate and is defined as:

$$\varepsilon_p = \frac{\tau_n}{\overline{\tau}_p}$$

It will be seen that the lower the local mean age of air at a point, then the better will be the supply of fresh air to that point whereas a value of local air change index greater than 1 indicates that the point in question is receiving air more efficiently than the average.

4.3 Contaminant Removal Effectiveness

(i) Local Air Quality Index, ε_p^c

Local air quality index is defined as the ratio between the steady state concentration of contaminant at the exhaust duct and the steady state concentration of contaminant at point p in the room.

$$\varepsilon_p^c = \frac{C_e(\infty)}{C_p(\infty)}.$$

Since contaminant may be injected anywhere within the room, for a point p, there are an infinite number of values depending on the location of the source.

(ii) Contaminant removal effectiveness, ε^c

Contaminant Removal Effectiveness is defined as the ratio between the steady concentration of contaminant at the exhaust duct and the steady state concentration of the room.

$$\varepsilon^c = \frac{C_e(\infty)}{< C(\infty) >}$$

This index gives an average performance for the whole room but its value also depends on the location of the contaminant source and hence there are also an infinite number of possible values.

Large values of Local Air Quality Index or Contaminant Removal Effectiveness are indicative of efficient removal of contaminant.

5 Experimental Strategy

5.1 The approach adopted was to select a simple mechanically ventilated space at Coventry University which, following predictive analysis, could be used for corroborative physical measurements. The room chosen was approximately rectangular with dimensions of 5.04m x 4.62m x 2.70m and is shown in Figure 1. Initially CFD analysis was undertaken to establish interzonal air flow rates having first set up a relatively fine grid consisting of 1664 cells. The results of this initial analysis are shown graphically in Figure 1.

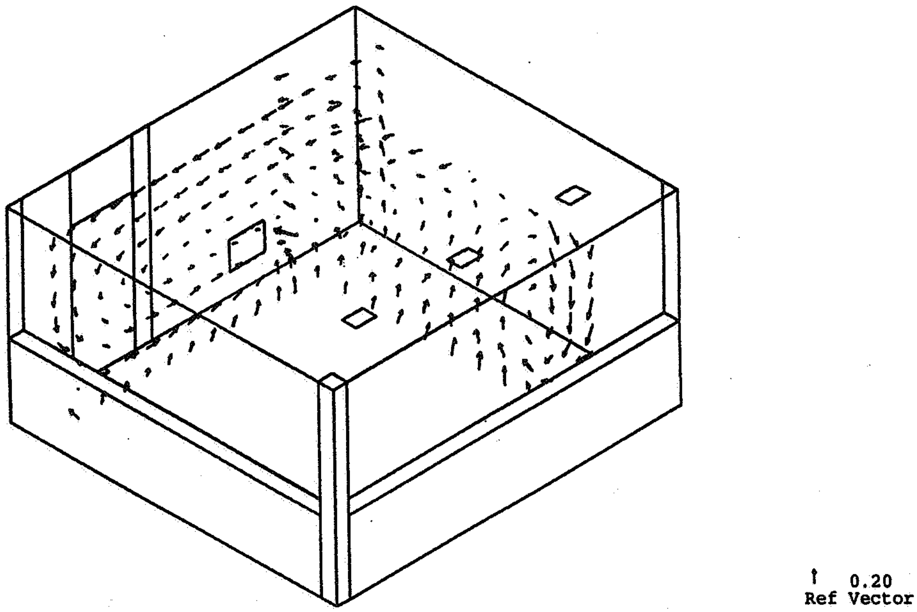

Figure 1 Air movement Pattern (Initial Model)

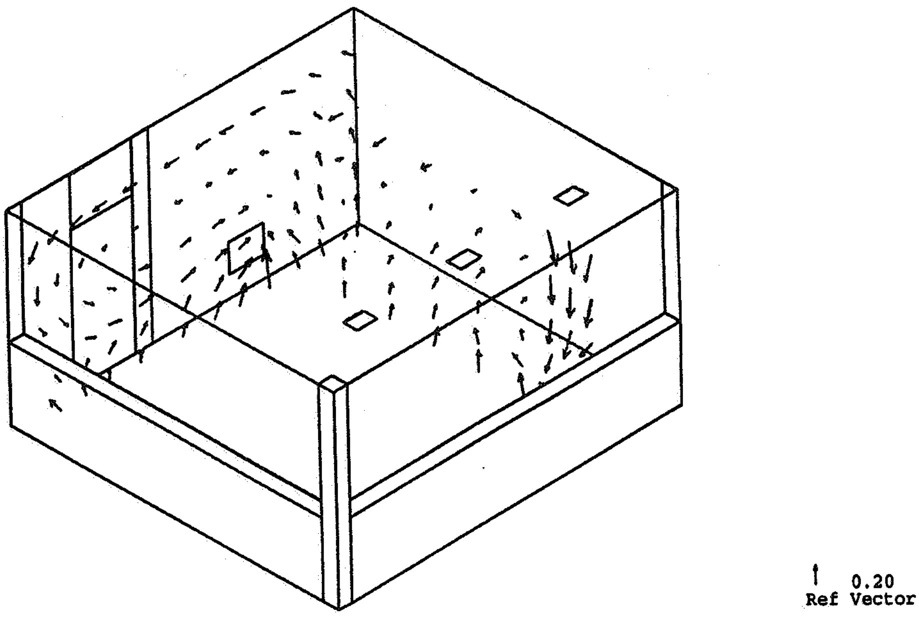

Figure 2 Air movement Pattern (Following First Cell Reduction)

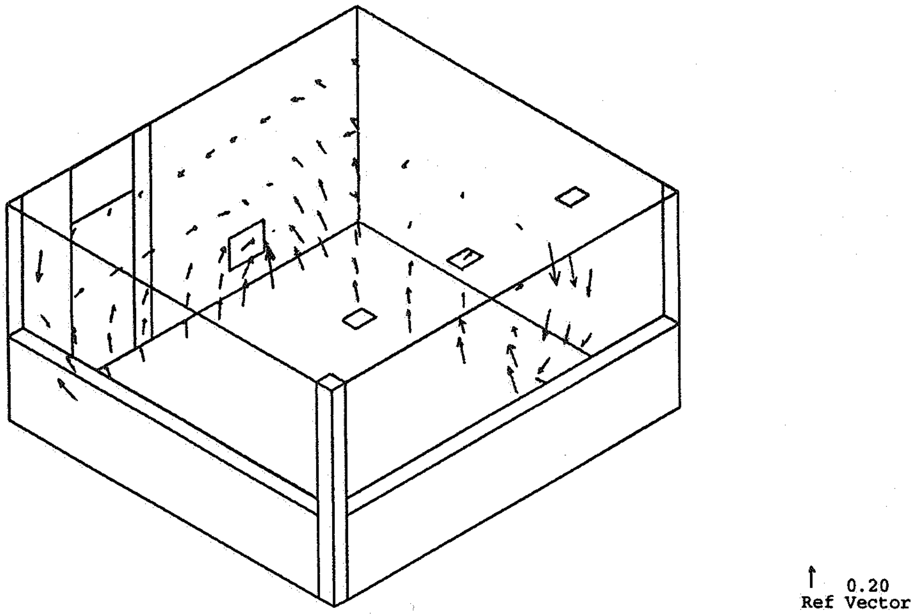

Figure 3 Air movement Pattern (Following Second Cell Reduction)

Since the objective was to reduce the space to a small number of measurement zones, the CFD was repeated for increasingly coarser grids whilst ensuring that the overall air flow pattern within the room remained unchanged. The result of this crudification can be seen in Figures 2 and 3. The latter, which consisted of a 5 x 8 x 11 grid of 440 cells, produced an essentially similar velocity vector pattern as the 1664 cell model, and was therefore used as the basis of the subsequent analysis. Studies have been carried out using a variety of mass flow rates. In this paper the results of a case where the mass flow rates at the 3 inlets were 0.114,0.117 and 0.145 kg/s with inlet air velocities of 1.89,1.95 and 2.42 m/s respectively is considered.

5.2 The ventilation effectiveness and contaminant removal effectiveness parameters can, in principle, be obtained by means of the CFD model. One way of doing this is to inject a contaminant at a suitable location and allow the model to compute the equilibrium concentrations throughout the space. These equilibrium concentrations may then be used to find the desired parameter. However, it is more efficient to convert the velocity vectors found by the CFD model to interzone flow rates, and hence produce the inter zone flow matrix of the of the equivalent multizone model of the problem. All the ventilation parameters may then be found by manipulation of this flow matrix. Furthermore, the equivalent multizone model can be simplified (i.e. "crudified") down to a much smaller number of zones than would be possible with a CFD model.

5.3 The CFD software used for the analysis was 'Flovent' by Flomerics, which does not provide output of interzonal flow data. However, additional software was made available from Flomerics to provide this data, and a conversion algorithm has been written to convert this data to the interzonal matrix of the equivalent multizone model. Unfortunately, the CFD model operates over an overall grid which includes cells of solid material. These cells appear as zones of zero air movement in the multizone model, and so a facility has been included in the conversion algorithm to remove these dead zones. The final flow matrix, after conversion and removal of dead zones, becomes the input to existing software at Coventry University which computes all of the ventilation effectiveness parameters and contaminant removal parameters.

5.4 In order to reduce the number of zones in the above model it has been necessary to establish a strategy for merging zones, i.e. for crudifying the model. The strategy adopted has been to select an appropriate parameter, e.g. local air change index, and combine adjacent zones which have similar values of the index.

The method is to divide the indices into a number of contour bands of appropriate intervals. This may be done by setting an equal band width in which case the number of zones within each band is not equal or by adjusting the band width to ensure an approximately equal number of zones within each band. The merged zone model has a smaller number of zones and hence a smaller interzonal flow matrix which is then used to recompute the ventilation effectiveness parameters.

Results have been obtained for the unmerged model consisting of 440 zones, as shown in Figure 3. Removal of dead zones, i.e. those occupied by solid material, reduced the 440 zone model to 384 zones, and this 384 zone model was subjected to four degrees of merger. In each case, the merging process was based on values of the local air change index. The values for the four cases were fitted into 9, 5, 4 and 3 bands, the band interval being selected in each case to ensure an approximately equal number of the original 384 zones in each band.

6 Consideration of Results

6.1 Figure 4 illustrates the values obtained from the 384 zone model of the local air change index in each of the zones within a section running the length of the room and situated between air inlet and extract grills. The differences between the high values of this parameter in the well ventilated part of this slice through the building and its low values in the central portion are clearly evident in this figure. The same information displayed in contour diagram form via Flovent is shown in Figure 5.

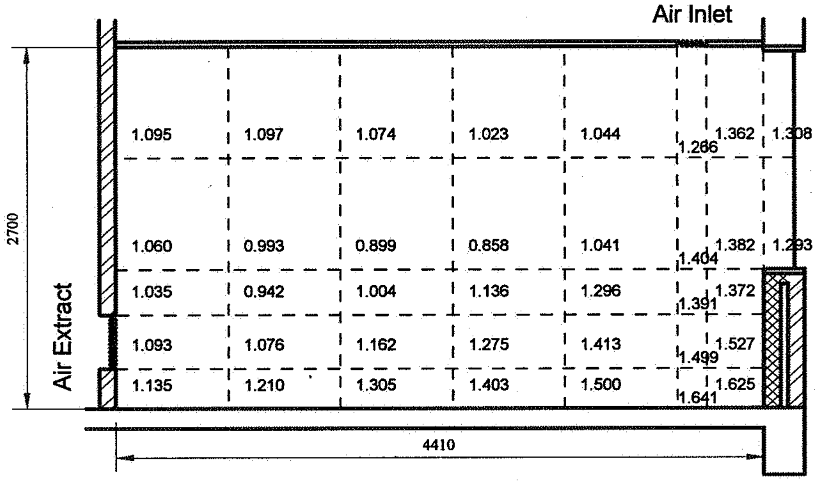

Figure 4 Local Air Change Index Within Each Zone

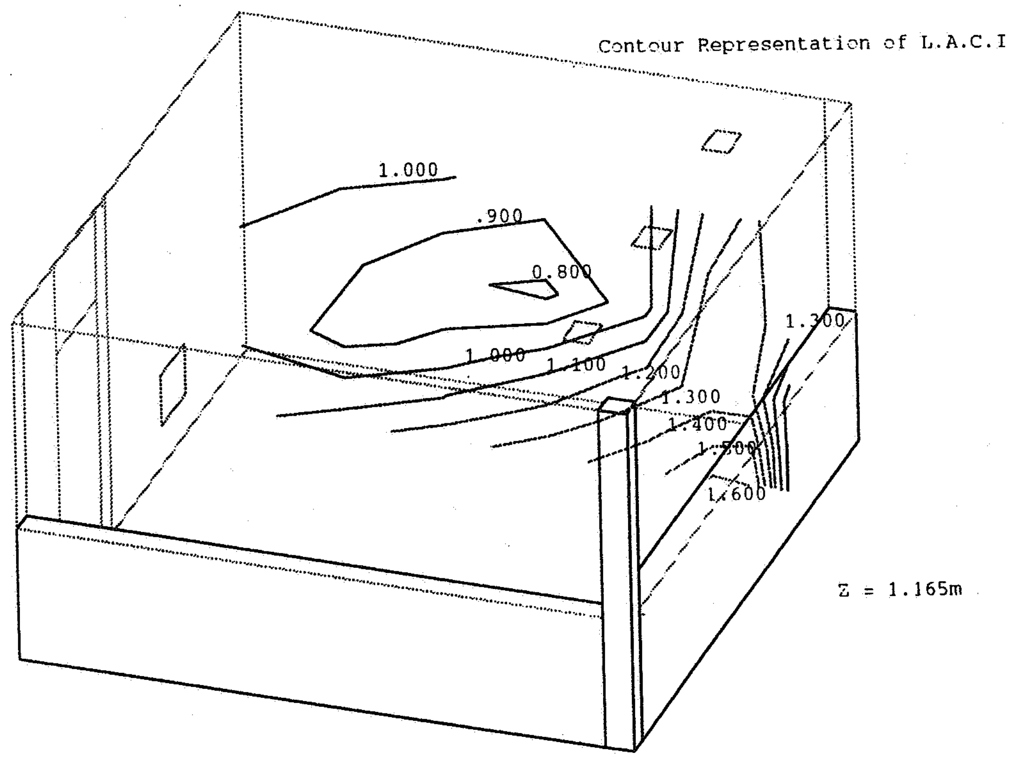

Figure 5 Contour Diagram Representation of Local Air Change Index Within Each Zone

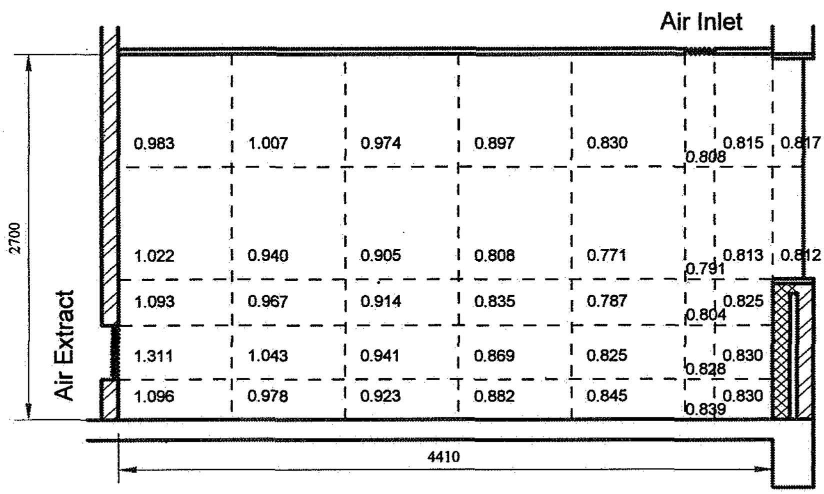

Figure 6 Contaminant Removal Effectiveness Within Each Zone

Figure 6 demonstrates variations in the contaminant removal effectiveness, i.e. how efficiently contaminant is removed from the whole room if subjected to injection into any one of the 37 cells within the slice of the room under consideration. This index of whole room performance indicates how much lower the concentration of contaminant would be if injection was close to the air extract, in which case much of the contaminant is removed directly with little or no circulation, compared with injection close to the inlet in which case contaminant is distributed efficiently throughout the whole space.

The above clearly demonstrate a technique whereby designers may predict spatial variations in ventilation effectiveness The values of a number of ventilation parameters in this and other sections of the space are shown in the poster display associated with this paper.

6.2 For the purposes of this report, zonal merger was based on the criterion of Local Air Change Index. Because of the relationship between Local Air Change Index and local Mean Age referred to in Section 4.2, it will be seen that analysis of the latter would have produced the same bands. Analysis could equally have been based on contaminant removal effectiveness, which would have produced different conclusions

The limits applied in the division into 9, 5, 4 and 3 bands are given below. This resulted in reductions from 384 to 88, 23, 15 and 5 zones respectively. It should be recognised that not all zones within each band are likely to be interconnected and hence it is always probable that the resulting number of zones will be greater than the number of bands into which the space has been divided.

The division of L.A.C.I. into bands for the current study was as follows;

9 bands		**5 bands**		**4 bands**		**3 bands**	
band limits	zones in band	band limits	zones in band	band limits	zones in band	band limits	zones in band
0.81		0.81		0.81		0.81	
	32		73		101		129
0.90		0.94		0.97		1.00	
	50		82		88		128
0.95		1.03		1.08		1.20	
	47		71		94		127
1.00		1.14		1.27		3.90	
	44		80		101		
1.05		1.35		3.90			
	33		78				
1.10		3.90					
	51						
1.20							
	49						
1.35							
	42						
1.60							
	36						
3.90							

The result of the subdivision is shown by way of block and contour diagrams in Figures 7 to 14. These clearly demonstrate how, as zonal reduction takes place:

(I) zones of similar Local Air Change Index are drawn together;

(ii) the basic pattern of the contour lines is retained; and

(iii) as would be expected, merger of the zones results in elimination of the highest and lowest values of the parameter when these are recalculated since the drawing together of similar values produces a result approaching the mean of its component parts.

The latter point is also clearly shown in Figure 15, where the value of Local Air Change Index based on the merged and unmerged cases are plotted for each of the original 37 occupied cells in the Section through the building shown in Figures 7 to 14. Figure 15 also serves to show how the variations in Local Air Change Index are retained throughout the merger process justifying the use of the merged model for the purpose of tracer gas sampling point location strategy.

Key to Figures 7 to 10.
x.xx(yyy) represents local air change index(zone number)

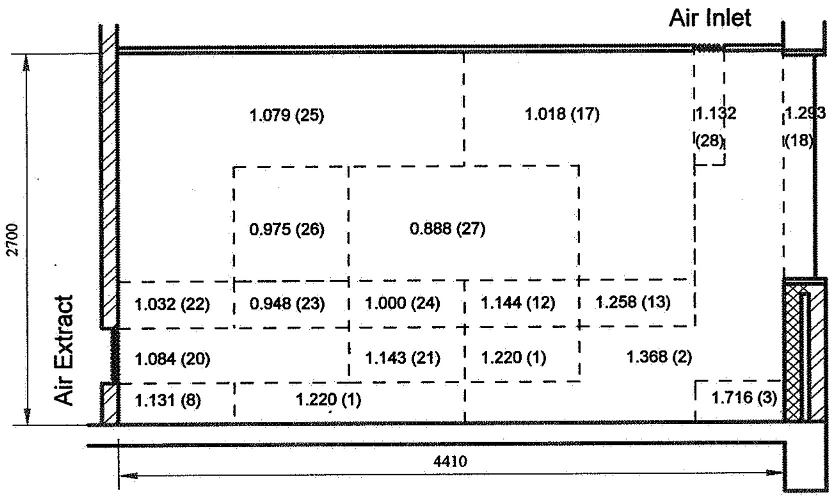

Figure 7 L.A.C.I. Following Reduction to 88 zones

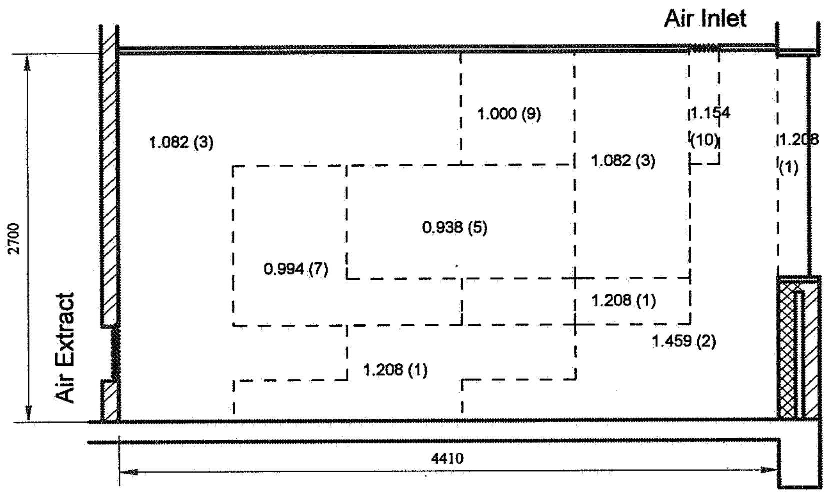

Figure 8 L.A.C.I. Following Reduction to 23 Zones

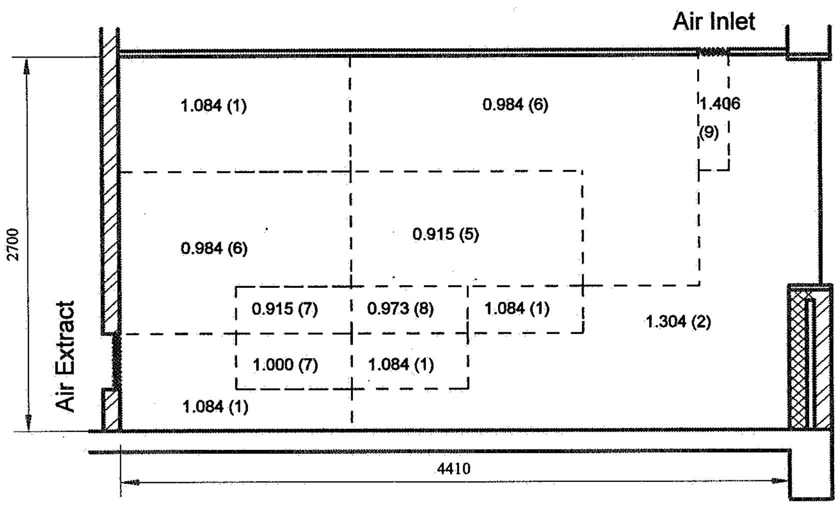

Figure 9 L.A.C.I. Following Reduction to 15 Zones

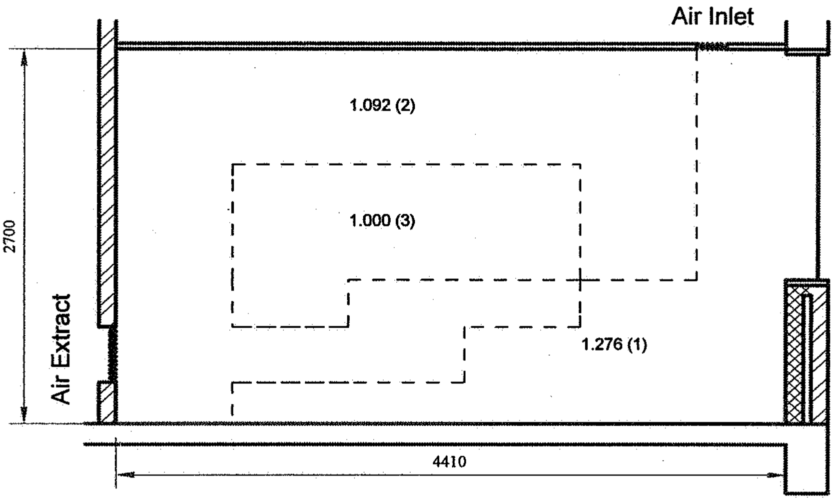

Figure 10 L.A.C.I. Following Reduction to 5 Zones

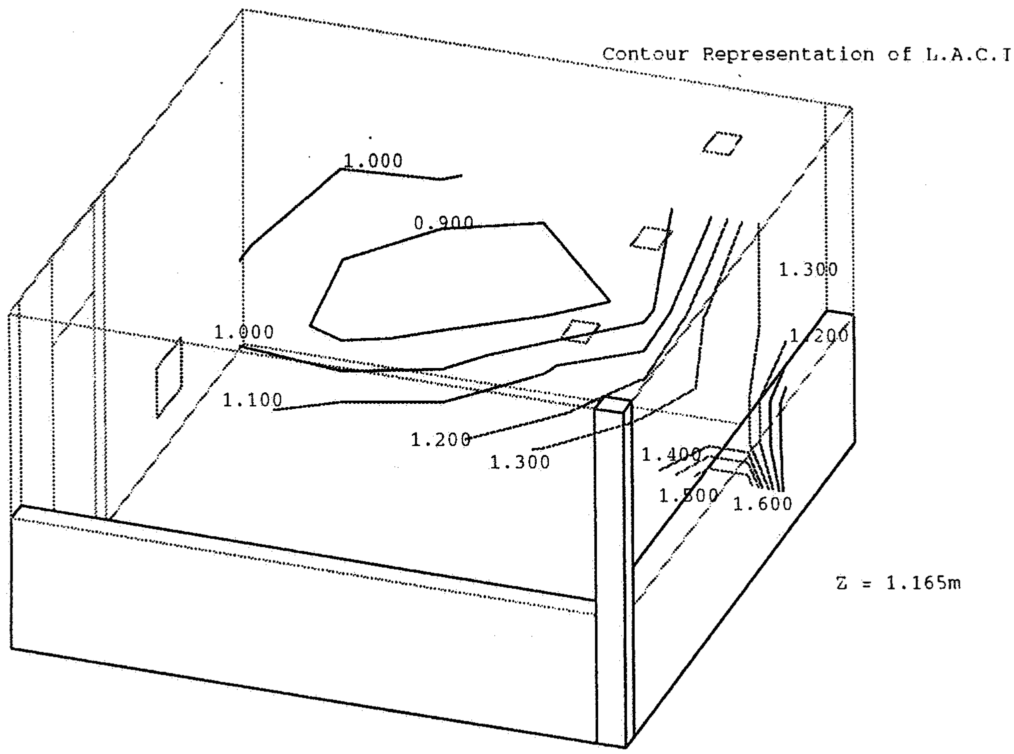

Figure 11 Contour Diagram of L.A.C.I. Following Reduction to 88 Zones

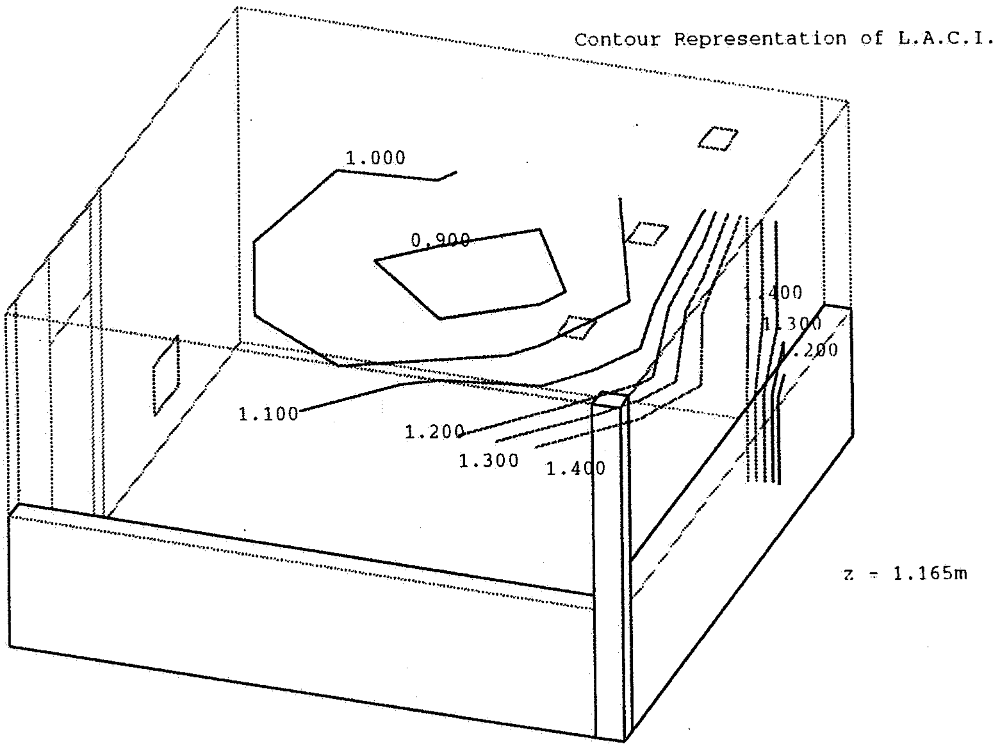

Figure 12 Contour Diagram of L.A.C.I. Following Reduction to 23 Zones

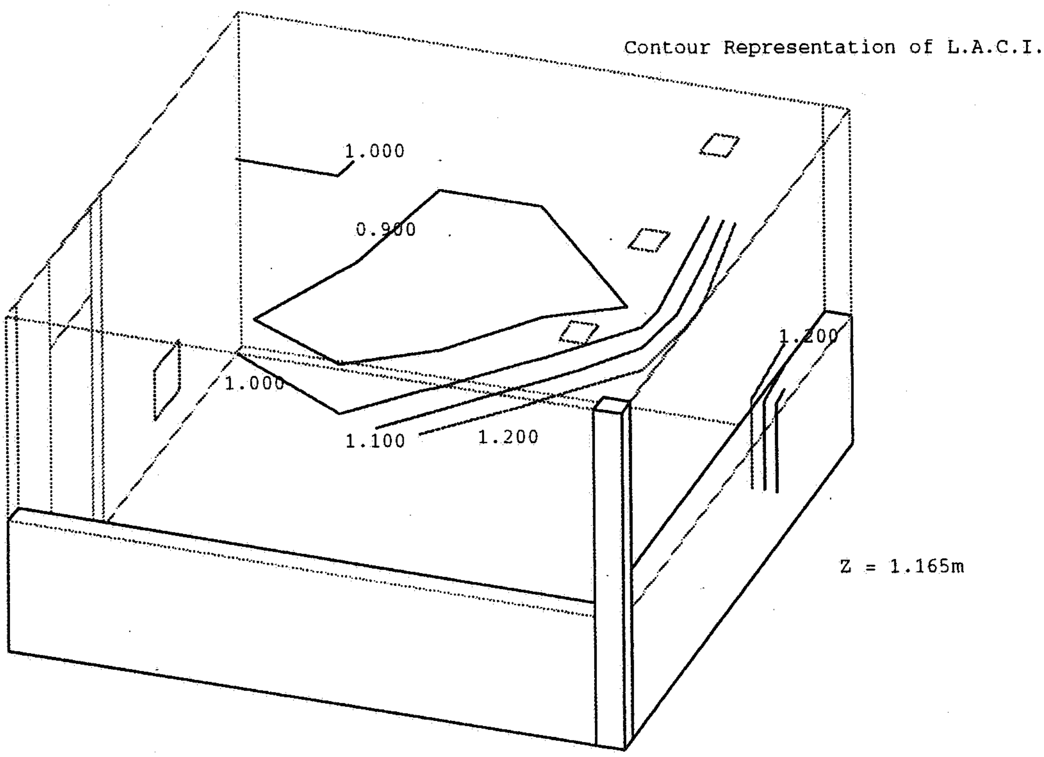

Figure 13 Contour Diagram of L.A.C.I. Following Reduction to 15 Zones

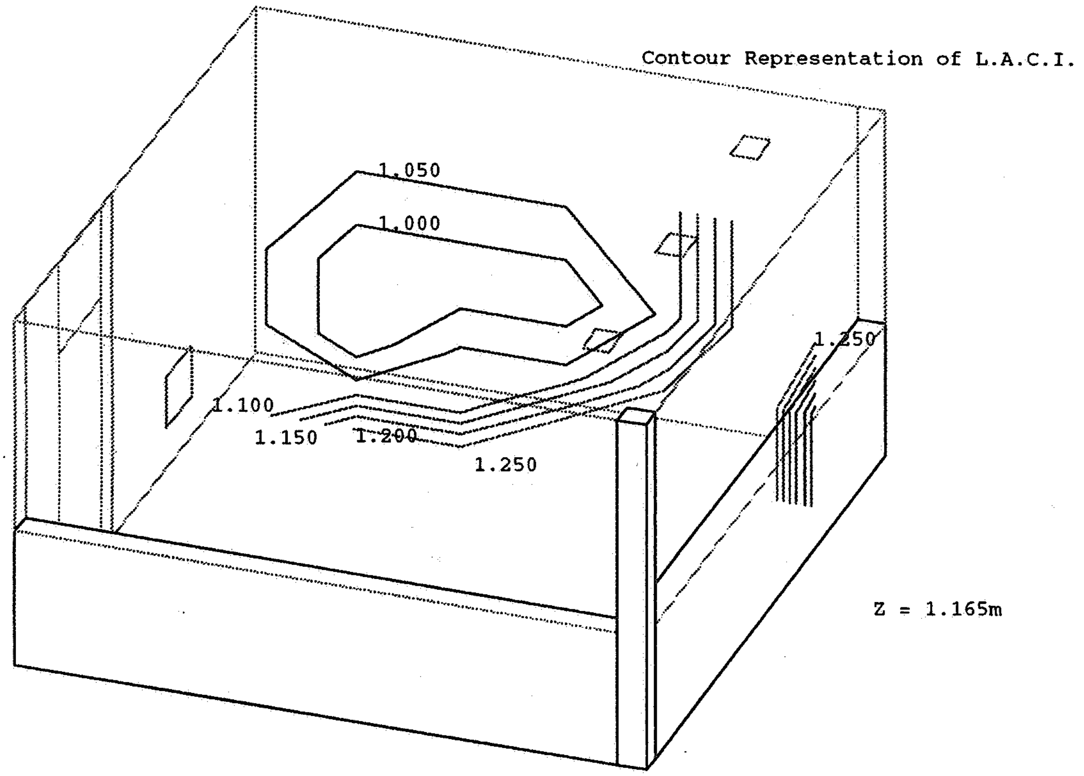

Figure 14 Contour Diagram of L.A.C.I. Following Reduction to 5 Zones

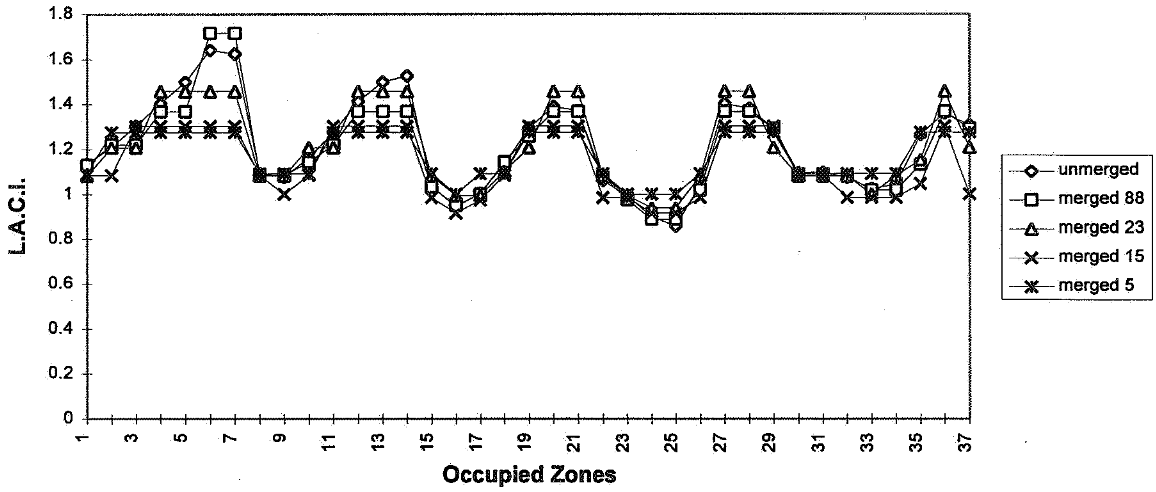

Figure 15 Variations in Initial and Merged Case Values of L.A.C.I.

7 Conclusions

Algorithms have been written to convert the output of a typical CFD model to an equivalent multizone model, which may then be used to compute all the usual ventilation effectiveness parameters. An additional algorithm has been written to reduce or "crudify" the multizone model to a smaller number of zones using any one of the ventilation effectiveness parameters as the criterion. Application of these algorithms to the computation of air movement in a typical mechanically ventilated room show that, in this case, a 384 zone representation of the space can be reduced to as little as a 5 zone representation without undue distortion of the computed values.

References

1 SIMONS, M.W., BROUNS, C.E. and WATERS, J.R.
'Flovent as an Aid to the Measurement of Air Movement Characteristics in Buildings'
Flovent User Meeting, May 1994

2 SUTCLIFFE, H.C.
'A Guide to Air Change Efficiency'
AIVC Technical Report 28, 1990

3 BROUNS, C.E. and WATERS, J.R.
'A Guide to Contaminant Removal Effectiveness'
AIVC Technical Report 28.2, 1991

Implementing the Results of Ventilation Research
16th AIVC Conference, Palm Springs, USA
19-22 September, 1995

The Use of Tracer Gas Methods for Detailed Airborne Moisture Transport Study in Buildings

D Ducarme, A Bossaer, P Wouters

Belgian Building Research Institute (CSTC/WTCB)
Division of Building Physics and Indoor Climate, Rue de la Violette, 1000 Brussels, Belgium

THE USE OF TRACER GAS METHODS FOR DETAILED AIRBORNE MOISTURE TRANSPORT STUDY IN BUILDINGS

Ducarme David, Bossaer Alain, Wouters Peter
Belgian Building Research Institute (CSTC-WTCB)
Division of Building Physics and Indoor Climate
Rue de la Violette 21-23
1000 Brussels, Belgium

SYNOPSIS

Three different examples illustrate the possibilities offered by the use of tracer gas methods for detailed airborne moisture transport studies in buildings. The first one concerns an individual dwelling with severe condensation problems, the second one gives an example of statistical data collection of humidity related parameters in 18 apartments and the last one focuses on the evaluation of the amount of water evaporating from the building materials of a recently built low energy dwelling and on the energy consumption required for drying the construction.

The paper deals on the one hand with the methodology employed for the measurements, on the other hand with the practical results that were obtained.

LIST OF SYMBOLS

V	volume of the space	[m^3]
S	source/sink in the space	[kg/s]
w_{inside}	absolute humidity inside	[kg/m^3]
$w_{outside}$	absolute humidity outside	[kg/m^3]
Q_{air}	air flow rate	[m^3/s]
$Q_{condensation}$	condensation rate	[kg/m^2.s]
β	vapour transfer coefficient	[s/m]
$p'_{surface}$	saturation vapour pressure on the surface of the profiled sheets	[Pa]
p_{cavity}	vapour pressure in the cavity	[Pa]
θ	temperature	[K]

1. INTRODUCTION

In the framework of three different projects, quite unique methods were used and data collected in relation to airborne moisture transport in buildings. This paper focuses on the one hand on the methodology employed and, on the other hand on the practical results obtained. It does not deal with humidity levels in spaces or with humidity transport in materials or constructions.

After a short discussion on the relevance of airborne moisture transport studies, available measurement techniques and schemes are presented. Then follow three applications.

The first one concerns an individual dwelling with severe condensation problems in the pitched roof structure. The combination of tracer gas techniques with accurate water vapour measurements permitted to qualify and quantify the causes of the problem and to propose appropriate solutions.

The second project [1] gives a good example of statistical data collection concerning the water vapour transport. Humidity and air change rate were measured during about 2 months in 18 apartments situated in Namur, Belgium with the specific aim of estimating the moisture production.

The third project focuses on the detailed evaluation of the overall energetical performances of a new low energy building. Detailed measurements were carried out during two periods of about one month. The recorded data permitted to accurately estimate the air change rates as well as the amount of water drying out from the construction.

Finally, some conclusions are given.

2. RELEVANCE OF AIRBORNE MOISTURE TRANSPORT MEASUREMENTS

2.1 MOISTURE PROBLEM

Moisture problems in dwellings often find their origin in an insufficient air renewal leading to high water vapour levels which provokes condensation on cold surfaces (single glazing, thermal bridges,...). These problems can generally be simply detected by humidity measurements possibly combined with surface temperature measurements.

However, other more complex problems require more than a simple humidity measurement to be understood. This is the case when there is a doubt on the origin of the water vapour which condenses. The use of tracer gas combined with humidity measurements can be the only way to understand the source of a problem and determine appropriate remedial actions.

2.2 STATISTICAL DATA

Nowadays, there are many simulation tools on the market that allow to simulate pollutant spreading in buildings (COMIS, CONTAM,...). These tools should be used by designers in order to evaluate the impact of different strategy (heating, ventilation,...) on the indoor climate (air quality and thermal comfort). However, the problem is as usual to feed the simulation tool with sufficiently representative/accurate input data so as to end up with valuable simulated values. In particular, the pollutant sources and sinks must be known as well as typical outside concentrations.

In this context, the collection of statistical data on water vapour is of high relevance since humidity is a major parameter for qualifying the indoor climate.

2.3 ENERGY CONSUMPTION FOR DRYING OUT CONSTRUCTIONS

New constructions contain important amounts of water stored in the building materials (plaster, concrete,...). The required energy to dry constructions and the time it can take are not well known. Humidity measurements combined with air flow rate measurements allow to follow the evolution of the water evaporation and to derive the energy consumption that it requires.

3. MEASUREMENT TECHNIQUES

3.1 BASIC EQUATIONS

The water vapour source/sink (production, condensation, evaporation, adsorption,...) in a building considered as a single zone is given by:

Eq. 1 $$S_{H_2O} = Q_{air} \cdot \left(w_{inside} - w_{outside}\right) + V \cdot \frac{dw_{inside}}{dt} \qquad [kg/s]$$

where the first term represents the water vapour flow rate extracted/supplied by the ventilation, that is:

Eq. 2 $$Q_{H_2O} = Q_{air} \cdot (w_{inside} - w_{outside}) \qquad [kg/s]$$

and the second term represents the variation of inside absolute humidity.

Thus, the study of airborne water vapour transport requires measurements of absolute humidities and air flow rates. The latter can be determined thanks to tracer gas techniques [2].

It must be noted that absolute humidities appear in the form of differences in those equations which implies that the measurement error on the absolute humidity strongly impacts the accuracy of the calculated results. This is for example shown by the next formula giving the error on the calculated water vapour extraction rate as a function of the measurement errors on the air flow rate and on the absolute humidity.

Eq. 3 $$\left|\frac{\Delta Q_{H_2O}}{Q_{H_2O}}\right|^2 = \left|\frac{\Delta Q_{Air}}{Q_{Air}}\right|^2 + 2 \cdot \left|\frac{\Delta w}{w_{inside} - w_{outside}}\right|^2$$

Equations 2 and 3 can easily be extended to multi-zone building models.

3.2 SENSORS

3.2.1 CLASSICAL HUMIDITY SENSORS

One of IEA Annex18 reports [3] provides a good overview of existing humidity sensors and their performances. The most commonly used are: the hair and polyethylene-strip hygrometer, the capacitive hygrometer, the conductance-film hygrometer and the lithium chloride sensor.

3.2.2 INFRARED GAS ANALYSERS

The measurement is based on the absorption of infrared light by the molecules of gas (water vapour or tracer gas) contained in the analysed air sample. The absorption can either be detected by the decrease of the light intensity after it has gone over a long path in the air sample (photometric type) or by the acoustic field created in a closed cavity filled with the gas when it is submitted to a pulsating light source (photoacoustic type).

By way of example, the accuracy of the Brüel&Kjaer type 1302 (employed for the first and the third project) is about 1% and a range drift of 2.5% over a 3 months period. This equipment permits to measure the concentrations of up to 5 different gases and the absolute humidity in a few minutes.

3.3 MEASUREMENT SCHEMES

To study the airborne humidity transport necessitates to measure absolute humidities at several places, at least one point inside and one point outside. Two schemes are possible: either a humidity sensor at each measurement point or a central sensor to which air samples collected at the different points are brought.

The use of an individual sensor for each point has the disadvantage that the unavoidable drifts affecting the measurement can be different for each of them. Accordingly, they have to be taken into account in the humidity measurement error (Δw in Eq. 3).

On the contrary, using a common sensor allows to eliminate (for a zero drift) or reduce (for a range drift) the drift error on the difference of two humidities and accordingly increase the accuracy on the calculated result. This point may be essential when absolute humidity differences are small which can be due to high ventilation rate (in summer for example).

4. EXAMPLE OF THE EXAMINATION OF A MOISTURE PROBLEM

4.1 DESCRIPTION OF THE PROBLEM

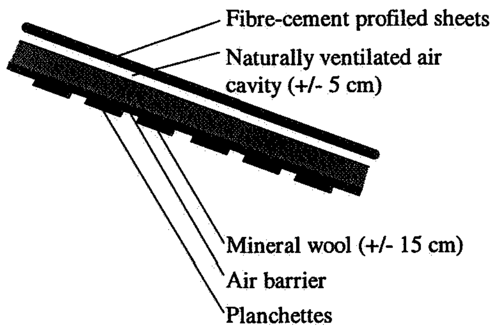

Figure 1: Structure of the pitched roof

The investigated dwelling is situated in Wommelgem, Belgium. It has a pitched roof made up of fibre-cement profiled sheets.

Often, water is dripping out of the roof structure into the dwelling. Usually this happens after a period of frost.

Figure 1 shows a sketch of the roof structure.

4.2 PERFORMED MEASUREMENTS AND OBJECTIVES

The main objective of the performed investigations was to determine where the water vapour condensing in the naturally ventilated air cavity was coming from. Indeed, it could originate from the dwelling where the absolute humidity is higher than outside and therefore could condense on the cold profiled sheets or it could come from the outside and, in this case could condense because of a supercooling effect on the profiled sheets (due to radiation exchange with a clear sky the temperature of a surface can be lower than the air temperature).

Pressurisation measurement, smoke visualisation and tracer gas measurement were performed.

The purpose of the tracer gas measurement is to determine the amount of indoor air leaving the house through the air barrier to the roof structure. Therefore a tracer (SF_6) is injected in the dwelling (constant concentration) and its concentration is measured continuously on different places in the air cavity. At the same time the temperature and the absolute humidity are measured on different places (inside, outside, in the cavity, on the profiled sheet).

4.3 RESULTS AND DISCUSSION

4.3.1 PRESSURISATION AND SMOKE VISUALISATION

The pressurisation gave an n_{50}-value of about 10 h^{-1}. This is not very good, but not extremely high for a Belgian dwelling. The smoke visualisation showed that the most important leakages are situated in the roof structure and at the windows.

4.3.2 TRACER GAS MEASUREMENT

Figure 2 shows the evolution of the ratio of the SF_6 concentrations in the air cavity and in the dwelling. This value directly indicates the proportion of inside air in the cavity. As one can see this is a rather fluctuating value (due to changing weather conditions). The average of the ratio is about 67%; this means that over the whole period the air in the cavity includes on average 2/3 of inside air and 1/3 of outside air. It is clear that the air barrier is far to be airtight.

The following step was the examination of potential condensation. One knows that the air in the cavity will condense against the profiled sheets if:

Eq. 4 $\theta_{surface} < \theta_{dew,cavity}$ [K]

The temperature on the surface is measured and the dewpoint in the cavity can be calculated from the measurement of the absolute humidity. The measured data showed that some condensation occurred during the measurement period.
To know the importance of this condensation the following equation can be used:

Eq. 5 $$Q_{condensation} = \beta \cdot \left(p_{cavity} - p'_{surface} \right)$$ [kg/m².s]

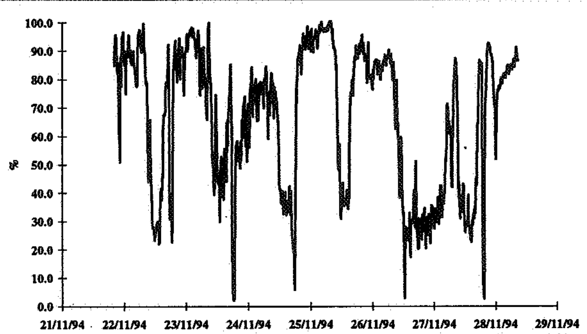

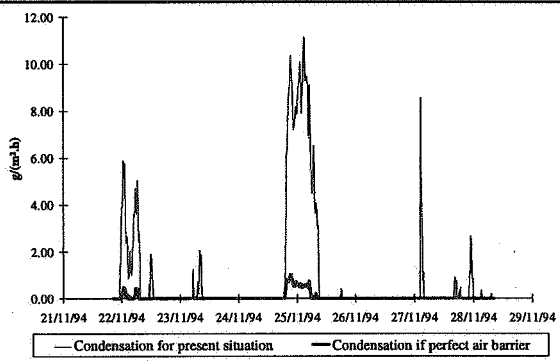

Figure 2: Ratio between the SF_6 concentrations in the cavity and in the dwelling
Figure 3: Condensation rates in present situation and for a perfect air barrier

This calculation has been made with the measured data (Figure 3) assuming a value of 22.10^{-9} s/m for the vapour transfer coefficient. The total amount of condensed water vapour over the considered period (6 days) is about 13 kg.
The reason why the problem mostly occurs after a period of frost, is that a buffer of frozen water is formed. When the roof surface temperature rises (because of the sun), this ice is melting very quickly and cannot be dried by the air in the cavity. As a consequence a large amount of water will be released in a short period, which causes the dripping of water into the dwelling.
The outside air flow rate to the air cavity can easily be determined from the tracer gas measurements if the assumption is made that all the air exfiltrating from the dwelling (measured) passes through the roof. The improvement brought by a perfect air barrier can then be evaluated. The result is also shown in Figure 3. The remaining part of condensation is caused by the effect of supercooling and is rather small compared to the present situation.
The problem is clearly due to the very bad airtightness of the air barrier and could be solved either by strongly improving the present air barrier or by placing a new airtight air barrier.
As conclusion it can be said that the studied problem clearly shows the relevance of airborne moisture transport study not only to find the origin of the problem, but also to simulate the effect of possible improvements.

5. EXAMPLE OF STATISTICAL DATA COLLECTION

5.1 THE CONTEXT

In the framework of an EC demonstration project [1] devoted to the field-testing of humidity controlled natural ventilation, a large amount of data was collected in 18 apartments situated in Namur, Belgium during about 70 days. Various parameters were continuously monitored (temperatures, air flow rates, CO_2 concentrations, absolute humidities,...) in the "humid spaces" (toilets, bathrooms and kitchens) in which natural extraction is taking place. One of the specific aims was to evaluate the water vapour extraction rate due to the natural ventilation.

5.2 THE MEASUREMENT TECHNIQUE

The MATE (Multi Purpose Automated Tracer Gas Equipment) system [2] was used to measure the extraction flow rates. Air samples were drawn successively from the different rooms and their tracer gas concentrations measured using infrared gas analysers as well as their humidity.

5.3 THE RESULTS

The next figures show some humidity related results from this project. Figure 4 shows the average outside absolute humidity as a function of the outside temperature. As one can see, the dependency is almost linear in the range -5 to 10 °C. Figure 5 shows histograms of the extracted water vapour rates through the ventilation ducts for 9 apartments with humidity controlled ventilation (hygro) and for 9 apartments without humidity controlled ventilation (reference). The average value is about 5 kg of water per day.

More information on the results of this study can be found in [1].

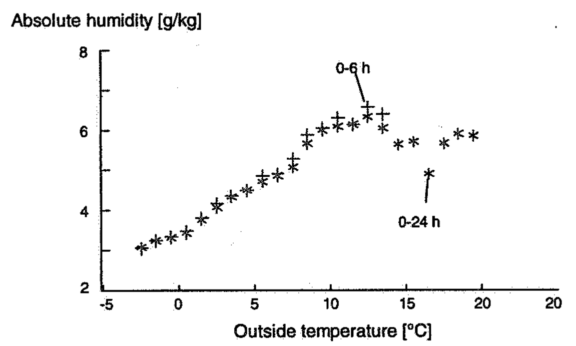

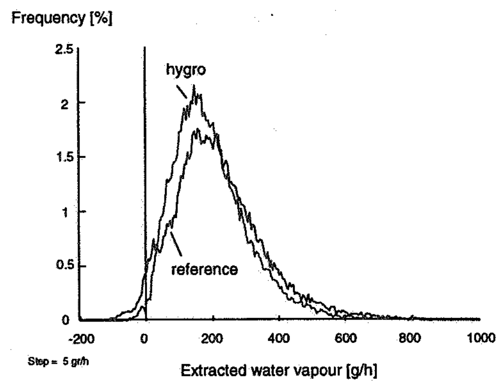

Figure 4 - Average outside absolute humidity as a function of the outside temperature
Figure 5 - Histogram of total extracted water vapour rates

6. EXAMPLE OF DETERMINING ENERGY CONSUMPTION FOR DRYING OUT WATER FROM CONSTRUCTION

6.1 THE OBJECTIVE OF THE STUDY

The PLEIADE dwelling is a low energy building situated in Louvain-La-Neuve, Belgium, recently built in the framework of IEA Task XIII, "Advanced Solar Low Energy Building".

An extensive monitoring was carried out in order to identify the performances of the dwelling (thermal performances, building airtightness, ventilation, air heating system...).

As part of it, detailed moisture measurements were performed with the objective to evaluate the energy consumption for drying out construction water in order to be able to make the heat balance of dwelling and to derive its thermal characteristics. On the other hand, it was also the intention to measure the amount of water that can be evaporated from a new construction during the first heating periods.

6.2 THE MEASUREMENT TECHNIQUE

As previously mentioned, a Brüel&Kjaer gas analyser type 1302 was used. The tracer gas concentrations were measured at 11 different places in the building as well as the absolute humidities (also measured outside). A two tracer gas technique was used so as to be able to differentiate the air coming from the outside and from the basement to the dwelling.

6.3 THE RESULTS

Figure 6 shows the evolution of the total air change rate of the dwelling. It should be noted that the mechanical ventilation system of the dwelling was switched off which explains the rather low values, only due to air infiltration.

The measured absolute humidities in the dwelling (average of 10 measurement points), in the basement and outside are shown on Figure 7. The higher inside values are due to the evaporation of construction water (no other source of water in the building). The variation of the humidity in the basement is due to the strong changes of its ventilation rate mechanically imposed for thermal identification purpose.

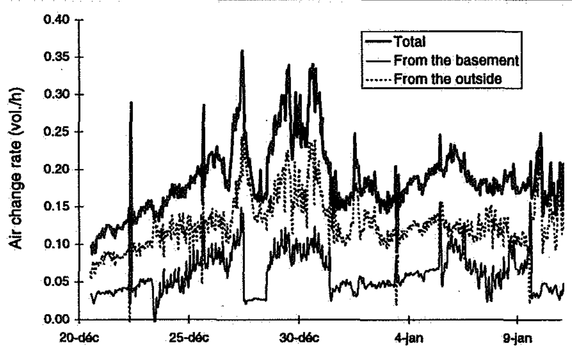

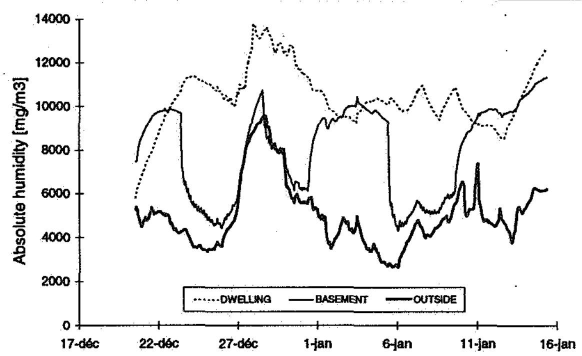

Figure 6 - Air change rate in the dwelling (from the outside and from the basement)
Figure 7 - Evolution of the absolute humidities (basement, dwelling and outside)

Knowing the air flow rates and the humidities in the time allows to derive the water vapour source in the building which is given in Figure 8.

Figure 9 gives the average air flow rates and absolute humidities during the measurement period (from 20-12-94 to 15-1-95).

In total, 312 kg of water were evaporated during a period of 25 days which corresponds with an energy consumption of about 700 MJ. On average, 500 g of water per hour evaporates from the construction which is equivalent to a cooling power of 300 Watt.

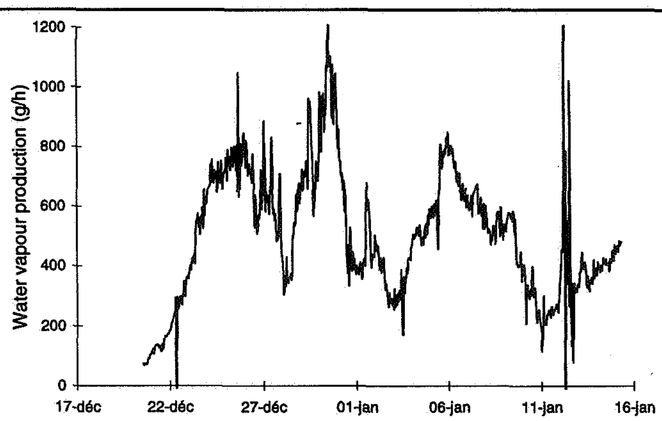

Figure 8 - Evolution of the water vapour production in the dwelling

Figure 10 gives, the distribution of thermal losses in its three components: the losses by transmission, the ventilation losses and the energy consumption due to the evaporation of the construction water. As it can be seen, about 10% of the whole heating energy injected in the building was consumed to evaporate construction water. It should be added that the building was protected from solar gains during this period.

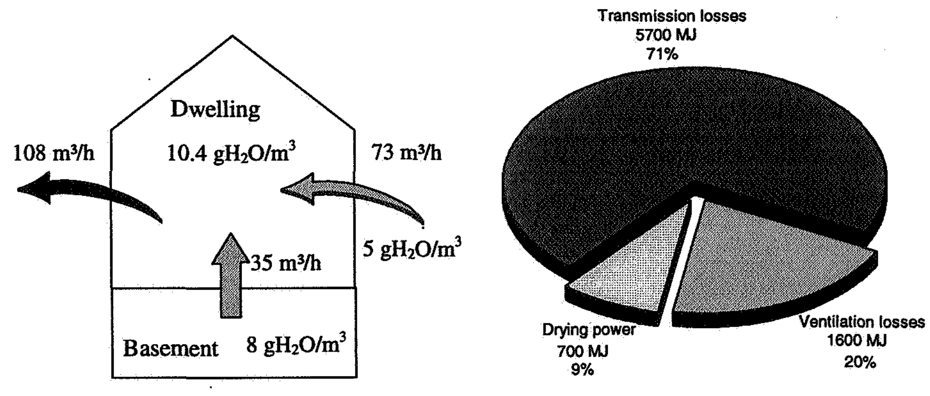

Figure 9 - Average air flow rates from 20-12-94 to 15-1-95
Figure 10 - Distribution of thermal losses

7. GENERAL CONCLUSION

This paper demonstrates by means of three examples that the combination of accurate absolute humidity measurements (with a common sensor for drift avoidance) and air flow rate measurements (by means of tracer gas) provides quite unique results for airborne moisture transport related problems.

ACKNOWLEDGEMENTS

The second project was partly financed by the European Community. The third project is financed by the Walloon Region of Belgium. The authors would like to express their gratitude to the sponsoring organisations.

REFERENCES

1. WOUTERS, P., GEERINCKX, B., L'HEUREUX, D.
'Natural Ventilation in 18 Belgian Apartments: Final Results of Long Term Monitoring'
14th AIVC conference Copenhagen, Denmark, 1993, proceedings pp369-378
2. ROULET, C.-A. and VANDAELE, L.
'Air Flow Patterns Within Buildings - Measurement Techniques'
Technical note 34, Air Infiltration and Ventilation Centre, Coventry, 1991.
3. RAATSCHEN, W.
'Demand Controlled Ventilation: State of the Art Review'
IEA Annex 18, Demand controlled ventilating systems, Final report, 1990

**Implementing the Results of Ventilation Research
16th AIVC Conference, Palm Springs, USA
19-22 September, 1995**

The Dutch E'Novation Program: Indoor Air Quality in Dwellings Before and After Renovation

P J M Op't Veld*, H G Slijpen**

* Cauberg-Huygen Consulting Engineers bv,
Maastricht, The Netherlands
** NOVEM bv, Sittard, The Netherlands

THE DUTCH E'NOVATION PROGRAM: INDOOR AIR QUALITY IN DWELLINGS BEFORE AND AFTER RENOVATION

P.J.M. Op 't Veld[1], H.G. Slijpen[2]

1) Cauberg-Huygen Consulting Engineers bv, Maastricht, The Netherlands
2) NOVEM bv, Sittard, The Netherlands

ABSTRACT

The Dutch "E'novation program" is a national demonstration program in which dwellings with high energy consumption, moisture and mold problems and poor indoor air quality were renovated, with special attention to the selection of the heating and ventilation systems, thermal insulation and the building physical details. A number of indoor air quality parameters were monitored before and after renovation, showing an important improvement in the indoor air quality. Moreover, energy consumption for space heating decreased by 39%, which, meets the targets of the Dutch National Environment Policy.

INTRODUCTION

In 1988 NOVEM (Dutch Company for Energy and Environment) started a national demonstration program in The Netherlands, involving the renovation of 2800 dwellings with high energy consumption, moisture and mold growth, poor indoor air quality etc. This program is called the "E'novation program". E'novation is a contraction formed by the two key words of this program: "Energy" and "Renovation". Many postwar buildings in The Netherlands have the above mentioned problems. The characteristics of these buildings are: no or insufficient thermal insulation, many air leakages, often no central heating, unvented geysers and inadequate physical details. The addition of thermal insulation often causes problems with moisture, ventilation and indoor air quality. The purpose of the E'novation demonstration program is to achieve both energy savings and good indoor air quality through an integrated handling of energy retrofitting, ventilation and heating systems and good physical details. In some projects special energy savings technics were applied, such as heat recovery, passive solar energy and demand controlled ventilation systems.

The Dutch Ministry of Economic Affairs has made available USD 3.800.000,-- for this program. This amount also includes the costs of a pre-study, the evaluation and measurement program and "knowledge-transfer" about this program. An amount of USD 1.100,-- per dwelling will be paid to the building corporations. NOVEM manages the program.

All the projects were supported by an extended program of measurement and evaluation. The measurement and evaluation program concerns:

- the performance of the ventilation, heating and heat recovery systems applied;
- the predicted and achieved energy consumption for space heating and warm water;
- the airtightness of the building envelope;
- evaluation of the overall quality of the renovation;
- evaluation of the experiences and opinions of the occupants.

In some projects a special measurement program was carried out to monitor indoor air quality. The measurements were taken before and after the renovation. The dwellings and the measured indoor air components and pollutants were chosen in such a way that the quality of the renovation process and its impact on the indoor air quality was measured as accurately as possible. Therefore any disturbing influence on the part of occupants (i.e. smoking) was eliminated.

This paper will focus on indoor air quality measurements in relation to energy savings and the results of airtightness measurements.

METHODS

The measurement program is set up as follows. In each dwelling the measurements were taken over the course of one week. CO_2, CO, CH_2O, TVOC (ref. to CH_4), relative humidity and temperature were continuously sampled and monitored in four rooms (living room, kitchen and two bedrooms) as well as outdoors by a B&K 1302 gas monitor and B&K 1303 sampler and doser unit combination. NO_2 was measured by passive sampling by means of Palmes diffusion tubes. Volatile organic compounds (VOC) were measured by active sampling and a G.C. analysis of aromatic hydrocarbons and halocarbons.
Respirable dust was measured continuously by a tyndallometer. Radon was measured for four months by passive sampling in the living room and in the crawl space.
The measured concentrations were checked with the guideline values of the WHO (1), and the target guidelines for VOC's (2).

RESULTS AND DISCUSSION

Indoor Air Quality

Before renovation most of the dwellings had unvented geysers in the kitchen. A number of these dwellings had local heating. During the renovation all unvented geysers were replaced by combi-boilers for heating and hot water supply with a closed combustion system (direct combustion air in take). The ventilation is improved by applying an individually controlled mechanical exhaust ventilation or by a balanced ventilation system.
In table 1 a summary is given of a number of measured indoor air quality parameters. It shows the averages during 1 week, measured in dwellings before and after renovation. In table 2 a summary is given of the measured concentrations of VOC before and after renovation.

Before renovation the indoor air quality was generally poor and in some cases even hazardous. The main sources were unvented geysers installed in most of the homes. It was known that these geysers could result in the guidelines for NO_2 and in some cases for CO and CO_2 being exceeded. Continuous measurements showed that CH_2O also frequently exceeded the guideline values.
After the renovation there was an obvious decrease in all measured indoor air quality parameters. The following was observed:

- The most significant decrease was the reduction in the NO_2 concentrations. Before renovation the weekly average values measured in kitchens exceeded the 24 h guideline value. After the renovation these values decreased to values much lower than the guideline values.
- The CH_2O concentrations also showed a large reduction. A comparison with the guideline value of 120 ug/m ^{3} is not quite correct because the filter reacts upon formaldehyde as well as upon a number of other aldehydes and upon C_5H_{12} and C_6H_{14}. Figure 1 shows a typical example of CH_2O concentrations measured in a kitchen before and after renovation. Before renovation extreme peak values occured during the moments that the unvented geyser was in use. After renovation these peaks disappeared.
- The measured CO concentrations were reduced by 50% or more in the renovated dwellings. Table 1 shows that the weekly averages measured did not exceed the guideline value. Nevertheless there were situations before the renovation in which this limit had been exceeded in shorter periods (about 10 to 12 hours) such as in the living room as a consequence of the flue gass backdraft from gas heaters.

Table 1. Measured indoor air quality parameters before and after renovation (mean values and standard deviations, n=16).

		before renovation			after renovation			
		living room	kitchen	bedrooms	living room	kitchen	bedrooms	guideline values
CO_2 (ppm)	mean std	1024 184	1013 277	927 193	882 160	836 122	672 148	1200
CO (mg/m^3)	mean std	3,9 0,4	4,3 0,2	4,2 1,6	2,2 1,0	2,0 0,5	1,4 0,5	10 (8h)
CH_2O* (ug/m^3)	mean std	665 214	577 51	530 234	405 167	357 153	231 188	120 (0,5h)
TVOC (ref CH_4) (mg/m^3)	mean std	- -	- -	- -	4,5 1,0	4,1 1,0	2,9 1,0	-
NO_2 (ug/m^3)	mean std	84 40	160 127	30 9	30 16	34 14	16 3	150 (24h)
Resp.dust (ug/m^3)	mean std	30 16	- -	- -	30 15	- -	- -	70 (PM10 24h)
RH(%)	mean std	42 4	41 6	57 9	45 4	44 3	45 4	30-70%

* including a.o. other aldehydes, C_5H_{12}, C_6H_{14}

Table 2. Concentrations of VOC in ug/m^3 before and after renovation.

	before renovation		after renovation	
	livingroom	kitchen	livingroom	kitchen
benzene	8,6	12,3	1,3	2,1
ethylbenzene	2,6	3,3	1,9	1,7
toluene	38,0	40,0	32,0	21,0
xylenes	3,0	7,0	1,3	1,4
styrene	1,1	0,9	0,6	0,4
n-propylbenzene	16,7	8,3	0,2	0,3
i-propylbenzene	0,2	0,2	<0,1	<0,1
1,2,4-trimeth.benz.	3,0	3,4	1,2	1,7
1,3,5-trimeth.benz.	1,4	1,5	0,7	0,6
naftalene	0,5	0,5	0,1	0,3
chlorobenzene	2,1	1,1	<0,5	<0,5
1,2 dichl.benzene	0,8	0,8	<0,5	0,5
1,3 dichl.benzene	<0,6	<0,6	<0,5	<0,5
1,4 dichl.benzene	0,8	0,8	<0,5	<0,5
1,2 dichl.ethene	2,1	1,3	0,7	0,7
dichloromethane	6,1	3,4	1,6	2,0
trichloromethane	2,1	2,1	1,7	2,3
1,2 dichl.ethane	<0,6	<0,6	<0,5	<0,5
trichl.ethene	11,5	11,5	7,3	7,7
tetra chl.ethene	6,6	7,8	5,9	6,2
tetra chl.ethane	1,4	1,4	<0,5	0,9
1,1,1.trichl.ethane	1,4	1,9	0,8	<0,5
1,1,2.trichl.ethane	1,4	<0,6	0,9	1,5

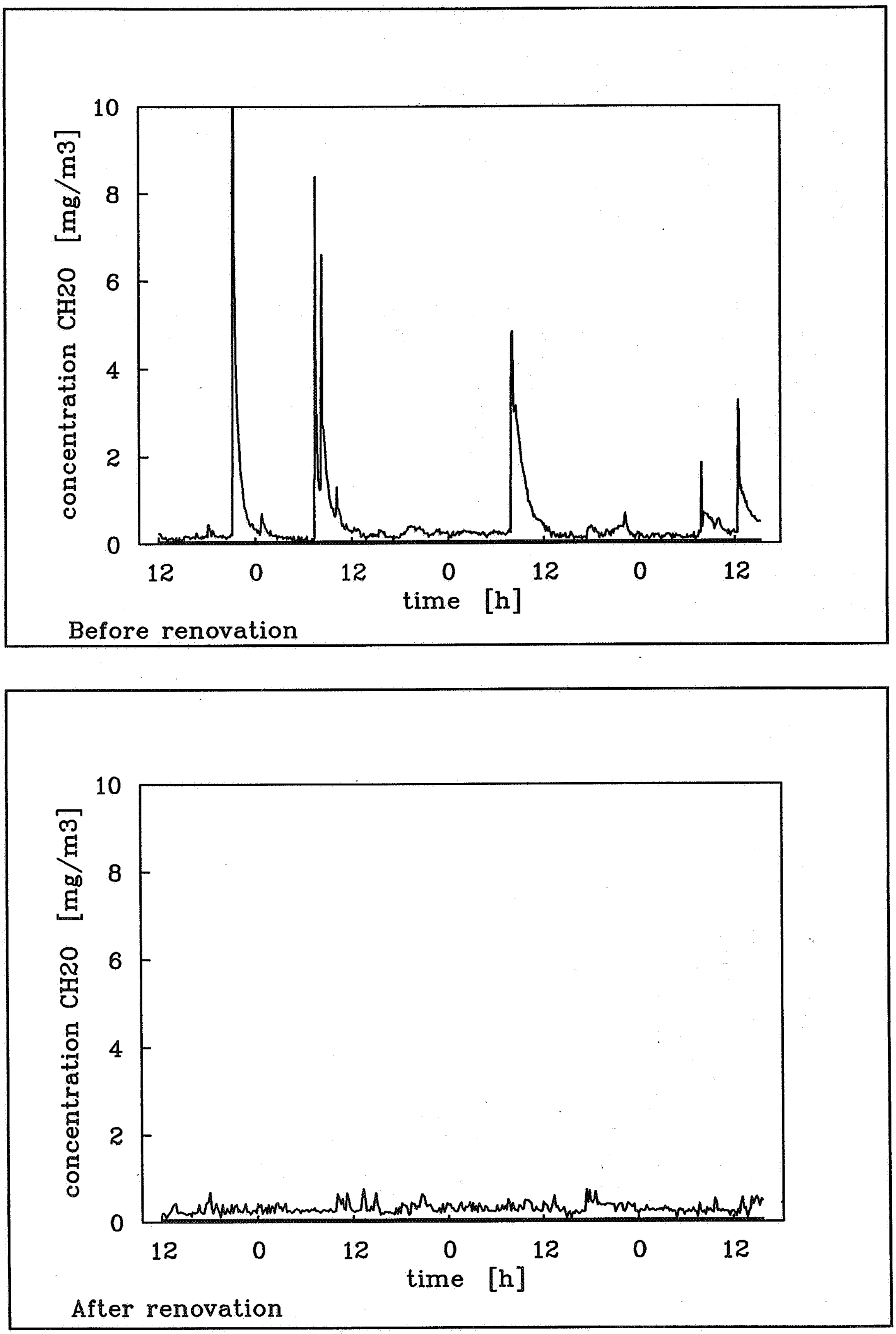

Figure 1. Concentrations of CH_2O (and o.a. other aldehydes, C_5H_{12}, C_6H_{14}) measured in a kitchen before and after renovation.

- Before and after renovation the weekly averages of the CO_2 concentrations were lower than the hygienic limit value.
  However in many shorter periods these limits were exceeded.
- The measured respirable dust concentrations appeared to be far below the limits both before and after the renovation.
- Almost all concentrations of VOC's showed a reduction. Before renovation the sum of the aromatic hydrocarbons exceeded the target value of 50 ug/m^3. In some dwellings benzene exceeded the guideline value of 12 ug/m^3. After renovation the target guidelines for the aromatic hydrocarbons and halocarbons were not exceeded.

Airtightness

An important part of the measurement program concerned the measurement and evaluation of the airtightness of the building envelope. In every project measurements took place before and after renovation. According to the Dutch standard NEN 2686 "Airpermeability of buildings. Method of measurement" airtightness is expressed as the airleakage flow in dm^3/s by a pressure difference of 10 Pa. Figure 2 shows the results of the measurements before and after renovation.
Before renovation the mean airtightness for the whole project was about 144 dm^3/s. For the single family houses the average was 290 dm^3/s; for the multi family houses 91 dm^3/s. After renovation airtightness improved with 25%. The average for the whole project after renovation was 107 dm^3/s. For the single family houses it was 185 dm^3/s; for the multi family houses it was 74 dm^3/s. These results meet easily the Dutch Building Code which demands a maximum airleakage flow of 200 dm^3/s by 10 Pa for new dwellings (this corresponds with a n50-value of 6 for a buildingvolume of 350 m^3).

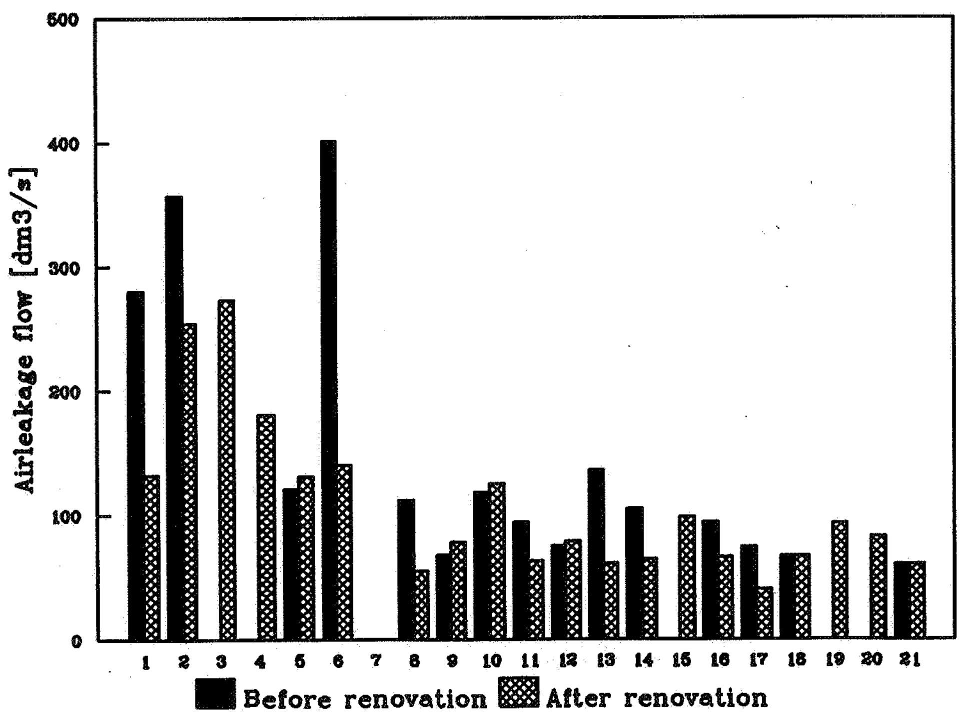

Figure 2. Measured airleakage flows in dm^3/s by 10 Pa.

Energy savings

As a part of the evaluation of the E'novation program, energy use has been calculated and monitored, both before and after renovation. The calculations concerned gas use for space heating, cooking and warm water and also electricity use. Before renovation expected decrease of 50% Figure 3 shows the measured gas consumption for space heating for the projects before and after renovation. The mean measured saving is about 39%. This is 11% less than the predicted decrease of gas use for space heating. While gas use for space heating decreased by 39%, gas use for warm water almost doubled. This was because in almost all the projects, the unvented geysers were replaced by combi-boilers for heating and hot water supply. This gives a large increase in the warm watersupply from 2,5 l/min to 5 to 7 l/min (60°C). Therefore the total measured gas use decreased only by 24% which is 13% less than the predicted decrease of 37%.
Figure 3 shows that the gas savings for space heating appear to be less in a number of projects. This is due to the fact that in these projects a local heating system was used before renovation (only a gas heater in the living room) and a central heating system after renovation. This meant that the average temperature of the dwelling and also thermal comfort increased.

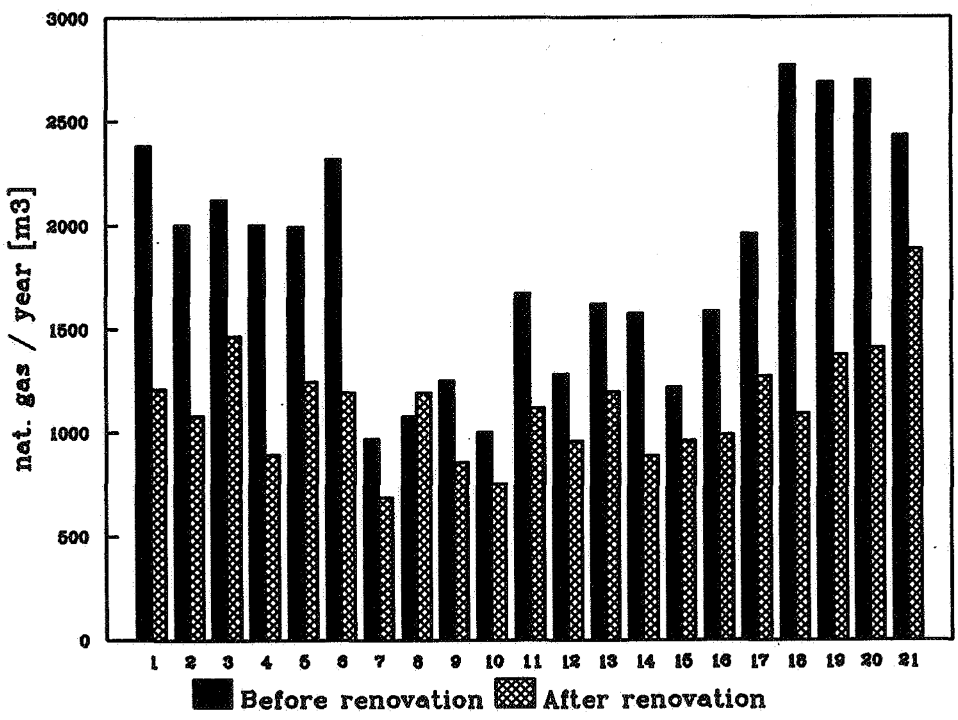

Figure 3. Measured energy consumption for space heating before and after renovation.

CONCLUSIONS

- The selected dwellings for the E'novation program had problems with high energy use and poor indoor air quality, often in combination with moisture and mold growth.
- The measurements carried out in all the dwellings did indeed show poor indoor air quality. For example NO_2 and CH_2O frequently exceeded the guideline values.
- The E'novation program, in which a well-considered choice has been made between various heating and ventilation installations in combination with improved physical details, results in significant improvement of indoor air quality.
- In all projects, problems with moisture and mold growth were consistently eliminated.
- The average airtightness increased by 25 %.
- The gas saving for space heating of 39% meets the target of the Dutch National Environment Policy. It appears that these savings are accompanied by an increase in thermal comfort, a larger warm water supply and improved indoor air quality. This also indicates that a renovation on "E'novation level" will be necessary if the same goals are to be achieved in most of the existing dwellings in The Netherlands.

REFERENCES

1. WHO (1987). Air Quality Guidelines for Europe. WHO Regional Publ., Europ.Series nl 23, Copenhagen
2. Seifert B. (1990). Regulating Indoor Air. Proceedings of Indoor Air 1990. 5:35-49, Ottawa.
3. Lebret E. (1985). Air pollution in Dutch homes. Department of Air Pollution and Department of Environmental and Tropical Health, Wageningen, Agricultural University, r-138.
4. Thijssen I. Korbee H. (1991). E'novatie kennisoverdracht in 1991, 369.1. Woon/Energie Gouda, The Netherlands.
5. Poel A., Eydems H. (1993). E'novation: A demonstration program for low energy retro-fitting. Proceedings of CIB Symposium Stuttgart 1993.

Implementing the Results of Ventilation Research
16th AIVC Conference, Palm Springs, USA
19-22 September, 1995

NRC Indoor Environment Research Facility

C Y Shaw, S A Barakat, G R Newsham, J A Veitch, J Bradley

Institute for Research in Construction, National Research Council Canada

The 16 th AIVC Annual Conference on Implementing the Results of Ventilation Research

Palm Springs, California, September 19-22, 1995

NRC INDOOR ENVIRONMENT RESEARCH FACILITY

C.Y. Shaw, S.A. Barakat, G.R. Newsham, J.A. Veitch and J. Bradley
Institute for Research in Construction
National Research Council Canada

Synopsis

This paper describes the new indoor environment research facility recently constructed at the Institute for Research in Construction, National Research Council Canada. This facility allows full-scale testing and physical modelling of office space lighting, thermal comfort, indoor air quality, airflow and contaminant-flow patterns, ventilation, acoustical characteristics, and occupants' reactions to these parameters. The facility consists of a test room, approximately, 12 m by 7 m by 2.74 m high, with adjustable interior partitions. The test area can range in size from a single large open area, to four identical single-office-sized test rooms.

The facility also has the option of including an exterior wall with windows to produce realistic boundary conditions created by wind and solar effects including daylighting. As well, the ceiling and floor are designed to allow the testing of different types and layouts of air diffusers and luminaires. To have an acoustically stable environment for special types of subjective experiments, noise from the HVAC systems and other external sources will not exceed NC 20 in the test rooms. Regulated and conditioned electrical power is available in the facility. Dedicated control systems provide a controlled environment for the test room and its various realistic boundary conditions.

Introduction

A significant ongoing challenge for building owners and managers is to balance the quality of office indoor environments against the savings in operating costs that are typically achieved through renovation and energy conservation programs. It is vital that energy savings not compromise occupant satisfaction and productivity, because the costs of lost productivity will always exceed the value of energy savings. Studies estimate that direct medical costs associated with indoor pollution in the US could range from US$500 million to over US$1 billion a year, while lost of productivity could cost tens of billions of dollars a year (Woods, 1989 and Leinster and Mitchell, 1992). Providing an acceptable indoor environment along with successful energy conservation depends on the performance of the building systems that heat, cool, ventilate, insulate and illuminate interior spaces. These systems must be properly designed and maintained in order to provide continuing comfort, environmental quality, and operating economy.

To help building owners and managers meet this challenge, it is necessary to develop techniques and measurement tools that can correctly diagnose shortcomings in any performance aspect, and can lead the building operator to correct them at the lowest cost. It is also necessary to explain the large difference between the occupants' perceptions and the physical assessment of a building's indoor air quality, acoustics and illumination. The best way to establish causal connections between physical parameters and human behaviour (e.g., perception, performance, mood) is to conduct systematic studies in a laboratory facility where each physical factor can be precisely varied, both individually and in combination, to assess its effect on the indoor environment and on the people in it. To facilitate such a study, the laboratory should be able to simulate offices and conference rooms of different sizes and layouts. It should also be able to simulate different ventilation system designs and operating conditions, lighting designs, and acoustical conditions.

Individual differences including age, gender, sensitivity, job satisfaction and job stress can also have significant effects on the occupant's perception of the indoor environment (e.g., Hedge et.al, 1992). Laboratory studies allow the researchers to examine the interactions of such personal characteristics and physical parameters in the workplace. Some of the social characteristics of workplaces can be created in the laboratory by having real office workers to serve as research subjects; this ensures results that are more representative of working organizations and their employees. This paper describes the indoor environment research facility constructed for this purpose at the National Research Council of Canada (NRC).

The Facility

The new facility is located at the west end of the second floor in a three storey laboratory-office building. It is the centrepiece of a multi-year research project on the indoor environment currently underway at the Building Performance Laboratory of the Institute for Research in Construction, NRC. It was designed to allow full-scale testing and physical modelling of office space lighting, thermal comfort, indoor air quality, airflow and contaminant-flow patterns, ventilation, acoustical characteristics, and occupants' reactions to these parameters. The architectural, mechanical and electrical designs are discussed in the following sections.

Architectural - Figure 1 shows that this facility consists of a test area, a control room and a reception area for the training and orientation of the test subjects. Inside the reception area, there is a visual acuity test room. The dimensions of the test area are 12 m by 7 m by 2.74 m high. The east, south and north walls are fixed internal walls with a sound transmission class of STC 55. The west wall is a double wall construction consisting of the exterior wall of the building and a removable interior wall. The exterior wall includes a removable panel to allow windows of different sizes and designs be installed for future investigations.

Partition walls of varying acoustical ratings can be installed to divide the test area into smaller spaces, ranging in size from a single large room to four identical single-office-sized rooms. At present, interior partitions for a five-zone configuration exist only above the suspended ceiling and below the raised floor (Figure 2). These partition tops and bottoms have an acoustical rating of STC 55. The remaining components of these interior walls can be installed with different acoustical ratings. Special fasteners have been installed in the tops and bottoms of the partitions above the ceiling and below the floor, to facilitate installation of these interior walls and to ensure that the required acoustical rating will be maintained at the joints. Also, the raised floor system can be removed completely to increase the ceiling height by 0.6 m for testing indirect lighting systems using suspended light fixtures.

Mechanical - The facility has a dedicated all-air, constant volume heating, ventilating, and air-conditioning (HVAC) system with multiple reheat. It consists of a supply air system and a return air system. The supply air system has an air pre-filter, a supply air fan, a chilled water cooling coil, a steam heating coil, a steam humidifier, and a high efficiency air filter (HEPA), all enclosed in the air handling unit (AHU). The AHU also has an internal by-pass to allow the supply air to by-pass all the components except the air filters. This feature will be particularly useful in assessing the contributions of these components to the overall contamination level in the test area.

The HVAC system is designed to provide the supply air to the test area at a constant flow rate adjustable between 0 and 1130 L/s or 15 air changes per hour, a constant temperature adjustable between 8°C and 30°C in the main supply air duct, and a constant relative humidity adjustable between 20% and 80%. It has the flexibility of using 100% outdoor air or a mixture of outdoor air and return air. Since the test area (Figures 1 and 3) can be divided into a maximum of five zones, the supply air system is divided into five zones, each with a steam reheat coil. Similarly, the return air system is also divided into five zones. There are two sets of the supply and return ducts for each zone: one set located in the ceiling space and the other set below the floor. The supply air can enter into each zone through either ceiling or floor mounted diffusers. As well, the return air can leave each zone through either ceiling or floor mounted air grilles. Balancing dampers and isolation dampers are installed in the ductwork to divert the airflows. The supply air diffusers and return air grilles can be installed in the removable panels in the ceiling and the floor. Using flexible ducts these diffusers and grilles can be placed anywhere in the ceiling or floor. Such a design will allow testing of almost any conceivable ventilation and air distribution systems intended for the office environment. An Energy Management and Control System (EMCS) is used to control and monitor the operation of the HVAC system.

Airflow control valves and dampers are used to control the airflow rates to and from each zone. As shown in Figure 3, all ducts to each zone have long and straight sections to facilitate installation of orifice plates for measuring the airflow rates in both the supply and return ducts of each zone.

Some acoustical experiments require that noise from the HVAC system and other external sources not exceed NC 20 in the test area. In addition to the STC 55 walls, duct silencers and vibration breakers are installed in the duct system. All ducts are acoustically lined with sound absorbing material which is wrapped completely with mylar film to prevent loose material from being released into the air stream. Also, no branch duct is used to serve more than one zone to avoid noise transmission from one zone to another through the air duct. The supply air flow to each zone can also be delivered through two diffusers, if needed, to lower the exit velocity to below 2.5 m/s or 500 ft/min. Furthermore, in tests where the subjective effects of varied ventilation noise levels are to be included, ventilation noises will be simulated in a controlled manner using loudspeaker systems located above the suspended ceiling of the test rooms.

Electrical - The electrical system allows installation and testing of almost all lighting designs suitable for the office environment. It has a dedicated, regulated power supply to ensure that the power supplied to the electrical systems being studied do not fluctuate uncontrollably with changes in the building electrical load. The regulated power supply provides power to four identical power source and dimmer sets: one for each of the four zones identified as test rooms. The fifth zone, the corridor area, can be connected to and supplied by any one of the other four zones.

Figure 4 shows the schematic diagram of one zone. Sixteen power outlets above the ceiling provide the power for ceiling or wall mounted lamp fixtures, and eight power outlets below the floor provide power for floor mounted lamp fixtures or task lamps for a total of 24 outlets per zone. There are eight dimmer switches, each with eight connectors. The 24 outlets can be connected to the 8 dimmers in any combinations. Thus, in each zone, it is possible to have eight groups of lamps, each with a different lighting level. Two sets of the dimmer switches are provided for each zone: one set located in the control room which is controlled by the researcher, while the other set located in the test room can be used by the test subject. The dimmer switch set in the control room also has an override controller which consists of five master switches to override the controls in individual test rooms. As shown in Figure 4, when the centre switch is engaged, the lighting level of all five zones will be the same. When one of the other master switches is engaged, the lighting level in the two adjacent zones controlled by the switch are identical.

Data Acquisition System - The facility has a 250-channel computerized data acquisition system for recording measured data. The flow rate, temperature and relative humidity are measured continuously in each duct using orifice plates, thermocouples and relative humidity sensors which have been installed in all supply and return ducts. The quality and amount of electrical power consumed by each lamp (and electrical appliance, e.g. computer display unit and printer) can be monitored continuously.

A computer controlled traversing system together with the data acquisition system will be used to measure and record the air temperatures, air velocities and turbulence intensities in the test area.

Research Plans

The first project to be conducted in this facility is a series of experimental investigations of lighting quality, preferences, and control effects on task performance and energy efficiency. The main objectives are:
(a) to characterize and quantify office lighting quality under different lighting designs, at lighting power densities relevant to existing and proposed codes and standards;
(b) to relate office worker task performance to lighting quality; and
(c) to determine the effect of the individual and automatic control over office lighting on worker satisfaction and performance.

The experiments will be carried out in this facility where subjects are exposed to various lighting conditions, and their preferences, mood, and task performance measured.

To make an efficient use of this facility, a five year research plan is being developed in consultation with a Steering Committee which includes representatives from government agencies and industry.

Summary

This paper describes the new indoor environment research facility recently constructed at the NRC. This facility allows researchers to assess the effects of the physical factors, either individually or in various combinations, on the occupant's task performance, mood, and perception of the quality of the indoor environment. These factors include illumination, building acoustics, ventilation, air distribution, thermal comfort conditions, and indoor air quality. It also enables the researcher to study systematically individual differences that can explain why some people are more affected than others by certain physical conditions.

This facility is the centrepiece of a multi-year research project on indoor environments currently underway at the Building Performance Laboratory, Institute for Research in Construction, NRC. The project's goal is to provide practical information to aid building owners and managers to satisfy the competing requirements for operating economy and occupant performance/productivity and comfort.

Acknowledgment

Funding for the facility was provided by the National Research Council Canada, Public Works & Government Services, Building Technology Transfer Forum (Provincial Public Works Departments), Ontario Hydro, Hydro Quebec, Industrial Technology Research Institute of Taiwan, and the Canadian Institute of Public Real Estate Companies.

Reference

A. Hedge, W. A. Erickson and G. Rubin. 1992. "Effects of Personal and Occupational Factors on Sick Building Syndrome Reports in Air-Conditioned Offices". Stress & Well-Being at Work, Assessments and Interventions for Occupational Mental Health (pp.286-298), Edited by J. Campbell Quick, L. R. Murphy and J. J. Hurrell, Jr., American Psychological Association, Washington, DC.

P. Leinster and E. Mitchell. 1992. "A Review of Indoor Air Quality and its Impact on the Health and Well-Being of Office Workers", Commission of the European Communities, Luxembourg, 1992.

J.E. Woods, 1989. "Cost Avoidance and Productivity in Owning and Operating Buildings", Occupational Medicine-State of the Art Review, V.4, No.4, October-December, 1989, pp.753-770.

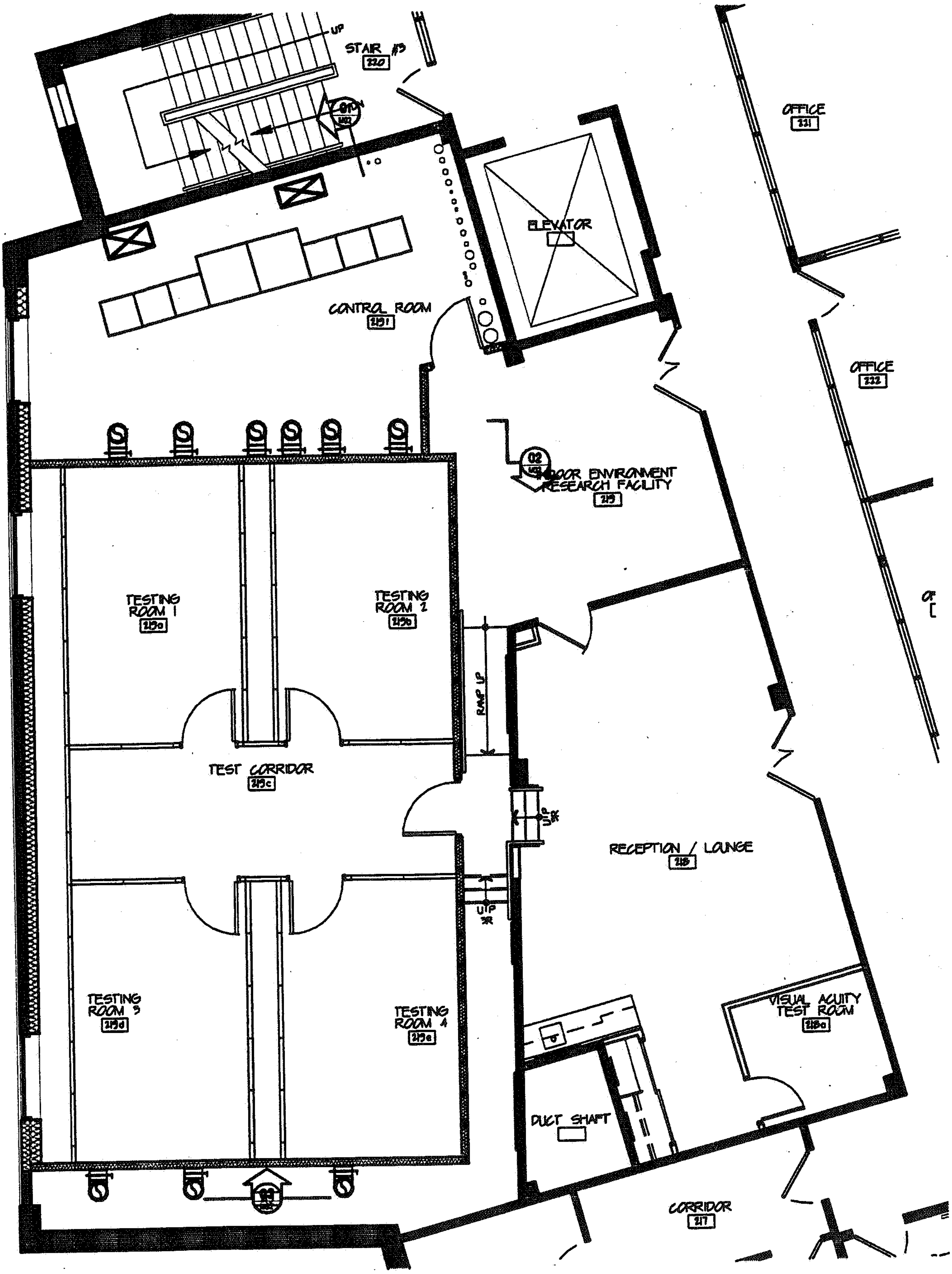

Figure 1 Floor plan

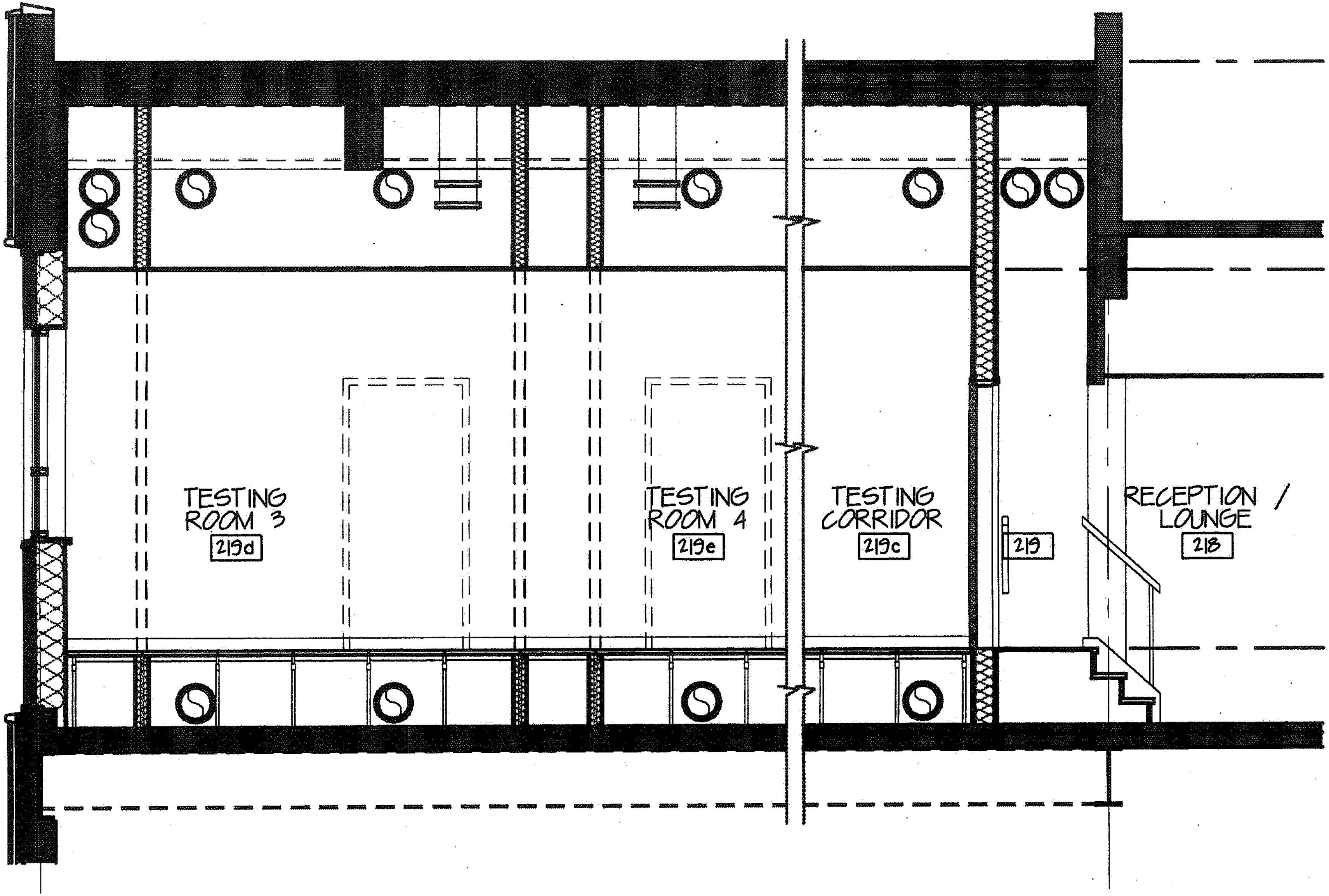

Figure 2 Elevation

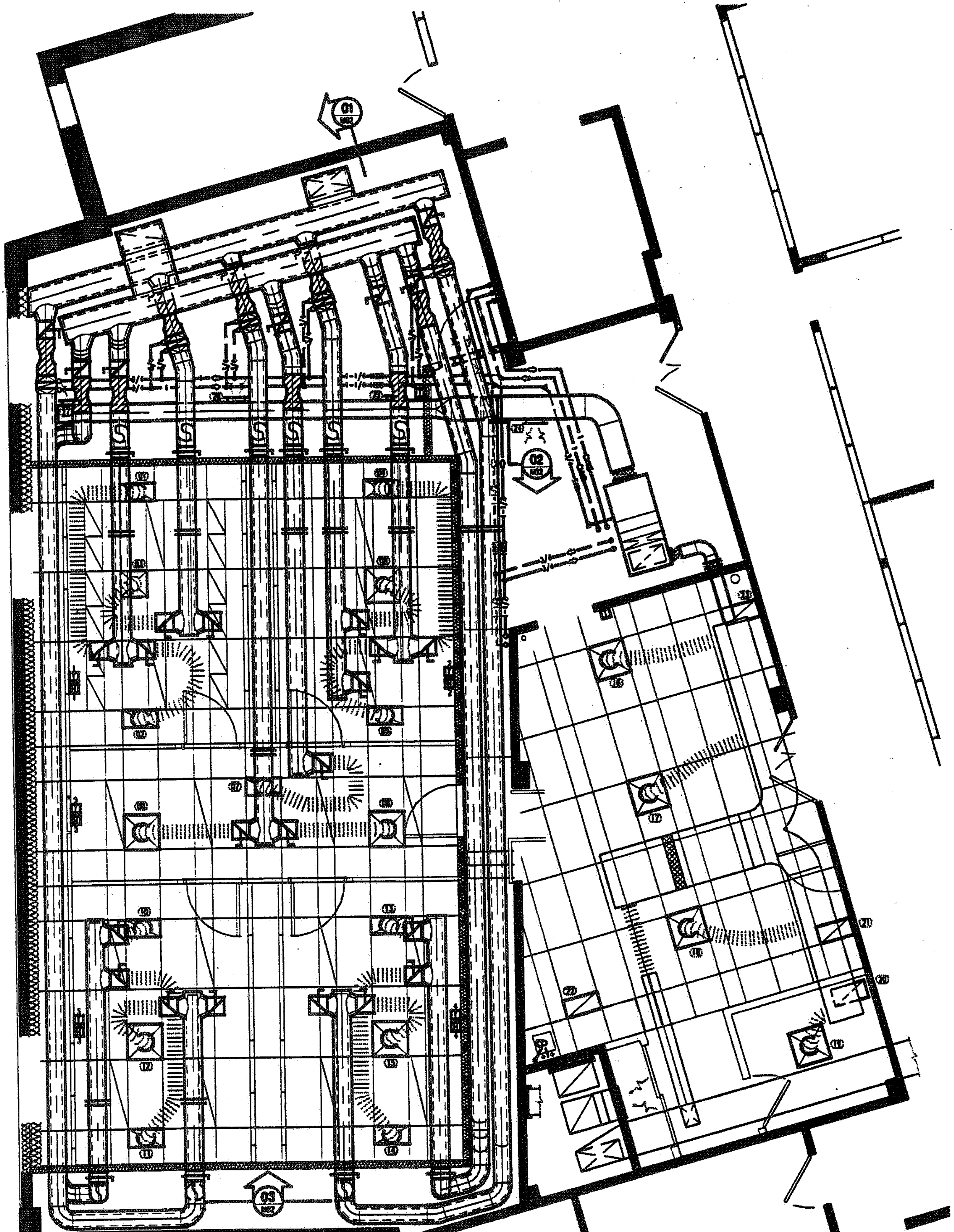

Figure 3 Schematic diagram of ductwork layout

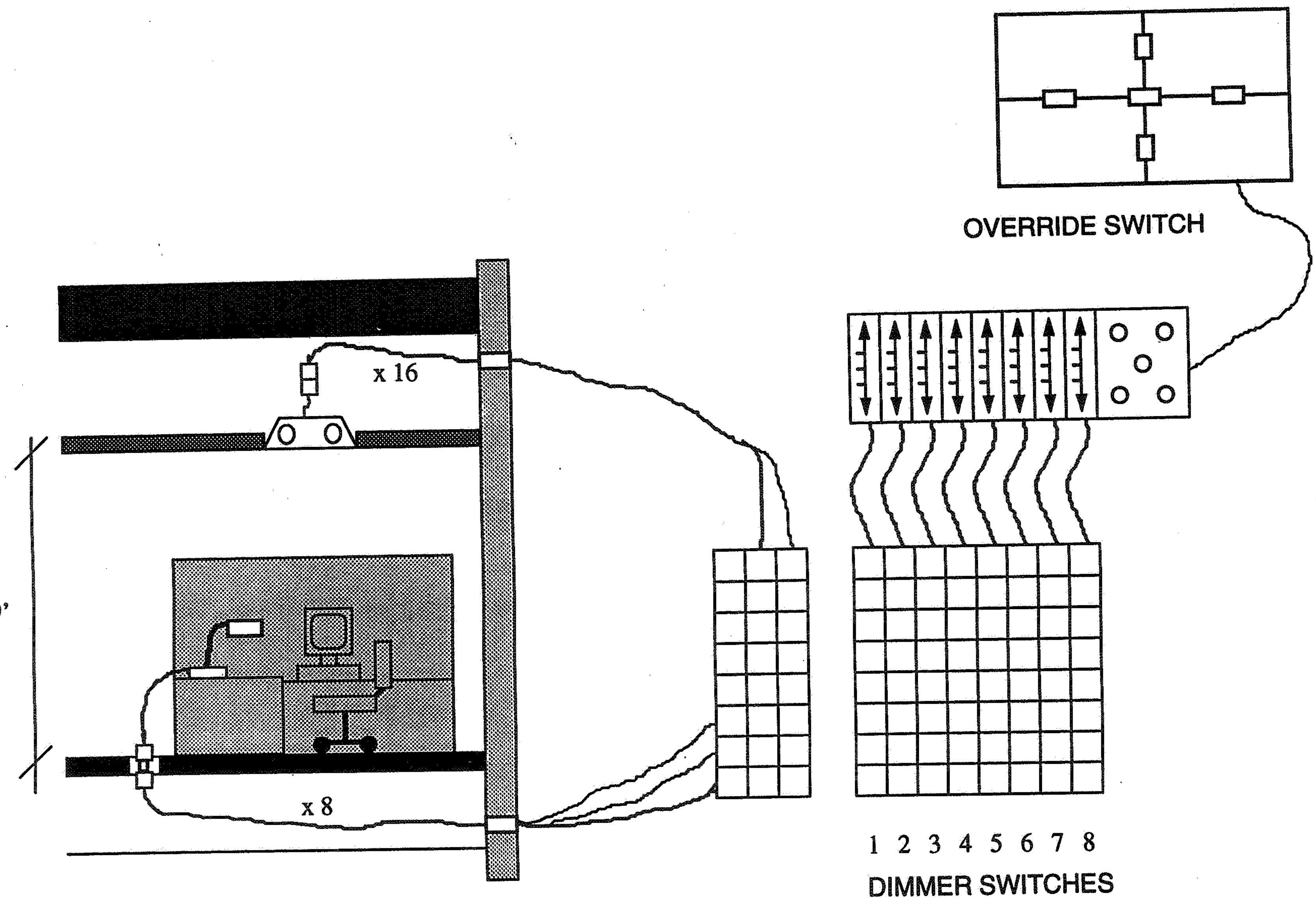

Figure 4 Schematic diagram of lighting controls

Implementing the Results of Ventilation Research
16th AIVC Conference, Palm Springs, USA
19-22 September, 1995

A Simple Calculation Method for Attic Ventilation Rates

I S Walker*, T W Forest**, D J Wilson**

* Energy Performance of Buildings Group, Energy and Environment Division, Lawrence Berkeley Laboratory, University of California, Berkeley, CA, USA
** Department of Mechanical Engineering, University of Alberta, Edmonton, Alberta, Canada

Synopsis

The ventilation of an attic is critical in estimating heating and cooling loads for buildings because the air temperature in the attic is highly sensitive to ventilation rate. In addition, attic ventilation is an important parameter for determining moisture accumulation in attic spaces that can lead to structural damage and reduced insulation effectiveness. Historically, attic venting has been a common method for controlling attic temperature and moisture, but there have been no calculation techniques available to determine attic ventilation rates. Current practice is to use rules of thumb for estimating attic vent areas.

Simple algebraic relationships are developed here, using functions fitted to an exact numerical solution for air flow through attic envelopes. This algebraic model (AVENT) was developed to be easy to use as diagnostic or design tool. Key factors included in the model are: climate (wind and stack effect), wind shelter, leakage distribution and total attic leakage.

This paper validates the model predictions by comparing to measured data from two attics at the Alberta Home Heating Research Facility (AHHRF). Average errors for the model are about 15% compared to the measured ventilation rates.

1 Introduction

The impact of attic venting on energy use and moisture control is well known. For example, in hot climates attic ventilation is used to cool the attic to reduce heating loads due to solar gain on the roof, and in cold climates attic venting is used to alleviate moisture problems. Methods for predicting attic ventilation rates are not well developed. For example, analyses of heat and moisture transport in attics by Gorman [1] and Peavy [2] used a single fixed value and simple empirical data correlations respectively. Other studies by Walker and Forest [3] have introduced a method for calculating attic ventilation rates using a numerical procedure to balance the flow equations through localised and attic envelope leaks. Walker and Forest's model works well for research level investigations, but is difficult to implement by other researchers or designers as a design or diagnostic tool.

The objective of this paper is to present a simple model that can be used to predict attic ventilation rates based on attic leakage, leakage distribution and weather conditions. Using this model for attic ventilation, building designers will be able to better optimise building performance. For example, the attic leakage may be placed at different locations (e.g. soffit, roof ridge or gable end vents) to find the effect on ventilation rate. To this end, the model developed here includes the effects of total attic venting, distribution of the attic vents and weather conditions.

2 Outline of AVENT model

The model is a set of algebraic equations that have been empirically fitted to the exact numerical solution of the flow equations for attic leaks. This is a procedure that has been used successfully by the authors for ventilation calculations for houses (see Walker and Wilson [4]). Because of the similarity of the model development procedure and the use of the same leakage and weather parameters, the empirical equations for attic ventilation have the same form as those in a house ventilation model, AIM2, developed previously by Walker and Wilson [4]. The differences will be discussed later in this paper.

The total attic leakage (determined by fan pressurization or combining vent sizes) is distributed at different locations on the attic envelope (e.g., the soffits). The leaks are separated because they are at different heights, which affects the stack effect, or because they have different surface pressure coefficients. The wind and stack induced pressures across each leak are calculated for each leakage site and the leakage coefficient and the pressures for each leak are combined to calculate flows using a power law pressure-flow relationship.

A mass balance is then performed on the sum of all leakage flows through the attic envelope. This involves a numerical solution of the non-linear pressure-flow equations. This mass balance is then used to determine empirical coefficients, stack factor, f_s, and wind factor, f_w, to multiply leakage distribution parameters and wind and stack induced pressures to determine the ventilation rate. The wind and stack effects are treated separately and then superposed to calculate the total ventilation rate.

3 Leakage Distribution

The leakage distribution determines where on the attic envelope leaks are located, and determines the stack and wind pressures they experience. The leaks are characterised by two parameters: C [m^3/sPa^n], the leakage coefficient and n, the pressure exponent that are used in the pressure-flow relationship $Q=C\Delta P^n$. For simplicity it is assumed that the same leakage exponent, n, can be applied to all the attic leaks. Using a single exponent means that the total attic leakage coefficient, C_{total}, is just the simple sum of all the separate leaks for the attic:

$$C_{total} = C_{floor} + C_{ridge} + C_{soffits} + C_{gables} + C_{pitched} \tag{1}$$

where

C_{floor} - the attic floor, the same as the ceiling of the house

C_{ridge} - the roof ridge vents

$C_{soffits}$ - the soffits under the eaves

C_{gables} - the gable end vents

$C_{pitched}$ - the pitched roof surfaces. This includes the background leakage and any vents on these surfaces (e.g., mushroom cap vents).

For stack effect calculations, the five leakage sites are differentiated by their height. The floor and gable leakage is at the bottom of the attic, the ridge vents are at the top and the pitched surface and gable end leaks are assumed to be distributed evenly with height. The information about leakage height is condensed into two parameters R and X given by Equations 2 and 3, and first suggested by Sherman and Grimsrud [5]. For an attic these are, for stack effect:

$$R_s = \frac{C_{floor} + C_{soffit} + C_{ridge}}{C_{total}} \tag{2}$$

$$X_s = \frac{C_{floor} + C_{soffit} - C_{ridge}}{C_{total}} \tag{3}$$

For wind effect, C_{floor} is exposed to the house interior pressure due to wind. Because attic floor (i.e., house ceiling) leakage rates are usually much smaller than the flow through soffit or eave vents, only a very rough approximation is required to estimate floor leakage. With this in mind, the house interior pressure is assumed to be the average of the pressure coefficients on the four walls of the house. C_{ridge} is assumed to have the same average pressure coefficient as the pitched roof surfaces. C_{soffit} and C_{gable} have the same pressure coefficients as the walls beneath them. This different grouping of leakage sites for wind effect means that R and X have to be redefined for wind effect by the following equations.

$$R_w = \frac{C_{floor} + C_{ridge}}{C_{total}} \tag{4}$$

$$X_w = \frac{C_{floor} - C_{ridge}}{C_{total}} \tag{5}$$

4 Wind Pressure Coefficients

The wind pressure coefficients for the attic floor, gable end vents and soffits are assumed to be the same as the wall beneath them. The pressure coefficients for these surfaces were taken from the wind tunnel measurements of Akins et al. [6]. This pressure coefficient data set was chosen because it presented results for many wind directions. Because Akins et. al. did not measure pressure coefficients on a range of pitched roof surfaces, the pitched roof pressure coefficients are taken from wind tunnel tests by Wiren [7]. For wind normal to the upwind side of the building, the upwind face has a Cp=0.65, the sides have Cp=-0.65 and the downwind face has Cp=-0.3. These coefficients are for an unsheltered building. Adjustments to these pressure coefficients for houses sheltering each other in a row have been discussed by Walker and Wilson [8]. An harmonic trigonometric function was developed by Walker and Wilson to interpolate between these normal values to fit the angular variation in pressure coefficients shown by Akins et. al. This function has been successfully applied to pressure coefficients for calculating attic ventilation by Walker and Forest [3] and Forest and Berg [9] using an exact numerical attic ventilation model.

For the rest of the attic leaks, the wind pressure coefficients taken from Wiren [7] are shown in Table 1.

Table 1. Roof pressure coefficients from Wiren [7].

Roof Pitch, degrees from horizontal	Upwind face	Downwind face
<10	-0.8	-0.4
10 to 30	-0.4	-0.4
>30	+0.3	-0.5

5 Stack Effect

The flow induced by stack effect, Q_s[m³/s], is assumed to have the power law form

$$Q_s = C_{total} f_s \Delta P_s^n \tag{6}$$

where f_s = stack flow factor and ΔP_s = stack effect reference pressure [Pa] given by

$$\Delta P_s = \rho_{out} g (H_p - H_e) \left(\frac{|T_a - T_{out}|}{T_a} \right) \tag{7}$$

where ρ_{out} = outdoor air density, [kg/m³]

g = gravitational acceleration [m/s²]

H_p = roof peak height above grade [m]

H_e = height of eaves or soffits above grade [m]

T_a = attic air temperature [K]

T_{out} = outdoor temperature [K].

The stack factor, f_s, was found by using a numerical solution to the attic flow equations to calculate the stack driven ventilation rate flowrate, Q_s. This was substituted into Equation 6, which was then solved for f_s. Q_s and f_s were calculated over a wide range of R_s, X_s and flow exponent, n. The algebraic approximation for stack factor was developed to give the same dependence of f_s on these parameters as the exact numerical solution. This approximation is given by Equation 8. The functional form of this approximation was selected to produce the correct limits of f_s when all leakage is concentrated in the pitched roof surfaces (i.e., no soffit or gable vents and $R_s = 0$), in the floor, eaves and roof ridge ($R_s = 1$), and for the ceiling-floor difference ratio limits of $X_s = 0$ and $X_s = +/- 1$.

$$f_s = \left(\frac{1 + nR_s}{n+1} \right) \left(\frac{1}{2} - \frac{1}{2} \left(\frac{X_s^2}{2 - R_s} \right)^{\frac{5}{4}} \right)^{n+1} \tag{8}$$

Equation 8 is the same as stack factor for a house with no furnace flue in AIM2, except that the leakage distribution coefficient definitions have changed to suit attic leakage locations. The stack factor calculated using Equation 8 is shown in Figure 1 together with the exact numerical stack factor. Figure 1 shows that the difference between exact and approximate f_s is typically a few percent, and that the stack factor (and therefore ventilation rate) is highly dependent on leakage distribution.

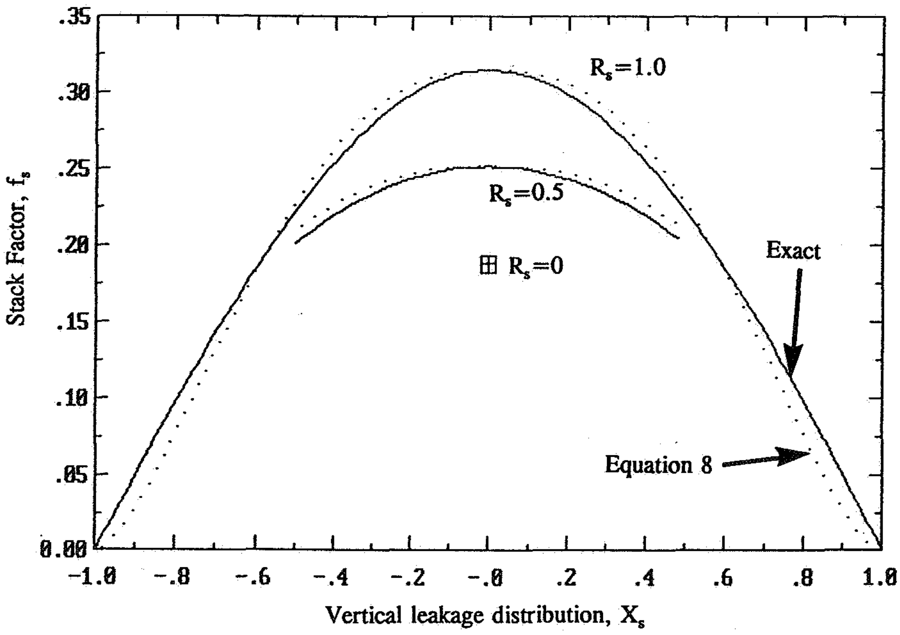

Figure 1. Comparison of stack factor, f_s, from exact numerical calculations and empirical approximation.

6 Wind Effect

The wind induced infiltration rate, $Q_w[m^3/s]$ is defined in terms of wind factor f_w by

$$Q_w = C_{total}\ f_w\ \Delta P_w^n \tag{9}$$

The reference wind pressure, ΔP_w is given by

$$\Delta P_w = \frac{\rho_{out}(S_w U)^2}{2} \tag{10}$$

where U = unobstructed wind speed (with no local shelter) at eaves height at the building site.

S_w = local wind shelter coefficient.

S_w is 1.0 for an unsheltered attic and 0 for a completely sheltered attic. Values of S_w must be estimated for the building location. Methods for estimating S_w are outlined by Walker and Wilson [8], including an interpolation method for calculating S_w for any wind direction.

The wind factor, f_w, was found by using the exact numerical solution to determine Q_w. This value for Q_w was then substituted into Equation 9, which was solved for f_w. As with the stack factor calculations, the approximating function for f_w was found by calculating f_w over a wide range of leakage parameters and finding functional forms that would reproduce the same characteristic dependence on these parameters. The wind factor, f_w, is given by

$$f_w = 0.15(2-n)\, X^* R^* \tag{11}$$

where

$$R^* = 1 - R_s\left(\frac{n}{2} + 0.2\right) \tag{12}$$

$$X^* = 1 - \left(\left(\frac{X_s - \left(\frac{1-R_s}{5}\right)}{2-R_s}\right)^2\right)^{0.75} \tag{13}$$

The main difference between the above relationship for f_w and that given by Walker and Wilson [4] for houses is the change in lead coefficient to **0.15** (from 0.19). This change is due to different pressure coefficients used for the attic. The value 0.15 is for roofs with pitches between 10 and 30 degrees (which covers most roofs). The change of pressure coefficients with roof pitch given by Table 1 changes this lead coefficient by typically less than 5%, except at extreme leakage distributions (i.e. no soffits, gable vents or floor leakage) where the change is about 25%. For simplicity a single value for this lead coefficient is adopted that covers a wide range of roof configurations.

Figure 2 compares the exact numerical and approximate value for f_w. This figure shows that typical differences between the exact and approximate f_w are about +/-5%. This figure also illustrates the strong dependence of f_w (and therefore ventilation rate) on leakage distribution.

The effect of wind angle on wind factor depends on how the pressure coefficients change with wind angle. Walker and Wilson [8] have discussed how wind pressure coefficients change with wind direction, and how to interpolate between normal pressure coefficients to determine pressure coefficients at intermediate wind angles. However, calculations using pressure coefficients measured by Akins et al. [6] for several wind directions have shown that large changes in pressure coefficient do not translate into large changes in f_w with wind angle. These calculations indicated that f_w has about a +/-15% variation with wind angle for an exposed attic. Calculations were also performed for an attic on a house sheltered by its neighbours, with reduced side wall pressure coefficients when the wind blows along the row of houses. These calculations had about the same variability and mean value over all wind directions as the exposed house. Because the change in f_w with wind angle is extremely complex and is not a dominant parameter it is neglected for simplicity. Its effect can be estimated in a particular situation by varying the lead coefficient in f_w from 0.13 to 0.17.

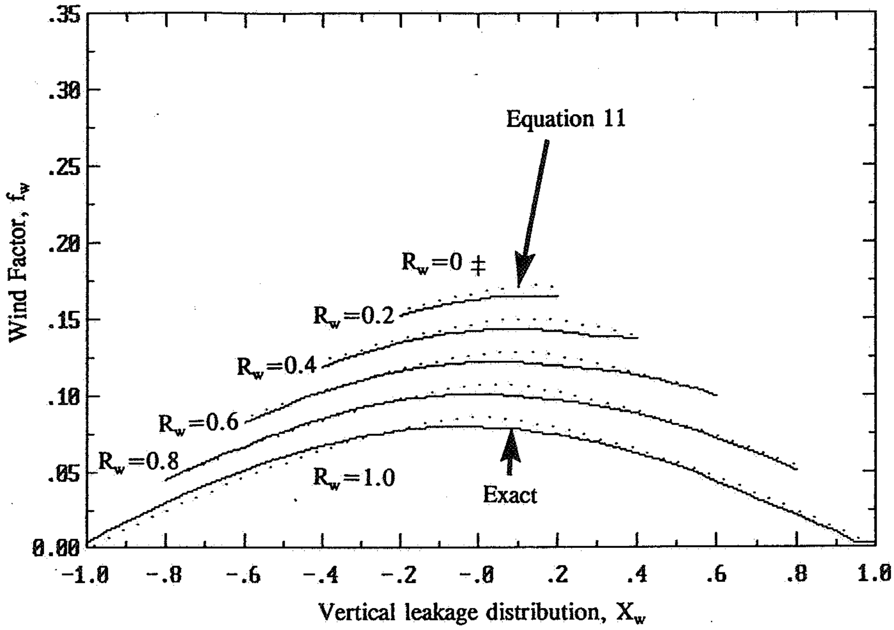

Figure 2. Comparison of wind factor, f_w, from exact numerical calculations and empirical approximation.

7 Combining Stack and Wind effects

The stack and wind driven ventilation rates given by Equations 6 and 9 must be combined to determine the total ventilation rate. This attic model, AVENT, uses the same superposition technique used before by the authors for calculating house ventilation rates. A detailed analysis of this and other superposition techniques is given by Walker and Wilson [10]. The superposition method used here is based on simple pressure addition for wind and stack effects and a simple first order interaction term:

$$Q = \left(Q_s^{\frac{1}{n}} + Q_w^{\frac{1}{n}} + B_1 (Q_s Q_w)^{\frac{1}{2n}}\right)^n \tag{14}$$

where Q = total flow due to combined wind and stack effects [m^3/s]

B_1 = interaction coefficient, assumed constant.

Analysis of data from the AHHRF test houses in many leakage configurations by the authors for periods where Q_s and Q_w were approximately equal suggests that a reasonable estimate for the interaction coefficient is B_1 =-0.33

8 Measurements and Model Verification

The measurements used to verify the model predictions were made at the Alberta Home Heating Research Facility (AHHRF). Two attics were monitored that had different leakage (by about a factor of four) and different leakage distributions. The two attics are labeled Attic 5 and Attic 6. Attic 5 is relatively tight in construction with few vents with a flow coefficient (C) of 0.044 [m^3/sPa^n] and exponent (n) of 0.71 and attic 6 has soffit vents and mushroom cap vents resulting in a much leakier construction with $C = 0.232$ [m^3/sPa^n] and $n = 0.6$. The ventilation rates were measured using a constant concentration tracer gas system. Attic temperatures and ambient weather conditions were also monitored. The measurements are described in greater detail by Walker and Forest [11].

A total of 3758 hourly averaged ventilation rate measurements were made in attic 5 and 3522 in attic 6. These measurements were made over a year so as to capture a large range of weather conditions. Analysis of these measurements showed that attic ventilation is a weak function of ambient temperature because the attics are not tall (2 m at the peak) and the temperature differences are smaller than for houses because the attics are unheated. This small height and temperature difference means that stack effect pressures are small and there is little stack effect ventilation. For this reason, the figures comparing measured and predicted ventilation rates will concentrate on wind effect. In addition, ventilation rates were normalised by attic volume to express them in air changes per hour (ACH).

The above relationships, in Equations 6 through 14, were used to predict attic ventilation rates for the two attics based on their total leakage, leakage distribution estimates and measured weather conditions for every hour of measurements. Figures 3 and 4 compare the measurements and model predictions for attics 5 and 6 respectively. For clarity in these figures, the measured ventilation rates were binned for every 1 m/s of windspeed. The average is shown by a square and the bars represent the standard deviation of the measured data within each bin. The predicted ventilation rates were also binned and averaged every 1 m/s and the averages are shown connected by a solid line in these figures.

Figures 3 and 4 show that the model predictions are close to the measurements on average with a mean difference of 13% for attic 5 and 15% for attic 6. The figures also show the large range of measured data for each windspeed bin. Some of this is due to having a range of windspeeds (and temperatures) within each bin, but is dominated by variations due to wind shelter (because the test houses are in an east-west row they shelter each other for east and west winds and are exposed for north and south winds). This shelter variation introduces a variation of approximately a factor of two in wind driven ventilation rates. Note that our model is able to account for this shelter variation using the shelter factor, S_w in Equation 10. Additional variation is the result of averaging measured values over an hour. Analysis by Walker and Forest [11] found that after accounting for given windspeed and wind direction there is still a standard deviation of about 30% in measured ventilation rates. For this reason it was essential to have the large data sets used here to evaluate the model predictions.

The above differences between measurements and model are averaged over the whole data set and indicate the precision of the model when applied to long time averages that would be typical when estimating energy losses for attics. The average absolute difference (which does not cancel positive and negative differences) is about 33% for attic 5 and 40% for attic 6. This is a typical difference between model and measurements for an individual hour. Given the hourly variation in measured ventilation rates and the simplicity of the model these average and absolute errors seem reasonable for design estimates.

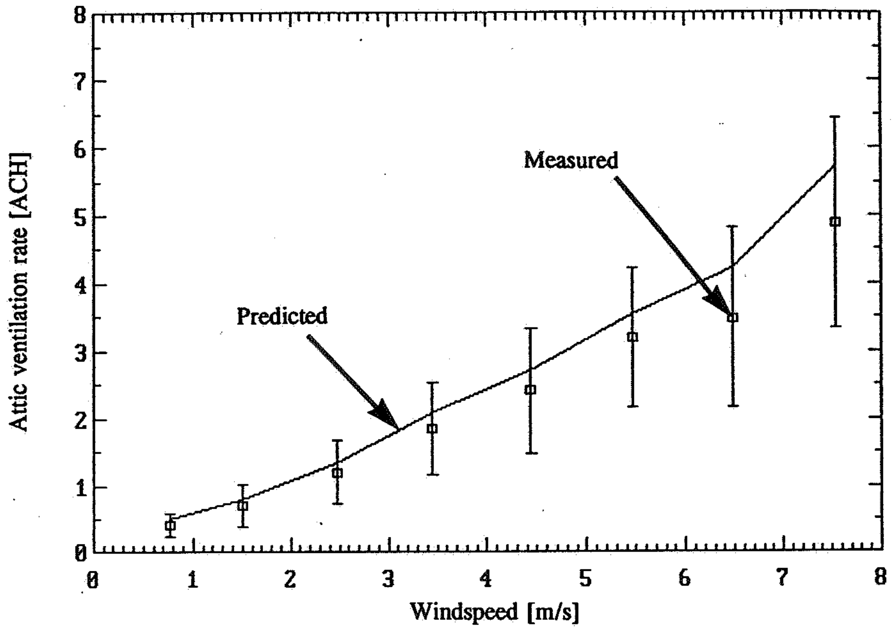

Figure 3. Measured and predicted attic ventilation rates for attic 5 at AHHRF (3758 hours). Bars represent one standard deviation of measured data.

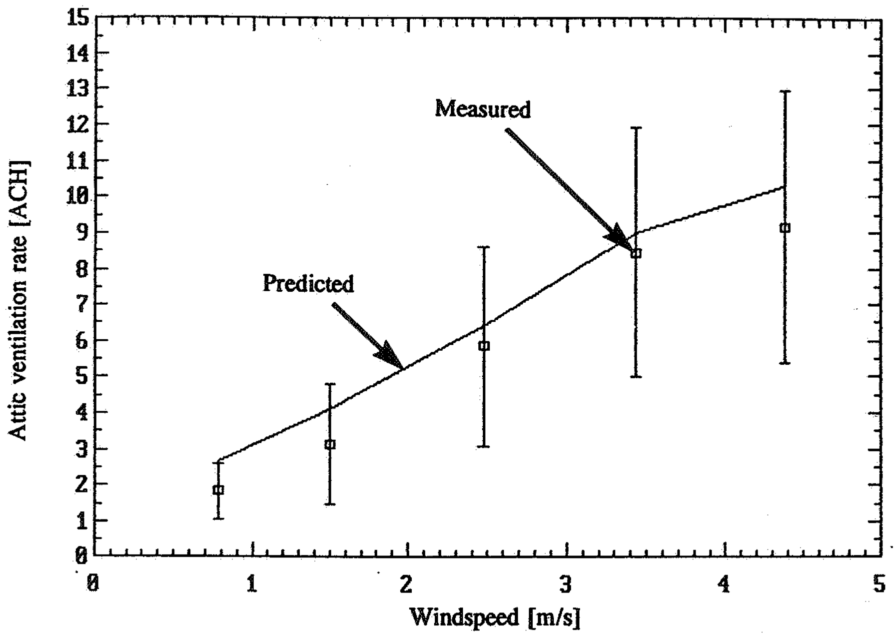

Figure 4. Measured and predicted attic ventilation rates for attic 6 at AHHRF (3522 hours). Bars represent one standard deviation of measured data.

9 Summary

The AVENT model presented here was developed to provide a simple method for estimating attic ventilation rates that is able to account for changing weather, leakage distribution (e.g. soffit, gable or roof ridge) and wind shelter.

This single zone attic ventilation model is based on easy to use algebraic relationships developed from exact numerical solutions to flow through the attic envelope. Model parameters for stack and wind effect were not found by fitting to measured data, but are based on exact theoretical relationships and wind tunnel measurements for pressure coefficients.

The model was validated by comparing predictions to measured data from two attics at AHHRF. The average differences were 13% and 15% for the two attics, which is acceptable given the simplicity of the model and the large variation in measured data.

10 Acknowledgments

The authors gratefully acknowledge the support of CMHC and NSERC. Additional support was provided by the Assistant Secretary for Conservation and Renewable Energy, Office of Building technologies, of the U.S. Department of Energy under Contract No. DE-AC03-76SF00098.

11 References

1. Gorman, T.M., "Modeling Attic Humidity as a function of Weather, Building Construction and Ventilation Rates", Ph.D. Dissertation, College of Environmental Science and Forestry, State University of New York, 1987.
2. Peavy, .A., "A Model for Prediction the Thermal Performance of Ventilated Attics", Summer Attic and House Ventilation, NBS Special Publication 548, 1979, pp.119-145.
3. Walker, I.S. and Forest, T.W., "Attic Venting and Moisture", CMHC report, 1993.
4. Walker, I.S., and Wilson, D.J., "Including Furnace Flue Leakage in a Simple Infiltration Model", Air Infiltration Review, Vol. 11, No. 4, AIVC, Coventry, U.K., September 1990, pp.4-8.
5. Sherman, M.H., and Grimsrud, D.T., "The Measurement of Infiltration using Fan Pressurization and Weather Data", LBL report number 10852, Lawrence Berkeley Laboratory, University of California, 1980.
6. Akins, R.E., Peterka, J.A. and Cermak, J.E., "Averaged Pressure Coefficients for Rectangular Buildings", Wind Engineering Vol. 1, Proc. 5th Int. Conf., 1979, pp. 369-380.
7. Wiren, B.G., "Wind Pressure Distributions and Ventilation Losses for a Single-Family House as Influenced by Surrounding Buildings - A Wind Tunnel Study", Proc. Air Infiltration Centre Wind Pressure Workshop, Brussels, 1984.
8. Walker, I.S. and Wilson, D.J., "Simple Methods for Improving Estimates of Natural Ventilation Rates", Proc. 15th AIVC Conference, Buxton, UK, September 1994.
9. Forest, T.W. and Berg, "Simulations of Attic Ventilation and Moisture", Canada Mortgage and Housing Corporation Report, 1993.
10. Walker, I.S. and Wilson, D.J., "Evaluating Models for Superposition of Wind and Stack Effect in Air Infiltration", Building and Environment, Vol. 28, No. 2, pp. 201-10, 1993, Pergamon Press.
11. Walker, I.S. and Forest, T.W., "Field Measurements of Ventilation Rates in Flat ceiling Attics", Accepted by Building and Environment, 1995.

Implementing the Results of Ventilation Research
16th AIVC Conference, Palm Springs, USA
19-22 September, 1995

Pressure Simulation Program

B Knoll, J C Phaff, W F de Gids

TNO Building and Construction Research,
Delft, The Netherlands

16 th AIVC Conference
Implementing the results of ventilation research

PRESSURE SIMULATION PROGRAM

B. Knoll, J.C. Phaff and W.F. de Gids
TNO Building and Construction Research
Delft, The Netherlands

SYNOPSIS

A computer program has been developed to predict the wind pressure coefficients C_p on facades and roofs of block shaped buildings.
The program is based on fits of measured data, including wind shielding by obstacles and terrain roughness.

Main advantages of the program are:

- it needs no expertise of its users on wind pressures;
- the input is simple. It exists of building and obstacles coordinates and orientations;
- generating C_p values for ventilation model calculations needs no separate action. By linking the pressure simulation program and the ventilation calculation program as well as their input, wider application of ventilation programs for non-experts becomes possible.

The accuracy of the predicted wind pressures in the first version of the pressure simulation program are promising. Especially complex building shapes and surroundings have to be dealt with more carefully, as well as increasing wind velocities in small passages. Also detailed improvements are necessary, e.g. to account for sloped roofs and the position of ventilation provisions above roof level.
Therefore, generation and implementation of additional wind tunnel data is planned, to improve the present version.

1. INTRODUCTION

A good prediction of wind pressure coefficients C_p, on facades and roofs with ventilation provisions, is vital for natural ventilation calculations. The accuracy of the ventilation calculations can highly depend on it, if wind is the dominant driving force.
The use of wind tunnel experiments to predict C_p-values is a proven, but expensive method. The use of C_p-estimations from data bases is a cheaper, but less accurate alternative and in case of surrounding obstacles almost impossible.
In both methods, generating C_p-values is an expert job, to be performed separately, primary to the actual ventilation calculations. This is found a disadvantage for operating applications with ventilation models by non-expert users.

The organisation for applied scientific research TNO is developing an automatic control system for natural ventilation of industrial buildings for the dutch ventilation company BRAKEL-ATMOS. The control system calculates and sets optimum grill positions, depending on meteo conditions, inside temperature, required ventilation flow and allowable draught.
For this application the need for implicit prediction of wind pressure coefficients became urgent. Due to the knowledge of most its users, the input needs to be simple data of the building to be ventilated and its surroundings.
The lack of such a tool lead to the development of the first version of a wind pressure simulation program, described in this paper.

The pressure simulation program is a computer program, written in Pascal and running under MS-DOS.
The pressure simulation program may be applied for:
- simple building structures (to be simplified to rectangular shaped facades with flat roofs);
- with ventilation provisions on variable positions within the facades and roof;
- in different surroundings per orientation;
- with common terrain roughnesses (z_0 = 0.35 to 7 m);
- and several local obstacles (also more or less block shaped).

2. BASICS OF THE PROGRAM

The pressure simulation program is based on measured data [1, 2]. It concerns wind tunnel experiments:
- on typical block shaped buildings,
- in different terrain roughnesses,
- with and without obstacles on systematically varying distances.

Because of the systematic set-up of these measurements, it was possible to fit the data by a set of mathematical expressions. For parameters describing the data additional references [3, 4 and 5] are applied.

The start of the fits is a formula, describing the general relation of wind pressure and wind direction for an unshielded object. This relation is presented by different researchers (Phaff

[1], Walker and Wilson [4] and ASHRAE).
With a set of additional formulas, containing the building dimensions and the terrain roughness as relevant parameters, the wind pressures on different spots of the roof and each facade are predicted.

The next stage was to add the influence of nearby obstacles.
For the main orientation of each obstacle to the building, a correction on the unshielded C_p was determined, using both the distance between obstacle and building and the leeward side C_p of the obstacle itself. The obstacle leeward C_p was calculated using the same procedure as used for the unshielded building, but now using of course the obstacle dimensions.
After calculating the C_p correction for the main obstacle direction, the correction for surrounding directions is determined, using the "shielding angle" of the obstacle to the building.

To ease the use of the program, a set of formulas has been added, calculating input parameters like dimensions and angles from a minimum of building and obstacle coordinates, to be entered by the user.

3. PROGRAM INPUT

To allow the program to be used by non-experts, the input is restricted to measurable dimensions of the building, nearby obstacles and their positions.

To prevent a time consuming, too detailed input, a simple instruction points out what kind of details are relevant. An example is the criteria for obstacles further away than 5 x their height. These are not considered to be of importance for the local shielding but may contribute to the terrain roughness.

An example of a part of the input is given in the text block and the building lay-out (figure 1).

```
obstacles(position in m(=meter))

terrain level above sea     : 0
roof height of the building: 8.2

    name: HOUSE
     x,y:  0,  0
  azimut:  270
   l,b,z:  22.6 8.5 8  {actual gutter
height=5.4}

    name:
     x,y:  20, -10
  azimut:  0
   l,b,z:  0.1, 0.1, 10

    name:
     x,y:  14.6, 0
  azimut:  270
   l,b,z:  22.6, 2.15, 3

    name:
     x,y:  18.3 ,0
  azimut:  270
   l,b,z:  8.5 34.2 8.5
```

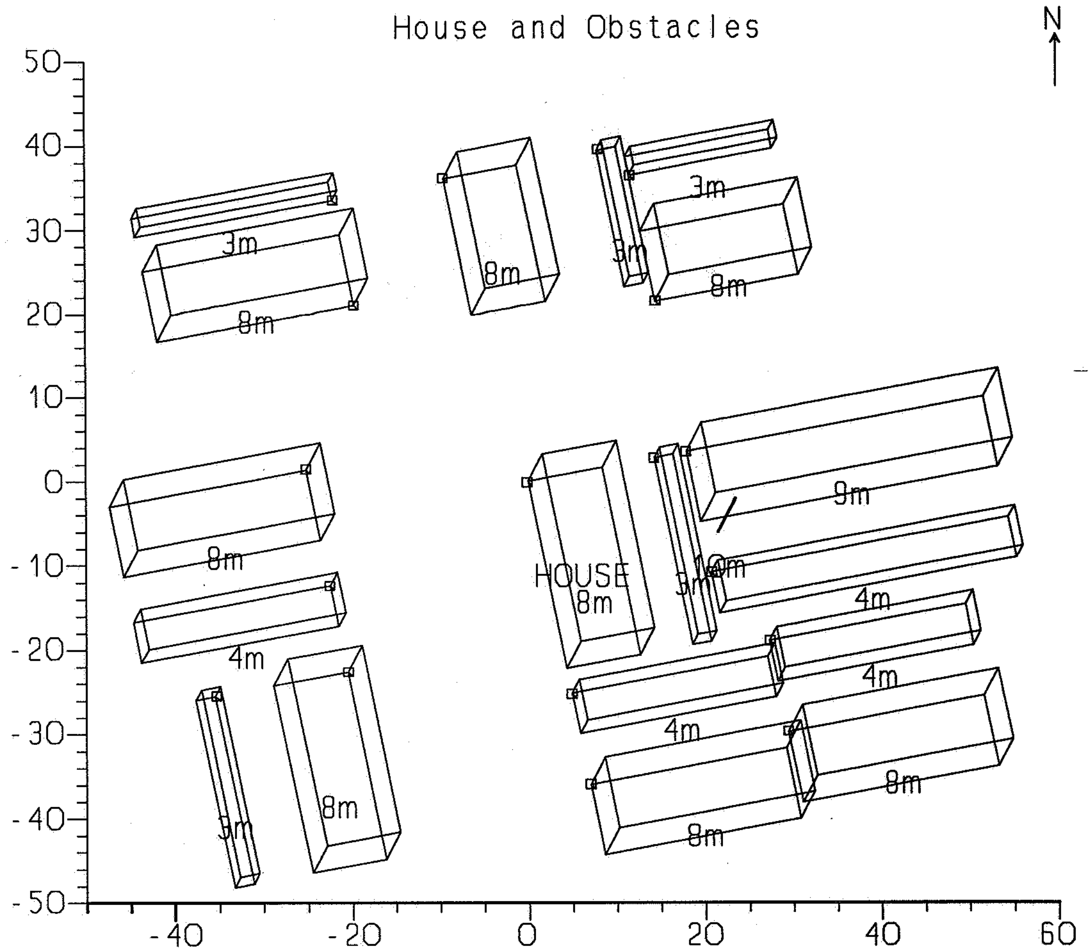

Figure 1 *Input lay-out with a marked edge on floor level of each building. Turning left first defines dimension x and secondly y. Azimuth is given for the first facade.*

4. PROGRAM OUTPUT

The output of the pressure simulation program is an array of pressure data. The pressure data files may be linked directly to a ventilation calculation program.

The output also may be expressed graphical. An example of a graphical output is given in figure 2.
The upper figures show the C_p-values per wind direction in the unshielded situation (imaginary), the local shielding correction (black filling) and their combined result, presenting the actual C_p-values. In the lower figures C_p is plotted polar on a map with the building lay-out. From this plot the influence of each obstacle on C_p may be seen directly.

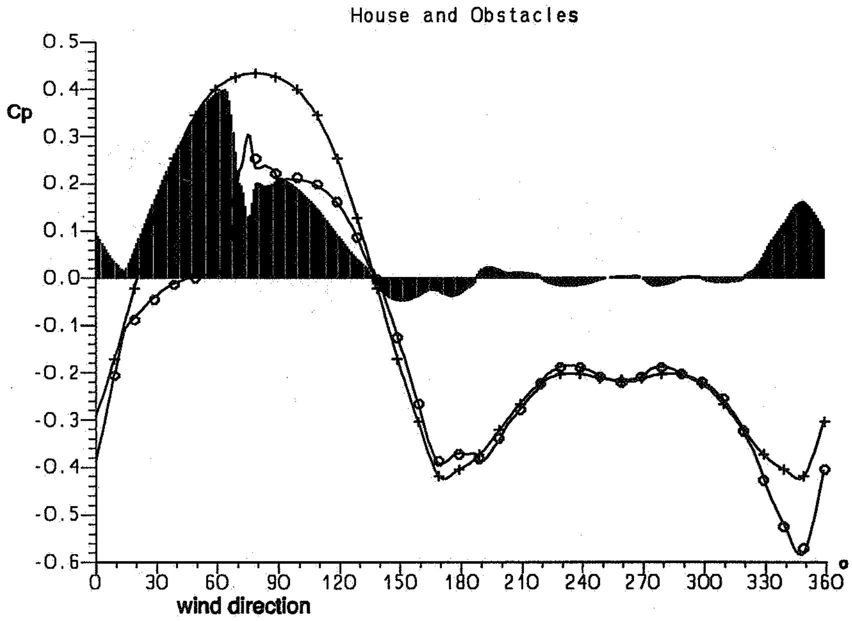

Figure 2 *Output graph for the rear facade. '+'= unshielded, Bar=obstacle correction 'o'= resulting C_p. Below given as a polar diagram.*

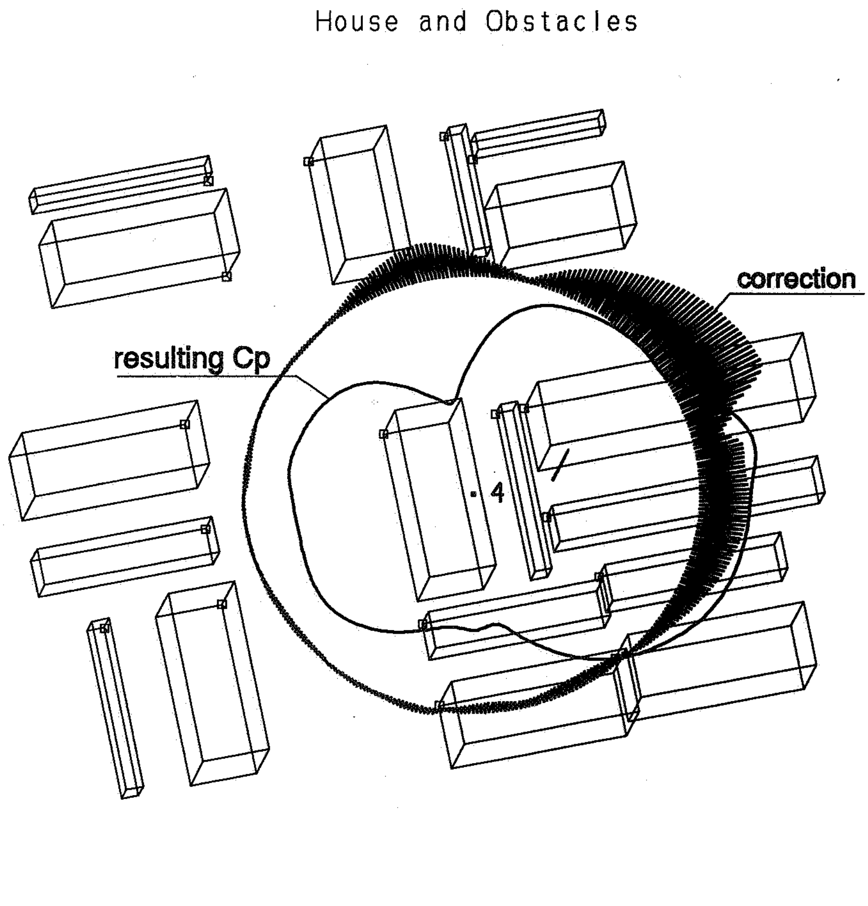

5. FIRST EVALUATION

For the output example shown, a data set of wind-tunnel C_p-values is available. The data set has proved to fit well with actual on-site measurements.
A comparison of these data and the C_p-values calculated with the pressure simulation program is presented in figures 3, 4 and 5.

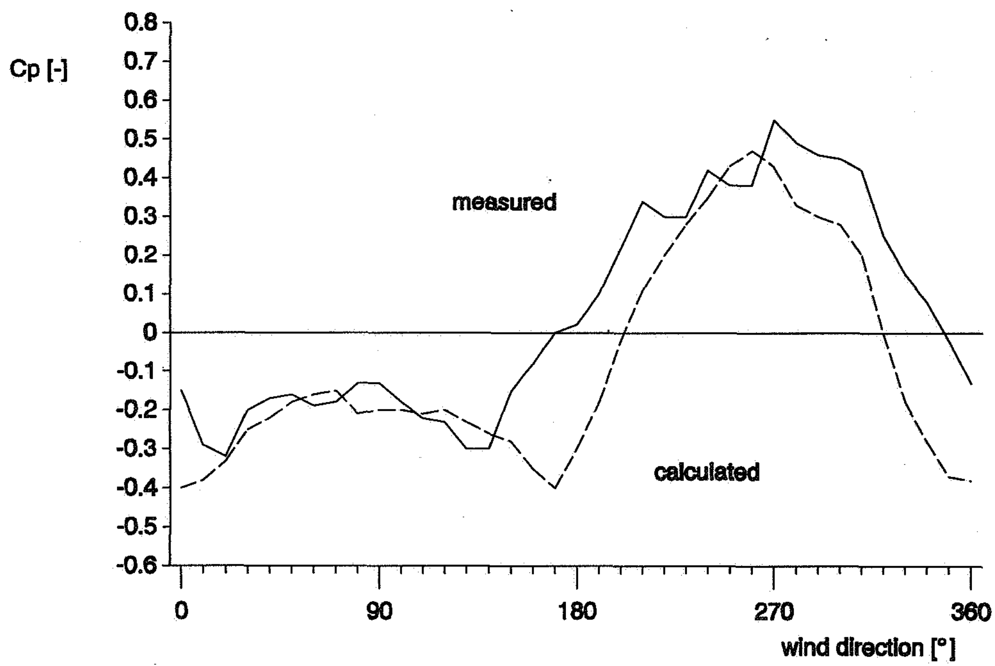

Figure 4 *Comparison measured and calculated C_p for the front facade*

The comparison shows a rather good agreement for both facades. Most remarkable in these characteristics is the change of calculated windward into leeward pressures happening too fast. An over-estimation of the contraction effect (under-estimation of the velocity increase) in case of small passages is held responsible for this.

The comparison for the roof pressure shows a worse agreement, especially for wind directions between 180° and 330°. The slope of the roof and the position of the ventilation duct within the roof is held responsible for this difference. The pressure simulation program doesn't account for sloped roofs yet.

One should realise that a rather preliminary tool is used and that a rather complex configuration of obstacles is concerned.

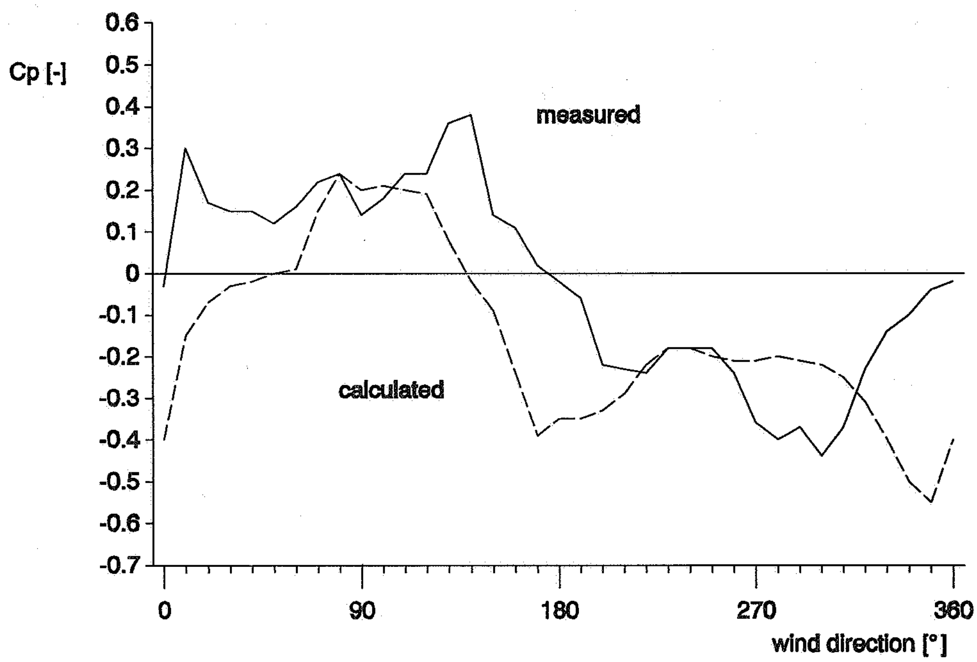

Figure 5 *Comparison measured and calculated C_p for the rear facade*

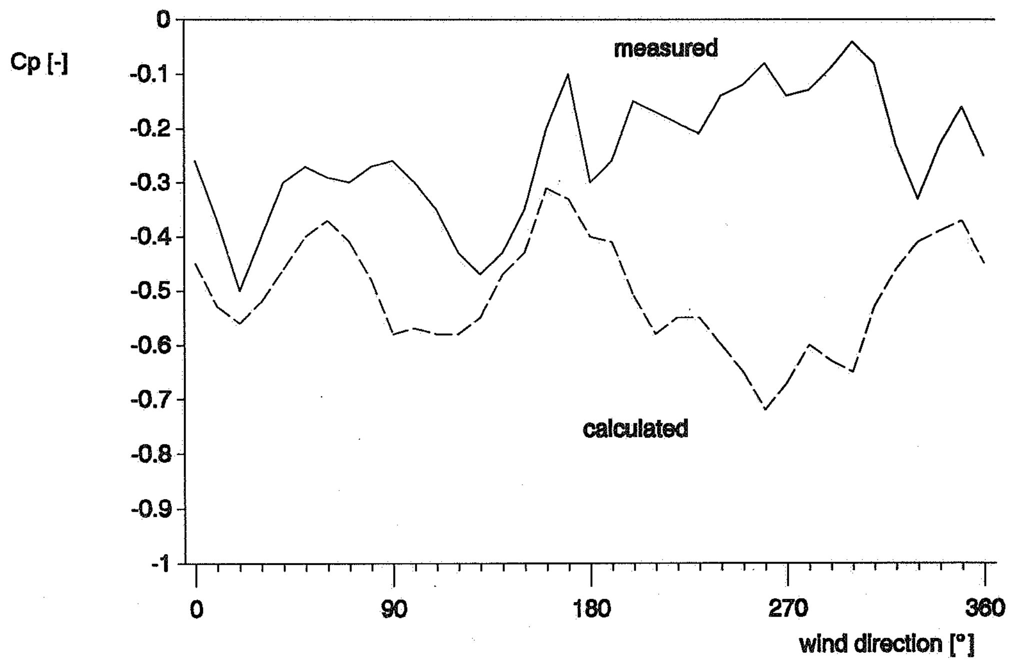

Figure 6 *Comparison measured and calculated C_p for the roof pitch*

Also, one should realise that minor differences in Cp, especially over a wind direction sector, and at steep changes, will have less effect in reality. This is due to normal fluctuations of the actual wind direction.

Therefore the results of the comparison are considered to be hopeful. If some essential corrections are added, the pressure simulation program is expected to be a useful tool. Hence, further development of the tool is recommended.

6. FUTURE IMPROVEMENTS

To end up with a useful and sufficient accurate pressure simulation program, improvements are recommended on:

- complex building shapes (non-block shaped, like sloped roofs, building extensions or combined blocks);
- complex surroundings (obstacle extensions or combined obstacles, sloped surfaces, seasonal corrections for vegetation);
- contraction effects depending on passage width.

Apart from this, extracting a version for correction of local meteo data is recommended. When local meteo data is used to control ventilation, the correction for local effects often is poor. This badly affects ventilation control. The obstacle corrections of the pressure simulation program may be utilised also to correct these data.

7. REFERENCES

[1] Phaff, J.C.
Model tests of the wind pressure distribution on some common building shapes.
Delft (NL), TNO report C403 (in Dutch), november 1977.

[2] Phaff, J.C.
Continuation of model tests of the wind pressure distribution on some common building shapes.
Delft (NL), TNO report C429 (in Dutch), june 1979.

[3] Bottema M.
Wind Climate and Urban Geometry.
TU Eindhoven (NL), 1993.

[4] Walker, I.S. and D.J. Wilson.
Practical Methods for Improving Estimates of Natural Ventilation Rates.
AIVC conference proceedings, 1994.

[5] Wolfseher, U. and K. Gertis.
Literature based estimation of the local wind distribution on shielded and unshielded surfaces ("Darstellung der lokalen Windverhältnisse über unbebauten und bebauten Flächen auf Grund vorhandener Literatur").
Gesundheits-Ingenieur 99, pages 321 - 352 (in German), 1978.

Implementing the Results of Ventilation Research
16th AIVC Conference, Palm Springs, USA
19-22 September, 1995

Determining IAQ Dynamic Response to Emissions

Milton Meckler, P E

President, The Meckler Group, Encino, California, USA

DETERMINING IAQ DYNAMIC RESPONSE TO EMISSIONS

Milton Meckler, P.E.

President, The Meckler Group
Encino, California, U.S.A.

ABSTRACT

To achieve acceptable indoor air quality (IAQ), ASHRAE Standard 62-1989 recommends the use of the alternative IAQ procedure.. The IAQ procedure can treat both constant-volume and variable-air-volume (VAV) with constant or proportional outside airflow rates. The relationships in Appendix E of the standard must be used in conjunction with the IAQ procedure to directly calculate indoor air contaminant concentrations in an occupied space. However, these relationships may not provide sufficient information to fully analyze system operation at part-load conditions, and particularly, to predict dynamic variations of contaminant concentrations during the day. Determination of indoor air contaminant concentrations vs. time of the day can be used as a design strategy to provide IAQ compliance in new construction and remodeling as well as a means to monitor whether maximum allowable concentrations are reached in old buildings.

This paper will first demonstrate the development of a dynamic model for each of the seven heating, ventilating and air-conditioning (HVAC) systems listed in the standard, and will apply this dynamic modeling to estimate the concentrations of formaldehyde and particulates (PM_{10}) as a function of time in an office occupancy for three types of filters.

1.0 INTRODUCTION

Emissions from indoor contamination sources such as building materials, consumer products, etc. are the primary determinant of IAQ. In achieving acceptable IAQ, ASHRAE Standard 62-1989 prescribes the use of the alternative IAQ procedure. This procedure can be used to treat both constant-volume and VAV with constant or proportional outside airflow rates.

Appendix E (Table E-1) of the standard also provides relationships to be used in conjunction with the IAQ procedure to directly calculate indoor air contaminant concentrations in an occupied space, and also to verify the adequacy of the outside ventilation airflow rates obtained by the Ventilation Rate (VR) procedure. However, these relationships may not provide sufficient information to fully analyze system operation at part-load conditions, and especially, to predict dynamic variations of indoor air contaminant concentrations throughout the day[1]. Determining dynamic variations can serve as a design strategy to provide IAQ compliance in new construction and remodeling as well as monitoring purposes. It provides a means to control indoor air contaminant concentrations cost-effectively than using excessive outside air (dilution).

In this paper, we will first develop a dynamic model for each of the seven most commonly used HVAC systems listed in ASHRAE Standard 62-1989, and then demonstrate how this dynamic modeling works by providing an example. In this example, we will estimate the concentrations of formaldehyde as a function of time in an office occupancy for three types of ASHRAE-rated filters, and outline how one can choose filters to decrease outside airflow requirement. Formaldehyde is the most dominant indoor air contaminant in newly constructed and remodeled buildings. Urea-formaldehyde-foam insulation (UFFI), particle boards, some paper products, fertilizers, chemicals, glass and packaging materials are the major sources of formaldehyde. In addition, we will estimate the indoor air contaminant concentrations of PM_{10} as a function of time for the same office occupancy for monitoring purposes.

2.0 DEVELOPING A DYNAMIC MODEL

Figure 1 shows a new model obtained by modifying the model in Appendix E of ASHRAE Standard 62-1989 to include diffusion. Applying a mass-balance for this model gives:

$$m_s = m_g + m_{v,in} - m_{r,out} - m_f - (m_{ia} - m_{ra}) \tag{1}$$

where

m_g: mass of contaminant generated in space,
$m_{v,in}$: mass of contaminant supplied with outside air,
$m_{r,out}$: mass of contaminant exhausted with return air,
m_f: mass of contaminant captured by filter,
m_{ia}: mass of contaminant absorbed by surfaces in space, and
m_{ra}: mass of contaminant re-absorbed.

In this model, it is assumed that densities of return air and outside air are the same, contaminant is generated continuously at a steady-rate, and no infiltration or leakage occurs. The filter is either located in the recirculated air (location A) or in the mixed air (location B). Eqn. (1) is further simplified by denoting the net effect of absorption (m_{ia} - m_{ra}) as m_a, where $m_{ia} > m_{ra}$. The ventilation effectiveness (E_v) is assumed to be 1.0 (perfect mixing). The concentration of a contaminant at any interval of time, *dt* in a space can be calculated by writing a differential equation for filter location A:

$$QdC_s(t) = Ndt + C_oV_odt - C_s(t)V_odt - C_s(t)(V_s - V_o)E_fdt - C_s(t)V_adt \tag{2}$$

and for filter location B:

$$QdC_s(t) = Ndt + (1-E_f)C_oV_odt - C_s(t)V_odt - C_s(t)(V_s - V_o)E_fdt - C_s(t)V_adt \tag{3}$$

where

$C_s(t)$: concentration of contaminant at time *dt*,
Q: volume of space,
N: contaminant emission rate,
C_o: concentration of contaminant in outside air,
V_o: flow rate of ventilation air,

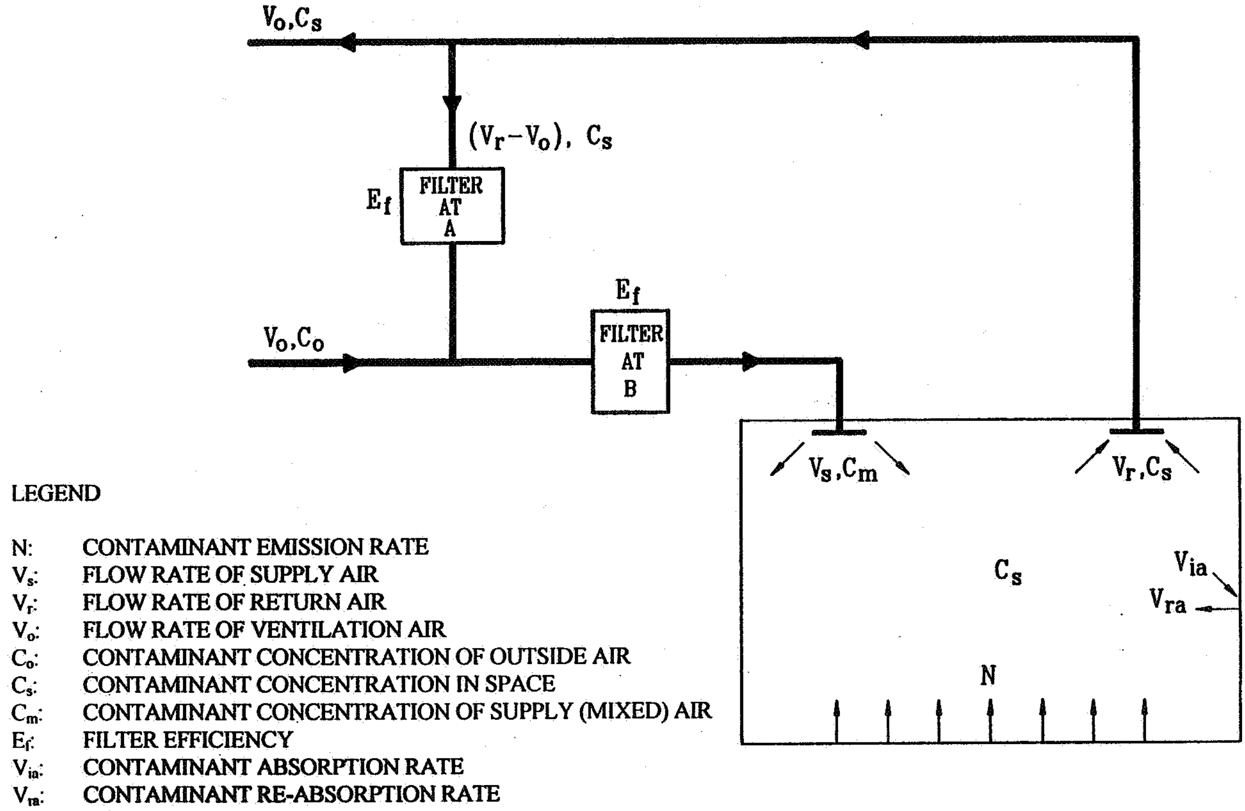

Figure 1. A Model to Determine Concentrations of Contaminants for Filter Locations A and B.

V_s: flow rate of supply air,
E_f: filter efficiency, and
V_a: flow rate of absorbed air.

Solving Eqn. (2) and Eqn. (3) above provides the general solutions in Eqn. (4) and Eqn. (5) for filter locations A and B, respectively.

$$C_s(t) = C_s(t-1)\exp\{-[V_o + V_a + E_f(V_s - V_o)]\,t/Q\} + [(C_oV_o + N) / (V_o + V_a + E_f(V_s - V_o))]\{1 - \exp\{-[V_o + V_a + E_f(V_s - V_o)]\,t/Q\}\} \quad (4)$$

$$C_s(t) = C_s(t-1)\exp\{-[V_o + V_a + E_f(V_s - V_o)]\,t/Q\} + \{[(1-E_f)\,C_oV_o + N] / (V_o + V_a + E_f(V_s - V_o))\}\{1 - \exp\{-[V_o + V_a + E_f(V_s - V_o)]\,t/Q\}\} \quad (5)$$

where

$C_s(t-1)$: initial concentration of contaminant in space.

Depending on the filter location, either Eqn.(4) or Eqn.(5) is then solved for $C_s(t)$ for each class of HVAC systems in Table E-1 of the standard, therefore, creating a distinct model for each class. The resulting dynamic equations are presented in Table 1 for Classes I through VII. Furthermore,

Table 1. Contaminant Concentration as a Function of Time for HVAC System Classes I through VII.

HVAC System Class	Filter Location	Flow	Temperature	Outside Air	Space Contaminant Concentration
I	None	VAV	Constant	100%	$C_s(t) = C_s(t-1) + [C_s(t-1) - C_o]\exp(-V_o t / Q) + \frac{N}{V_o}[1 - \exp(-V_o t / Q)]$
II	A	Constant	Variable	Constant	$C_s(t) = C_s(t-1)e^{-x} + \frac{C_o V_o + N}{V_0 + E_f(V_s - V_o)}(1 - e^{-x})$
III	A	VAV	Constant	Constant	$C_s(t) = C_s(t-1)e^{-y} + \frac{C_o V_o + N}{V_0 + E_f(F_r V_s - V_o)}(1 - e^{-y})$
IV	A	VAV	Constant	Proportional	$C_s(t) = C_s(t-1)e^{-z} + \frac{C_o F_r V_o + N}{F_r V_0 + F_r E_f(V_s - V_o)}(1 - e^{-z})$
V	B	Constant	Variable	Constant	$C_s(t) = C_s(t-1)e^{-x} + \frac{(1-E_f)C_o V_o + N}{V_0 + E_f(V_s - V_o)}(1 - e^{-x})$
VI	B	VAV	Constant	Constant	$C_s(t) = C_s(t-1)e^{-y} + \frac{(1-E_f)C_o V_o + N}{V_0 + E_f(F_r V_s - V_o)}(1 - e^{-y})$
VII	B	VAV	Constant	Proportional	$C_s(t) = C_s(t-1)e^{-z} + \frac{(1-E_f)F_r C_o V_o + N}{F_r V_0 + E_f F_r(V_s - V_o)}(1 - e^{-z})$

Note: Exponents x, y and z above are computed as follows:

$x = \frac{t}{Q}[V_o + E_f(V_s - V_o)]$ $\quad y = \frac{t}{Q}[V_o + E_f(F_r V_s - V_o)]$ $\quad z = \frac{tF_r}{Q}[V_o + E_f(V_s - V_o)]$

the net effect of absorption and re-absorption (or "sink" effects) in Eqn. (4) and Eqn. (5) is omitted because data gathered to date indicate that the sink effects are negligible.

2.1 Evaluating IAQ in New Construction and Remodeling

We will now demonstrate how dynamic modeling can be used in estimating the concentration of formaldehyde in new construction or remodeling. In this example, formaldehyde is assumed to be emitted from resilient flooring, painted surfaces and furniture. The contaminant emission rate of formaldehyde is estimated to be approximately 4.44 $\mu g/m^3$-min per Table H-1 of the draft ASHRAE Standard 62-19XX.

Consider an office occupancy of 93 m^2 with a Class VI HVAC system. A maximum occupancy of 7 people per 93 m^2 is assumed in accordance with ASHRAE Standard 62-1989. Referring to Table 1, the Class VI HVAC system has a VAV system with a filter at location B, and constant temperature and constant outside ventilation airflow rate.

The Class VI HVAC system may have various filter types with different efficiencies. Figure 2 shows the contaminant removal efficiencies of several ASHRAE-rated filters on a mass-mean-diameter (MMD) basis of particulates in microns. For example, the contaminant removal efficiency of an ASHRAE-rated (40%) filter at an MMD of 2.0 microns, is 15%. In our calculations, we will use Type 1 (40%, ASHRAE-rated), Type 2 (60%, ASHRAE-rated) and Type 3 (90%, ASHRAE-rated) filters with corresponding contaminant removal efficiencies of 15%, 50% and 95%.

Table C-1 of the draft ASHRAE Standard 62-19XX provides target concentration guidelines for most common indoor air contaminants. For this example, the target (maximum allowable) concentration of formaldehyde is approximately 0.1 parts per million (ppm) (or 122 $\mu g/m^3$). Based on this allowable concentration, the calculated outside airflow requirement for the office occupancy is 154 L/s (or 22 L/s/person) for new construction and 84 L/s (or 12 L/s/person) for remodeling, if dilution is the only method used to decrease formaldehyde concentrations to allowable levels. These rather high and, therefore costly outside air requirements (in comparison to 9.5 L/s/person for an office occupancy per ASHRAE Standard 62-1989) may be significantly decreased by the use of air-cleaning in combination with proper filtration. Air-cleaning refers to removal of particulates in both gaseous and vapor phases.

To demonstrate a sample calculation, the following variables are used:

$E_f = 0.15$ (15%)
$C_o = 0.0\ \mu g/m^3$
$V_s = 708$ L/s
$V_o = 154$ L/s
$Q = 255\ m^3$
$N = 4.44\ \mu g/m^3$-min (at full occupancy)
$F_r =$ flow reduction factor

The C_s of formaldehyde as a function of time can be calculated by solving the following equation in Class VI of Table 1.

$$C_s(t) = C_s(t-1)\exp(-y) + \{[(1-E_f)\,C_oV_o + N] / [V_o + E_f\,(F_rV_s - V_o)]\}\,[1 - \exp(-y)]$$

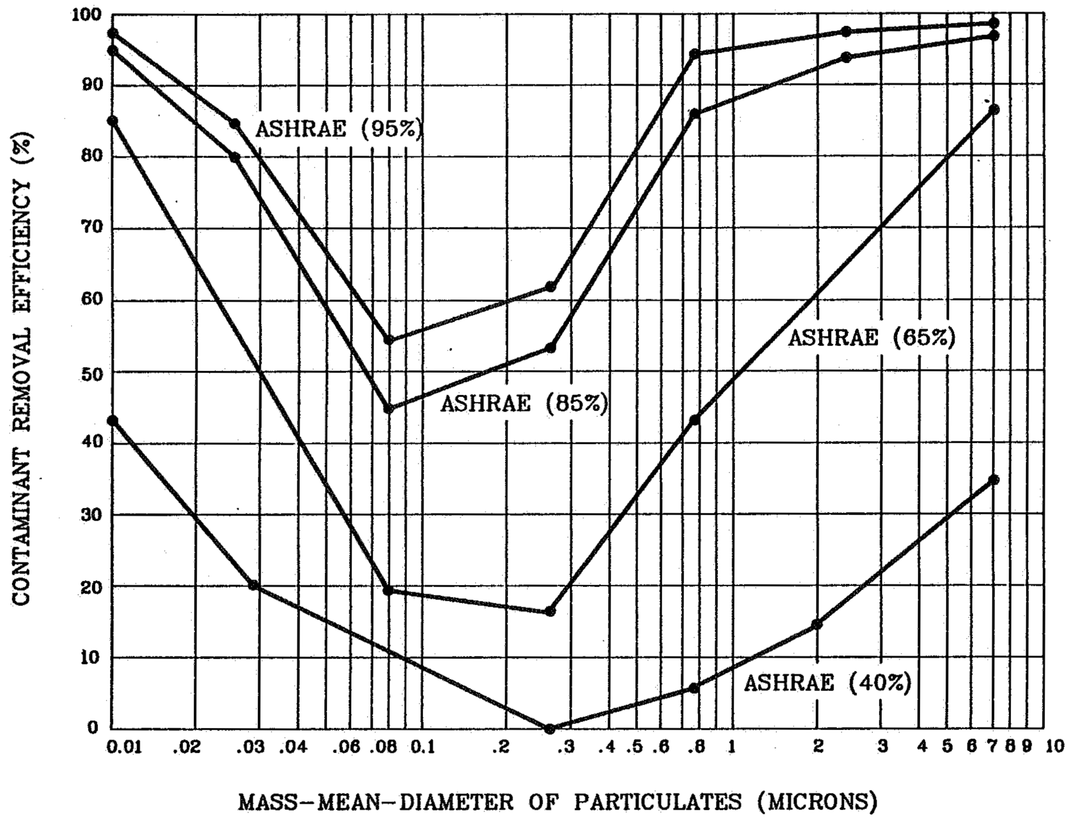

Source : EPA Research Triangle

Figure 2. Contaminant Removal Efficiency of Several ASHRAE-Rated Filters.

where

$$y = [t/Q]\,[V_o + E_f\,(F_r V_s - V_o)]. \qquad (6)$$

Figure 3 shows how the C_s of formaldehyde various hourly depending on the Type 1, Type 2 and Type 3 filter efficiencies during the day with variable occupancy. For comparison purposes, Figure 3 also shows the projected performance with dilution air but without an air-cleaning system. As can be seen from Figure 3, filters with higher contaminant removal efficiencies result in considerably decreased indoor air contaminant concentrations in new construction or remodeling.

Dynamic modeling can be used as a design strategy to deal with high concentrations of formaldehyde in new and remodeled buildings. Not only does this strategy verify the compliance of contaminant concentrations obtained by dilution, it also determines the time of day at which maximum concentrations occur. In Figure 3, maximum formaldehyde concentrations occur between 7:00 am and 9:00 am, and 5:00 pm and 6:00 pm for all three types of filters.

To avoid these maximum concentrations while decreasing the outside air requirement to around 9.5 L/s/person, one needs to use a higher efficiency filter. In this case, holding everything constant, same calculations need to be performed with V_0 = 9.5 L/s/person to observe how these curves behave, and choose the curve with a filter efficiency that will eliminate or minimize the period of time in which maximum concentrations occur. The dynamic modeling described here provides a method to ensure compliance with allowable contaminant concentrations at all times;

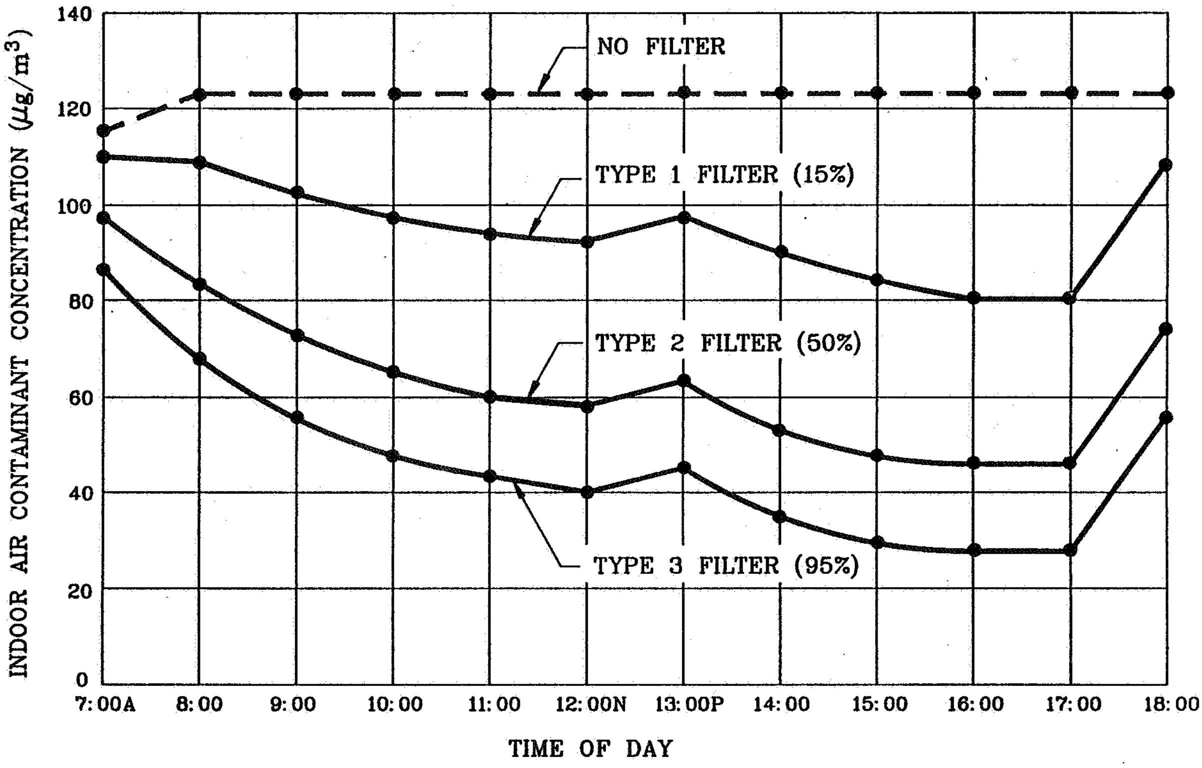

Figure 3. Concentration of Formaldehyde in an Office Occupancy with a Class VI HVAC System and Type 1, Type 2 and Type 3 Filters.

emphasizes the very important role air-cleaning and filtration play in attaining allowable contaminant concentrations and, therefore, acceptable and cost-effective IAQ; and provides a useful means to evaluate HVAC system operation, especially for VAV systems at part-load conditions.

2.2 Monitoring Indoor Air Contaminant Concentrations by Dynamic Modeling

Considering the same office occupancy with a Class VI HVAC system as before, let us now estimate $C_s(t)$ of PM_{10} for Type 1 (40%, ASHRAE-rated), Type 2 (60%, ASHRAE-rated) and Type 3 (90%, ASHRAE-rated) filters with corresponding contaminant removal efficiencies of 18%, 56% and 95%. Again, contaminant removal efficiencies of ASHRAE-rated filters in this example are based on an MMD of particulates in microns. The emission rate of PM_{10} is estimated to be approximately 0.018 $\mu g/m^3$-min per Table H-1 of the draft ASHRAE Standard 62-19XX. Per Table C-1 of the draft ASHRAE Standard 62-19XX, the maximum allowable C_s of PM_{10} is approximately 50 $\mu g/m^3$.

The C_s of PM_{10} as a function of time can be calculated by again solving Eqn.(6). Figure 4 shows how the C_s of PM_{10} varies hourly depending on the Type 1, Type 2 and Type 3 filter efficiencies during the day with variable occupancy. For comparison purposes, Figure 4 also shows the projected performance with dilution air but without an air-cleaning system. In this example again (refer to Figure 4), filters with higher contaminant removal efficiencies result in considerably decreased C_s of PM_{10}.

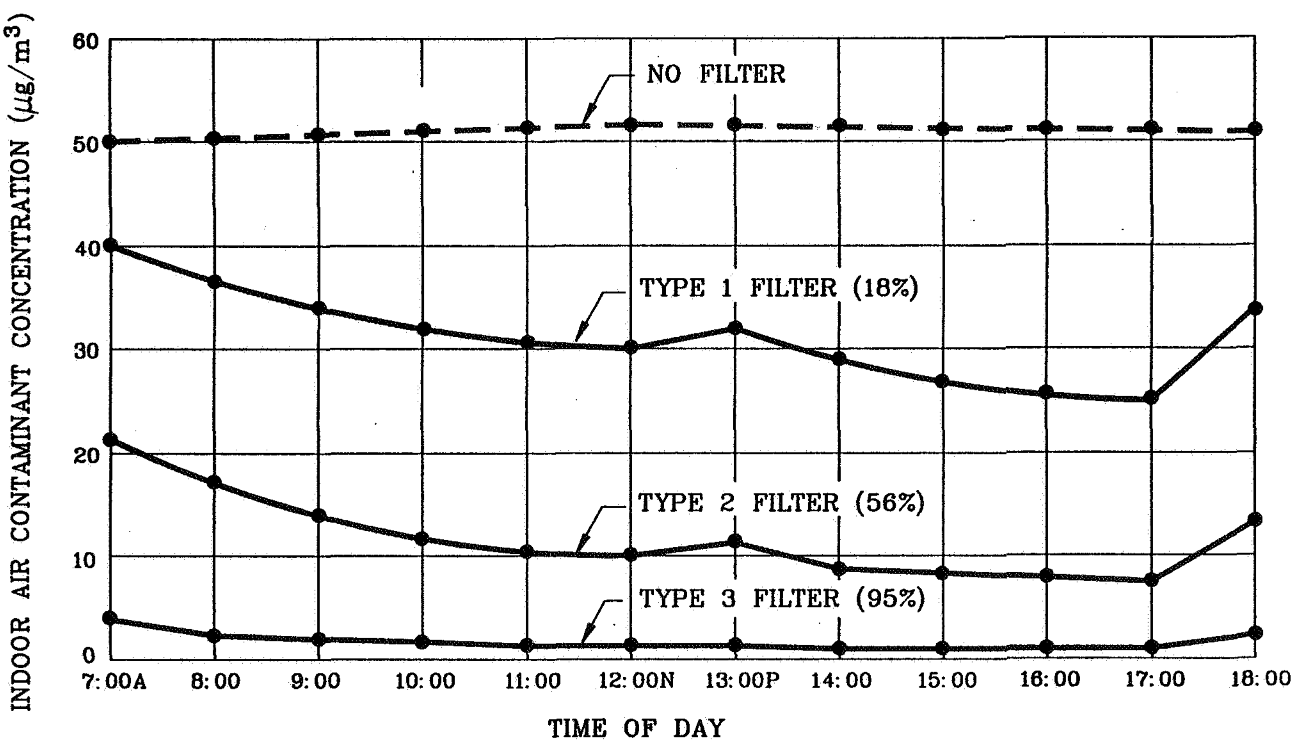

Figure 4. Concentration of PM_{10} in an Office Occupancy with Class VI HVAC System and Type 1, Type 2 and Type 3 Filters.

As can be seen from Figure 4, the monitored maximum PM_{10} concentrations occur between 7:00 am and 9:00 am, and 5:00 pm and 6:00 pm for all three types of filters and they are in compliance with allowable levels. Should these concentrations become significant or exceed the allowable levels, they may be eliminated or minimized simply by choosing a higher efficiency filter. Choosing an appropriate high-efficiency filter can help outside ventilation airflow rate decrease, resulting in significant energy saving while providing acceptable IAQ.

3.0 REFERENCE

[1]MECKLER, M.
"Dynamic Response Models for IAQ Performance Evaluation"
ASHRAE Winter Meeting, Seminar 01, 1995.

Implementing the Results of Ventilation Research
16th AIVC Conference, Palm Springs, USA
19-22 September, 1995

Modelling Coupled Heat and Air Flow: Ping-Pong Vs Onions

Jan Hensen

University of Strathclyde, Energy Systems Research Unit, Montrose Street, Glasgow G1 1XJ, Scotland, UK

SYNOPSIS

By means of a case study involving a severe case of coupled heat and air flow in buildings, this paper aims to quantify the differences resulting from different methods (ping-pong and onion approach) for linking heat and air flow models.
The main conclusion is that when used improperly, the onion method will have implications in terms of computing resources, but - more seriously - the ping-pong method may generate substantial errors.

1 INTRODUCTION

In building energy prediction it is still common practice to separate the thermal analysis from the estimation of air infiltration and ventilation. Although this might be a reasonable assumption for many practical problems, this simplification is not valid for cases involving relatively strong couplings between heat and fluid flow. Passive cooling by increasing natural ventilation to reduce summertime overheating is a typical example.

Given the increased practical importance of such applications, there is a growing interest in practice and academia to establish prediction methods which are able to integrate air infiltration estimation and building thermal simulation (see eg Heidt and Nayak 1994).

There are various approaches for integrating heat and air flow calculations, each having specific consequences in terms of computing resources and accuracy. One way to actually quantify this, is to use a simulation environment which supports these various approaches, and to compare the results of the approaches for a typical case study. This topic is elaborated in the current paper, after a brief outline of the background and implementation details.

2 BACKGROUND

Starting from the observation that it is not very effective to set up single equations describing both fluid and heat flow*, we see in practical applications two basic approaches for integrating or coupling a thermal model with a flow model:
1) the thermal model calculates temperatures based on fixed flows, after which the flow model recalculates the flows using the calculated temperatures, or
2) the flow model calculates flows based on fixed temperatures, after which the thermal model recalculates the temperatures using the calculated flows.
This means that either the temperatures (case 2) or the flows (1) are different in both models, and something needs to be done in order to ensure the thermodynamic integrity of the overall solution.

In case the thermal model and the flow model are actually separate programs which run in sequence, the above procedure can not even be done on a per time step basis. This is the so-called sequential coupling as described by Kendrick (1993) and quantified with case study material by Heidt and Nayak (1994). For many applications, the thermodynamic integrity of this type of coupling should be seriously questioned and will undoubtedly generate relative large errors in predicted temperatures and flows.

---

* other opions exist (see eg Axley and Grot 1989)

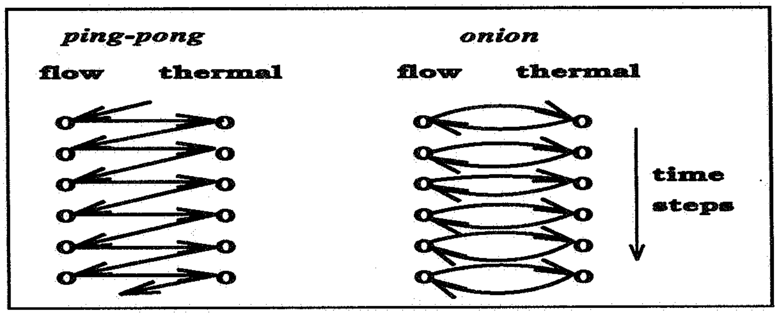

Figure 1 Schematic representation of ping-pong vs onion approach

In case the thermal and flow model are integrated, the above procedure is possible for each time step and thermodynamic integrity can be guarded by:

1 the "ping-pong" method in which the thermal and flow model run in sequence (ie each uses the results of the other model in the previous time step)#, and

2 the "onion" method in which the thermal and flow model iterate within one time step until satisfactory small error estimates are achieved.

Obviously the final results in terms of evolution of the thermodynamic integrity, will depend on how fast boundary values and other external variables to the models change over time. Therefore length of the simulation time step is also an issue which needs to be considered.

The above has some bearing on computational fluid dynamics approaches as well. However, the current paper focusses on combining a nodal network flow method with a comprehensive thermal model.

3 IMPLEMENTATION

Although, the above is a quite generic problem, in order to generate quantitative results, it is necessary to become specific in terms of implementation of the methods.

In earlier publications a full account has been given of the internal workings of the ESP-r building and plant simulation environment both with respect to energy simulation in general (Clarke 1985) and with respect to simultaneous heat and mass flow simulation (Hensen 1991).

ESP-r features both a mass balance network approach and a CFD approach. The latter approach is described in a separate paper (Clarke et al. 1995). The former approach is used for the studies in the current paper.

An outline of the mass balance network approach could be: during each simulation time step, the mass transfer problem is constrained to the steady flow (possibly bi-directional) of an incompressible fluid (currently air and water are supported) along the connections which represent the building/ plant mass flow paths network when subjected to certain boundary conditions regarding (wind) pressures, temperatures and/ or flows. The problem therefore reduces to the calculation of fluid flow through these connections with the internal nodes of the network representing certain unknown pressures. A solution is achieved by an iterative

in Figure 1 (and in our implementation) the air flow calculations use air temperatures calculated in the previous time step. Obviously the other way around is also possible.

mass balance technique in which the unknown nodal pressures are adjusted until the mass residual of each internal node satisfies some user-specified criterion.

Each node is assigned a node reference height and a temperature (corresponding to a boundary condition, building zone temperature or plant component temperature). These are then used for the calculation of buoyancy driven flows (or stack effect) which are obviously of importance in the current context. The approach for buoyancy calculations has already been described in a previous paper (Clarke and Hensen 1991).

Coupling of building heat flow and air flow - and building moisture flow and plant heat flow and plant fluid flow(s) and lighting and electric power and ....- models in a mathematical/ numerical sense, effectively means combining all matrix equations describing these processes. (Referred to as 'full integration' by Kendrick (1993).)
While in principle it is possible to combine all matrix equations into one overall 'super-matrix', this is not done within ESP-r, primarily because of the advantages which accrue from problem partitioning.
The most immediate advantage is the marked reduction in matrix dimensions and degree of sparsity - indeed ESP-r never forms two dimensional arrays for the above matrices, but instead holds matrix topologies and topographies as sets of vectors. A second advantage is that it is possible to easily remove partitions as a function of the problem in hand; for example when the problem incorporates building only considerations, plant only considerations, plant + flow, and so on. A third advantage is that, potentially, different partition solvers can be used which are well adapted for the equation types in question - highly non-linear, differential and so on.

It is recognised however that there are often dominating thermodynamic and/ or hydraulic couplings between the different partitions. If a variable in one partition (say air temperature of a zone) depends on a variable of state solved within an partition (say the air flow rate through that zone), it is important to ensure that both values are matched in order to preserve the thermodynamic integrity of the system.

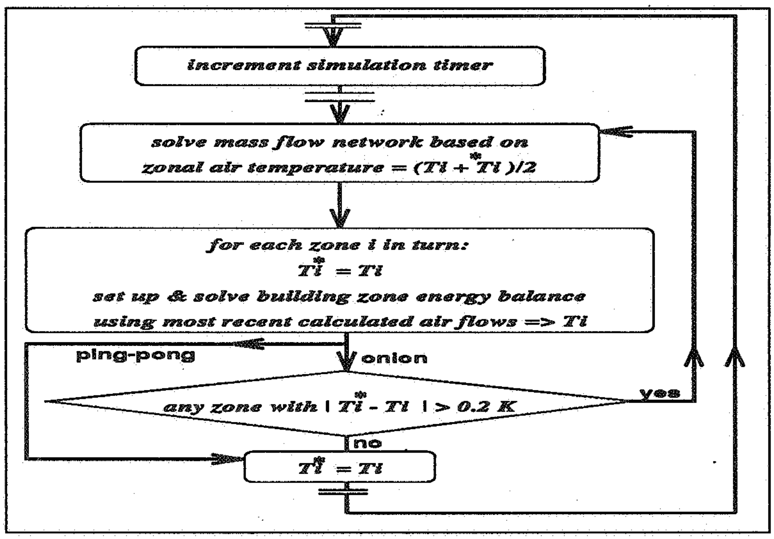

Figure 2 Schematic flow diagram showing the implementation of resp. pinp-pong and onion coupling of air flow and energy balance calculations

As explained in more detail elsewhere (Clarke et al. 1995), the ESP-r building and plant energy simulation environment is a virtual laboratory for energy modelling issues. For research reasons, ESP-r features various ways of coupling heat and air flow. Figure 2 schematically shows the implementation of respectively pinp-pong and onion approaches to coupling of air flow and energy balance calculations.

The flow diagram shows that in ping-pong mode, within a time step, the air flows are calculated using the zonal air temperatures (T_i) of the previous time step; during the first pass through a time step, T_i equals T^{*i} (history variable). In onion mode, the first pass through a time step also uses the zonal air temperatures of the previous time step. However, each subsequent iteration uses $(T^{*i} + T_i)/2$, which basically means successive substitutions with a 0.5 relaxation factor.
Not shown in the diagram is that during the simulation start-up period, the onion method reverts to the ping-pong approach to avoid unnecessary iterations.

In line with ESP-r's virtual laboratory philosophy, the system also supports various modes of time step control, for example: boundary condition look ahead (monitors user specified control variable(s) and reduces time-step value if rate of change greater than user specified value), time-step reduction by iteration (reduces time-step value until diference in control variable for current time-step and previous time-step is within user specified limit), user specified time-step value, iteration without time-step reduction (this is the onion method in essence), simulation rewind (rewind simulation clock to user specified start period if user specified control variable is outside user specified limit).

3 CASE STUDY

One of the most severe cases of coupled heat and air flow in our field involves a free running building (no mechanical heating or cooling) with air flow predominately driven by temperature differences caused by a variable load (eg solar load). A frequently occuring practical example is an atrium using passive cooling by increasing natural ventilation to reduce summertime overheating.
Although it would be interesting to consider other cases, this is not possible here due to space constraints.

3.1 Model & Simulations

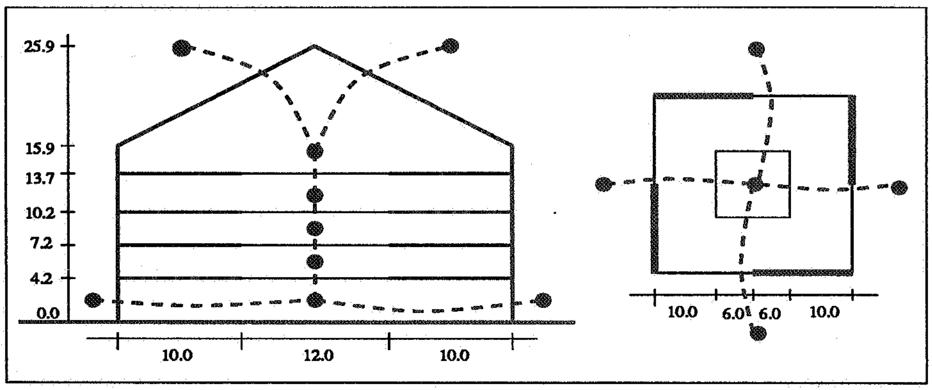

Figure 3 Cross-section and plan of atrium with air flow network

The current case concerns the central hall of a 4-wing building located in central Germany. This central hall is in essence a 5 storey atrium, of which a cross-section and plan are sketched in Figure 3. Each floor has a large central void of 144 m^2. The floors and opaque walls are from concrete, while the transparent walls and the roof consist of sun-protective double glazing.
In order to increase the infiltration, there are relatively big openings at ground and roof level. The 8 building envelope openings (2 m^2 each) are evenly distributed and connected as indicated in the flow network. For the present study, all openings are continuously opened. Apart from solar gains, there are no other heat gains.
There is no control (heating, cooling, window opening, etc.) imposed on the building.

The ambient conditions are taken from a climatic test reference year for Wüerzburg, Germany. The simulation period (28 August until 2 September) consists of a 6 day period with increasing outdoor air temperature to include a range of medium to maximum temperatures.

As indicated above, ESP-r features various modes of time step control. However, in order to avoid 'interferences' which might make it difficult to interpret certain results in the current case, it was decided not to activate time step control other than to achieve the onion type of coupling. Instead of time step control, two time step lengths of respectively one hour and one tenth of an hour were used during simulation.

3.2 Results & Discussion

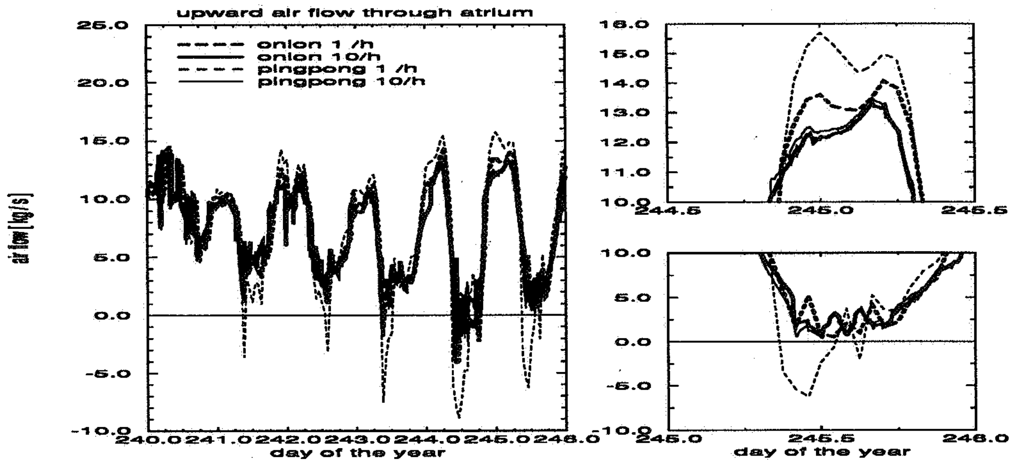

Figure 4 Simulation results for vertical air flow through atrium

Figure 4 shows the simulation results for the vertical air flow through the atrium. The right hand side of the figure shows two blown up parts of the graphs, in order to focus on the differences between the various methods. In the blow-ups, the different methods can clearly be distinguished, and it can be seen that the ping-pong method with 1 hour time steps is clearly an outlier relative to the other cases. For the 6 minute time steps, the onion and pinp-pong approaches give almost identical results.
In general, the flows tend to be higher during the night, and become less during the day. This effect is less pronounced during the first day which has relatively low ambient air temperatures and levels of solar radiation.

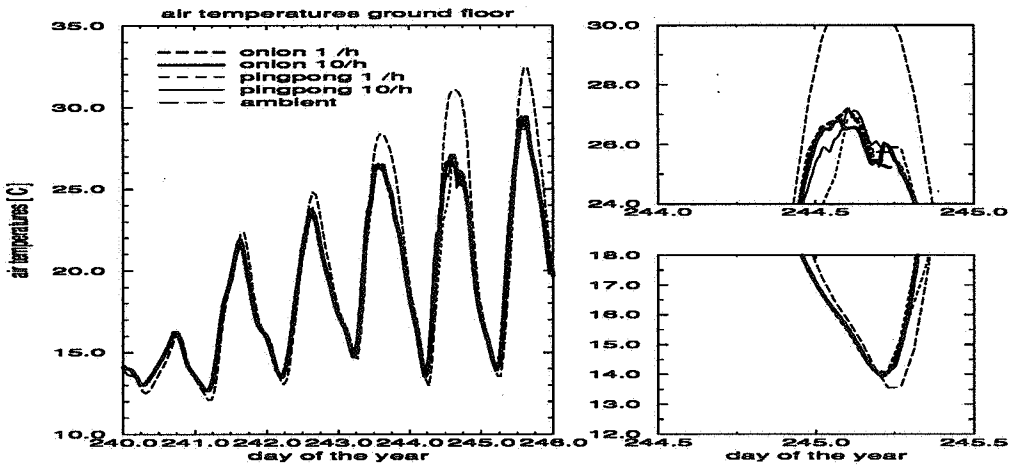

Figure 5 Simulation results for ground floor air temperatures

Figure 5 shows the simulation results for the air temperatures on the ground floor. The general graphs and the blow-ups show very little difference between the various approaches. This is probably due to the fact the incoming air temperature (= ambient) is equal in all cases, and because of the large thermal capacity of the ground floor.

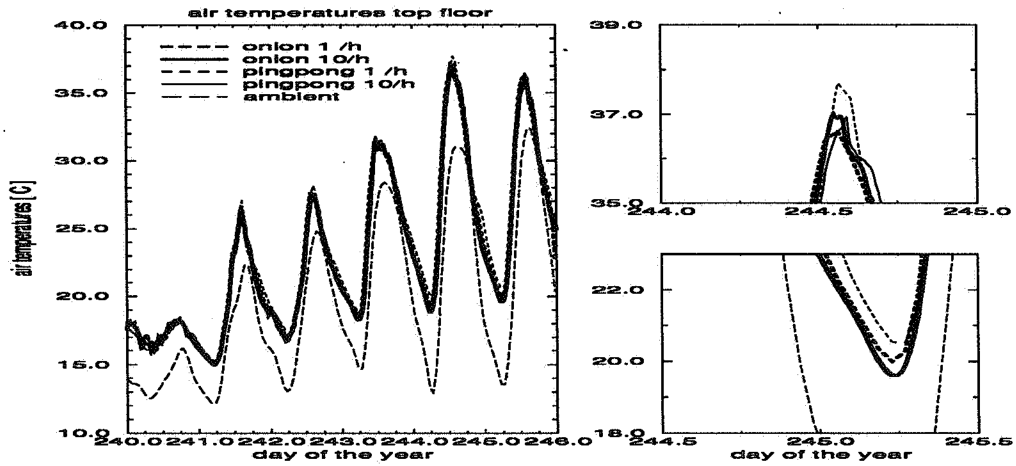

Figure 6 Simulation results for top floor air temperatures

Figure 6 shows the simulation results for the air temperatures on the top floor. Here the general graph and the blow-ups show larger differences between the various approaches. This is due to the succession of differences occuring at the lower floors, and due to the fact that the top floor has a much higher solar gain (via the transparent roof) than the other floors.
It is interesting to compare Figure 6 with Figure 4, because it shows that the flow increases with difference between zonal and ambient temperatue and not with zonal temperature itself. Obviously the temperature difference depends on the amount of air flow, and the amount of air flow depends on temperature difference. As clearly shown in the graphs, it takes an integrated approach to predict the net result.

Table 1 holds a statistical summary of the results. Included are number of hours above certain temperature levels, since such parameters are used in certain countries to assess summer overheating. For the ground floor air temperature there are relative big differences in hours > 27°C between the once per hour and the 10 per hour time step cases. This is because the maximum air temperature for that zone is close to 27°C (hours > 27°C becomes very

Table 1 Statistical summary of air flow and temperature results for the various methods (On = onion, PP = ping-pong)

		On-1	On-10	PP-1	PP-10
vertical flow					
max	kg/s	14.51	14.19	15.69	13.49
min	kg/s	-4.21	-3.60	-8.90	-3.67
mean	kg/s	7.35	7.26	7.04	7.05
std.dev.	kg/s	4.37	3.71	5.93	3.87
range	kg/s	18.72	17.79	24.58	17.16
ground temperature					
max	$°C$	29.21	29.42	28.87	29.37
min	$°C$	12.67	12.63	12.66	12.63
mean	$°C$	18.95	18.93	18.64	18.84
hours > 27 $°C$	h	2	5.3	1	6.3
hours > 30 $°C$	h	0	0	0	0
top floor temperature					
max	$°C$	36.63	37.00	37.70	36.94
min	$°C$	15.24	15.06	15.16	14.91
mean	$°C$	23.19	22.96	23.27	22.83
hours > 27 $°C$	h	36	34.6	38	34.3
hours > 30 $°C$	h	22	22.9	24	23.4
iterations	–	429	1028	-	-

sensitive),
In general, the ping-pong once per hour case is a bit of an outlier in terms of the air flow and the maximum top floor temperature. The other results are relatively close.

On its last line, Table 1 shows the number of iterations needed by the onion approach. Obviously this has computing resource implications. Since the amount of code involved in the iteration is much smaller than the code which needs to be processed for a time step, the number of iterations can not be compared directly to the number of ping-pong time steps. In the the current case, the onion once per hour needed approximately the same total amount of processing time than the ping-pong 10 per hour case.

4 CONCLUSIONS

The case study presented here, involves a severe case of coupled heat and air flow in buildings. Two different methods (ping-pong and onion method) of linking heat and air flow models have been considered using two different time step lengths.

It was found that the differences in air flow are larger than the differences in air temperatures. The temperature differences between the various methods grow with the number of stacked zones.
The results indicate that when properly used, each method will give satisfactory results. In this context the term "properly" is mainly related to the time step issue. When used improperly in terms of time step, the onion method will have implications in terms of computing resources, but - more seriously - the ping-pong method may generate substantial errors.
Which method to choose depends on the required accuracy. In general it is advisable to be careful with the ping-pong approach in combination with long time steps for problems with strongly coupled heat and air flow.

Although the coupled heat and air flow results are for an imaginary (but realistic) building the observed trends are expected to be valid for many cases. The actual consequences for a particular building configuration will be the result of many complicated interactions with opposite effects. This makes it extremely difficult - if not impossible - to create simplified design-aids for this purpose. Detailed building performance evaluation can be achieved through an integral building & systems simulation approach.

References

Axley, J. and R.A. Grot 1989. "The coupled airflow and thermal analysis problem in building airflow system simulation," in *ASHRAE Transactions*, vol. 95:2, pp. 621-628, Atlanta, GA.

Clarke, J.A. 1985. *Energy simulation in building design,* Adam Hilger Ltd, Bristol (UK).

Clarke, J.A. and J.L.M. Hensen 1991. "An approach to the simulation of coupled heat and mass flow in buildings," in *Proc. 11th AIVC Conf. Ventilation System Performance held at Belgirate (I) 1990,* vol. 2, pp. 339-354, IEA Air Infiltration and Ventilation Centre, Coventry (UK).

Clarke, J.A., J.L.M. Hensen, and C.O.R. Negrao 1995. "Predicting indoor airflow by combining network, CFD, and thermal simulation," in *Proc. 16th AIVC Conf. "Implementing the Results of Ventilation Research", Palm Springs, Sep 1995*, pp. ??-??, IEA Air Infiltration and Ventilation Centre, Coventry (UK).

Heidt, F.D. and J.K. Nayak 1994. "Estimation of air infiltration and building thermal performance," *Air Infiltration Review*, vol. 15, no. 3, pp. 12-16.

Hensen, J.L.M. 1991. "On the thermal interaction of building structure and heating and ventilating system," Doctoral dissertation Eindhoven University of Technology (FAGO).

Kendrick, J. 1993. "An overview of combined modelling of heat transport and air movement," Technical Note AIVC 30, Air Infiltration and Ventilation Centre, Coventry UK.

Implementing the Results of Ventilation Research
16th AIVC Conference, Palm Springs, USA
19-22 September, 1995

Effectiveness of a Heat Recovery Ventilator, an Outdoor Air Intake Damper and an Electrostatic Particulate Filter at Controlling Indoor Air Quality in Residential Buildings

Steven J Emmerich, Andrew K Persily

National Institute of Standards and Technology, Bldg 226, Room A313, Gaithersburg, MD 20899, USA

Synopsis

A preliminary study of the potential for using central forced-air heating and cooling system modifications to control indoor air quality (IAQ) in residential buildings was performed. The main objective was to provide insight into the potential of three IAQ control options to mitigate residential IAQ problems, the pollutant sources the controls are most likely to impact, and the potential limitations of the controls. Another important objective was to identify key issues related to the use of multizone models to study residential IAQ and to identify areas for follow-up work. The multizone airflow and pollutant transport program CONTAM93 (1) was used to simulate pollutant concentrations due to a variety of sources in eight houses with typical HVAC systems under different weather conditions. The simulations were repeated after modifying the systems with three IAQ control technologies - an electrostatic particulate filter, a heat recovery ventilator (HRV), and an outdoor air intake damper (OAID) on the forced-air system return. Although the system modifications reduced pollutant concentrations in the houses for some cases, the HRV and OAID increased pollutant concentrations in certain situations involving a combination of weak indoor sources, high outdoor concentrations, and indoor pollutant removal mechanisms. Also, limited system run-time during mild weather was identified as a limitation of IAQ controls that operate in conjunction with forced-air systems. Recommendations for future research include: simulation of other buildings, pollutants, and IAQ control technologies; model validation; sensitivity analysis; and development of a database of important model inputs.

1. Introduction

Central forced-air heating and cooling systems can have a significant impact on IAQ in residential buildings because they circulate large volumes of air, spreading pollutants generated in one room to the rest of the house. They also can act as a source of indoor air pollution, for example, due to dirty ductwork. However, forced-air system modifications have the potential to improve IAQ through the addition of air cleaners or devices to introduce outdoor air into the house. Evaluating the effectiveness of such modifications could require extensive field testing. Computer modeling can provide insight without the time and effort required to perform field tests. Such a modeling effort requires a whole building approach that accounts for the multizone nature of airflow and pollutant transport in residential buildings and considers all relevant factors - air leakage paths in the building envelope and interior walls, wind pressure coefficients, pollutant sources, HVAC system airflows, filter efficiencies, pollutant sinks, pollutant decay or deposition, and ambient weather and pollutant concentrations. Many residential IAQ studies have employed simplified approaches to studying buildings and their HVAC systems. For example, some studies have ignored the multizone nature of the problem (2,3) and others have not rigorously modeled building airflow (4,5). A few studies have employed a whole building modeling approach (6,7).

In this effort, a multizone airflow and pollutant transport model was used to conduct a preliminary assessment of the potential for using central forced-air heating and cooling systems to control IAQ in residential buildings. The objective of this effort was to provide insight into the use of state-of-the-art IAQ models to evaluate such modifications, the potential of these modifications to mitigate residential IAQ problems, the pollutant sources they are most likely to impact, and their potential limitations. This study was not intended to determine definitively whether the IAQ control options studied are reliable and cost-effective.

Another important objective was to identify key issues in the use of multizone airflow and pollutant transport models to study IAQ in residential buildings.

2. Modeling Method and Parameters

The program CONTAM93 (1) was used to simulate the pollutant levels due to a variety of sources in eight houses with typical HVAC systems. CONTAM93 is a multizone airflow and pollutant transport model employing a graphic interface for data input and display. Multizone models take a macroscopic view of airflow and IAQ by calculating average pollutant concentrations in the different zones of a building as contaminants are transported through the building and its HVAC system. The multizone approach is implemented by assembling a network of elements describing the airflow paths between the zones of a building. The network nodes represent the zones containing pollutant sources and sinks and are modeled at a uniform temperature and pollutant concentration.

Simulations were performed for a hot, mild, and cold day for each location using Weather Year for Energy Calculation (WYEC) data (8). Each simulation consisted of a one-day cycle repeated until peak concentrations converged to a specified tolerance. The HVAC systems were then modified with three IAQ control technologies including an electrostatic particulate filter, a heat recovery ventilator, and an outdoor air intake damper. Altogether, 96 simulations were performed to evaluate the impact of these controls on pollutants from the following sources: a constant-emission volatile organic compound (VOC) source, intermittent-emission (burst) VOC sources, combustion pollutant sources, and elevated outdoor pollution.

2.1 Buildings

The CONTAM93 description of buildings includes the building zones, characteristics of leakage paths connecting zones, and the wind pressure coefficients of leaks through the building envelope. The buildings were described in an earlier paper (9), and in greater detail in reference 10. The study included eight buildings - a ranch and a two-story house, located in two sites (Miami and Minneapolis), with typical and low levels of air leakage. The ranch and two-story house floorplans and zone labels (in all capitals) are shown in Figures 1 and 2, respectively. The Minneapolis houses have basements (zone BMT) not shown in the figures.

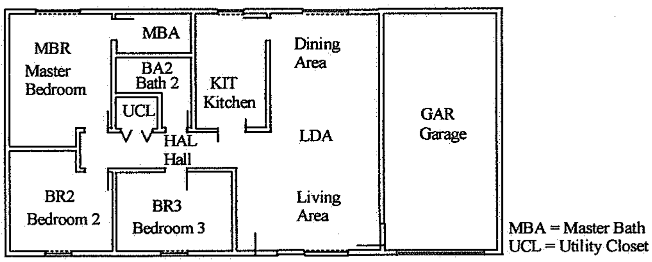

Figure 1 - Ranch House Floorplan and Zones

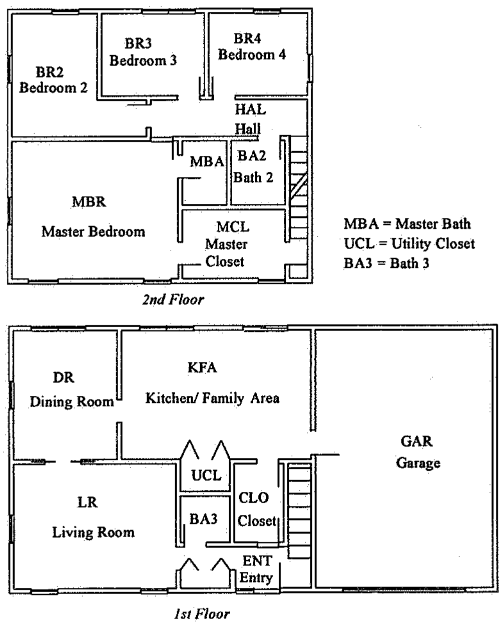

Figure 2 - Two-story House Floorplan and Zones

The air leakage of the house envelopes and interior partitions was modeled by including elements for leakage paths typically found in residential buildings. Most of the leakage values were based on Table 23-3 of ASHRAE (11). All doors connecting interior zones other than closets were modeled as open. The wind pressure coefficients for the building walls and the flat garage roof were based on Equation 23-8 and Figure 14-6 of ASHRAE (11), respectively. Wind shielding effects can be important but were not considered.

2.2 HVAC Systems

The CONTAM93 description of HVAC systems includes the total system airflow, supply and return locations and flow rates, outdoor air supply flow rates, and operating schedules. The buildings were modeled with typical residential central forced-air heating and cooling systems with modest duct leakage and no outdoor air intake. System operation schedules were determined by calculating the fractional on-time required to meet the cooling or heating load. The baseline systems included standard furnace filters with constant efficiencies of 5% for fine particles (diameter less than 2.5 μm) and 90% for coarse particles (diameter greater than 2.5 μm). The systems are described in greater detail in references 9 and 12.

2.4 Pollutant Factors

The pollutants of interest for this study were nitrogen dioxide (NO_2), carbon monoxide (CO), particulates, and volatile organic compounds (VOC). Based on a literature review of reports quantifying residential sources of these pollutants (12), the pollutant sources included eight VOC burst (short duration) sources, a constant VOC area source, and combustion sources of CO, NO_2, and fine particles. The concentrations due to each source of the same pollutant were calculated separately. Table 1 lists information on these sources including the zones in which they are located, source strengths, and time-patterns.

Table 1 - Pollutant Sources

Source	Pollutant	Zone(s)	Source strength	Schedule
Burst (medium)	TVOCs	Several	300 mg/h	9 - 9:30 am 7 - 7:30 p.m.
Burst (high)	TVOCs	GAR and BMT	1100 mg/h	9 - 10 am 7 - 8 p.m.
Flooring material	TVOCs	All but GAR, ATC	7.0 mg/h m2	constant
Oven	CO	KIT (ranch house), KFA (two-story house)	1900 mg/h	7 - 7:30 am 6 - 7 p.m.
Oven	NO2	KIT (ranch house), KFA (two-story house)	160 mg/h	7 - 7:30 am 6 - 7 p.m.
Oven	Fine particles	KIT (ranch house), KFA (two-story house)	0.2 mg/h	7 - 7:30 am 6 - 7 p.m.
Heater	CO	GAR and BMT	1000 mg/h	7 - 10 am (GAR) 7 - 9 p.m. (BMT)
Heater	NO2	GAR and BMT	250 mg/h	7 - 10 am (GAR) 7 - 9 p.m. (BMT)
Heater	Fine particles	GAR and BMT	2 mg/h	7 - 10 am (GAR) 7 - 9 p.m. (BMT)

Typical outdoor pollutant concentrations were used to account for pollution entering the dwelling from outside and provide background levels for the indoor sources. The CO and NO_2 concentrations were selected to have a diurnal pattern with morning and afternoon peaks, and varied from 1 to 3 ppm for CO and 20 to 40 ppb for NO_2 based on a review of US EPA air quality documents (13-15). A constant fine particle concentration of 13 $\mu g/m^3$ is based on reference 16, and a constant TVOC concentration of 100 $\mu g/m^3$ is based on reference 17.

Elevated outdoor concentrations of CO, NO_2, and coarse particles were also simulated to evaluate the impact of the IAQ control technologies on pollutants brought into residences from outside. These elevated pollutant concentrations were also based on EPA air quality documents (13-15). The elevated CO and NO_2 concentrations also had a diurnal pattern with morning and afternoon peaks, and varied from 4 to 12 ppm for CO, and 200 to 400 ppb for NO_2. The coarse particle concentration was constant at a level of 75 $\mu g/m^3$.

Reversible sink effects for the VOC were modeled with sink elements based on a boundary layer diffusion controlled (BLDC) model with a linear adsorption isotherm (18). The model parameters include the film mass transfer coefficient, the adsorbent mass, and the isotherm partition coefficient. Little data is available for these parameters which depend on airflow rates, gas diffusion properties, and adsorbent material. The values used for the parameters were 35 $\mu m/s$ for the film mass transfer coefficient, 0.5 g-air/g-sorbent for the partition coefficient, and 3 kg per m^2 of zone interior surface area for the adsorbent mass.

NO_2 decay and particle deposition were modeled as single-reactant first order reactions with a single, constant value in all zones. NO_2 decay depends strongly on the materials present in a house (e.g. floor and wall coverings, furnishings), and a wide range of measured values have been reported. The kinetic rate coefficient used for NO_2 decay was 0.87 h^{-1} based on the average of measurements in a contemporary research house (19). Particle deposition depends on the size and type of particles, particle concentration, airflow conditions, and surfaces available for deposition. The fine particle deposition rate used was 0.08 h^{-1} based on particles from a wood-burning stove in a test house (20). The coarse particle deposition rate used was 1.5 h^{-1} based on the lower value reported for 4 μm particles in a test room (21).

2.5 IAQ Control Technologies

The IAQ control technologies considered for the study were limited to commercially available equipment that can be used with typical forced-air systems. Ventilation systems and IAQ controls that operate independently of a forced-air system (e.g. whole-house exhaust ventilation systems) were not considered. The three control technologies were electrostatic particulate filtration, heat recovery ventilation, and an outdoor air intake damper on the forced-air system return. This report discusses only the important modeling details. More information including duct drawings, cost estimates, and thermal loads is in reference 10.

The electrostatic particulate filter (EPF) has a filter efficiency of 30% for fine particles (emitted by the combustion sources in these simulations) and 95% for coarse particles (associated with the elevated outdoor pollution). The EPF was modeled by replacing the standard furnace filters in the baseline HVAC systems. The filter efficiency was modeled as constant over time with no impact on airflow through the system.

The heat recovery ventilator (HRV) draws air from the return side of the forced-air system and replaces it with outdoor air drawn through the heat exchanger. The actual outdoor airflow rate during operation was selected to provide an air change rate of 0.35 h^{-1} through the HRV. The HRV was modeled by setting the outdoor airflow rate for each HVAC system to the appropriate fraction of the system supply airflow rate. Thus, outdoor air will be supplied by the HRV whenever the HVAC system is operating. Other control options were not studied (e.g. demand control). A standard furnace filter was included in the intake path of the HRV.

The outdoor air intake damper (OAID) draws outdoor air into the return side of the forced-air system. The OAID was modeled similarly to the HRV by modifying the HVAC system to include a constant fraction of outdoor air to provide an air change rate of 0.35 ach through the system during operation. A standard furnace filter was also included. The primary difference between the OAID and the HRV is that the OAID does not include an exhaust duct. Thus, the OAID will tend to pressurize the house. This effect was modeled by reducing the HVAC return flows from the house by an amount equal to the outdoor air supplied to the system.

3. Results

3.1 *Outdoor Air Change Rates*

The impact of the HRV and OAID may be evaluated by comparing the resulting air change rates in the houses with those required by ASHRAE Standard 62 (21). Standard 62 requires a minimum outdoor air change rate of 0.35 h^{-1} or, if greater, 7.5 L/s (15 cfm) per person with an assumption of 2 people for the first bedroom and 1 person for each additional bedroom. Therefore, the minimum outdoor air change rates are 0.41 h^{-1} for the Miami ranch house, and 0.35 h^{-1} for all other houses.

Figure 3 shows the 24-hour average air change rates for the houses for all baseline, HRV, and OAID cases. The Minneapolis air change rates were calculated including the volume of the basement. The baseline average air change rate is below the ASHRAE minimum air change rate for all tight houses under all weather conditions. While the HRV and OAID do increase the building air change rates for all cases, the benefit is limited by the HVAC system run-time. With the HRV, the tight Miami houses meet the ASHRAE minimum air change rate on the hot day but still fall short on the cold and mild days. The tight Minneapolis houses meet the requirement on the cold day but still fall short on the mild and hot days.

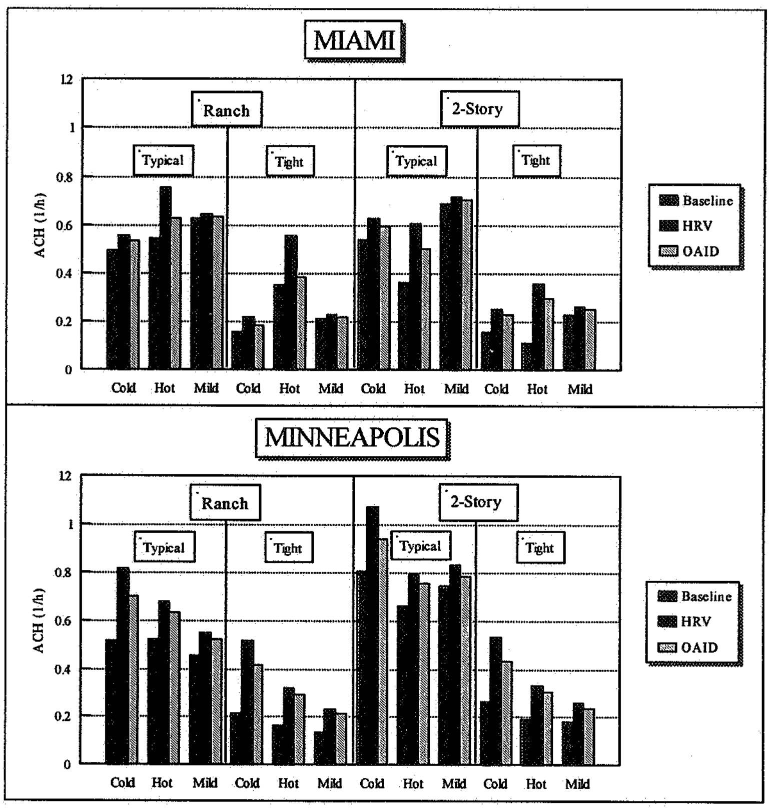

Figure 3 - 24-hour Average Building Air Change Rates

Figure 3 also demonstrates an important difference between the HRV and the OAID. In all cases, the OAID increases the building air change rate by a smaller amount than the HRV. Because the OAID does not have an exhaust path, the air entering the house through the OAID pressurizes the building and reduces infiltration through envelope leaks. This reduction of envelope infiltration partially offsets the increase in building air change rate due to the outdoor air entering through the OAID, causing a smaller overall increase than the HRV.

The Miami results also show one impact of duct leakage.

The baseline ranch and 2-story house results are quite close for the cold and mild days. However, for the hot day, the baseline air change rate in the 2-story house is substantially smaller than in the ranch house. The difference between the two is the a 10% supply duct leak in the attic of the ranch house (no duct leakage was included for the two-story house because the ducts are all within the conditioned space). Since the system runs most of the time on the hot day, duct leakage has a significant impact on the air change rate of the ranch house. The contribution of duct leakage to the air change rate of the Miami ranch house is less noticeable on the cold and mild days as the system operates much less.

3.2 *Sample Transient Results*

Figure 4 shows the impact of the HRV and OAID on the living-space average TVOC concentrations due to the LDA burst source for the tight Miami ranch house, cold day case. The living-space average includes the kitchen, living room, dining room, and all bedroom zones. When the HVAC system comes on, the concentration drops suddenly due to the additional outdoor air brought in through the HRV and the OAID. When the system is off, the concentration decreases at a lower rate due to infiltration. Both the HRV and OAID had small impacts on the concentration peaks (reductions of 2.5% and 3.4%, respectively) but more substantial impacts on the 24-hour average concentrations (reductions of 14% and 17%, respectively). The small reductions in peak concentrations indicate an inability of the modest increase in ventilation rate to mitigate concentration spikes due to a short-term source. [Note: Figure 4 shows the TVOC concentration rising at 9 a.m. when the source is scheduled to begin emitting. This occurred for all cases because the program interpreted the scheduled sources to begin one time step (five minutes) before the scheduled time.]

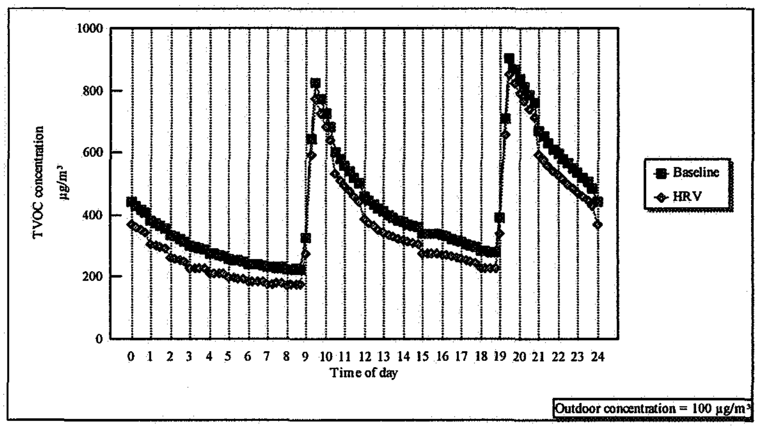

Figure 4 - Transient Living-space TVOC Concentration Cue to LDA Burst Source (Tight Miami Ranch House on Cold Day)

Figure 5 shows the living-space average concentrations due to the floor TVOC source for the tight Miami ranch house in cold weather. Since the floor source is constant, the concentration changes are due primarily to changes in the building air change rate with

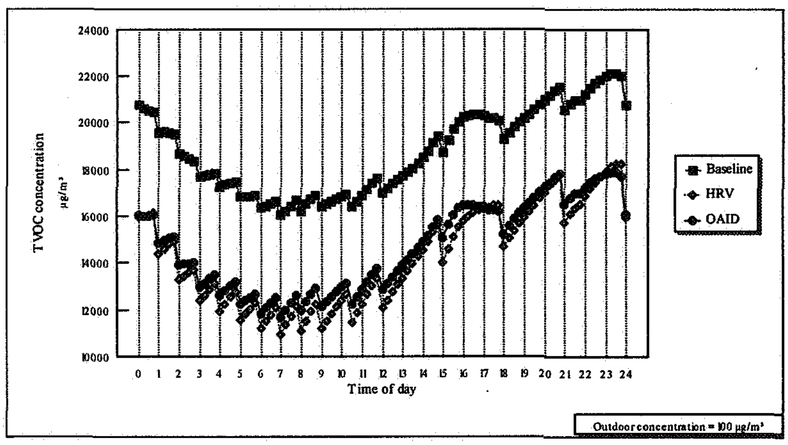

Figure 5 - Transient Living-space TVOC Concentration Due to Floor Source (Tight Miami Ranch House on Cold Day)

the outdoor conditions and with HVAC system operation. In general, the TVOC concentration gradually increases when the system is off and then drops sharply when the system turns on due to the higher air change rate. Overall, the concentrations are higher during the latter part of the day because the system operates less frequently and the infiltration driving forces are lower, both resulting in a lower air change rate. As explained earlier, system operation increases the outdoor air change rate in this house due to the supply duct leak in the attic. The HRV and the OAID reduced both peak (19% and 18%, respectively) and average TVOC concentrations (22% and 24%, respectively) for the floor source by a greater amount than for the burst source. The IAQ controls have a greater impact on the peak concentration for the floor source than for the burst sources because the floor-source peak is due to a gradual build-up of pollutant through the day rather than a short-term event.

3.3 *Impact of IAQ Controls on Average Pollutant Concentrations*

Figure 6 shows the ratio of the 24-hour, living-space average concentrations to the 24-hour average outdoor concentration for the baseline, EPF, HRV, and OAID cases in the tight, Miami ranch house on the cold day. The indoor/outdoor ratios are shown on a log scale as they range over five orders of magnitude depending on the source. The VOC burst source results shown use the average of the concentrations due to all eight burst sources to represent the average impact of the IAQ controls on localized sources in different rooms of the house. The variation in the indoor/outdoor ratio among the sources is due to the relative values of the source strength, indoor decay mechanisms and outdoor pollutant concentrations. The controls themselves have much less impact on these ratios, but the effects can still be seen.

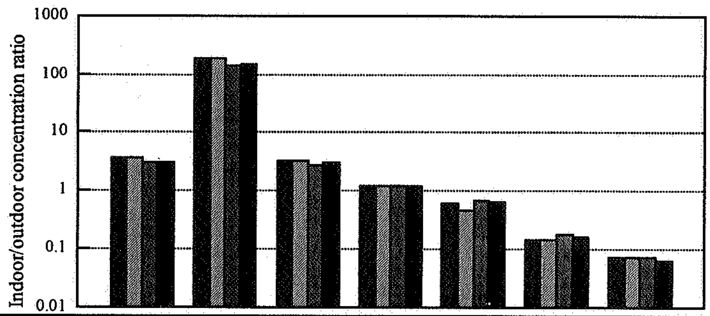

Source	Burst-VOC	Floor-VOC	Oven-CO	Oven-NO2	Oven-fine	OA-NO2	OA-coarse
Baseline	3.7E+00	1.9E+02	3.2E+00	1.2E+00	6.2E-01	1.4E-01	6.9E-02
EPF	3.7E+00	1.9E+02	3.2E+00	1.2E+00	4.4E-01	1.4E-01	6.8E-02
HRV	3.0E+00	1.4E+02	2.7E+00	1.2E+00	6.8E-01	1.8E-01	7.1E-02
OAID	3.0E+00	1.5E+02	3.0E+00	1.2E+00	6.5E-01	1.6E-01	6.1E-02

Figure 6 - Indoor/outdoor Ratios of Average Concentrations Due to Various Sources (Tight Miami Ranch House on Cold Day)

The average impact of the IAQ controls for all pollutant sources are shown in Figure 7 as percent reductions in baseline concentrations. In general, both the HRV and OAID reduced the concentrations due to indoor sources of the pollutants without non-ventilation removal processes (CO and VOC) and increased, or had little impact, on the concentrations of pollutants with decay/deposition and filtration removal processes (NO_2 and particles). The HRV and OAID had the greatest reduction for the constant, distributed source (Floor-VOC), which was also the source resulting in the largest indoor/outdoor concentration ratio. In general, the HRV and OAID increase NO_2 and particle concentrations because, as shown in Figure 6, the baseline average indoor concentration is below the average outdoor concentration. Therefore, the additional outdoor air brought in by these controls increases the indoor concentration. Figure 7 shows that this trend was true on average. However, whether

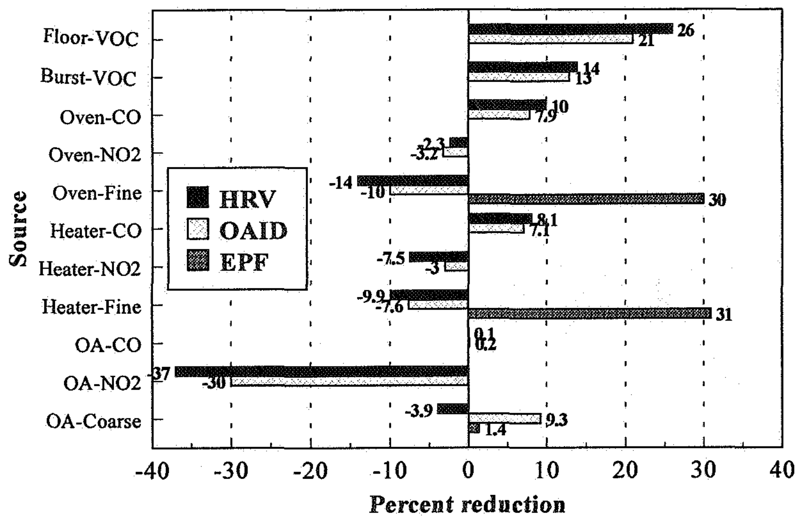

Figure 7 - Average Reductions in Living-space Average Concentrations

an increase or decrease occurred for an individual case depended on several factors including the building air change rate, the indoor source strength, the outdoor pollutant concentration, decay/deposition rates, and the timing of the source, system operation, and outdoor peaks.

The impact of the OAID was nearly always similar to but slightly smaller than the impact of the HRV because, as shown in Figure 3, it increases the average building air change rate by a smaller amount than the HRV. As discussed previously, this smaller increase in building air change rates is due to the pressurization effect of the OAID. However, the HRV and OAID did not always have similar impacts, as seen in the case of coarse particle concentrations due to elevated outdoor air pollution. For this pollutant, the OAID reduced the baseline concentration by an average of 9.3% while the HRV increased the baseline concentration by an average of 3.9%. This impact is believed to be due to the pressurization effect of the OAID. Both devices include a standard furnace filter with filtration efficiency of 90% for coarse particles in the intake path. However, no penetration factor was included for infiltration air and, therefore, the filtered air entering through the OAID and HRV has a lower particle concentration than the unfiltered air entering through the envelope. Since the operation of the OAID results in less infiltration than the baseline and HRV cases, it reduces the indoor coarse particle concentration.

In general, the EPF had a small impact on the already low coarse particle concentrations with an average reduction of only 1.4%. This small impact is due to the small change in coarse particle filtration efficiency from 90% to 95%. Figure 7 shows that the EPF was more effective at reducing the fine particle concentrations with reductions of 30% and 31% for the oven and heater sources, respectively. It should be noted that, as indicated by the indoor/outdoor ratios, the conditions simulated provided only a modest challenge to the EPF.

3.4 Factors Influencing Impact of IAQ Controls

In addition to the pollutant and source dependent variations, the impact of the IAQ controls on the concentration due to a single source varied greatly from case to case. For example, the reduction for the floor source ranged from 3% to 69%. One reason for the variation was dependence on HVAC system run-time.

Figure 8 shows both the average percent reduction in baseline Floor-VOC concentration due to the HRV and the average percent system run-time for the Miami cases. As shown by the building air change results, the system run-time is an important factor for these IAQ controls

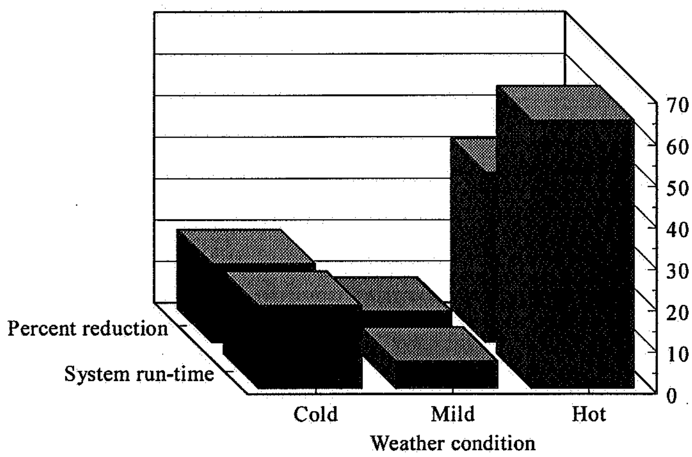

Figure 8 - Influence of System Run-time on IAQ Control Impact (Floor-VOC for Miami HRV Cases)

which were specified to operate only in conjunction with the system. On the mild day, the system operated an average of 7% of the time to meet the low thermal load and reduced the baseline concentration by only 8%. On the hot day, the system operated 65% of the time to meet the high heating load and reduced the baseline concentration by 41%. Although this influence was observed for most sources and cases, other factors, such as timing of system operation, also become important for short-duration sources.

Often, the conditions (small indoor-outdoor temperature difference) causing low system run-time also correspond to low infiltration and high pollutant concentrations. Therefore, days with high concentrations due to low infiltration could receive the least help from the HRV or OAID due to low system run-time. For example, the tight Miami ranch house in mild weather has the second highest baseline 24-hour average TVOC concentration (20,700 $\mu g/m^3$) but, after modest reductions due to the HRV and OAID, it ends up having the highest TVOC concentrations for the modified cases with concentrations of 16,800 $\mu g/m^3$ and 18,600 $\mu g/m^3$, respectively. The effectiveness of the central forced-air modifications could also be limited if the cooling and heating equipment is oversized. Although it was not explored in this study, oversized equipment would further reduce the HVAC system run-time. The system run-time limitation could be overcome through other control options (e.g. constant operation, demand control, or scheduled operation) or through other approaches to residential ventilation.

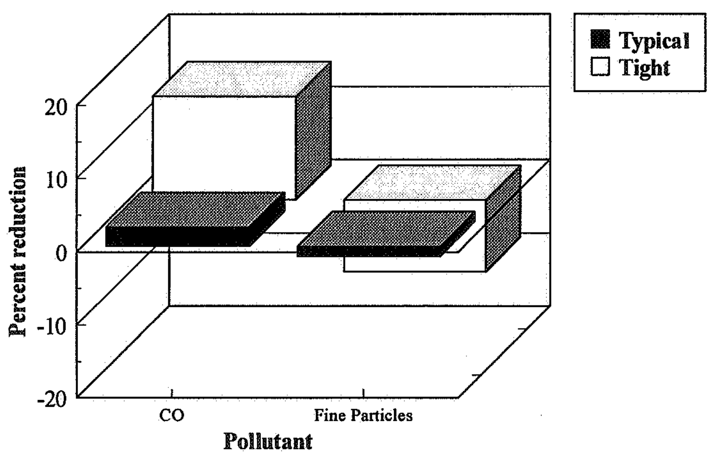

Figure 9 - Influence of envelope airtightness on IAQ control impact (average percent reduction of oven pollutants due to HRV)

Another factor showing a consistent influence on the IAQ control impacts was envelope airtightness. Figure 9 shows the average impact of the HRV on baseline CO and fine particle concentrations due to the oven. The HRV consistently had a larger impact, whether positive or negative, in the tight houses due to a greater relative change in the average building air change rates for the tight houses.

4. IAQ Modeling Issues and Follow-up Activities

An important goal of the project was to identify issues related to the reliability and usefulness of multizone IAQ models and to identify important areas for follow-up work. Several such issues were identified in planning the study, performing simulations, and analyzing the results. Follow-up activities to address these issues are discussed briefly below.

- Model validation - A systematic approach to multizone model validation that considers the types of models, building features, pollutants and sources is needed. Although absolute validation of a program such as CONTAM is impossible, empirical evaluation of a model's predictions is important to establish its range of applicability, to reduce the potential for large errors, and to verify that it correctly predicts trends of interest. While a number of multizone airflow and pollutant transport model validation efforts have been conducted, the efforts to date have not been sufficient to identify the situations in which such models will perform reliably and the situations where they are expected to be less reliable.
- Experimental evaluation - An issue related to model validation but specific to this project is the experimental evaluation of the IAQ controls that were modeled. Even a limited experimental effort would lend support to the model results or indicate deficiencies in the modeling method or details.
- Sensitivity analysis - The modeling results show that the outcome of a simulation varies dramatically for different input values due to the complexities of airflow and pollutant transport in multizone systems, and that the relationships between model inputs and outputs can be unexpected and difficult to understand based only on one's intuition. In this study, attempts were made to select reasonable values for all of the inputs, but the range of reasonable values is quite large for many inputs and some uncertainty in the input values will always exist. Therefore, it is critical to understand which model inputs are most important to the results of a given simulation.
- Development of database for model parameters - In the process of setting up the houses in CONTAM93, difficulties were encountered in obtaining data for many model parameters. Specific inputs that were particularly problematic include, but are not limited to, leakage areas of building components, wind pressure coefficients, particle and NO_2 decay rates, VOC source strengths, and VOC sink characteristics. The lack of a reliable database for model inputs is not a new problem, but it can limit the usefulness of airflow and IAQ models. Existing knowledge gaps need to be identified and analyzed, and a strategy should be developed to obtain the information needed to make modeling a more useful tool.
- Investigation of options to identify/eliminate input errors - Describing a building as a multi-zone system of airflow and pollutant transport elements can be a very complex process, depending on the configuration of the building and the factors being considered in the simulation. Use of any simulation program involves the risk of inputting erroneous numerical values or neglecting to input an individual element. Given the fact that the results of a simulation may not be intuitive, it may be far from obvious that an input error has occurred. This problem is particularly serious for the less experienced modeler who is more likely to make an error and less likely to recognize its existence. It is not clear

what features could be developed to identify input errors, but this issue merits attention as these programs are more widely used.

- Simulation of other buildings, pollutants, and IAQ control technologies - The factors included in the simulations were limited by project resources and because it was a preliminary assessment. The modeling approach could be used to investigate many other factors including other house characteristics, pollutants and sources, IAQ controls, and side-effects of implementing the controls. These control options could and ultimately need to be evaluated in several other respects including equipment and installation costs, energy impact, and the potential impacts on the concentrations of other pollutants such as indoor humidity. The consideration of side-effects is important to evaluating the appropriateness of IAQ controls. Some of these issues could be addressed with the current version of CONTAM93, while others may require the development of additional simulation capabilities as discussed below.
- Development of representative building set - It will always be difficult to generalize the results of such simulations or to predict their impact on the residential building stock without considering the wide variety of house types and building features. Development of a set of houses to represent the building stock of a particular region or country based on a statistical analysis of important residential buildings features would make such generalizations more appropriate.
- Development of additional simulation capabilities - Despite the limitations of IAQ modeling discussed here, these programs have the potential to provide valuable insight into a range of IAQ issues. The IAQ issues that can be studied by a program are determined by its simulation capabilities. In addition, these capabilities determine the ability of the model to consider the potential side-effects of an IAQ control method. All models are limited in their capabilities, and opportunities exist to expand these models to consider other issues, or to consider them more thoroughly. Some important additional capabilities include more complete treatment of chemical reaction and absorption phenomena, more detailed HVAC system models to enable realistic consideration of system interactions, thermal analysis to enable the determination of energy impacts, and exposure analysis.

5. Conclusions

The multizone program CONTAM93 was used to simulate the impact of several modifications to typical residential HVAC systems on pollutant concentrations due to a variety of sources in eight houses under different weather conditions. Although the system modifications reduced pollutant concentrations in the houses for some cases, the HRV and OAID increased pollutant concentrations in certain situations involving a combination of weak indoor sources, high outdoor concentrations, and indoor pollutant removal mechanisms. Limited system run-time during mild weather was identified as a limitation of IAQ controls that operate in conjunction with typical forced-air systems. However, this limitation could be overcome through other control options for these devices or through other approaches to residential ventilation. Recommendations for future research include: additional simulations for other buildings, pollutants, and IAQ control technologies; model validation; model sensitivity analysis; and development of a database of important model inputs.

Acknowledgements

This work was sponsored by the US Consumer Product Safety Commission under Interagency Agreement No. CPSC-IAG-93-1124. The authors wish to acknowledge the efforts of Roy Deppa and Lori Saltzman of CPSC in support of this project, Cherie Bulala, Kent Holguin, and Dave VanBronkhorst for performing simulations and analyzing results, and George Walton for assistance with the CONTAM93 model.

REFERENCES

1. Walton GN. *CONTAM93 - User Manual* (1994) NISTIR 5385, National Institute of Standards and Technology (NIST).

2. Hamlin T and Cooper K. "CMHC Residential Indoor Air Quality - Parametric Study" (1992) Proc of the 13th AIVC Conference, Air Infiltration and Ventilation Centre (AIVC).

3. Novosel D, McFadden DH and Relwani SM. "Desiccant Air Conditioner to Control IAQ in Residences" (1988) Proc. of IAQ 88, American Society of Heating, Refrigerating, and Air-Conditioning Engineers (ASHRAE).

4. Owen MK, Lawless PA, Smith DD, Ensor DS and Sparks LE. "Predicting Indoor Air Quality with IAQPC" (1992) Proc. of the 5th International Jacques Cartier Conference, Center for Building Studies, Concordia University.

5. Sparks LE, Tichenor BA, Jackson MD and White JB. "Verification and Uses of the EPA Indoor Air Quality Model" (1989) Proc. of ASHRAE IAQ 89, ASHRAE.

6. Li Y. "Prediction of IAQ in Multi-room Buildings" Proc of Indoor Air 93, Vol. 5.

7. Yuill GK, Jeanson MR, and Wray MR. "Simulated Performance of Demand-Controlled Ventilation Systems Using Carbon Dioxide as an Occupancy Indicator" (1991) ASHRAE Transactions Vol. 97 Pt. 2, ASHRAE.

8. Crow LW. *Development of hourly data for weather year for energy calculations (WYEC), including solar data, at 29 stations throughout the United States and 5 stations in southern Canada* (1983) ASHRAE RP 364, Bulletin; ASHRAE.

9. Emmerich SJ, Persily AK, and Walton GN. "Application of a Multi-zone Airflow and Contaminant Dispersal Model to Indoor Air Quality Control in Residential Buildings" (1994) Proc. of the 15th AIVC Conference, AIVC.

10. Emmerich SJ and Persily AK. *Indoor Air Quality Impacts of Residential HVAC Systems Phase II.A Report: Baseline and Preliminary Simulations* (1995) NISTIR 5559, NIST.

11. ASHRAE. Handbook of Fundamentals (1993) ASHRAE.

12. Emmerich SJ and Persily AK. *Indoor Air Quality Impacts of Residential HVAC Systems Phase I Report: Computer Simulation Plan* (1994) NISTIR 5346, NIST.

13. EPA. *National Air Quality and Emissions Trends Report, 1992* (1993a) US. Environmental Protection Agency.

14. EPA. *Air Quality Criteria for Carbon Monoxide* (1991) US. Environmental Protection Agency.

15. EPA. *Air Quality Criteria for Oxides of Nitrogen, Volume I of III* (1993b) US. Environmental Protection Agency.

16. Sinclair JD, Psota-Kelty LA, Weschler CJ and Shields HC. "Measurement and Modeling of Airborne Concentrations and Indoor Surface Accumulation Rates of Ionic Substances at Neenah, Wisconsin" (1990) Atmos Env 24A:627-638.

17. Shields HC and Fleischer DM. "VOC Survey: Sixty-eight Telecommunication Facilities" (1993) Proc. of Indoor Air '93, Vol. 2.

18. Axley JW. "Adsorption Modeling for Building Contaminant Dispersal Analysis" (1991) Indoor Air 1:147-171.

19. Leslie NP, Ghassan PG and Krug EK. Baseline Characterization of Combustion Products at the GRI Conventional Research House (1988) GRI-89/0210, Gas Research Institute.

20. Traynor GW, Apte MG, Carruthers AR, Dillworth JF, Grimsrud DT, and Gundel LA. "Indoor Air Pollution due to Emissions from Wood-Burning Stoves" (1987) Environ Sci Technol 21:691-697.

21. Byrne MA, Lange C, Goddard AJH, and Roed J. "Indoor Aerosol Deposition Measurements for Exposure Assessment Calculations" (1993) Proc of Indoor Air '93.

22. ASHRAE. *Ventilation for Acceptable Indoor Air Quality* (1989) Standard 62-1989, ASHRAE.

Implementing the Results of Ventilation Research
16th AIVC Conference, Palm Springs, USA
19-22 September, 1995

A Laboratory for Investigation of the Air Quality in Simulated Indoor Environments

L E Ekberg, J B Nielsen

Danish Building Research Institute, P O Box 119,
DK-2970 Horsholm, Denmark

A LABORATORY FOR INVESTIGATION OF THE AIR QUALITY IN SIMULATED INDOOR ENVIRONMENTS

Synopsis

A laboratory, designed to form the basis for research aiming at increasing the knowledge concerning the interactions between indoor pollution sources and the indoor environment, has been taken into operation. One long term purpose of the activities in the laboratory is to develop theoretical models, based on experimental data, for the prediction of the air quality in real buildings. At present, the experiments focus on the relationship between the emission of pollutants from building materials and the environmental parameters, i.e. air temperature, air humidity, air velocity and pollutant concentration in the air. The measurements include sensory assessments by panels of air quality judges, as well as chemical analyses of a variety of gaseous and vaporized organic compounds.

The air-conditioning and ventilation system enables the environment in the laboratory to be controlled with high accuracy, as regards the thermal climate. The temperature and the air humidity in the laboratory can be varied within wide ranges. Low concentrations of polluting gases, vapours and particles in the supply air are ensured by the use of a charcoal filter in combination with a high-grade fine filter. The conditioned and filtered supply air enters the laboratory by a displacement ventilation system, which can be operated either with constant or variable airflow rates.

The present paper gives a description of the air quality laboratory and outlines the approach for the indoor air quality research at the Danish Building Research Institute (SBI).

1. Introduction

The quality of the indoor environment is determined by several factors which influence the comfort and well-being of humans. One such factor is the presence of polluting substances in the indoor air, i.e. the indoor air quality. The major sources of indoor air pollution can be found among building materials, ventilation system components (e.g. deteriorated filters), office equipment, people and the outdoor air. The prerequisites for a good indoor air quality are set in the process of the design and construction of a building and in the maintenance of the building in operation.

It is a common viewpoint that the preferred measure to minimize the risk of poor indoor air quality is to reduce the strength of the indoor pollution sources rather than increasing the ventilation rates. To realize this, research is needed to increase the knowledge about the factors which influence the interaction between the pollution sources and the indoor air. One main goal is to provide professionals involved in the building design process with tools to aid an appropriate building design. This can, for example, be achieved by providing projectors the opportunity to select materials with low emissions of pollutants under all of the physical conditions conceivable in the indoor environment being projected. Emissions from building materials are of special concern since this type of pollution has been found to cause a lasting sensation of odours, as opposed to, for example, the sensory effects, caused by human bio-effluents, which usually disappear a few minutes after the start of the exposure, due to adaptation [1]. The emission of organic compounds from various materials used indoors can be studied using environmental chambers of different sizes [2,3]. Full-scale chambers can be used for testing large structures, combinations of materials and furniture, while small-scale chambers can be used for testing small samples of larger materials.

2. Lay-out and construction of the laboratory at SBI

The laboratory facilities consist of two adjacent ventilated full-scale rooms, of which the main room has a total volume of 96 m^3 and the ante-room has a volume of 32 m^3. The walls and the ceilings of the rooms consist of panes of glass mounted in aluminum frames and the floor consists of high-pressure laminated fibreboard. The main purposes for selecting these materials were to ensure a negligible sink effect and a negligible emission of pollutants from the inner surfaces of the laboratory. The two full-scale rooms are located in a 1800 m^3 hall, which is ventilated with an outdoor air change rate of about 4 h^{-1}. Figure 1 shows a photograph of the exterior of the air quality laboratory.

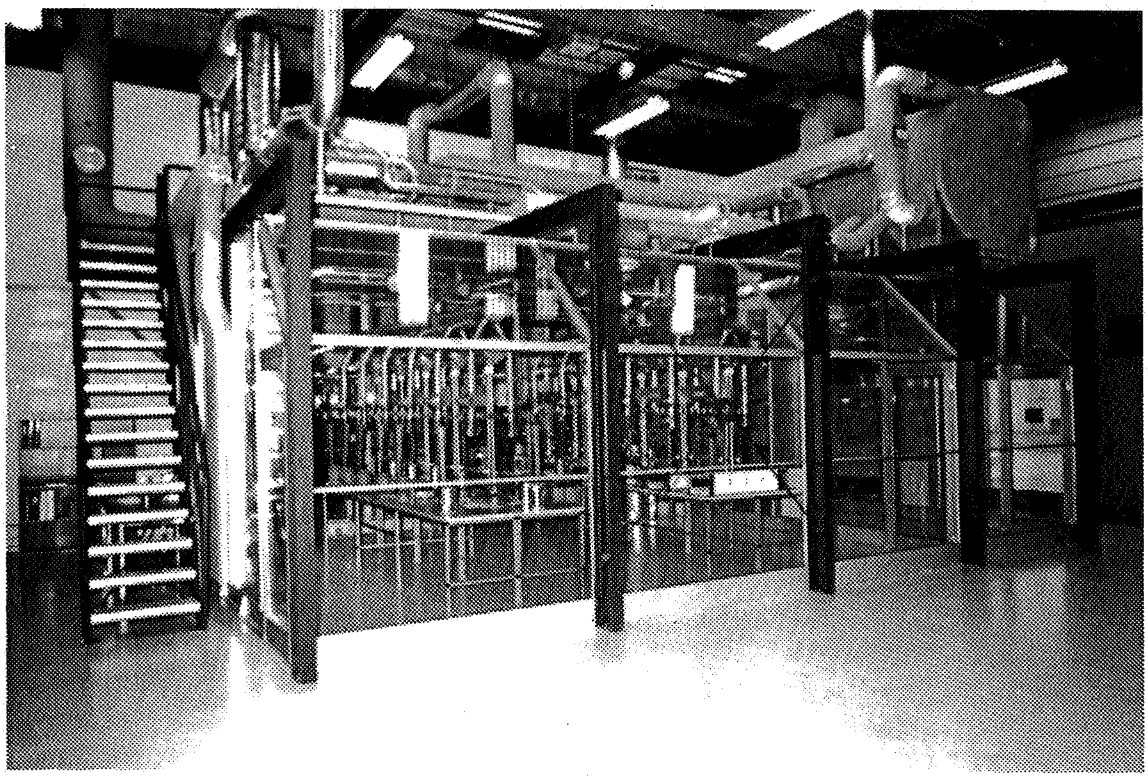

Figure 1. The exterior of the air quality laboratory with the main room to the left and the ante-room to the right. The ventilation and air conditioning system and the duct-work are located at the roof of the laboratory.

Small-scale test chambers
The laboratory is prepared for the simultaneous use of up to 24 small-scale test chambers in order to facilitate the investigation of a large number of building materials, studied under different environmental conditions. These small-scale chambers, of the type CLIMPAQ (Chamber for Laboratory Investigations of Materials, Pollution and Air Quality), are made of glass and have each an internal volume of 50,9 litres. The CLIMPAQs can be removed from the laboratory in order to enable full-scale experiments with large structures or combinations of materials. Details about the construction and operation of the CLIMPAQ can be found elsewhere [4]. Figure 2 shows a photograph of one group of CLIMPAQs in the main room. Up to twelve CLIMPAQs can be installed in each of two groups.

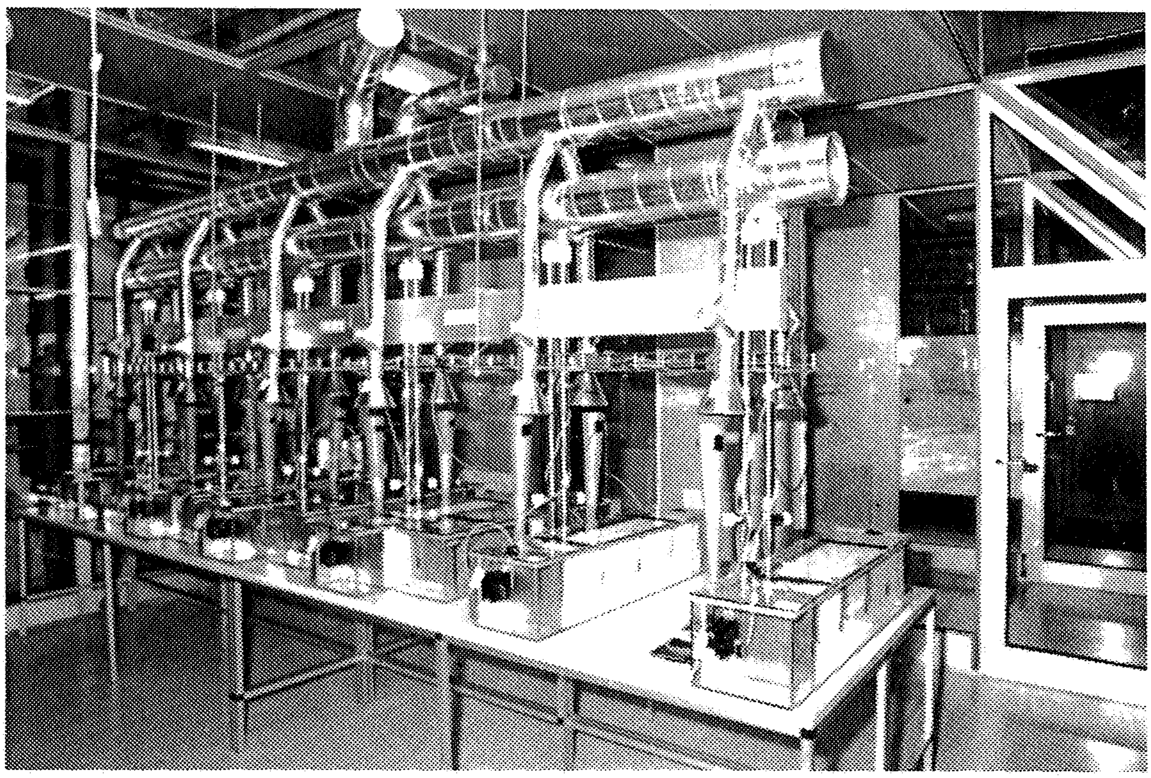

Figure 2. The interior of the main room with one of the two CLIMPAQ-groups.

Air-conditioning and ventilation system
The air-conditioning and ventilation system enables the temperature and the air humidity in the laboratory to be varied within wide ranges. The temperature in the main room and the ante-room can be varied between 10°C and 30°C, while the possible temperature range in the CLIMPAQs is 10-40°C. The relative humidity can be varied in the range 30-70 %RH. The stability of the airflows to the CLIMPAQs is within ±2%, while the temperature in the rooms and in the CLIMPAQs are controlled with an accuracy greater than ±0.5°C. The stability of the humidity control is ±5%RH at a relative humidity of 50%RH.

Low concentrations of polluting gases, vapours and particles in the supply air are ensured by the use of a particle filter of class EU5, a charcoal filter and a fine filter of class EU7. The conditioned and cleaned supply air enters the laboratory by a displacement ventilation system, which can be operated either with constant or variable airflow rates. The laboratory is operated at an overpressure of about 10-15 Pa relative to the hall in which it is located. Some technical data for the air quality laboratory and the CLIMPAQ are presented in table 1.

Table 1. Some technical data for the air quality laboratory and the CLIMPAQ. The air change rates and the airflow rates are specified as the maximum capacities obtainable in both rooms simultaneously.

		Main room	Ante-room	CLIMPAQ
Volume	[m^3]	95.3	31.8	0.0509
Floor area	[m^2]	34.0	11.4	0.200
Maximum air change rate	[h^{-1}]	9.5	11.5	127
Maximum airflow rate	[l/s]	250	100	1.80

3. Methods for measurements of air quality and experimental parameters

There are several types of sources, conceivable for investigation in the laboratory, each emitting a variety of chemical compounds. At present the focus is on volatile organic compounds (VOCs) emitted from building materials and on how pollutants from materials are perceived by humans. Therefore the air quality measurements include both chemical analyses of the emitted compounds and sensory assessments of the air quality.

Chemical analysis

Identification and quantification of volatile organic compounds are carried out by sampling on adsorbents, subsequently desorbed and analyzed with gas chromatography, flame ionization detection and mass spectrometry. The adsorbent material is normally Tenax TA filled in stainless steel tubes for active sampling of VOCs. After the adsorbents have been exposed they are transported to a chemical laboratory for analysis. This method gives detailed information about the individual substances present. However, of practical and economical reasons the method can only give results with relatively low time-resolution.

The total concentration of VOCs (TVOC) is measured with high time-resolution using an instrument based on photo-acoustic spectroscopy. This method cannot give any information about individual VOCs, but gives the opportunity for screening the TVOC concentration in all of the 24 small-scale chambers as well as in the full-scale rooms and in the supply air. The measurement system, which is controlled by a personal computer, includes automatic logging of the measured concentrations and automatic switching between all of these sampling locations. The minimum time-interval between two samples including purging of the sampling tube is about 1 minute. In addition to the TVOC concentration, the instrument can measure, for example, the total concentration of aldehydes.

Sensory assessments
The human perception of air pollutants from materials may be measured using sensory panels of judges assessing the air quality [5,6]. The sensory assessment may be based on the use of trained panels of about 10 persons. Each panel member is trained to assess the perceived air quality in the decipol unit. The decipol-scale is related to known concentrations of the reference gas 2-propanone. The perceived air quality can also be measured using an untrained panel of at least 40 judges. The air quality in the CLIMPAQ is assessed using a diffuser mounted at the air outlet of the CLIMPAQ. To ensure a low background concentration in the laboratory where the CLIMPAQs are located, this space is ventilated with the maximum airflow rate shown in table 1, when the panel members are carrying out their air quality assessments.

Experimental parameters
The supply airflow rates and the air temperature in each CLIMPAQ are monitored automatically and stored by a personal computer. The airflow rates are measured with temperature compensated hot-wire anemometers mounted in the supply air ducts to the CLIMPAQs. The inaccuracy of the measured airflow rate is typically less than ±5% of the measured value. The temperatures in the CLIMPAQs, in the supply air and in the main room are measured with thermocouples with an inaccuracy of about ±0.2°C. The air humidities in the CLIMPAQs are measured with the photo-acoustic gas analyzer described above.

4. Selection of airflow rates for the CLIMPAQ tests

The test parameters used during experiments are selected to represent realistic indoor conditions. In order to get a realistic concentration of pollutants the airflow rate is chosen based on a model room, so that the ratio between the ventilation rate and the material area, i.e. the area specific airflow rate in the CLIMPAQ is equal to the ratio in the model room. Table 2 shows an example of the calculated area specific airflow rates for different material types, using the Nordtest Model Room [7] ventilated with an air change rate of 2.0 h^{-1}.

Table 2. Surface areas and area specific airflow rates for different material types in the Nordtest Model Room [7] ventilated with 2.0 h^{-1}.

Material type	Surface area in the model room [m^2]	Area specific airflow rate at 2.0 h^{-1} in the model room [m^3/h per m^2]
Floor/Ceiling	7	4.83
Wall	24	1.41
Sealant	0.2	169

5. Studies recently carried out in the laboratory

This section summarizes the test-design and aim of two projects that recently have been carried out in the air quality laboratory. The purpose of presenting the test design is to give an indication of the approach and the extent of the experiments.

The influence on emission rate of the air velocity and the concentration
Five different new materials were tested under different conditions regarding the air velocity over the material surface and the concentration of the emitted pollutants. The materials were selected to represent frequently used indoor materials of different types, as regards the material thickness and surface structure. The test specimens were samples of an acrylic wall paint on gypsum board, waterborne varnish on beech-wood parquet, PVC floor, carpet of tufted nylon and an acrylic sealant. The tests were performed using three different airflow rates with a factor 10 between the minimum and the maximum values. The air velocities over the test specimens ranged from 0.05 to 0.20 m/s. Throughout the tests the air temperature and the relative humidity in the CLIMPAQs were held constant at 23°C and 50%, respectively.

The tests were carried out during three subsequent two-month periods involving the simultaneous use of 12 CLIMPAQ-chambers. Sampling for detailed chemical analyses and sensory assessments were carried out at days 1, 7, 14, 28 and 60.

Selection of flooring materials for a planned building
Five floor coverings, competing for installation in a new airport terminal, were tested with respect to their inclination to emit pollutants to the air. The materials were newly produced and they were tested during a one month period under constant environmental conditions. The experiments included a study of the effect of cleaning agents on the indoor air quality.

6. Future research areas and projects

This section gives a brief presentation of various research projects that will be carried out in the air quality laboratory.

Indoor climate labelling of building materials
The danish standard for determination of emissions from building materials was adopted in 1994. The standard forms the basis for the activities within the Danish Indoor Climate Labelling of Materials [8], which is operated in collaboration with building material producers. The aim is to provide manufacturers with standardized methodologies for the development of "healthy" materials for indoor use. At present, the focus is on emission of organic compounds from newly produced building materials, and the method is based on both chemical analyses and sensory assessments in combination with mathematical modelling. The main feature of the approach is the calculation of an "indoor climate relevant" time value, which is an expression of the time required for the emission to decline sufficiently to result in an acceptable concentration of pollution in a standard room. The acceptable concentration thresholds are established from evaluations of the

thresholds for both irritation and odour. The indoor air quality laboratory at SBI is a fundamental tool for further development and refinement of the labelling system.

Sorption processes, pollution sources and sinks

It has been shown that sorption of pollutants on indoor surfaces may be of importance to the indoor air quality. Adsorption on surfaces may reduce the maximum indoor concentration, but when the compound, at a later stage, is desorbed the result will be an extended time-period required for the decay of the concentration of the pollutant in question (i.e. a prolonged exposure to pollutants). Future research will aim at an increased knowledge about the influencing parameters and the sorption characteristics of various indoor materials. The basic knowledge will be obtained by the use of micro-balance studies, based on gravimetric weighing of small material samples. The transfer to real conditions will be obtained by studies based on concentration measurements in the CLIMPAQ chambers and full-scale experiments.

Mould growth on building materials

Growing knowledge on the impact of mouldy materials in water damaged buildings in relation to human health has resulted in model studies in CLIMPAQs. Type of mould as well as their metabolic products, which may have health implications, have been identified. Observations, such as irritation from eyes, skin and mucosa have been experienced by the test panels assessing the air quality in the chambers with mouldy materials.

Further development of methods for sensory characterization of emissions

It has been shown that the exposure-response relationship between the concentration of air pollutants from materials and the perceived air quality differs between materials and that the relation may differ from the corresponding relation for human bio-effluents [6]. Furthermore, the sensory emission rates determined by sensory assessments are not constant, but may depend on the concentration level they are determined at. In order to be able to model the perceived air quality, in spaces where concentrations may vary, the exposure-response relationship needs to be known. This is achieved by assessing the air quality at least at two different concentration levels for each material type. For this purpose a dilution system, for use in combination with the CLIMPAQ, is under development. The system enables mixing of the polluted exhaust air from the CLIMPAQ with unpolluted supply air. In this way it is possible to produce different concentration levels of the pollutants emitted from a certain material.

Full-scale experiments

The smaller of the two rooms in the laboratory, the ante-room, is used as a reference chamber for the passive tracer gas technique (PFT-technique) developed and used by SBI [9]. Moreover, in the future, there will be an increased need for a full-scale laboratory facility, e.g. when the models developed by the use of results from small-scale emission testing are to be verified by comparison to full-scale experiments. To meet these future demands, the CLIMPAQs can be removed from the laboratory, which creates a full-scale laboratory facility, consisting of two test chambers of 32 m^3 and 95 m^3, respectively. With this flexible solution it is also possible to carry out experiments in the field of air distribution in rooms.

7. Conclusions

In the air quality laboratory at the Danish Building Research Institute the main parameters of importance to the indoor air quality can be controlled and monitored with high accuracy. Independent experiments can simultaneously be carried out in up to 24 small-scale test chambers. The high test capacity makes it possible to perform detailed and extensive studies of the interaction between the indoor air and the indoor building materials. Due to the flexible design, the laboratory can easily be prepared for a wide variety of investigations within the fields of indoor air quality and ventilation.

Acknowledgements

The work related in this paper is a result of the efforts of several of the colleagues at the SBI. The authors wish to thank the following persons for their valuable contributions: U. Kjær, L. Gunnarsen, J. Lauridsen, H.N. Knudsen and S. Gravesen. The development and construction of the air quality laboratory was financed by the Danish Ministry of Housing, National Building and Housing Agency. L.E. Ekberg gratefully acknowledges the financial support from the Danish Research Academy and the Swedish Institute.

References

[1] Gunnarsen, L. "Adaptation and ventilation requirements", Proceedings of the Indoor Air '90 Conference, V1, pp 599-604, Toronto, 1990.

[2] Commission of the European Communities, "Guideline for the characterization of volatile organic compounds emitted from indoor materials and products using small test chambers", Report EUR 13593 EN, 1991.

[3] Commission of the European Communities, "Determination of VOCs emitted from indoor materials and products, Interlaboratory comparison of small chamber measurements", Report EUR 15054 EN, 1993.

[4] Gunnarsen, L., Nielsen, P.A. and Wolkoff, P. "Design and characterization of the CLIMPAQ chamber for laboratory investigations of materials, pollution and air quality", Indoor Air, 4, pp 56-62, 1994.

[5] Bluyssen, P.M. "Air quality evaluated by a trained panel", Ph.D. Thesis, Laboratory of Heating and Air Conditioning, Technical University of Denmark, Lyngby, 1990.

[6] Knudsen, H.N, Clausen, G. and Fanger, P.O. "Sensory characterization of emissions from materials", Submitted to Indoor Air, 1995.

[7] Nordtest Method, "Building materials: Emission of volatile organic compounds, chamber method", NT Build 358, Esbo, 1990.

[8] Wolkoff, P. and Nielsen, P.A. "Indoor climate labelling of building materials: Chemical emission testing, modelling and indoor relevant odour thresholds", National Institute of Occupational Health, Copenhagen, 1993.

[9] The Nordic Building Research Cooperation Group, NBS-I, "The development of the PFT-method in the Nordic Countries", Ed. Säteri, J., The Swedish Council for Building Research, Stockholm, 1991.

Implementing the Results of Ventilation Research
16th AIVC Conference, Palm Springs, USA
19-22 September, 1995

Measurement and CFD Modelling of IAQ Indices

M Regard, F R Carrie, A Voeltzel, V Richalet

Ecole Nationale des Travaux Publics de l'Etat,
Departement Geniem Civil et Batiment, URA CNRS
1652, Rue Maurice Audin, 69518 Vaulx en Velin Cedex,
France

MEASUREMENT AND CFD MODELLING OF IAQ INDICES

M. REGARD, F.R. CARRIÉ, A. VOELTZEL, V. RICHALET
Ecole Nationale des Travaux Publics de l'Etat,Département Génie Civil et Bâtiment, URA CNRS 1652
Laboratoire des Sciences de l'Habitat, Rue Maurice Audin 69518 Vaulx en Velin Cedex FRANCE

SYNOPSIS

So as to better understand and predict IAQ problems, the velocity field and distribution of local mean age of air were determined experimentally with three-dimensional anemometry and decay-mode tracer gas measurements inside a classroom. We also performed 3-D numerical simulations of the velocity field in this room, using a CFD code. The time dependent concentration decay of tracer gas was simulated using the previously determined flow field in the pollutant transport equation. Relatively good agreement was found between the simulated and experimental concentration decay curves. From those curves, a map of local mean age of air was built, allowing us to quantify the ventilation efficiency in the classroom.
Our analyses show that the use of a CFD code to quantify air quality indices and/or to identify indoor air quality issues can be of particular interest for design and diagnostic of sensitive areas with regard to IAQ problems.

LIST OF SYMBOLS

$c_e(t)$	pollutant concentration at exit opening and time t (kg/m^3)
$c_o(t)$	pollutant concentration at supply opening and time t (kg/m^3)
$c_p(t)$	tracer gas concentration at point P and time t (kg/m^3)
k	kinetic energy of turbulence (m^2/s^2)
Q	ventilation rate (m^3/s)
t	time (s)
V	room volume (m^3)
ε	kinetic energy of turbulence dissipation rate (m^2/s^3)
$\varepsilon_{c,p}$	pollutant removal efficiency at point P (dimensionless)
$\tau_n = V / Q$	nominal time constant of the room (s)
τ_p	local mean age of air at point P (s)
$\tau'_p = \tau_p / \tau_n$	normalised local mean age of air at point P (dimensionless)

1. INTRODUCTION

Richalet *et al.* (1994) performed field measurements in 4 classrooms located near Lyon (France) in order to assess the quality of indoor climate and to try to better understand occupants' behaviour regarding windows opening [1]. The survey included measurements of CO_2 concentration, relative humidity, temperature, openings duration, and aerobiological load together with outdoor climate and questionnaires to the occupants. Results have shown very high CO_2 levels coupled with significant aerobiological loads at some time of the day, even in one mechanically ventilated building. In some cases, not only the air exchange rate is insufficient according to the French national standards (that require a ventilation rate of 15 m^3/h per person in classrooms), but also the location of supply and return openings is not appropriate. These observations were in good agreement with the feeling of stuffy climate revealed by the occupants' interviews. From this alarming report, we decided to perform a larger-scale field testing in classrooms in order to better assess the extent of IAQ problems in French schools and in turn, to try to improve the existing situation. In parallel, in this paper, we study the assessment of ventilation systems effectiveness in terms of IAQ. Here, our

investigations focus on experiments performed in one of the previously monitored classrooms (Collège de St Genis Laval, see [1]).
After some background information and a description of our experiments, the fourth and fifth parts of this paper are dedicated to the numerical simulations we performed to predict IAQ indices and dynamic pollutant removal behaviour in this room.

2. BACKGROUND

Literature was reviewed to take a census of the many indices available at present to predict air quality and comfort in a room [2]. It appears that researchers take an increasing interest in IAQ indices such as local mean age of air (τ_p, defined as the average time for air to travel from a supply outlet to point P in a room) and pollutant removal efficiency ($\varepsilon_{c,p} = \frac{c_e - c_o}{c_p - c_o}$) ([3], [4], [5]).
Recently, Gan and Awbi (1994) performed numerical predictions of the local mean age of air in a room using the steady-state approach. To this end, they directly solved the transport equation for the local mean age of air.
They obtained good agreement with experimental data. They also simulated CO_2 emissions generated by occupants and found that the age of air was not appropriate to indicate the air quality in spaces with contaminant sources.

Another limitation of the use of such an index to qualify IAQ lies in the fact that the effect of a given pollutant concentration with respect to health or comfort is essentially non-linear. As a matter of fact, for most pollutants, doubling their concentration or the exposure time does not double their effect on human beings and thus temporal fluctuations of their concentration can have a major impact. As a result, it appears particularly interesting to study the dynamic behaviour of a pollutant concentration.

To this end, we chose to simulate decay-mode tracer gas measurements with a commercially-available CFD code (Fluent) and to compare our results with field measurement data. This way it is possible to compare predicted and measured concentration levels as a function of time and to assess the adequacy of using this CFD code to predict time-dependent pollutant transport. Comparisons between the predicted and measured local mean age of air at different locations in the room were performed using the following equation:

$$\tau_p = \int_0^\infty \frac{c_p(t)}{c_p(0)}\, dt \tag{1}$$

Thus, local or global pollutant removal efficiencies were assessed numerically. Finally, so as to better understand possible discrepancy in the results, we also performed anemometry measurements with a 3D probe and three omni-directional sensors.

3. EXPERIMENTS

3.1 Description of the classroom

Our experiments were carried out in a full-scale classroom in a secondary school near Lyon (France). The cell studied is shown in figure 1.
The classroom is mechanically ventilated, with the possibility of blowing air at medium or high speed. The inlet air is a mixture of fresh air from outside, heated during the cold season, with polluted return air. Another specificity of the ventilation system in this room is that both air supply and return openings are located on the same vertical wall at the same height. Intuitively,

the existence of a short-circuit of the air flow between supply and return in the upper part of the room, with dead zones in the lower part seems possible, particularly at low inlet air velocities. It is worth noting that our experiments were carried out with the ventilation system turned on maximum speed in order to reach measurable velocities in the classroom.

3.2 Velocity measurements

We performed velocity measurements using 3 hot film omni-directional probes, together with an ultrasonic 3-D sensor. The 3-D sensor acquisition frequency was 80 Hz, the measurement being averaged over the acquisition period. Its accuracy is ± 2 cm/s for velocity magnitude and ± 2° for direction. The omni-directional probes perform continuous acquisition, and give results with an accuracy of ±1.5 % over the range [0 -1 m/s]. A few acquisitions were taken at each location and then averaged.
Simultaneously, air temperature was measured at the inlet incoming jet as well as at several other locations in the room for possible velocity correction. Surface temperatures at walls and windows were measured too. All of these temperature measurements were performed using PT100 probes.

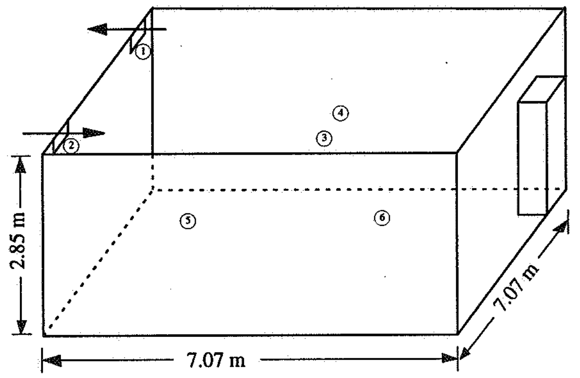

Fig. 1. Classroom dimensions and location of sampling points for tracer gas measurements.

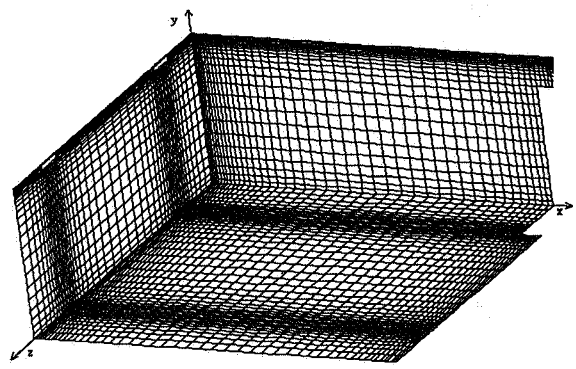

Fig. 2. 3 D computational grid (50 x 26 x 51).

3.3 Tracer gas measurements

To evaluate the distribution of local mean age of air in the room, we carried out a decay mode tracer gas experiment using SF_6. As shown in figure 1, 2 injection points were imposed in the center of the room at a height of 2.70 m. 4 sampling points were distributed over the room (points 4 to 6 at y = 1.20 m, point 3 at y = 2.70 m), and 2 additional sampling points were located at air supply and return so as to evaluate the ventilation system recycling rate. It was found to be 20% with a standard deviation of 2%.
During a first period, SF_6 was injected in the room with all openings sealed, and fans were used to ensure a good mixing. When the tracer gas concentration over the room seemed homogeneous, injection was stopped, fans were turned off, inlet and return openings were unsealed and the ventilation system was turned on maximum speed. Then SF_6 concentration started to decrease, and the experiment was continued until quasi zero concentrations were reached.

4. SIMULATIONS

The finite volume CFD code Fluent version 4.31 was used to solve the non-linear time-averaged Navier-Stokes equation to obtain the flow field in the room. From this converged flow field, the time-dependent transport equation of the tracer gas (here, $SF6$) was solved to simulate the decay of the pollutant concentration after injection. The computational grid (51 x 27 x 52 cells) is an irregular cartesian grid with refinement at walls and at air supply and return (fig. 2). Calculations were led using the SIMPLE solution algorithm and the Renormalization Group k-ε turbulence model [6].

Boundary conditions :

- At air supply, a uniform velocity profile at 24°C was applied, deduced from our tracer gas and temperature measurements. Thus, the average supply air speed was set to 1.24 m/s. It is noteworthy that the measured velocity magnitudes near the supply are in good agreement with our tracer gas measurement. However the jet profile, which includes somewhat higher velocities near the center than near the walls of the register was not taken into account. As for the velocity direction, it was deduced from the measured velocity map near the supply register. The supply air jet orientation with respect to the horizontal plane was found to be 27°.
No turbulence characteristics were measured experimentally. However, referring to previous full-scale experimental studies reported in [7], a uniform turbulent intensity profile (10%) was imposed. The turbulence length scale was calculated from the characteristic dimension at the inlet flow equal to the opening hydraulic diameter.
- At walls, a no-slip condition was applied as well as a constant surface temperature of 24°C. Turbulence conditions at walls were the RNG k-ε model built-in conditions for k and ε [6].
- At the flow exit, we set the static pressure to zero.

5. EXPERIMENTAL AND NUMERICAL RESULTS

5.1 Velocity field in the classroom.

Figure 3 illustrates the simulated velocity field obtained at $z = 0.67$ m, $z = 5.64$ m, and $y = 0.51$ m. The flow directions of the numerically predicted velocity field are in general in good agreement with our measurements (see figure 4). However, significant discrepancy in the results can be observed at some locations (see figure 5). Velocity magnitudes tend to be somewhat underestimated in the central part of the room (figures 4 to 6). This may be explained by the boundary conditions imposed at flow inlet. As previously mentioned, although the uniform velocity profile set ensures the correct ventilation rate, the peak value of velocity is not taken into account, which can lead to the prediction of lower velocities within the room.

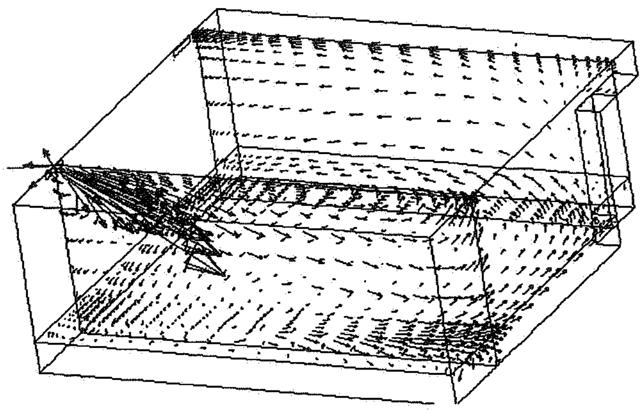

Fig. 3. Velocity vectors at z= 0.67 m, z = 5.64 m, and y = 0.51 m.

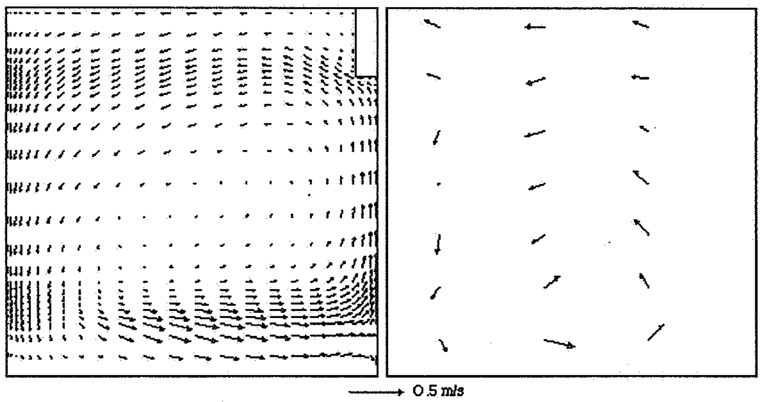

(a) (b)
Fig. 4. Horizontal velocity in a horizontal plane.
(a) Numerical results : z=1.34 m. (b) Experimental results : z= 1.23 m.

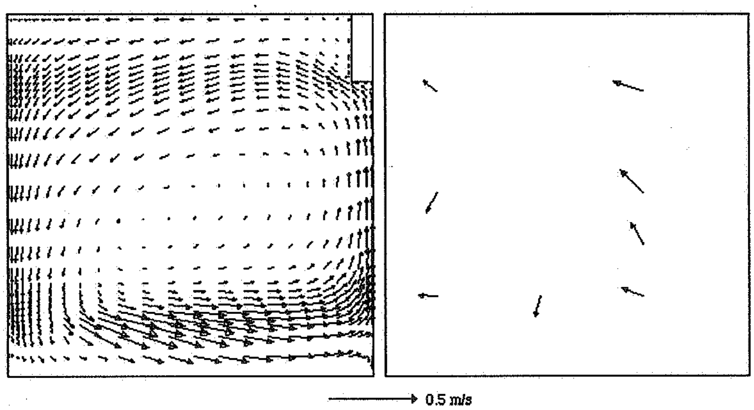

(a) (b)
Fig. 5. Horizontal velocity in a horizontal plane.
(a) Numerical results : z=1.59 m. (b) Experimental results : z=1.60 m.

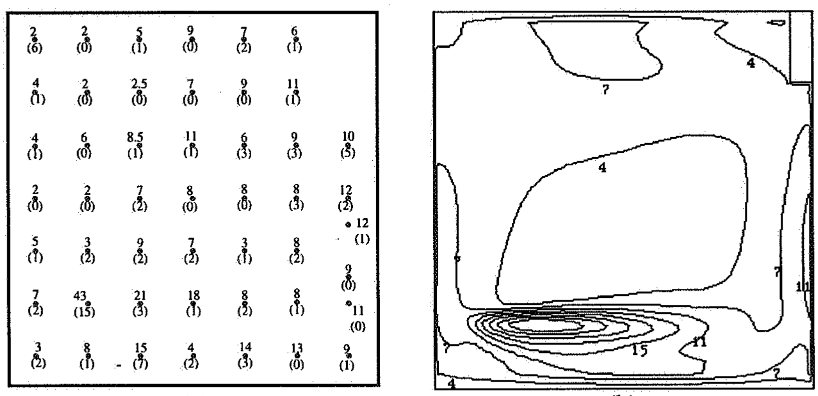

(a) (b)
Fig. 6. Velocity magnitude (cm/s) in a horizontal plane. (a) Experimental results : z=1.80 m. The figure in brackets is the standard deviation. (b) Numerical results : z=1.82 m.

5.2 Air quality in the classroom

From our tracer gas experiment, we observed a great homogeneity of concentration inside the room (figure 7a). It is worthwhile to note that sampling points 4 to 6 were located inside the occupation zone in the room, and so no measurements were performed at corners. As a result, within the occupied zone of this classroom all seats are ventilated with the same efficiency. The reader should note that the ventilation rate set during our experiments (roughly 200 m^3/h) is twice the ventilation rate usually prevailing in the classroom, and that was prevailing during the survey of Richalet *et al.* (1994). Therefore, in the present conditions, it is not surprising that the mixing of air appears better than what we could expect from this previous study [1].

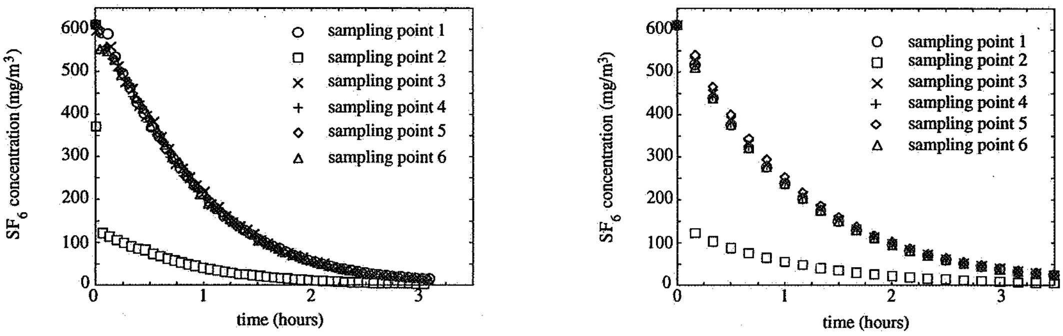

(a) (b)

Fig. 7. SF6 concentration in the classroom. (a) Experimental results. (b) Numerical results.

Predicted concentration decays are displayed in figure 7b. It is noteworthy that the decays are homogeneous (the curves are superposed), which is in agreement with our experimental observations. However, the predicted decontamination of the room appears to be too slow (predicted concentration levels up to 20% more than measured concentrations) (figure 8). One of the explanations of this observed discrepancy lies in the underestimated velocity magnitudes in the room, suggesting that this result could be improved if we better predict the flow field. Also, we can observe in figure 8 that the total amount of tracer gas crossing the return opening slightly differs from its expected value (14 % difference between the areas the concentration decay curves). One explanation lies in the uncertainty associated with the evaluation of the homogenisation concentration (and thus, the initial concentration at the return register) from the 4 sampling points in the room (points 3 to 6 in figure 1).

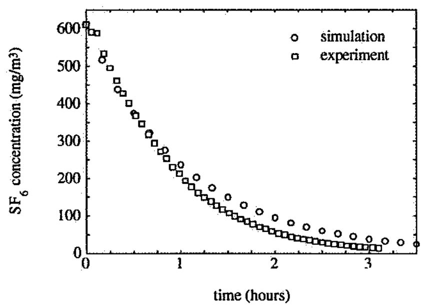

Fig. 8 : Tracer gas concentration at return opening during the decay period

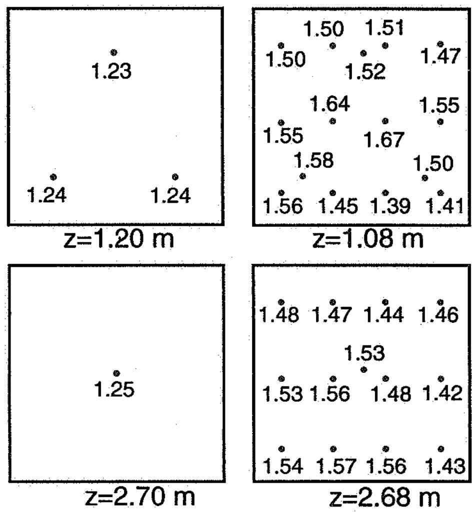

(a) (b)

Fig. 9 : Normalised local mean age of air distribution. (a) Experimental data. (b) Numerical results.

Nevertheless, the numerical results can provide extensive data, and give information about ventilation efficiency at different locations in the room, particularly in terms of local mean age of air distribution (fig. 9).The predicted local mean ages of air, normalised with respect to the nominal time constant of the room, are up to 25% more than those calculated from our experiments. In addition, it can be seen that the experimental age of air field seems uniform in contrast with the predicted results : the variation of the predicted normalised age of air is within 15%.
Moreover, our simulation of concentration decay in a room after injection of a pollutant can give an idea of the way the classroom is decontaminated from occupants pollutant production (CO_2, water vapor) after they leave the classroom, at the end of a class for example.

6. CONCLUSION

From experimental velocity and tracer gas measurements, we were able to estimate the air quality in a classroom in terms of local mean age of air at different location in the room. In addition, we found that the dynamic behaviour of the decontamination of a given pollutant could be simulated with a CFD code, and that the agreement between observed and predicted time-dependent pollutant concentration behaviour is relatively good. As a result, temporal fluctuations of a pollutant concentration can be determined to better assess its impact on man. However, we found that in our case the velocity field that is used to solve the pollutant transport equation is extremely sensitive to the boundary conditions (e.g. airflow direction) at the supply register and it appears that a more detailed modelling of inlet boundary conditions may lead to better agreement with experimental observations. In the future, we plan to focus on this issue and investigate the role of pollutant sources in dynamic concentration levels.

ACKNOWLEDGEMENTS

The presented work is part of a CNRS / ECOTECH research program on ventilation and indoor air quality. The authors would like to thank CNRS for their financial support during this project, and the executive staff of Collège de St Genis Laval for their kind assistance. We also thank Dr. Gérard Guarracino of ENTPE / LASH for his support.

REFERENCES

1. **Richalet, V., Beheregaray, B., Guarracino, G., Janvier, L., and Dornier, C.** *Effectiveness of ventilation systems in classrooms: a case study.* In *European Conference on Energy Performance and Indoor Climate in Buildings.* Lyon, France. École Nationale des Travaux Publics de l'État. 1994. p. 237-242.
2. **Voeltzel, A.** *Appréciation de la qualité des ambiances en terme de confort et de qualité de l'air.* DEA: ENTPE, 1995.
3. **Sandberg, M.** What is Ventilation Efficiency? *Building and Environment.* 1981, Vol. 16, N° 2, p. 123-135.
4. **Davidson, L. and Olsson, E.** Calculation of age and local purging flow rate in rooms. *Building and Environment.* 1987, Vol. 22, N° 2, p. 111-127.
5. **Gan, G. and Awbi, H.B.** *Numerical prediction of the age of air in ventilated rooms.* In *Roomvent '94 - Fourth International Conference.* Krakow, Poland. 1994. p. 15-28.
6. **Fluent Incorporated,** Fluent User's guide. Version 4.3, jan. 1995
7. **Jouini, D.B., Saïd, M.N., Plett, E.G.,** Measurement of room air distribution in a ventilated office environment. *Building and Environment.* 1994, Vol. 29, N° 4, p. 511-521.